

THE CASIMIR FORCE IN THE SEMI-CLASSICAL REGIME: A MICROSCOPIC THEORY

THÈSE N° 3585 (2006)

PRÉSENTÉE LE 21 JUILLET 2006
À LA FACULTÉ SCIENCES DE BASE
Groupe de mécanique quantique
SECTION DE PHYSIQUE

ÉCOLE POLYTECHNIQUE FÉDÉRALE DE LAUSANNE

POUR L'OBTENTION DU GRADE DE DOCTEUR ÈS SCIENCES

PAR

Pascal BUENZLI

physicien diplômé EPF
de nationalité suisse et originaire de Maur (ZH)

acceptée sur proposition du jury:

Prof. H. Brune, président du jury
Prof. Ph. A. Martin, directeur de thèse
Dr N. Macris, rapporteur
Prof. J. S. Høye, rapporteur
Prof. B. Jancovici, rapporteur



ÉCOLE POLYTECHNIQUE
FÉDÉRALE DE LAUSANNE

Lausanne, EPFL

2006

Abstract

The present thesis is devoted to a detailed study of the Casimir force exerting between two parallel metallic plates whose conducting behaviour is described on the microscopic level. In the semi-classical regime, which corresponds to large separations and high temperatures, the theoretical value of this force — which exhibits a universal character — is subject to a controversy revolving around a factor 2.

Current theories describe the plates macroscopically or semi-macroscopically and impose perfect boundary conditions to the field at their interface. In a statistical mechanical framework, we perform a direct calculation of the average force exerting between the fluctuating charges of a two-slab system in the semi-classical regime. In a first model, the charges are classical. The calculation is then generalised to quantum plasmas coupled to the radiation field, by means of path integral formalism. Relying on these accurate models, we can pronounce on the correct value of the force. In addition, we explain its universality as being the result of perfect screening mechanisms reflecting the effective shielding of the charges in the conductors. We conclude that although shielded, charge fluctuations inside the conductors cannot be neglected.

Keywords: Casimir forces, thermal quantum electrodynamics, field fluctuations, classical plasmas, quantum plasmas.

Version abrégée

Cette thèse est consacrée à une étude détaillée de la force de Casimir s'exerçant entre deux plaques métalliques parallèles dont le comportement conducteur est modélisé sur le plan microscopique. Dans le régime semi-classique, qui correspond à de grandes séparations et de hautes températures, la valeur théorique de cette force — qui présente un caractère universel — est sujette à une controverse portant sur un facteur 2.

Les théories actuelles font appel à une description macroscopique ou semi-macroscopique des conducteurs et imposent au champ des conditions de bord parfaites à leur interface. Partant des principes de la mécanique statistique, nous exposons un calcul direct de la force moyenne s'exerçant entre deux systèmes composés de charges fluctuantes, dans le régime semi-classique. Dans un premier modèle, les charges sont traitées classiquement. Puis, par le biais du formalisme des intégrales de chemin, le calcul est généralisé à des plasmas quantiques en interaction avec le champ de radiation. Sur la base précise de tels modèles, nous sommes en mesure de nous prononcer sur la valeur correcte de la force. De plus, nous expliquons l'origine de son universalité comme étant le fait de règles de somme reflétant l'écrantage effectif que subissent les charges. Nous concluons que bien qu'écrantées, les fluctuations de charge à l'intérieur des conducteurs parfaits doivent être prises en compte.

Mots-clefs: Forces de Casimir, électrodynamique quantique à l'équilibre thermique, fluctuations de champ, plasmas classiques, plasmas quantiques.

Contents

Abstract, Version abrégée, Keywords	i
1 Introduction	1
1.1 Fluctuation-induced forces	1
1.2 The Casimir effect	3
1.3 Thermal effects — the semi-classical regime	6
1.4 Overview of the present thesis	13
2 General settings and outline of the method	15
2.1 Microscopic setting of the particles and the field	16
2.1.1 Hamiltonian	18
2.2 Statistical description	20
2.2.1 Bohr–van Leeuwen theorem	20
2.2.2 Correlation functions	22
2.3 Macroscopic properties of the system	25
2.3.1 Stability of matter and existence of the thermodynamic limit	26
2.3.2 Some physical parameters at stake in Coulomb systems . .	26
2.3.3 The weak-coupling regime	28
2.3.4 The semi-classical regime, and the Casimir force	28
2.3.5 Debye screening and sum rules	29
2.3.6 Perfect vs ideal conductors	31
2.4 The Casimir force	32
2.4.1 Main result of the thesis	33
2.5 Outline of the calculation	34
2.5.1 Expressing the force in terms of the Ursell function (The force as a two-body observable)	35
2.5.2 Introduction to Mayer graphs and their resummation . . .	41
2.5.3 Asymptotic correlations between the plasmas	44
2.5.4 Validity of the perfect screening sum rules	50
2.5.5 The asymptotic force	52
2.5.6 Generalisation of the method to quantum plasmas and field- coupled quantum plasmas	54

3	The Casimir force between classical plasmas	59
	Microscopic origin of universality in Casimir forces, <i>J. Stat. Phys.</i> , 119, 273–307 (2005)	63
3.1	Introduction	63
3.2	Description of the model	67
3.3	Mayer series for inhomogeneous charged fluids	69
3.4	Debye-Hückel theory	72
3.5	Contributions of the other graphs	78
3.6	Plasma in front of a macroscopic dielectric medium	83
	Appendix 3.A: Slab of finite thickness	87
	Appendix 3.B: Bounds for the Debye-Hückel potential	89
	Appendix 3.C: Decay of Mayer graphs at large slab separation	91
	References	93
3.7	Decay analysis of Mayer graphs	95
	3.7.1 Decay of Mayer graphs at large separation	95
	3.7.2 Illustration on a specific example	96
	3.7.3 Determination of the factor $d^{-2I} = d^{-2(L-C)}$	98
3.8	Towards subleading orders of the force	100
	3.8.1 Leading and subleading orders of the Ursell function	100
	3.8.2 On subleading contributions to the classical force	103
4	Field-coupled quantum plasmas: path integral representation	107
	Equilibrium correlations in charged fluids coupled to the radiation field, <i>Phys. Rev. E</i> , 73, 036113, 1–14 (2006)	115
4.1	Introduction	115
4.2	The model	118
4.3	The gas of charged loops and the effective magnetic interaction	120
4.4	Two quantum charges in a classical plasma	125
4.5	Particle correlations in the many-body system	128
4.6	Transverse field correlations	132
4.7	Bose and Fermi statistics	136
4.8	Concluding remarks	138
	Appendix 4.A	140
	Appendix 4.B	141
	Appendix 4.C	141
	Appendix 4.D	142
	References	142
5	The Casimir force between field-coupled quantum plasmas	145
	The Casimir force at high temperature, <i>Europhys. Lett.</i> , 72, 42–48 (2005)	147
	References	155

5.1	The force expressed in the loop formalism	157
5.1.1	The free energy of the full system and its differentiation	157
5.1.2	The force expressed in terms of the loop-correlation	161
5.2	Quantum Mayer graphs	167
5.2.1	Resummation of the “classical” contribution V^{el}	168
5.3	Asymptotic correlations between the plasmas	170
5.3.1	The Debye–Hückel potential Φ_{AB} at large separations	170
5.3.2	The potential W_{AB}^c at large separations	171
5.3.3	The magnetic potential W_{AB}^m at large separations	171
5.3.4	Behaviour of the Mayer bonds	173
5.3.5	Dominant graphs and asymptotic behaviour of h_{AB}	174
5.3.6	Perfect screening sum rules	176
5.4	The Casimir force in the semi-classical regime: final result	178
5.4.1	Final result	179
	Appendix 5.A: Properties of V^c and W^m regarding loops’ origin	180
	Appendix 5.B: Large-distance behaviour of $\overline{W_{AB}^m}$	181
	Appendix 5.C: Brownian path integrals on slab geometries	183
6	Conclusions and outlook	187
	Appendix A: Resummation of Mayer graphs in density	193
	Appendix B: Some Fourier transforms	195
	Bibliography	197
	Acknowledgments	205
	Curriculum Vitae	207

Chapter 1

Introduction

Contents

1.1	Fluctuation-induced forces	1
1.2	The Casimir effect	3
1.3	Thermal effects — the semi-classical regime	6
1.4	Overview of the present thesis	13

1.1 Fluctuation-induced forces

The first evidence of a force between macroscopic bodies which is generated by the fluctuations of their surrounding media is likely to be found in the maritime domain. In the early 19th century, the frigate captain of the French royal navy P. C. Caussé describes in his book *l'Album du Marin : contenant les diverses positions du bâtiment à la mer* (Caussé, 1836) that two ships in a big swell but no wind (“*Calme avec grosse houle*”; see Figure 1.1) experience a certain attractive force when they happen to be at a close distance to each other. The rigs of the rolling ships would eventually disastrously entangle if strong crews rowing in the sloops would not tow the ships out of reach of one another. This force originates in the asymmetry (due to the presence of the other vessel) of the pressure exerted on the ships’ sides by the smaller waves produced by the rolling (Boersma, 1996).¹

In an entirely different field, H. B. G. Casimir (1948) was the first to predict the existence of an attractive force between two neutral parallel metallic plates at a distance d apart, induced by electromagnetic field fluctuations. The presence of

¹Very recently, however, Boersma’s statement has been qualified as a myth (Ball, 2006) in a news at news@nature.com.

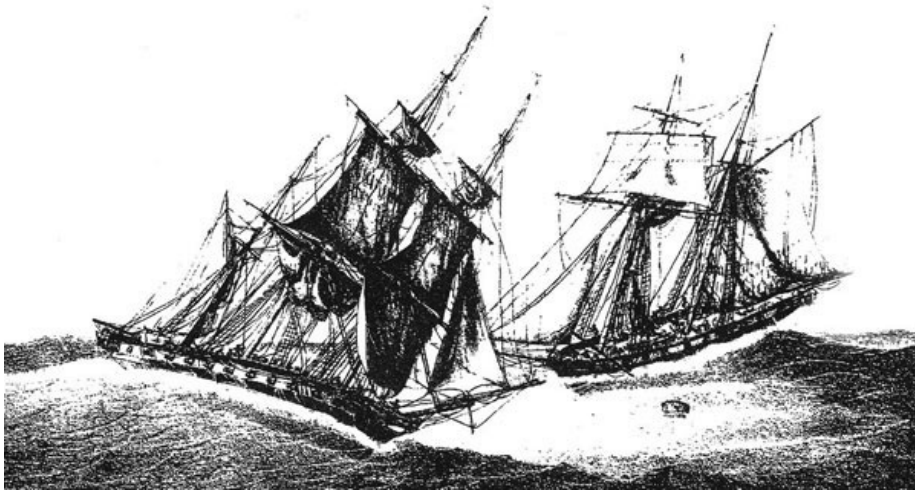


Figure 1.1: Two frigates in a big swell without wind attract each other.

this force can be similarly understood as being provoked by an asymmetry of the field radiation pressure between the inner space delimited by the plates and the outer spaces (Milonni, Cook, & Goggin, 1988).

Other fluctuation-induced forces have been observed and understood before Casimir's prediction: the London–van der Waals force between neutral atoms or molecules in a fluid (London, 1930). Even when atoms or molecules exhibit no permanent dipole moment in average, the quantum-mechanical fluctuations (deviations to the average value) of the latter still lead to an interaction potential, decaying as $1/r^6$ with the separation distance r . In fact, Casimir's paper on the two parallel plates follows a work of Casimir and Polder (1948) showing that retardation effects (the finiteness of the speed of light) accelerates the decay of the London–van der Waals interaction to a $1/r^7$ behaviour at very large distances (*i.e.*, much larger than atomic transition wavelengths).

Looking for a more elementary calculation for this result, and after a suggestion of Bohr,² Casimir discovered that the modification in the zero-point electromagnetic energy provoked by the presence of two metallic plates in the vacuum engenders a macroscopic force between them. Later, he could reinterpret the result about retarded van der Waals forces as being similarly due to a change of the zero-point energy induced by the presence of the second particle (Casimir, 1949).

Van der Waals forces, besides their implication in fluids, have everyday macroscopic implications too, such as the one observed by Aristotle (350 B.C., Book IX,

²See, *e.g.*, Milonni, (Milonni, 1994, Chap. 7)

part 9), who noticed the ability of gecko-lizards to adhere to tree trunks “even with the head downwards”. Geckos do not produce secretions; the unusually strong adhesive force of their feet (they are able to hang from a ceiling with one toe only!) has been asserted only a few years ago to be of van der Waals type, although capillarity effects from residual air humidity enhance its strength (Autumn et al., 2000, 2002; Huber et al., 2005). Carbon nanotubes have recently been used, with spectacular results, to imitate the gecko’s elastic foot-hairs, able to intimately establish contact with the surface so as to induce enough van der Waals type intermolecular interactions (Yurdumakan, Ravivakar, Ajayan, & Dhinojwala, 2005).

Many other fluctuation-induced effects can be found in nature. Their presence always reveals the incessant motion of what otherwise seems still. Let us, at last, mention — as a concrete application of their manifestation — that sound waves or noise in air can induce such a force between parallel metal plates, an interesting property of which is that it can be repulsive due to the limited bandwidth of the noise’s spectrum, suggesting nonresonant means of acoustic levitation (Larrazza & Denardo, 1998).

1.2 The Casimir effect

The original idea of Casimir’s calculation is based on the fact that two metallic plates that impose the vanishing of the electromagnetic field at their location restrain its allowed frequency modes $\omega_{\mathbf{K}}$. In particular, these frequencies, which correspond to the energies $\hbar\omega_{\mathbf{K}}(n + \frac{1}{2})$ of the quantized field, are dependent on the separation d between the plates. Even in the absence of photons ($n = 0$; “vacuum”, or zero-point, zero temperature), the residual total energy of the field $\frac{1}{2} \sum_{\mathbf{K},\lambda} \hbar\omega_{\mathbf{K}}$ due to its quantum fluctuations — and usually left behind because of its problematic infinite value — is the source of a force between the plates. Plates closer to each other “lower” the infinity of this quantity. As forces are defined only by differences of energy, Casimir could give to such a difference a well-defined value:³ the attractive *Casimir force* between the plates, whose strength by unit surface is

$$f(d) = -\frac{\pi^2 \hbar c}{240 d^4} \quad (1.1)$$

(\hbar is Planck’s constant, c the speed of light, and the minus sign denotes attraction). In spite of its apparently very theoretical character and its weakness (the force between two plates of 1cm^2 surface at a distance $1\mu\text{m}$ apart is of about 10^{-7}N), it is the strongest force between two neutral macroscopic objects at micrometer distances, and it has been observed experimentally.

³A regularization technique is necessary, however.

Casimir's pioneering calculation has raised whole new branches of research in many different fields:

- It poses the general problem of the “structure of the vacuum” in all quantum field theories in the presence of external sources or geometrical constraints. Understanding the properties of the vacuum leads to fundamental questions on the structure of the space-time. It is of crucial importance, *e.g.*, in cosmology, and in attempts to unify the four fundamental forces of nature.

Zero-point fluctuations of the electromagnetic field are also, for example, at the onset of the spontaneous emission of a photon by the decay of an excited atom.

- In quantum chromodynamics, the Casimir effect has been proposed as a confining mechanism for quarks and gluons, known as the “bag model” of hadrons.
- Attempts to explain sonoluminescence (intense light pulses arising from collapsing bubbles in alternatively compressed fluids) by means of this effect have given rise to the dynamical Casimir theory, in which effects with moving boundaries or constraints are investigated. An accelerated mirror, for example, should emit light as a consequence of it reflecting the vacuum fluctuations it encounters.
- In critical phenomena, forces between boundaries or layers can be generated at critical points, where the range of the interactions becomes long. These forces present similitudes with the Casimir force. In particular, they exhibit a universal character.
- Still in its very formulation — concerned more specifically by the forces due to the fluctuations of the electromagnetic field between conductors and dielectric bodies, or between atomic entities — a number of questions have been investigated, like the influence of geometry, of finite conductivity, of imperfect boundaries and their roughness. Some remain poorly understood, or even controversial, especially the influence of *finite temperature*. This last topic will be the main concern of the present work.
- On the technological level, the Casimir force can cause small elements in nanoscale structures and microelectromechanical systems to stick together. These devices are indeed fabricated at the micron and submicron scale. But the force can also be used to control the mechanical motion of such devices (Chan, Aksyuk, Kleiman, Bishop, & Capasso, 2001).

The literature on the Casimir effect is huge, and expanding every few days. It is impossible to be exhaustive in mentioning even general references. Among widespread text books and reviews are those of Milonni (1994), Duplantier and Rivasseau (2003), Levin and Micha (1993), Mostepanenko and Trunov (1997), Milton (2001), Plunien, Müller, and Greiner (1986), Elizade and Romeo (1991), Mahanty and Ninham (1976), *etc.* For more recent accounts on developments and controversies, see, *e.g.*, (Bordag, Mohideen, & Mostepanenko, 2001), and (Milton, 2004).

The scope of this effect's implications is equally hard to delimit and novel ideas may arise in the future. As an illustration, it has been asked very recently whether it might be a way of explaining the preservation of Cooper pairs in high-temperature superconductors (Kempf, 2006).⁴

Experiments

As soon as one comes to probing the Casimir force in experiments, the ideal case considered by Casimir has to be enhanced so as to include the other effects mentioned above.

Attempts to measure the force date back to the middle 1950s, but several technical problems prevented net conclusions to be drawn. The principal difficulties in the experiment of, *e.g.*, Sparnaay (1958) consisted in the cleaning and flattening of the surfaces, as well as in estimating the surface potentials of the capacitor's plates. The parallelism of the plates was controlled by "judging by eye" (!) the shaft of light of two 6W lamps placed in the plane of the interface (for two perpendicular directions to look at). They assessed the difference between the maximum and minimum separation to be at most $0.4 \pm 0.1\mu\text{m}$, for an average separation $d = 5\mu\text{m}$. Clearly, such a technique — in spite of its pleasant and appealing simplicity — is not really transposable at shorter distances and for more precise measurements. Most experiments are nowadays performed on systems made of a sphere in front of a metallic plate to overcome this serious difficulty. The Derjaguin approximation (Derjaguin, 1934) (also called "proximity force theorem") is used to modify the result (1.1) to this geometry [see, *e.g.*, (Bordag, 2006) or Refs. therein for first corrections; see also (Milton, 2004, Sec. 3.5)].

The advent of new technologies allowed to improve substantially experimental setups about a decade ago. First conclusive demonstrations of the Casimir force (to a few percents) have been performed by Lamoreaux (1997), and Mohideen and Roy (1998). They have been followed by many others, see, *e.g.*, (Milton, 2004, Sec. 3.6) for a short review. The only measurement reported on after Sparnaay in

⁴The idea is that the parallel Cu-O layers of such materials, isolating at temperatures higher than the critical value and superconducting below, would induce the formation of Cooper pairs so as to become superconducting and as such retrieve the Casimir energy.

the experimentally difficult (but theoretically simpler) two parallel plates geometry is that of Bressi, Carugno, Onofrio, and Ruoso (2002), who obtained a 15% precision level.

Yet, finite conductivity, and finite temperature corrections (among others) have been taken into account in these recent experiments, sometimes in a controversial manner. It is of importance to have at disposal precise theoretical formulae for them.

In this context, for example, it would also allow the experimental testing of Newton's inverse-square law of gravitation at micron length scales — after proper subtraction of the Casimir force. These tests are important because many theories attempting to unify the four fundamental forces predict the existence of yet undiscovered forces that would act at such scales (Fischbach & Talmadge, 1999).

1.3 Thermal effects — the semi-classical regime

Macroscopic theories

Calculations considering the thermal fluctuations of the field while still imposing its vanishing on ideally conducting plates (*i.e.*, on plates considered as *macroscopic objects without internal structure*), have been performed by Fierz (1960) and Mehra (1967). Two asymptotic regimes can be retrieved depending on the value of the dimensionless parameter

$$\alpha = \frac{\hbar c}{k_B T d} \quad (1.2)$$

(k_B is the Boltzmann constant), which measures the ratio of the thermal photon wavelength to the separation distance (see Section 2.3.2). For $\alpha \gg 1$ (short distances, low temperature), Casimir's result (1.1) is recovered. The next terms are the black body radiation pressure ($\propto T^4$) and exponentially small corrections in the parameter α . For $\alpha \ll 1$ (high-temperature, large-distances), up to exponentially small terms in $1/\alpha$, the result is found to be

$$f(d) = -\frac{k_B T \zeta(3)}{4\pi d^3}, \quad (1.3)$$

where $\zeta(3) = \sum_{n=1}^{\infty} n^{-3} \approx 1.202$ is the zeta Riemann function evaluated at 3. The latter force is still attractive, and has the remarkable property of being *classical*: it does neither depend on \hbar nor on c . Quantum mechanical fluctuations of the field that were inducing a force decaying as $\propto d^{-4}$ are taken up by thermal fluctuations and modify its decay to a $\propto d^{-3}$ behaviour. We will refer to this regime as **the semi-classical regime** of the Casimir force.

A calculation has been performed similarly by Schaden and Spruch (2002a, 2002b), but starting with a classical field from the beginning. The same result (1.3) is obtained.

Semi-macroscopic/semi-microscopic theories

Before the calculations of Fierz and Mehra, Lifshitz (1955) formulated a general theory of forces between *thermalised dielectrics*, including thus both effects of imperfect conductivity and finite temperature. It is based on the introduction in the Maxwell equations of an additional “random” field, thought of as reflecting the fluctuations of the plates’ microscopic constituents, exactly in the spirit of Langevin’s stochastic force in the theory of Brownian motion. The correlations of this random field are set to be local in space and homogeneous in time. They involve the dielectric susceptibility $\epsilon(\omega)$ of the media, Planck’s constant and the temperature all in one, as in the theorem of fluctuation-dissipation (Landau, Lifshitz, & Pitaevskii, 1984, Chap. 8). The random field — which represents the polarization and magnetization of matter — gives the material sources of the Maxwell equations. These equations are then solved for the total, stochastic, field according to the geometry of the problem, by imposing macroscopic Maxwell boundary conditions at the surfaces of the dielectric plates. The force by unit surface is retrieved as the Maxwell stress tensor, and its average is calculated from the given correlations of the added random field.

Lifshitz’ theory is very rich, and, to the present, the most complete and used theory (in its various reformulations) for Casimir-related experiments. At strictly zero temperature, it is capable of recovering Casimir’s result (1.1) for large distances and for an infinite dielectric constant corresponding to metallic plates; for short distances and dilute media, it reduces to the van der Waals–London force between polarizable molecules. When temperature is nonzero, at small separations — small but still large with respect to a characteristic length involved in the absorption spectra of the metal —, again (1.1) is found for metal plates, with first corrections in temperature. Going to large distances instead ($\alpha \ll 1$) yields the result

$$f(d) = -\frac{k_B T \zeta(3)}{8\pi d^3}. \quad (1.4)$$

This result differs from (1.3) by a factor 2.

This observation led Schwinger and his group (Schwinger, 1975; Schwinger, DeRaad, & Milton, 1978) to reformulate the theory in terms of Green’s dyadics (response functions relating the electromagnetic field to a microscopic polarization source). They found that Lifshitz’ general formula was correct, but prescribed

another way of taking the limits to recover the conducting case, which was leading to (1.3) instead of (1.4).

For a nice presentation and comparisons of the different derivations leading to Lifshitz' formula, see (Milonni, 1994). A shorter account can be found in the lecture notes of Ph. A. Martin prepared for the 1st Warsaw school of Statistical Physics, Kazimierz, Poland (Martin & Buenzli, 2006).

The controversy

To date, the factor 2 controversy between the value (1.3) and (1.4) still holds. After a long period of rest, it has naturally regained in strength since the experiment of Lamoreaux, and still results in actual dense debates. In fact, these debates also concern the low temperature corrections to Casimir's result (1.1). As such, it is not clear — depending on the author — whether temperature effects have been important in the experiments so far achieved, which have aimed at investigating the purely quantum force (1.1) but have been performed at room temperature.

The controversies arising in both regimes in Lifshitz-like theories reduce to knowing whether the reflection coefficient of the transverse electric (TE) mode of the field $r^{\text{TE}}(\omega, \mathbf{k})$ vanishes or not in the limit of zero frequency.

In the *low-temperature, small-separation regime*, this difference adds — or not — the linear temperature correction term $+\zeta(3)k_B T/8\pi$:⁵

$$f(d) \sim \begin{cases} -\frac{\pi^2 \hbar c}{240d^4} + O(T^4), & r^{\text{TE}}(0) = 1 \\ -\frac{\pi^2 \hbar c}{240d^4} + O(T^4) + \frac{\zeta(3)k_B T}{8\pi d^3}, & r^{\text{TE}}(0) = 0. \end{cases} \quad (1.5)$$

In the *semi-classical regime*, it changes the amplitude of the force by a factor 2:

$$f(d) \sim \begin{cases} -\frac{\zeta(3)k_B T}{4\pi d^3}, & r^{\text{TE}}(0) = 1 \\ -\frac{\zeta(3)k_B T}{8\pi d^3}, & r^{\text{TE}}(0) = 0. \end{cases} \quad (1.6)$$

The reflection coefficient is expressed in terms of the frequency-dependent dielectric susceptibility $\epsilon(\omega)$. Different models of an explicit dielectric function have been proposed. The question then reduces in knowing which of the two

⁵In his calculation, Lifshitz missed this $\propto T$ correction term by using the Euler–McLaurin sum formula on a discontinuous function. See (Høye, Brevik, Aarseth, & Milton, 2003, Sec. II).

proposed models:

$$\epsilon(\omega) = 1 - \frac{\omega_p^2}{\omega^2} \quad \text{“Plasma model”} \implies r^{\text{TE}}(0) = 1 \quad (1.7)$$

$$\epsilon(\omega) = 1 - \frac{\omega_p^2}{\omega(\omega + i\gamma)} \quad \text{“Drude model”} \implies r^{\text{TE}}(0) = 0 \quad (1.8)$$

represents adequately the physics of real conductors at small frequencies. This has led to several studies, both theoretical and numerical, and to re-analyses of experimental data.

Rather than citing the long list of all articles related to this controversy, and since no net result seems to have broken through in this context, let us briefly mention only a few works of the last developments.

- Brevik, Aarseth, Høye, and Milton (2005); Høye, Brevik, and Aarseth (2005) argue, on the basis of an analysis of optical data of real metals that the TE zero mode does not contribute, thus, in particular, that (1.4) is correct.
- On the other hand, Mostepanenko et al. (2005) rule out the Drude model which they say violates the third law of thermodynamics (the Nernst heat theorem) and contradicts experimental data (facts refuted by the former group).
- By taking into account the effects of spatial dispersion on the field’s modes, *i.e.*, by allowing a wavevector-dependent dielectric function, Sernelius (2005, 2006) says he resolves the controversy and finds (1.4) in the semi-classical regime. His work is criticized by Klimchitskaya and Mostepanenko (2006) who point out that he assumed a translation invariant space in all directions in writing the wavevector-dependent dielectric susceptibility, so that his conclusion is not reliable.

One of the last articles in this series is (Brevik, Ellingsen, & Milton, 2006).

These theoretical investigations are all based on Lifshitz’ formula, which proves to be at the same time powerful, but also insidious. Thermal effects in the Casimir force surprisingly seem to push this theory to its limits.

More refined analyses are needed. *In the following, we concentrate only on the factor 2 controversy occurring in the semi-classical regime.* In a joint letter with Jancovici and Šamaj (2005), we have stressed, on the firm basis of purely *microscopic models* of conductors (see below), the importance of taking into account the charge fluctuations inside the conductors (Buenzli & Martin, 2005b). We agree on saying that the correct result is (1.4).

As a last remark, let us note that an experiment in a cylinder–plane geometry is currently being developed by Brown-Hayes, Dalvit, Mazzitelli, Kim, and Onofrio

(2005) with the hope, in particular, to investigate larger distances and as such, to be able to discriminate from the experimental point of view the factor 2 problem.

Microscopic theories

Theories aimed at retrieving the Casimir force by modeling the plates on the atomic level have been relatively scarce, and are almost never mentioned in text books — except for the (unjustified) pairwise summation of van der Waals forces that led Lifshitz to develop his theory. This may be explained by the fact that these theories in general recovered Lifshitz' formula. In view of the preceding, and as we will see, microscopic theories might renew interest for future developments in Casimir forces.

Universality: an as yet not discussed remarkable characteristic of the Casimir force is its universality: the results for the force at zero temperature (1.1) or in the semi-classical regime (1.3)–(1.4) exerting between two *conductors* have in common that they are independent of the material constitution of the latter.

However, it could not really have been otherwise, because this constitution never entered fully in play in the modelling: in Casimir's original calculation, as well as in that of Fierz and Mehra, the plates consist only in perfect boundary conditions to the field. The coupled system of interacting matter and field has been reduced to field's degrees of freedom only. Matter's degrees of freedom are thought of having been integrated out so as to result in the enforcement of perfect conductor boundary conditions to the field, which are not made dependent on the plates' constitution. In Lifshitz-like theories, the material constitution of the plates is indeed taken into account by the dielectric susceptibility. However, the limit $\epsilon \rightarrow \infty$ is eventually taken to recover perfect conducting plates. This quantity disappears “by hand” from the result.⁶

It is the challenge of theories modeling the plates on the *microscopic* level to *understand the emergence of this universality*. In the case of the force between dielectrics, it is of note that Lifshitz' general force depends on their material constitution only by the dielectric susceptibility (which is, furthermore, a bulk quantity), which consists already in an extraordinary simplification of the microscopic processes at stake in the media.

⁶A form of universality was, however, noted by Lifshitz, in the sense that the force between dielectrics at large separations (for both zero and nonzero temperature) only depends on the static dielectric constant $\epsilon(\omega = 0)$. This has the consequence that the static conductivity $\sigma = \omega_p^2/(4\pi\gamma)$ and the plasma frequency ω_p occurring respectively in the Drude and plasma models (1.7)–(1.8) do not show up in the corresponding asymptotic results (1.3)–(1.4).

In the following, we mention some works performed on the microscopic level, and finally turn to the main subject of this thesis.

Dielectrics:

- An early microscopic calculation that retrieved the Lifshitz formula at zero temperature is that of Renne (1971a). It relies on a previous calculation (Renne, 1971b) expressing the energy of an arbitrary system of harmonic oscillators (atoms) in interaction with the radiation field as a sum of 2-particle, 3-particle, *etc.*, retarded van der Waals interactions. This interaction energy is written in terms of the dielectric constant of the medium, and the result compares to Lifshitz' formula for the force upon differentiation with respect to d .
- A quantum statistical model of polarizable fluids allowed Høye and Brevik (1998) to recover Lifshitz' formula at finite temperatures. The fluids are modeled by fluctuating dipole moments (harmonic oscillators) whose interaction with the field is assimilated to a “spin”-field coupling term. The path integral formalism is used to represent the quantum mechanical partition function in a classical-like form and field's degrees of freedom are integrated out, with the effect of yielding an effective interaction between the dipoles (Høye & Stell, 1981; Brevik & Høye, 1988). By considering Kubo's formula and the Ornstein–Zernike relation, they emphasize a correspondence between the Green functions of the macroscopic electromagnetic problem and the correlation functions of the microscopic system. This correspondence makes the connection between their average force and the Lifshitz force.
- Recently, Valeri and Scharf (2005) have formulated a microscopic theory for the force between dielectrics based on the photon-exciton Hamiltonian — representing the polarizable atoms interacting with the field. Using many-body techniques, they evaluate the Green function of the total electromagnetic field entering into the Maxwell stress tensor and retrieve Lifshitz' formula.

They emphasize that their model does not give an adequate description of metals (divergent series might occur in the metallic limit). However, they stress that at vanishing frequencies, their microscopic theory gives a vanishing reflection factor for the TE mode, supporting in this sense the value (1.4) of the force in the semi-classical regime. They also find that imposing hard boundary conditions in the macroscopic theory of the Casimir effect is not well-defined for it includes infinite self-energy contributions by disregarding the finite distances between the atoms.

Metals: The preceding microscopic theories all retrieve the Lifshitz force between dielectric media. Nevertheless, the factor 2 controversy concerns the force between perfect metals. We have seen that calculations in which no fluctuations at all of the field were allowed inside the metallic plates resulted in the value (1.3) of this force in the semi-classical regime. Lifshitz-like theories, which use an intermediate scheme — between taking into account these fluctuations, but still enforcing macroscopic boundary conditions to the field — are capable of retrieving both results (1.3) and (1.4) in the metallic limit. We will see that microscopic models of *conducting plates*, in which charge fluctuations are fully taken into account and no particular conditions are imposed to the field yield the result (1.4):

- In the study of universality properties of Coulomb systems, Forrester, Jancovici, and Téllez (1996) have investigated the case of a statistical system of classical charges confined to a two-dimensional plane parallel to a macroscopic, nonfluctuating, conductor (ideal conductor). They express the potential's correlations in terms of the Green function of the Poisson equation (which corresponds to a kind of Debye–Hückel approximation) and thus evaluate the stress tensor. The force between the two conductors is found to be Formula (1.4). Precisely, it does not depend on the microscopic charges. Jancovici and Téllez (1996) show that for this force observable, the macroscopic conducting plate can be thought of as a fluctuating system.
- Still in the framework of classical Coulomb systems, we provided in (Buenzli & Martin, 2005a) an exact calculation to retrieve the Casimir force (1.4) beyond the Debye–Hückel approximation in the large-separation asymptotics. The *universality* of the force has been found to be a direct consequence of *perfect screening sum rules* expressing the shielding of charges in conducting phases. At about the same time, Jancovici and Šamaj (2004) studied (in the Debye–Hückel theory) the screening of the Casimir force by an additional electrolyte filling the interspace.
- With a view to settle the debate about the factor two, we published a letter jointly with Jancovici and Šamaj (2005), based on analyses of the physical parameters at stake in the semi-classical regime of charged systems, and on exact calculations performed in their framework. In particular, our letter (Buenzli & Martin, 2005b) more specifically presents the calculation where matter is treated quantum-mechanically and is coupled to a radiation field. The main result is that the force (1.4) is retrieved, and that universality originates from the perfect screening sum rules satisfied by the charge correlations.

Although classical models already recover this force, this calculation is an important check that the force is not modified by the inclusion of retardation

effects, which we know — since Casimir and Polder — can have nonperturbative implications in fluctuation-induced forces.

These above-mentioned works are the ingredients of the present thesis, of which an overview is presented hereafter.

1.4 Overview of the present thesis

The present thesis has the purpose of investigating in detail the Casimir force between metals modelled by statistical systems of fluctuating charges in a two-slab geometry and in the semi-classical regime. Models of increasing complexity are presented, from classical Coulomb systems to quantum systems coupled to the radiation field.

The main results are the following. The force (1.4) is invariably retrieved. Its universality is the result of perfect screening sum rules satisfied by the correlations, that reflect the effective shielding of charges in the conductors. Our conclusion is that even though shielded, fluctuations of charges inside the conductors cannot be neglected in the calculation of the Casimir force in the semi-classical regime (at least), to retrieve correctly its value.

Each chapter will contain a detailed description of its own. The general structure and content of the document is as follows.

In the first part of Chapter 2, the microscopic and statistical description of the various systems investigated throughout this work are presented in detail. Then (Section 2.5), the main methods used to calculate the large-distance asymptotic force (beyond the Debye–Hückel theory) are illustrated by carrying them out on the simplest case of classical charges interacting via the Coulomb potential. The result already shows the above-mentioned microscopic origin of the universality of the force and has made the object of an article (Buenzli & Martin, 2005a), reproduced in Chapter 3. This chapter is supplemented by a few considerations about subleading contributions to the asymptotic force.

Matter and field decouple when they are both treated classically so that the field is inoperative on the Casimir force in such a case. In order to include the magnetic Lorentz forces between the slabs, we expose in Chapter 4 the formalism used to treat matter quantum-mechanically and include the coupling with the (classical) radiation field. The article (Boustani, Buenzli, & Martin, 2006) written on this subject is included. This formalism uses the Feynman–Kac–Itô path integral to represent the full statistical system in terms of a classical system of charged loops, whose random extension represents the quantum fluctuation of position of the particles. The field’s degrees of freedom can be integrated out exactly, resulting in an additional pairwise interaction exerting between the loops. In the article,

we also calculate the large-distance density correlations and large-distance field correlations of this quantum charged system.

In Chapter 5, we apply the formalism developed in the precedent chapter to the two-plate situation: the Casimir force in the semi-classical regime exerting between field-coupled systems of quantum charges is calculated using the same methods as in the classical case. We recover the result (1.4), even though new terms — of magnetic origin — arise in the asymptotic interplasma correlations. These new terms are shielded away by the screening mechanisms of the Coulomb fluids. The calculation details of this result presented in the letter (Buenzli & Martin, 2005b), also included in the chapter, are given.

Finally, Chapter 6 sums up the conclusions of this work and gives some perspectives.

Degree of rigour of the developments — asymptotic analyses:

The calculations carried out are not rigorous in the sense of pure mathematics. They rely on a certain number of assumptions physically plausible. Still, we do not have recourse to intermediate approximations. Among assumptions made, are the validity of the thermodynamic limit, the approach as $d \rightarrow \infty$ of physical quantities pertaining to one of the slab to their isolated-slab counterpart, the integrable speed of approach to bulk values of the density, the relevance of the resummed Mayer graph series. At times, limits and integrals have been freely interchanged (especially in the loop formalism). Whenever possible within reason, they have been rigorously justified by dominated convergence.

Throughout the document, we have made use of the notations $O(\cdot)$, $o(\cdot)$, and $\overset{d \rightarrow \infty}{\sim}$. These notations have a precise mathematical meaning, see, *e.g.*, (Olver, 1974). As an example,

$$f(d) \overset{d \rightarrow \infty}{\sim} -\frac{\zeta(3)}{8\pi\beta d^3} \quad \text{means} \quad \lim_{d \rightarrow \infty} d^3 f(d) = -\frac{\zeta(3)}{8\pi\beta}. \quad (1.9)$$

Chapter 2

General settings and outline of the method

Contents

2.1	Microscopic setting of the particles and the field	16
2.1.1	Hamiltonian	18
2.2	Statistical description	20
2.2.1	Bohr–van Leeuwen theorem	20
2.2.2	Correlation functions	22
2.3	Macroscopic properties of the system	25
2.3.1	Stability of matter and existence of the thermodynamic limit	26
2.3.2	Some physical parameters at stake in Coulomb systems	26
2.3.3	The weak-coupling regime	28
2.3.4	The semi-classical regime, and the Casimir force	28
2.3.5	Debye screening and sum rules	29
2.3.6	Perfect vs ideal conductors	31
2.4	The Casimir force	32
2.4.1	Main result of the thesis	33
2.5	Outline of the calculation	34
2.5.1	Expressing the force in terms of the Ursell function (The force as a two-body observable)	35
2.5.2	Introduction to Mayer graphs and their resummation	41
2.5.3	Asymptotic correlations between the plasmas	44

2.5.4	Validity of the perfect screening sum rules	50
2.5.5	The asymptotic force	52
2.5.6	Generalisation of the method to quantum plasmas and field-coupled quantum plasmas	54

The first part of this chapter aims to present the framework of the basic physical model that we consider, and its different refinements. As announced in the introduction, we model Casimir's metallic plates on the atomic level by two slabs containing moving interacting charges. In a fluid state, such slabs behave as conductors. In particular, they exhibit screening effects, which will prove to lie at the heart of universality in the high-temperature Casimir force. Yet, several laws of mechanics can be considered ruling these plasmas. They lead to different regimes of validity and degrees of complexity in the calculation of the total force between the plates. Since the high-temperature/large-distance force (1.4) or (1.3) has a classical value, one expects to be able to retrieve it already within a *classical* description of the plasmas. This force is, however, usually obtained as a limiting case of quantum field models. Moreover, depending on the specific model or the way the limiting case is obtained, its amplitude varies by a factor 2. It is therefore of strong interest to investigate the force in our microscopic framework when the plasmas are also *quantum-mechanical*, and *coupled to the electromagnetic field*.

The force acting between the thermalised plates will be defined in general by the derivative of the free energy with respect to the separation distance d . In classical and quantum plasmas, this corresponds to average the microscopic Coulomb forces exerting between the charges; for field-coupled plasmas, the whole Lorentz forces are taken into account.

In the second part of the chapter, we outline the main method employed to calculate the asymptotic Casimir force at large distances by illustrating it in the classical case. We comment on the tools by which this method can be generalised to the other cases. Explicit calculations and details will be found in the subsequent chapters and articles.

2.1 Microscopic setting of the particles and the field

A widely used model to describe conducting electrons in a metal is the one-component plasma, also known as jellium. It consists of electrons moving on a positively charged uniform background representing the crystallized ions. A more realistic representation of the microscopic entities at stake consists in replacing the neutralizing ionic background by positive point charges. We will be considering such systems of negative and positive moving charges (plasmas) to describe conducting matter.

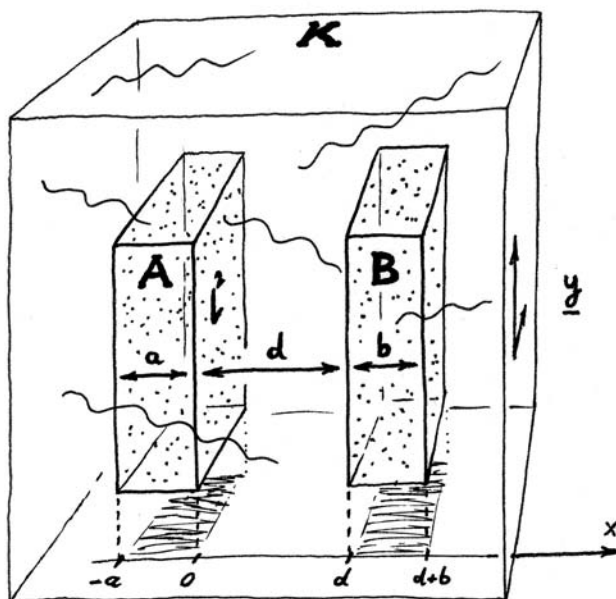


Figure 2.1: The two plasmas A and B of thickness a and b , surface L^2 , set at a distance d apart. They interact with the radiation field enclosed in the box K .

We represent the two metallic plates of Casimir's basic setting by a system consisting of two interacting plasmas A and B , set at a distance d apart. Their respective thickness is a and b and their surface L^2 (Figure 2.1).

We suppose these plasmas to be composed of nonrelativistic point charges of several species γ . At the detail level of the microscopic framework we are interested in, these species account for the negative and positive atomic entities mentioned above, typically electrons and ions. They can also represent positive and negative ions in an electrolyte. We denote by e_γ the charge, and by m_γ the mass of a particle of species γ .

The particles, constituting the plates, are confined by wall potentials to the two separate regions A and B , delimited by

$$-a < x < 0, \quad \text{and} \quad d < x < d + b \quad (2.1)$$

along the x axis, as shown in Figure 2.1. These confining potentials are considered steep, so that particles of plasma A stay in region A , and particles of plasma B in region B . As a consequence, particles in one plate are always distinguishable from alike particles in the other. The species index set $S \ni \gamma$ is split into two disjoint contributions S_A and S_B (for species in A and B), even though same characteristics of mass and charge can be found on either side. To ensure the global neutrality of

each plate, we impose

$$\sum_a e_{\gamma_a} = \sum_b e_{\gamma_b} = 0, \quad (2.2)$$

where the sums are carried over every particle of A and B , respectively.

This system of charges is coupled to an electromagnetic field which is itself enclosed into a larger box K englobing the plates. This field is not an external electromagnetic field. Rather, it contains also radiation created by the moving charges.

2.1.1 Hamiltonian

We will be using the **Coulomb gauge** so that electrostatic (longitudinal) effects remain separate from radiative (transverse) ones. It is commonly used when matter is nonrelativistic and high-energy processes are neglected (Cohen-Tannoudji, Dupont-Roc, & Grynberg, 1989, Sec. II.C.5). In this gauge, the N -particles Hamiltonian is known to read, in Gaussian units¹

$$H_{K,L} = \sum_{i=1}^N \frac{1}{2m_{\gamma_i}} \left(\mathbf{p}_i - \frac{e_{\gamma_i}}{c} \mathbf{A}(\mathbf{r}_i) \right)^2 + \sum_{i<j} \frac{e_{\gamma_i} e_{\gamma_j}}{|\mathbf{r}_i - \mathbf{r}_j|} + \sum_{i=1}^N V^{\text{walls}}(\mathbf{r}_i, \gamma_i) + H_0^{\text{rad}}. \quad (2.3)$$

Namely, the charges interact via the pairwise electrostatic (instantaneous) Coulomb potential

$$e_{\gamma_i} e_{\gamma_j} v(\mathbf{r}_i - \mathbf{r}_j) \equiv \frac{e_{\gamma_i} e_{\gamma_j}}{|\mathbf{r}_i - \mathbf{r}_j|}, \quad (2.4)$$

and the radiative contributions are contained in the particles' kinetic energy, which builds up the only matter–field coupling of this description. The vector potential $\mathbf{A}(\mathbf{r})$ is divergence free, and the term H_0^{rad} is the free field energy. The field is supposed to satisfy periodic boundary conditions on the sides of the box K , for simplicity.

The wall potential $V^{\text{walls}}(\mathbf{r}_i, \gamma_i)$ confines the particles either to A , if $\gamma_i \in S_A$, or to B , if $\gamma_i \in S_B$. We neglect spin–field couplings.

¹Electrostatic Gaussian units are most often used in atomic physics. They correspond to cgs (centimeters, grams, seconds) and the additional charge unit of statcoulomb (statC, or esu), defined by the requirement that the force between two unit charges at a distance of 1 cm apart is 1 dyne (1 g cm/s²). The Coulomb potential therefore reads $1/r$. See, e.g., (Jackson, 1998; Schwinger, DeRaad, Milton, & Tsai, 1998; Sommerfeld, 1948).

Throughout this work, the field will be treated classically. This will be justified for the calculation of the Casimir force in the semi-classical regime by the fact that only long wavelengths of the field are relevant for interactions across large distances d . Such modes are expected to be correctly described classically (like in Planck's radiation law). We will be dealing with two ways of treating the particles' mechanics:

- **Classical plasmas:** in this case, the dynamics induced by the Hamiltonian (2.3) corresponds to the coupled system of Maxwell equations (with sources given by the particles), and Newton's law (with the Lorentz force). The Casimir force due to classical plasmas is the object of Chapter 3.
- **Quantum plasmas:** in this situation, the particles will obey Fermi or Bose statistics, depending on their species. At least one fermionic species in each plasma will be assumed for stability. The Hamiltonian (2.3) acts on the Hilbert space of N -particle states, symmetrized accordingly. We note that we still assume particles with same characteristics in plasmas A and B to be distinguishable by their strict confinement.² The Casimir force due to field-coupled and quantum plasmas is investigated in Chapter 5.

Although being rather fundamental, the microscopic description given by the Hamiltonian (2.3) neglects a certain number of effects. Indeed, the quantum nature of the field, and relativistic effects of the particles, for example, are not included. Interaction processes of the field with matter involving high energy modes — leading to high velocities or even particle creations, like in electron-positron pair productions — are not described correctly in this nonrelativistic Hamiltonian regarding the particles. This leads to the introduction of a form factor in the Fourier mode expansion of the radiation field, cutting off wavelengths κ such that $\hbar c|\kappa| \gtrsim mc^2$. Doing so improves the consistency of the model and naturally removes ultraviolet divergencies.

By the omission of the spin–field coupling $-\mu_{\gamma_i}\sigma_i \cdot \mathbf{B}(\mathbf{r}_i)$, the Hamiltonian (2.3) is independent of the spin variables (μ_{γ_i} are the magnetic moment amplitudes containing the gyromagnetic factor, and σ_i the spin operators). The spin degrees of freedom of the particles can, however, still be taken into account. They are then involved in the symmetrization of the states, accordingly to Pauli's principle.

We emphasize that the formation of neutral atoms is not presupposed. In that respect, treating the field classically is not contradictory with the quantum-mechanical nature of the particles (in the weak-coupling regime at least). The moving charges may radiate at any wavelength.

²This is justified for example when the external potential is taken infinite in the whole space between the plates, preventing any tunneling effect between the two plasmas.

More generally, other fundamental forces than the electromagnetic one considered in this Hamiltonian are found in nature. Among them, the force one encounters most in its everyday experience is the gravitational force. However, the ratio of this force to the electrostatic force is very small in atomic matter; it ranges from 10^{-38} – 10^{-43} among protons and electrons. The remaining forces are the strong force, which holds the nuclei together but is of a very short range (10^{-15} m, about the size of a nucleus), and the weak force, changing the flavour of quarks. The weak force is necessary, in particular, for the buildup of heavy nuclei; it is of even shorter range (10^{-18} m, or 0.1% of a proton's size). All forces but the electromagnetic force are thus not relevant for the interactions taking place at the atomic level between the charged entities we consider.

2.2 Statistical description

The above setting is used as the microscopic basis for the calculation of the average force acting between the two plasmas. In the semi-classical regime, this force depends on temperature. The thermalised macroscopic states of our system are defined within the theory of statistical mechanics. We consider that matter and field are in thermal equilibrium, and in contact with a heat reservoir of temperature T . Statistical averages, denoted by $\langle \dots \rangle$, are taken with the Gibbs weight

$$\exp(-\beta H_{K,L}), \quad \beta = (k_B T)^{-1}, \quad (2.5)$$

according to standard statistical mechanics formulae (canonical or grand-canonical). The free energy $\Phi_{K,L,d}$ of the total system is defined by

$$\Phi_{K,L,d} = -k_B T \ln Z_{K,L,d}, \quad (2.6)$$

where $Z_{K,L,d}$ is the partition function integrating the Gibbs weight over all microscopic configurations of matter and field.

We will take the **thermodynamic limit** of this system in two stages. We let first the enclosing space for the field $K \rightarrow \mathbb{R}^3$, and then extend the plates' surfaces $L^2 \rightarrow \mathbb{R}^2$ in the transverse \mathbf{y} plane (see Figure 2.1). Finitely thick as well as semi-infinite ($a, b \rightarrow \infty$) plasmas will be considered.

The plasmas will be supposed in a fluid state (see Section 2.3). Macroscopic states as defined above will be invariant under translations and rotations in the transverse \mathbf{y} plane. Furthermore, by the microscopic constraints (2.2), each plasma will be globally neutral, carrying no average total charge.

2.2.1 Bohr–van Leeuwen theorem

An important difference between classical and quantum matter emerges at this point. The so-called Bohr–van Leeuwen theorem states that matter and field de-

couple in thermalised states when they are both treated *classically*. As a consequence, the free energy of the total system becomes the sum of the free energy of the electrostatic Coulombic matter, and the free energy of the free radiation field.

Classical partition function

Indeed, consider the phase space integrals of the classical Gibbs weight defining the total partition function:

$$Z_{K,L,d} \equiv \int \frac{d\alpha}{\pi} \int d\mathbf{r} d\mathbf{p} e^{-\beta H_{K,L}}. \quad (2.7)$$

We have denoted by $d\alpha/\pi$ the integral over all field's mode amplitudes, and, symbolically, by $d\mathbf{r} d\mathbf{p}$ the spatial and impulsions integrals of all particles (their exact form depends on the ensemble chosen). The simple shifts $\mathbf{p}_i \mapsto \mathbf{p}_i - \frac{e\gamma_i}{c} \mathbf{A}(\mathbf{r}_i)$ in particles' impulsions (at fixed positions and field amplitudes) render the kinetic energy of the particles in the integrand independent of the vector potential $\mathbf{A}(\mathbf{r})$. The coupling terms between matter and field are suppressed in the Hamiltonian (2.3), so that the Gibbs weight factorizes into the product $e^{-\beta H_0^{\text{rad}}} e^{-\beta H_L^{\text{mat}}}$, with

$$H_L^{\text{mat}} = \sum_{i=1}^N \frac{\mathbf{p}_i^2}{2m_{\gamma_i}} + \sum_{i<j} \frac{e_{\gamma_i} e_{\gamma_j}}{|\mathbf{r}_i - \mathbf{r}_j|} + \sum_{i=1}^N V^{\text{walls}}(\gamma_i, \mathbf{r}_i) \quad (2.8)$$

corresponding to the Hamiltonian of electrostatic matter. The partition function of the total system becomes

$$Z_{K,L,d} = Z_{0,K}^{\text{rad}} \Xi_{L,d}^{\text{mat}}, \quad (2.9)$$

where

$$Z_{0,K}^{\text{rad}} = \int \frac{d\alpha}{\pi} e^{-\beta H_0^{\text{rad}}}, \quad \Xi_{L,d}^{\text{mat}} = \int d\mathbf{p} d\mathbf{r} e^{-\beta H_L^{\text{mat}}} \quad (2.10)$$

are the partition function of the free field, and of the electrostatic particles. Finally, the free energy (2.6) splits into

$$\Phi_{K,L,d} = \Phi_{0,K}^{\text{rad}} + \Phi_{L,d}^{\text{mat}}. \quad (2.11)$$

Since the field's free energy $\Phi_{0,K}^{\text{rad}}$ is obviously independent on d , it plays no role in the calculation of the Casimir force. The field will therefore be omitted from the description from the beginning in Chapter 3, and only electrostatic matter will be considered.

Quantum partition function

The partition function in the quantum case reads

$$Z_{K,L,d} = \int \frac{d\alpha}{\pi} \text{Tr}_{\text{mat}} e^{-\beta H_{K,L}}. \quad (2.12)$$

As before, all (classical) Fourier amplitudes of the field are integrated over. The trace is carried over all particle wave functions with appropriate statistics. A decoupling between field and matter no longer holds.

2.2.2 Correlation functions

The free energy constitutes a very important function in the statistical mechanics of thermalised systems. It is related, in the thermodynamic limit, to the free energy defined by the phenomenological laws of thermodynamics. Macroscopic observables involved in mechanical or heat processes, such as the pressure, the entropy, *etc.*, are obtained as derivatives of it (for the aforementioned observables: with respect to the (specific) volume, and to temperature).

However, correlation functions — especially density and charge correlation functions — play a not less important role. We briefly present their main characteristics in what follows.

Their knowledge allows to calculate mean values of a number of observables defined on the microscopic stage. In particular, the observables one is usually mostly interested in are one-particle observables (like the density) or two-particles observables (like the total energy, or the total force between the plasmas A and B , in our two-plasma system), for which only the one-point and the two-point density correlations need to be known. Moreover, these correlation functions can be accessed directly through experiments. The one-point correlation function is no more than the mean density itself. Two-point correlation functions can, *e.g.*, be measured by neutron or X-ray scattering (Hansen & McDonald, 1986; Stanley, 1971).

The one-point correlation function (the density)

The microscopic density of particles of species γ at point \mathbf{r} is defined by

$$\hat{\rho}(\mathbf{r}, \gamma) = \sum_{i=1}^N \delta_{\gamma\gamma_i} \delta(\mathbf{r} - \mathbf{r}_i) \quad (2.13)$$

(N is the total number of particles, $\delta_{\gamma\gamma_i}$ the Kronecker symbol, and $\delta(\mathbf{r} - \mathbf{r}_i)$ the Dirac distribution.) The mean density, or one-point correlation function, corre-

sponds to the statistical average of this microscopic observable:

$$\rho(\mathbf{r}, \gamma) = \langle \hat{\rho}(\mathbf{r}, \gamma) \rangle. \quad (2.14)$$

The two-point correlation function

One may ask in a system of interacting particles how the density of particles of species γ at a point \mathbf{r} of the space correlates to (is influenced by) the known presence at \mathbf{r}' of another particle, of species γ' (Figure 2.2).

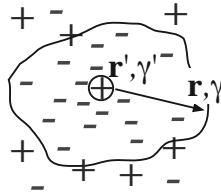


Figure 2.2: Because of interactions, the presence at \mathbf{r}' of a particle of species γ' influences the particle density of species γ at \mathbf{r} .

One can show that this conditional density reads, in average,

$$\langle \hat{\rho}(\mathbf{r}, \gamma) |_{\mathbf{r}', \gamma'} \rangle = \frac{\langle \hat{\rho}(\mathbf{r}, \gamma) \hat{\rho}(\mathbf{r}', \gamma') \rangle}{\langle \hat{\rho}(\mathbf{r}', \gamma') \rangle}, \quad (2.15)$$

where $\langle \hat{\rho}(\mathbf{r}, \gamma) \hat{\rho}(\mathbf{r}', \gamma') \rangle$ is called the *two-point density* or the *density-density correlation function*, and gains its meaning through the relation (2.15). This correlation function includes the contribution of coincident points: it describes correctly for the conditional density the situation in which $\mathbf{r} = \mathbf{r}'$ and $\gamma = \gamma'$. When this coincident point contribution is extracted out, we will speak of the *two-point correlation function* or *density correlation function* $\rho(\mathbf{r}, \gamma; \mathbf{r}', \gamma')$. One has

$$\langle \hat{\rho}(\mathbf{r}, \gamma) \hat{\rho}(\mathbf{r}', \gamma') \rangle = \rho(\mathbf{r}, \gamma; \mathbf{r}', \gamma') + \delta_{\gamma\gamma'} \delta(\mathbf{r} - \mathbf{r}') \rho(\mathbf{r}, \gamma). \quad (2.16)$$

In a noninteracting particle system, the conditional density simply results in the mean density $\rho(\mathbf{r}, \gamma)$. Indeed, nothing can tell at point \mathbf{r} what is happening at point \mathbf{r}' . The two-point density factorizes into $\langle \hat{\rho}(\mathbf{r}, \gamma) \rangle \langle \hat{\rho}(\mathbf{r}', \gamma') \rangle$. The same is expected to happen in effect when the two points \mathbf{r} and \mathbf{r}' become very distant from one another. Often, for that reason, one considers *truncated correlation functions*, where the factorized product is further subtracted. In a fluid state, such truncated correlations tend rapidly to zero as $|\mathbf{r} - \mathbf{r}'| \rightarrow \infty$. On the other hand, in a crystallized phase, they will rather oscillate according to the lattice structure (Hansen & McDonald, 1986).

The mean-value of a one-body observable can be expressed as an integral over the density. Similarly, the mean-value of a two-body observable can be expressed as a double integral over the two-point correlation function. Consider, e.g., the average of the Coulomb potential energy $U_C = \sum_{i < j} e_{\gamma_i} e_{\gamma_j} / |\mathbf{r}_i - \mathbf{r}_j|$. Rewriting the double sum as $\frac{1}{2}(\sum_i \sum_j - \sum_{i=j})$, one can express each of the latter sums as an integral carried on Dirac functions: precisely the microscopic density. Using the linearity of the expectation value $\langle \dots \rangle$, one has, in view of (2.16),

$$\begin{aligned} \langle U_C \rangle &= \frac{1}{2} \left\langle \sum_{\gamma, \gamma'} \int d\mathbf{r} \int d\mathbf{r}' \hat{\rho}(\mathbf{r}, \gamma) \hat{\rho}(\mathbf{r}', \gamma') \frac{e_{\gamma} e_{\gamma'}}{|\mathbf{r} - \mathbf{r}'|} - \sum_{\gamma} \int d\mathbf{r} \hat{\rho}(\mathbf{r}, \gamma) \frac{e_{\gamma}^2}{|\mathbf{r} - \mathbf{r}|} \right\rangle \\ &= \frac{1}{2} \sum_{\gamma, \gamma'} \int d\mathbf{r} \int d\mathbf{r}' \rho(\mathbf{r}, \gamma; \mathbf{r}', \gamma') \frac{e_{\gamma} e_{\gamma'}}{|\mathbf{r} - \mathbf{r}'|} = \frac{1}{2} \int d\mathbf{r} \int d\mathbf{r}' c(\mathbf{r}, \mathbf{r}') \frac{1}{|\mathbf{r} - \mathbf{r}'|}. \end{aligned}$$

In the last equation, we have defined the *charge correlation function* $c(\mathbf{r}, \mathbf{r}') = \sum_{\gamma, \gamma'} e_{\gamma} e_{\gamma'} \rho(\mathbf{r}, \gamma; \mathbf{r}', \gamma')$. Such developments can be done the same way for any two-body observable (except for the last equality).

Let us finally introduce the dimensionless, truncated correlation function defined by

$$h(\mathbf{r}, \gamma; \mathbf{r}', \gamma') \equiv \frac{\rho(\mathbf{r}, \gamma; \mathbf{r}', \gamma')}{\rho(\mathbf{r}, \gamma) \rho(\mathbf{r}', \gamma')} - 1. \quad (2.17)$$

It is called the **Ursell function** and is of particular importance, for it is subject to a formal expansion in the density by means of Mayer graphs. It will be the centrepiece investigated in this work, once the Casimir force will be expressed as a microscopic two-body observable.

As a last remark, note that in classical statistical mechanics, calculating the average of the microscopic density — or the average of products of the density — with the Gibbs weight in the canonical ensemble, say, the properties of the Dirac distribution and the fact that the Hamiltonian is symmetric under permutations of alike particles yield the representations

$$\rho(\mathbf{r}, \gamma) = \frac{1}{\Xi_{\text{mat}}} \int d\mathbf{p} \int d\omega_{N-1} e^{-\beta H(\mathbf{r}, \gamma, \mathbf{p}; \mathbf{r}_2, \gamma_2, \mathbf{p}_2; \dots; \mathbf{r}_N, \gamma_N, \mathbf{p}_N)}, \quad (2.18)$$

$$\rho(\mathbf{r}, \gamma; \mathbf{r}', \gamma') = \frac{1}{\Xi_{\text{mat}}} \int d\mathbf{p} \int d\mathbf{p}' \int d\omega_{N-2} e^{-\beta H(\mathbf{r}, \gamma, \mathbf{p}; \mathbf{r}', \gamma', \mathbf{p}'; \mathbf{r}_3, \gamma_3, \mathbf{p}_3; \dots; \mathbf{r}_N, \gamma_N, \mathbf{p}_N)}, \quad (2.19)$$

sometimes posed as definition of the correlation functions. In (2.18) and (2.19), $d\omega_{N-1}$ and $d\omega_{N-2}$ are the particles' integration elements on the $N-1$ and $N-2$ last particles, respectively (they contain, respectively, factors $N_{\gamma} / \prod_{\gamma''} N_{\gamma''}!$ and $N_{\gamma} N_{\gamma'} / \prod_{\gamma''} N_{\gamma''}!$ if $\gamma \neq \gamma'$, $N_{\gamma}(N_{\gamma}-1) / \prod_{\gamma''} N_{\gamma''}!$ otherwise). Correlation functions of higher order (three-point, four-point, *etc.*) are naturally defined similarly. We will not use them in this work.

2.3 Macroscopic properties of the system

Charged systems as defined above depict an accurate microscopic description believed to give an account of many states of matter. They incorporate, for nonrelativistic matter, the principal energies in play on the atomic level.

At high temperature, low density — in the fluid state —, they obviously describe electrolytes (ionic solutions), and weakly relativistic plasmas. In this phase, these models exhibit perfect conductor behaviours on the macroscopic scale. In particular, the *screening effects* originating from the signed and long-range Coulomb interaction are known to hold. A fixed charge in the plasma surrounds itself, in average, with opposite charges, with the effect of reducing its effective strength above a certain distance (the screening length) (see Figure 2.3). We will come back to this property below.

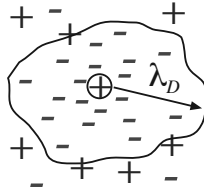


Figure 2.3: The screening length λ_D measures the extension of the screening cloud around a fixed charge.

As temperature is decreased, one expects the freely moving charges to recombine into neutral entities at low density. In a bulk quantum system (without radiation field), it has been shown by Fefferman (1985) that in a coupled limit of low density and low temperature, the equation of state of the electron–proton plasma tends to the ideal gas law of recombined Hydrogen atoms in their fundamental state. This result is called the *theorem of atomic limit*. The conducting behaviour of the system is lost in this limit. The charged fluid becomes isolating.

At non-strictly-zero temperature and density, there is still a fraction of ionized charges. When these charges and the recombined atoms are in thermal equilibrium (the Saha regime) it is possible to calculate the large-distance correlations occurring between them. They lead to effective van der Waals–London-like interactions in dilute systems between every species (even though charged), that take into account many-body collective effects (Alastuey, Cornu, & Martin, n.d.).

One of the grand successes of statistical mechanics is that, from invariable microscopic fundamental interactions, it provides a way of describing phase transitions between macroscopic regimes of very different properties, like gas–liquid, or ferromagnetic–paramagnetic transitions. In the statistical theory, these phase transitions correspond mathematically to nonanalyticities in the thermodynamic

functions, occurring within the thermodynamic limit. In the particular system of electrons and protons, when density is increased, the atomic or molecular gas phase of the model discussed above turns into a liquid, and eventually a solid. At very high density, one even expects a metallic Hydrogen phase to occur, showing up fully delocalized electrons, thus, again conducting.

Let us discuss further some properties of the fundamental description of our system, and introduce its main characteristic lengths.

2.3.1 Stability of matter and existence of the thermodynamic limit

The Coulomb interaction, its fundamental character notwithstanding, is difficult to deal with in statistical mechanics for essentially two reasons: its long range and the $1/r$ singularity at its origin. Concerns regarding the long range are resolved by the establishment of screening processes (see Section 2.3.5).

In **classical plasmas**, the collapse of opposite charges brought about by the Coulomb divergency at the origin needs to be overcome by adding a short-range repulsive potential

$$v_{\text{SR}}(\mathbf{r} - \mathbf{r}', \gamma, \gamma') \quad (2.20)$$

between the particles in the Hamiltonian (2.3). At high temperatures and low density, its specific form is irrelevant. It intervenes at ranges much smaller than the mean interparticle distance and the screening length (defined below).

This collapse does not occur in **quantum plasmas** containing at least one fermionic species due to Pauli's exclusion principle, which is the reason why we assumed each of our plasmas to contain at least one such species.

Although the particles' confining regions in our two-plasma system are not extended to the bulk in the x direction, we assume that the partial thermodynamic limit $L \rightarrow \infty$ yields well-defined equilibrium states and well-defined thermodynamic potentials as in the bulk situation (Lieb, 1976).

An account on recent results about the stability of matter coupled to the (classical or quantum) electromagnetic field can be found in Lieb (2004), and results on their thermodynamic limit (for a bulk system) in Lieb and Loss (2005). See also references therein.

2.3.2 Some physical parameters at stake in Coulomb systems

We introduce a number of parameters with the help of which specific regimes of the plasmas will be characterized.

Classical: the following parameters occur in classical plasmas already. They characterize the electrostatic plasma and its screening properties. They will be relevant to quantum plasmas too:

- the **mean interparticle distance** a_ρ , which corresponds to the mean density according to $a_\rho \approx \rho^{-1/3}$;
- the **Landau length** βe^2 (also called **Bjerrum length**). It can be thought of as a transition range above which electrostatic interaction is dominated by thermal fluctuations (e is a typical charge of the system, say, that of an electron);
- from the above lengths, one defines the **coupling parameter** $\Gamma = \frac{\beta e^2}{a_\rho}$. It consists in the ratio between the Coulomb and thermal energies, and measures the strength of the interaction, relatively to temperature;
- a length of considerable importance is the **screening length** or **Debye length** $\lambda_D \equiv \kappa^{-1} \approx (\beta e^2 \rho)^{-1/2}$: this length shows up once screening induced by the long range of the Coulomb interaction is systematically dealt with. The effective, mean-field interaction between classical charges in the bulk system is an exponentially damped potential e^{-kr}/r : the Debye length characterizes the range of the screening cloud surrounding a charge (Figure 2.3). One has $\lambda_D \approx a_\rho / \Gamma^{1/2}$.

Specifically quantum-mechanical: some additional relevant lengths and parameters specific to the quantum plasmas and to the field-coupled quantum plasmas are:

- the **thermal de Broglie wavelength** $\lambda_{\text{part}} = \hbar \sqrt{\beta/m}$, which measures the amplitude of the position fluctuations of the thermalised particles;
- the quantity $\frac{\lambda_{\text{part}}}{a_\rho}$, corresponding to a measure of the overlap of the wave functions. It characterizes the degree of degeneracy (at temperature T) of the quantum plasma;
- when the field is taken into account, an additional important length is the **photon thermal wavelength** $\lambda_{\text{ph}} = \beta \hbar c$. It is the wavelength of the field's mode whose energy is of the order of the thermal energy $k_B T$;
- the **relativistic parameter** $\lambda_{\text{part}} / \lambda_{\text{ph}} = 1 / \sqrt{\beta m c^2}$ will measure the strength of physical corrections brought by the inclusion of the radiation field. For consistency in our nonrelativistic model, this parameter must be considered small.

2.3.3 The weak-coupling regime

The weak-coupling regime is defined as the physical situations corresponding to small values of the coupling parameter:

$$\Gamma \ll 1. \quad (2.21)$$

This regime characterizes dilute systems in a fluid state, close to the ideal gas. It is attained for low densities and high temperatures, when the strength of the Coulomb interaction is weak. In terms of the screening length, it is equivalent to $a_p \ll \lambda_D$: the mean interparticle distance is much smaller than the screening length, so that the effective interactions are indeed screened, and the plasma behaves as a conductor.

Another parameter used to characterize this regime is $\Gamma' = \frac{1}{2}\beta e^2/\lambda_D \approx \Gamma^{3/2}$. The latter coupling parameter is better adapted to the consideration of weak-coupling expansions of the density profiles in inhomogeneous plasmas (J.-N. Aqua & Cornu, 2001b).

2.3.4 The semi-classical regime, and the Casimir force

Semi-classical regimes, in our microscopic theory, correspond to weakly degenerate plasmas $\lambda_{\text{part}}/a_p \ll 1$, and to relevant field modes of long wavelengths with respect to λ_{ph} . The relativistic parameter $\lambda_{\text{part}}/\lambda_{\text{ph}} = 1/\sqrt{\beta mc^2}$ is also $\ll 1$.

Let us investigate how these quantities relate to the different regimes usually considered for the Casimir force. The relevant parameter distinguishing the quantum and (semi-)classical regimes in the calculation of, *e.g.*, Lifshitz, is

$$\alpha = \frac{\hbar c}{k_B T d} = \frac{\lambda_{\text{ph}}}{d}. \quad (2.22)$$

In the event that $\alpha \gg 1$, the zero temperature Casimir force (1.1) is recovered. The classical value (1.3) or (1.4) of the force between the metallic plates is obtained when $\alpha \ll 1$. We will naturally regain this result in the *semi-classical regime* of the plasmas as specified right above. However, we also see that $\alpha \ll 1$ can correspond to the *weak-coupling regime* too, which is coherent with the conducting fluid state assumed for the metallic plates.

Indeed, $\alpha \ll 1$ can be attained by high temperatures and large separation distances. In our calculations, we will expand the force for large distances at a “high” but fixed temperature, so that the following parameter magnitudes are satisfied:

- $\Gamma \ll 1$ and $a_p/d \ll 1$, $\lambda_D/d \ll 1$. The plasmas are in a conducting fluid state (weak-coupling);

- $\lambda_{\text{part}}/a_\rho \ll 1$. The plasmas' particles are weakly degenerate;
- $\lambda_{\text{ph}}/d = \alpha \ll 1$. This ensures that among the modes of the thermalised field, only ones with very large wavelengths — of the order of d — may induce sizeable effects for interplasma interactions. Such modes are usually well-described classically (as in Planck's radiation law), which justifies the use of a classical treatment of the radiation field;
- $\lambda_{\text{part}}/\lambda_{\text{ph}} = 1/\sqrt{\beta mc^2} \ll 1$. The plasma is weakly relativistic. This has to be ensured for the consistency of our nonrelativistic model. Temperature can not be arbitrarily high, which is coherent with fixing temperature and letting $d \rightarrow \infty$.

For these reasons, the framework of our calculation and the assumptions about its regime (weak-coupled, fluid, conductive, semi-classical) agree with the high temperatures, large separations of the classical result (1.4)–(1.4) for the Casimir force. The fact that the plasmas are weakly degenerate and that the field can be treated classically in the limit $d \rightarrow \infty$ at a high temperature also indicates (by Bohr–van Leeuwen's theorem) that the pure classical model presented in Chapter 3 asymptotically captures the correct expression. Corrections naturally contain quantum and radiative contributions, but they only build up subdominant $\propto d^{-4}$ terms.

2.3.5 Debye screening and sum rules

We have already mentioned that in the fluid phase, the statistical charged system exhibits perfect conducting behaviours. One of the reasons is that the effective interaction arising from the classical Debye–Hückel mean-field theory is an exponentially damped potential with a range (λ_D) much larger than the mean interparticle distance (a_ρ), at weak-coupling. One interprets this reduction of the interaction range as the result of the screening of charges in the plasma. This is supported by the fact that the mean potential satisfies integral constraints, so-called *sum rules*. Perfect conducting behaviour of the system, whether classical or quantum-mechanical, is associated to alike relations holding more generally for its full correlation functions, especially the *perfect screening sum rule* (also called *electroneutrality* or *charge sum rule*). This rule expresses explicitly the fact that a fixed charge in the system is perfectly shielded away by a cloud of opposite charges.

Let us recall the simple reasoning of Debye and Hückel (1923a, 1923b) establishing the mean-field theory of a charged bulk system [see also (Balescu, 1975, Sec. 6.5)]. It naturally leads to the settlement of the perfect screening rule in the mean-field approximation already.

The mean-field electrostatic potential $\Psi(\mathbf{r})$ is defined in such a way that a particle of charge e_γ at \mathbf{r} experiences an average potential $e_\gamma\Psi(\mathbf{r})$ summing up the collective effects of all other particles of the system. The potential energy of the system thus reads $U(\mathbf{r}_1, \gamma_1, \dots, \mathbf{r}_N, \gamma_N) = \sum_{i=1}^N e_{\gamma_i}\Psi(\mathbf{r}_i)$. Then the conditional density at $\mathbf{r} \neq \mathbf{0}$ given that there is a particle e_{γ_0} at $\mathbf{0}$ is [see (2.15) and (2.19)]

$$\langle \hat{\rho}(\mathbf{r}, \gamma) |_{\mathbf{0}, \gamma_0; \mathbf{r}, \gamma \neq \mathbf{0}, \gamma_0} \rangle \equiv \frac{\rho(\mathbf{r}, \gamma; \mathbf{0}, \gamma_0)}{\rho(\gamma_0)} = \rho(\gamma)e^{-\beta e_\gamma \Psi(\mathbf{r})}, \quad (2.23)$$

where $\rho(\gamma)$ is the homogeneous density far from the origin ($\Psi(\mathbf{r}) \rightarrow 0$, $r \rightarrow \infty$). On the other hand, the macroscopic electrostatic potential at \mathbf{r} experienced around the fixed charge at $\mathbf{0}$ can be said to also correspond to the mean-field potential $\Psi(\mathbf{r})$. From this perspective, $\Psi(\mathbf{r})$ satisfies the Poisson equation with the conditional mean density (2.23) as source (taking into account the fixed charge):

$$\nabla^2 \Psi(\mathbf{r}) = -4\pi \sum_\gamma e_\gamma \langle \hat{\rho}(\mathbf{r}, \gamma) |_{\mathbf{0}, \gamma_0} \rangle = -4\pi e_{\gamma_0} \delta(\mathbf{r}) - 4\pi \sum_\gamma e_\gamma \frac{\rho(\mathbf{r}, \gamma; \mathbf{0}, \gamma_0)}{\rho(\gamma_0)}. \quad (2.24)$$

Inserting the mean-field expression (2.23) into (2.24), linearising the exponential (weak-coupling regime), and using the bulk neutrality $\sum_\gamma e_\gamma \rho(\gamma) = 0$, the potential reads as the solution of the (linear) Poisson–Boltzmann equation

$$[\nabla^2 - \kappa^2] \Psi(\mathbf{r}) = -4\pi e_{\gamma_0} \delta(\mathbf{r}), \quad \kappa^2 = \lambda_D^{-2} = 4\pi\beta \sum_\gamma e_\gamma^2 \rho(\gamma). \quad (2.25)$$

With bulk boundary conditions, its resolution yields

$$\Psi(\mathbf{r}) = e_{\gamma_0} \frac{e^{-\kappa r}}{r} \equiv e_{\gamma_0} \Phi(\mathbf{r}). \quad (2.26)$$

A common approximation then consists in replacing, in a nonconstrained system, the potential energy U by $\sum_{i < j} e_{\gamma_i} e_{\gamma_j} \Phi(\mathbf{r}_i - \mathbf{r}_j)$, on the ground that the two-point Ursell correlation function (2.17) of the bulk system reads, by (2.23),

$$h^{\text{DH}}(\mathbf{r}, \gamma; \mathbf{0}, \gamma_0) = -\beta e_\gamma e_{\gamma_0} \Phi(\mathbf{r}) \quad (2.27)$$

(as before, the exponential is linearized by assuming a weak-coupling regime). We will not restrict to such an approximation in our work, but, instead, will make use of an exact expansion of the Ursell function, still involving the Debye–Hückel potential.

It is an easy task from (2.23) and (2.26) to see that the mean charge density $c_{e_{\gamma_0}}(\mathbf{r})$ around the fixed charge explicitly reads

$$c_{e_{\gamma_0}}(\mathbf{r}) = -\frac{\kappa^2}{4\pi} e_{\gamma_0} \frac{e^{-\kappa r}}{r} = -\frac{\kappa^2}{4\pi} e_{\gamma_0} \Phi(\mathbf{r}), \quad (2.28)$$

so that the total amount of charge carried by the cloud is

$$\int d\mathbf{r} c_{e_{\gamma_0}}(\mathbf{r}) = -e_{\gamma_0} \int d\mathbf{r} \frac{\kappa^2}{4\pi} \Phi(\mathbf{r}) = -e_{\gamma_0}. \quad (2.29)$$

This integral relation satisfied by the mean-field potential is the **perfect screening sum rule**: the fixed charge is surrounded by a charge density screening it exactly. Expressed in terms of the Ursell correlation function in the Debye–Hückel regime (2.27), this sum rule (2.29) can be reexpressed as

$$\sum_{\gamma} \int d\mathbf{r} e_{\gamma} \rho(\gamma) h^{\text{DH}}(\mathbf{r}, \gamma; \mathbf{0}, \gamma_0) = -e_{\gamma_0}. \quad (2.30)$$

It can be shown, that the perfect screening sum rule holds in full generality for the exact Ursell correlation function. The integrated amount of the cloud charge density surrounding a fixed charge in the plasma compensates it exactly:

$$\sum_{\gamma} \int d\mathbf{r} e_{\gamma} \rho(\gamma) h(\mathbf{r}, \gamma; \mathbf{0}, \gamma_0) = \int d\mathbf{r} \sum_{\gamma} e_{\gamma} \langle \hat{\rho}(\mathbf{r}, \gamma) |_{\mathbf{0}, \gamma_0} \rangle = \int d\mathbf{r} c_{e_{\gamma_0}}(\mathbf{r}) = -e_{\gamma_0} \quad (2.31)$$

(a globally neutral plasma is assumed for the first equality). This result holds in classical as well as in quantum plasmas in a fluid state (Martin, 1988). Furthermore, it will also be valid for the “inhomogeneous” plasmas considered in our two-plasma system (*i.e.*, of finite or semi-infinite width, and infinite surface), whether they be classical, or field-coupled and quantum-mechanical.³

2.3.6 Perfect vs ideal conductors

The above description of *perfect* conductors in equilibrium with the radiation field differs fundamentally from that of what we call *ideal* conductors, which are defined on the macroscopic scale only. Ideal conductors represent objects without internal structure. Their interaction with the electromagnetic field is simplified to merely imposing Maxwell boundary conditions to the field at their interfaces. In our microscopic viewpoint of perfect conductors, no particular boundary conditions on the field are imposed there. One expects of course the macroscopic

³Taking the limit of infinite extension in at least one direction is important in the interpretation of the result (2.31): in finite systems, this sum rule means nothing more than the conservation of the total charge in the finite volume, whereas in our case, any macroscopic excess of charge can be repelled to infinity and the plasma acts (in average) as a grounded conductor. The fact that the screening cloud bears an opposite total charge while having an escape at infinity becomes nontrivial and is really a property peculiar to conductors.

boundary conditions to be valid in average in a region close to the surfaces (Jackson, 1998, Sect I.6). Ideal conductors are sometimes seen as perfect conductors of vanishing screening length. However, the charge fluctuations present in perfect conductors (and disregarded in ideal ones) are responsible for a quantitative change in the high-temperature Casimir force strength and in this respect, the crossover from perfect to ideal has to be treated with care. Ideal conductor limits of confining metallic walls for a classical Coulomb system have been investigated in (Jancovici & Téllez, 1996). Potential correlations and the Maxwell stress tensor (but not the total force integrating it) have been found to differ in the two ways of treating the metallic walls.

2.4 The Casimir force

At the root of the basic concept of energy lies the wish of explaining the forces observed in the nature by a general principle: if a system exhibits the freedom of occupying different states, its natural tendency is to be drawn by the one of lowest energy. The relative (potential) gain of energy it can acquire defines the force.

Like Casimir did in its original calculation, the force between the metallic plates at zero temperature is defined by the derivative of the energy of the whole system. At nonzero constant temperatures, the relevant energy function to that purpose becomes the free energy, as advocated by the laws of thermodynamics.

Having introduced the microscopic model and specified its macroscopic thermalised states, the mean force by unit surface between the finite-volume slabs is defined by the rate of change occasioned in the free energy $\Phi_{K,L,d}$ (2.6) by varying the separating distance d :

$$f_{K,L}(d) \equiv -\frac{1}{L^2} \frac{\partial}{\partial d} \Phi_{K,L,d}. \quad (2.32)$$

It corresponds to the thermodynamic *internal pressure* of the two-plasma system. Applying external forces to the material volume $V \approx L^2(a + d + b)$ of the system, this volume can be “compressed” or “expanded” — keeping the plates’ shape untouched — by changing d : $\partial V = L^2 \partial d$, and $P = -\frac{\partial}{\partial V} \Phi_{K,L,d} = -\frac{1}{L^2} \frac{\partial}{\partial d} \Phi_{K,L,d}$. A negative value of the internal pressure $f_{K,L}(d)$ will tend to press the plates together: the force between the plates is attractive. Conversely, if the pressure is positive, the force between the plates is repulsive.

On the microscopic level, using the form of the free energy $\Phi_{K,L,d}$ specific to the different natures of the model, one can relate this pressure to thermal averages of elementary forces acting between the microscopic entities:

- **classical plasmas:** differentiating the free energy with respect to d gives the average value of the **electrostatic forces** exerting between each pair of par-

ticles constituted by one particle in A and one particle in B . In consideration of our sign convention, one can regard them as being the total electrostatic force (along the x axis) acting on plasma B .

Due to the Bohr–van Leeuwen decoupling of matter and field (2.11), the force between the field-coupled *classical* plasmas receives no possible contribution from the radiation field from the beginning;

- **quantum plasmas:** when the radiation field is not taken into account, the Casimir force again corresponds to the microscopic **electrostatic forces** exerting between the A and B plasmas;
- **field-coupled quantum plasmas:** the inclusion of the radiation field into the description of the system introduces new contributions in addition to the former electrostatic forces. They correspond to the missing parts (the radiative electric part and the magnetic part) of the whole **Lorentz forces** due to the coupled system of field and matter that act on the system B , and that take support on its particles.

We finally define **the Casimir force** as being the force $f_{K,L}(d)$ (2.32) in the thermodynamic limit, *i.e.*,

$$f(d) \equiv \lim_{L \rightarrow \infty} \lim_{K \rightarrow \mathbb{R}^3} f_{K,L}(d). \quad (2.33)$$

2.4.1 Main result of the thesis

The essential result presented in this thesis is that, starting from the above premises, the Casimir force at any fixed (high) temperature has the large-distance asymptotic behaviour

$$f(d) = -\frac{\zeta(3)}{8\pi\beta d^3} + \mathcal{O}(d^{-4}), \quad d \rightarrow \infty, \quad (2.34)$$

independently of the model chosen. The constant $\zeta(3) \approx 1.202$ is the value of the Riemann zeta function $\zeta(s) = \sum_{n=1}^{\infty} n^{-s}$ at $s = 3$.

This result agrees with a number of authors on the asymptotic value of the Casimir force at high-temperature. However, a large controversy about this value is found in the literature, as said in the introduction, the debate revolving around whether $-\zeta(3)/(4\pi\beta d^3)$ or $-\zeta(3)/(8\pi\beta d^3)$ is the correct result. The first value arises naturally in macroscopic approaches imposing ideal conductor boundary conditions to the field at the plates' surfaces. When fluctuations of the field inside the plates are taken into account, like in the semi-microscopic (mesoscopic) approach of Lifshitz or Schwinger, both values can be retrieved, depending on how the metallic limit is extrapolated from dielectric media.

By the truly microscopic and elaborate framework of our calculation, we thus settle on a firmer basis the validity of the value $-\zeta(3)/(8\pi\beta d^3)$, supporting in this respect the use of the Drude model of the dielectric function (*i.e.*, in turn, the vanishing of the TE (transverse electric) field mode) at zero frequency, at least in the semi-classical regime. We also conclude that when calculating the Casimir force at nonzero temperature, charge fluctuations inside the conductors cannot be ignored.

The most noteworthy property of the asymptotic result (2.34) is that it is *universal*, *i.e.*, it does not depend on the material constitution of the plates, like their density, and the microscopic charges and masses. This observation is rather natural in models not taking into account such quantities in their formulation, like Casimir's calculation, as well as Lifshitz' or Schwinger's ones — for which the dielectric function $\epsilon(\omega)$ is taken infinite to recover metallic behaviour of the plates. It is, however, not a straightforward feature in microscopic models, like ours. From the calculation of the asymptotic force, we will see that this universality is the result, in the conductive phase, of the perfect screening sum rule in each plasma. Its origin thus receives within our treatment a more satisfactory explanation, based on microscopic mechanisms.

Since the perfect screening sum rules arising in the force involve the screening of charges close to the inner surfaces of the plates, we also understand why the force is independent of the plates' thickness a and b . This holds provided that a and b are finite and large enough to allow the screening clouds to form (*i.e.*, not microscopic).

Note that the asymptotic, universal, term in (2.34) does not depend on any electric or magnetic quantity. Its form is identical in electrostatic Gaussian units or in the MKSA international system of units (see Footnote 1).

Depending on the refinement of our model, the $O(d^{-4})$ subdominant terms in (2.34) may contain finite widths, temperature, quantum, and field corrections. We will comment on these higher-order contributions at the end of Chapter 3, and in the Conclusions (Chapter 6).

2.5 Outline of the calculation

In this section, we give an account of the method used to calculate the asymptotic Casimir force (2.34) from the microscopic premises presented in the earlier sections. We will carry out the calculation assuming *classical plasmas*, for simplicity. The presentation found here will differ slightly from that of the article in Chapter 3 in regards to the method used to retrieve asymptotic information on the Debye–Hückel mean-field potential, defined by the resummation of the long-ranged Coulomb potential. Although not as rigorous, this method is simpler to

generalise to the further models.

In a first stage, we also present how, by differentiating the free energy with respect to d , one is led to the calculation of the average electrostatic forces between the charges of the plasmas, which has been the starting point of the article.

In the last part, some hints will be given on how to treat the problem when quantum mechanics and the field are added. The formalism adapted to that purpose makes use of the Feynman–Kac–Itô representation. The strategy to generalise the validity of the classical result is then essentially the same as the classical one presented below. This formalism will be presented in Chapter 4. The details of its application to the Casimir force problem are postponed until Chapter 5.

Strategy

The strategy of the calculation is as follows: in a first stage, the Casimir force (2.33) is expressed as the average value of a two-body observable, which is rewritten as an integral over the Ursell correlation (2.17). The knowledge of the asymptotic correlations between the two slabs as $d \rightarrow \infty$ is required. This asymptotic analysis is carried out on the Ursell function by representing it in its series expansion in Mayer graphs. Resummation of the Coulomb potential is needed to overcome nonintegrabilities due to its long range. This exact resummation process systematically introduces the Debye–Hückel potential in replacement of the Coulomb potential in the resummed graphs, which thereby encompass the screening effects occurring in the plasmas. The next task is to analyse the asymptotic behaviour of this screened Debye–Hückel potential, so as to deduce its implication in the Ursell function and, finally, in the force.

2.5.1 Expressing the force in terms of the Ursell function (The force as a two-body observable)

From the decoupling of matter and field in the classical case — implying the separation (2.11) of the total free energy — the force (2.32) (at finite volume) between the two plasmas is given by

$$f_{K,L}(d) = f_L(d) = \frac{k_B T}{L^2} \frac{\partial}{\partial d} \ln \Xi_{L,d}^{\text{mat}} = \frac{k_B T}{L^2} \frac{\frac{\partial}{\partial d} \Xi_{L,d}^{\text{mat}}}{\Xi_{L,d}^{\text{mat}}}, \quad (2.35)$$

where $\Xi_{L,d}^{\text{mat}}$ is the partition function of the purely electrostatic matter, as given by (2.10). Integrating out the impulsions' degrees of freedom, this partition function reads as the positional integral of a Gibbs weight $\exp(-\beta U)$, where the potential energy U can be written as

$$U = U_A + U_B + U_{AB} + V_A^{\text{walls}} + V_{B,d}^{\text{walls}}. \quad (2.36)$$

The quantities U_A and U_B are the interaction potentials associated to the individual plasmas, and

$$U_{AB} = \sum_a \sum_b \frac{e_{\gamma_a} e_{\gamma_b}}{|\mathbf{r}_a - \mathbf{r}_b|} + v_{\text{SR}}(\mathbf{r}_a - \mathbf{r}_b, \gamma_a, \gamma_b) \quad (2.37)$$

is the sum of the pair interactions between particles in A (indexed by “ a ”) and particles in B (indexed by “ b ”). We have split the wall potentials $\sum_i V_i^{\text{walls}}(\mathbf{r}_i, \gamma_i)$ of the Hamiltonian (2.3) explicitly into an A and a B contribution

$$V_A^{\text{walls}} + V_{B,d}^{\text{walls}} = \sum_a V_A^{\text{walls}}(\mathbf{r}_a, \gamma_a) + \sum_b V_{B,d}^{\text{walls}}(\mathbf{r}_b, \gamma_b). \quad (2.38)$$

The dependence upon d in the partition function $\Xi_{L,d}^{\text{mat}}$ originates only from the particles’ confinement to plasma B , filling the region $d < x < d + b$.

Contact theorem

There are two ways of taking the derivative with respect to d of the partition function $\Xi_{L,d}^{\text{mat}}$ in (2.35). In the first, the derivative is taken directly on the ideally confining factor $\exp(-\beta V_{B,d}^{\text{walls}}) \propto \prod_b \Theta(x_b - d)\Theta(d + b - x_b)$ (up to \mathbf{y}_b dependencies; Θ is the Heaviside step function). It will thus relate the Casimir force to the average value of sums of terms $\propto \delta(d + b - x_b) - \delta(x_b - d)$, precisely, to the mean densities evaluated at the interfaces $x = d$ and $x = d + b$ of the plate B . This constitutes a version of the so-called *contact theorem*, usually relating the bulk pressure to the density at the walls. This kind of calculation has been carried out in the Debye–Hückel approximation (at first order around piecewise-flat densities) by Jancovici and Šamaj (2004), to show that a third party plasma of charges (in a conductive state) filling the empty space between the plates screens the Casimir force.

Microscopic electrostatic forces

We will take another route to compute the force, more suitable in our setting to overcome the restriction to the Debye–Hückel theory. Before taking the derivative of the partition function, we perform the change of variable

$$x_b \mapsto \tilde{x}_b \equiv x_b - d \quad (2.39)$$

in every positional integral concerning the particles of plasma B . Doing so measures the positions of the particles of plasma B from the inner side of the latter (see Figure 2.4). As an effect, the confining factor $\exp(-\beta V_{B,d}^{\text{walls}})$ becomes obviously independent on d : the new variables are constrained by $0 < \tilde{x}_b < b$. The

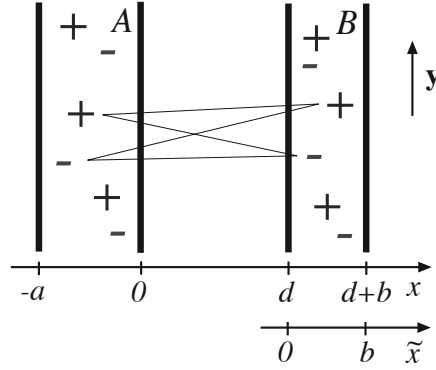


Figure 2.4: The Casimir force as the average value of all electrostatic forces exerting between plasma A's and plasma B's particles. The positions along x in plasma B are measured from its inner surface by virtue of (2.39).

d dependence is ported explicitly and exclusively into the AB interactions, which still must occur at a minimal distance d . The interaction potential U_{AB} (2.37) in the partition function $\Xi_{L,d}^{\text{mat}}$ is changed into

$$\sum_a \sum_b \frac{e_{\gamma_a} e_{\gamma_b}}{[(x_a - \tilde{x}_b - d)^2 + (\mathbf{y}_a - \mathbf{y}_b)^2]^{1/2}} + v_{\text{SR}}(x_a - \tilde{x}_b - d, \mathbf{y}_a - \mathbf{y}_b, \gamma_a, \gamma_b). \quad (2.40)$$

By differentiating the Gibbs weight in the integrand, a factor $(-\beta)$ times the derivative of (2.40) with respect to d drops from the exponential. Since $\frac{\partial}{\partial d} \Xi_{L,d}^{\text{mat}}$ is normalised by $\Xi_{L,d}^{\text{mat}}$ in (2.35), one reconstructs the average value

$$f_L(d) = \frac{1}{L^2} \left\langle \sum_a \sum_b e_{\gamma_a} e_{\gamma_b} (\partial_x v)(x_a - \tilde{x}_b - d, \mathbf{y}_a - \mathbf{y}_b) \right\rangle, \quad v(x, \mathbf{y}) = \frac{1}{\sqrt{x^2 + \mathbf{y}^2}}, \quad (2.41)$$

after neglecting the contribution of the short-range forces. They will be irrelevant at large separations (as soon as d is larger than their range). The expression (2.41) represents the average value of all microscopic Coulomb forces exerting between the particles of plasma A and the particles of plasma B (Figure 2.4).⁴

One can check from this microscopic interpretation that a negative value of $f_L(d)$ effectively corresponds to attracting plates. Equivalently, $f_L(x)$ represents the x component of the total force exerting on plasma B.

Notations

Before going further, we introduce a few short-hand notations:

⁴In Formula (2.41), positions in plasma B are still measured from its inner border; the reverse shifts (2.39) can be performed if wished.

- We regroup the species γ_1 and the position variable \mathbf{r}_1 of a particle under the common symbol “ $\mathbf{1}$ ”:

$$\mathbf{1} \equiv (\mathbf{r}_1, \gamma_1), \quad \int d\mathbf{1} \dots \equiv \sum_{\gamma_1} \int d\mathbf{r}_1 \dots \quad (2.42)$$

Three-dimensional positions are further split along the x axis and the \mathbf{y} plane of the plates (as shown in Figures 2.1 and 2.4) according to $\mathbf{r}_1 = (x_1, \mathbf{y}_1)$. We thus also introduce the variable “ $\mathbf{1}$ ” to denote the gathering of γ_1 and the x component, only, of the position:

$$\mathbf{1} \equiv (x_1, \gamma_1), \quad \int d\mathbf{1} \dots \equiv \sum_{\gamma_1} \int dx_1 \dots \quad (2.43)$$

- From now on, the positions along x of the particles of plasma B will always be counted from the inner surface of the latter (*i.e.*, on the axis \tilde{x} of Figure 2.4). (This is needed when taking the limit $d \rightarrow \infty$ on properties pertaining to plasma B . These properties become independent of plasma B 's position in space.)
- Unless otherwise specified, sums over species and integrals over positions run over the whole two-plasma system. Nevertheless, indexing one-point and two-point functions by indices A or B will mean that their argument is compelled to reside in A or B . For example, the mean density in plasma B is $\rho_B(\mathbf{2}) \equiv \mathbb{1}_B(\mathbf{2})\rho(\mathbf{2})$, where $\mathbb{1}_B(\mathbf{2})$ is the characteristic function of plasma B (situated at the origin): this function ensures that $0 < x_2 < b$, and it vanishes if $\gamma_2 \notin S_B$. Similarly, $\rho_{AA}(\mathbf{1}, \mathbf{2}) \equiv \mathbb{1}_A(\mathbf{1})\mathbb{1}_A(\mathbf{2})\rho(\mathbf{1}, \mathbf{2})$.

However, for two-point “ A – B ” functions, interactions must consistently be taken to exert across a minimal distance d along the x axis [according to the change of variable (2.39)]. Concretely, the function $v_{AB}(x_1, \tilde{x}_2, \mathbf{y})$ (reintroducing tildes over B variables on the axis \tilde{x} for a moment) corresponds to the Coulomb potential between A and B with a least interaction distance d :

$$v_{AB}(x_1 - \tilde{x}_2, \mathbf{y}) \equiv v(x_1 - (\tilde{x}_2 + d), \mathbf{y}) \stackrel{(2.39)}{=} v(x_1 - x_2, \mathbf{y}), \quad (2.44)$$

with the constraints $-a < x_1 < 0$, and $0 < \tilde{x}_2 < b$, $d < x_2 < d + b$.

As well, $\rho_{AB}(\mathbf{1}, \tilde{\mathbf{2}}) = \mathbb{1}_A(\mathbf{1})\mathbb{1}_B(\tilde{\mathbf{2}})\rho(\mathbf{1}; \tilde{\mathbf{2}} + d) \stackrel{(2.39)}{=} \mathbb{1}_A(\mathbf{1})\mathbb{1}_{B,d}(\mathbf{2})\rho(\mathbf{1}; \mathbf{2})$, where $\mathbb{1}_{B,d}(\mathbf{2})$ confines x_2 to $d < x_2 < d + b$.

- At the limit $d \rightarrow \infty$, the interaction between the two plasmas vanishes. Quantities particular to the individual, isolated, plasmas will be superscripted by “ 0 ”. For instance, the local density $\rho_B(\mathbf{2})$ becomes, in the limit, that of a single slab of width b situated at the origin, denoted by $\rho_B^0(\mathbf{2})$.

Expressing the force in terms of the A – B correlation function

The finite-volume force in the form (2.41) can be conveniently expressed as an integral weighted by the density correlation function $\rho(\mathbf{1}, \mathbf{2})$ (see Section 2.2.2). One replaces the sums in (2.41) by integrals over A and B of the microscopic density $\hat{\rho}(\mathbf{i}) = \sum_{j \in A \cup B} \delta(\mathbf{i}, \mathbf{j})$ (2.13) at point \mathbf{i} . By the linearity of $\langle \cdot \cdot \cdot \rangle$, this leads to

$$\begin{aligned} f_L(d) &= \frac{1}{L^2} \sum_{\gamma_1} \int d\mathbf{r}_1 \sum_{\gamma_2} \int d\mathbf{r}_2 e_{\gamma_1} e_{\gamma_2} (\partial_x v)(x_1 - x_2 - d, \mathbf{y}_1 - \mathbf{y}_2) \\ &\quad \times \mathbb{1}_A(\mathbf{r}_1, \gamma_1) \mathbb{1}_B(\mathbf{r}_2, \gamma_2) \langle \hat{\rho}(\mathbf{r}_1, \gamma_1) \hat{\rho}(x_2 + d, \mathbf{y}_2, \gamma_2) \rangle \\ &= \frac{1}{L^2} \int d\mathbf{1} \int d\mathbf{2} e_{\gamma_1} e_{\gamma_2} (\partial_x v_{AB})(\mathbf{1}, \mathbf{2}) \rho_{AB}(\mathbf{1}, \mathbf{2}). \end{aligned} \quad (2.45)$$

Note that since $\mathbf{1} \in A$ and $\mathbf{2} \in B$, these points can never meet. There are never coincident points contributions in AB correlations.

Truncation of the correlation function in the thermodynamic limit

To obtain the Casimir force (2.33), the thermodynamic limit $L^2 \rightarrow \mathbb{R}^2$ of $f_L(d)$ is taken at this stage. The correlation function $\rho_{AB}(\mathbf{1}, \mathbf{2})$ in (2.45) tends to a function $\rho_{AB}(1, 2, \mathbf{y}_1 - \mathbf{y}_2)$, invariant under translations in the \mathbf{y} -plane. Hence, one of the transverse \mathbf{y} -integrals present in (2.45) cancels with the plates' surface L^2 in the limit, resulting in

$$f(d) = \int d\mathbf{1} \int d\mathbf{2} \int d\mathbf{y} e_{\gamma_1} e_{\gamma_2} (\partial_x v_{AB})(1, 2, \mathbf{y}) \rho_A(1) \rho_B(2) h_{AB}(1, 2, \mathbf{y}), \quad (2.46)$$

where h_{AB} is the Ursell function (2.17) of the infinitely extended plates. The truncation in h_{AB} does not affect the force, due to the global neutrality of the plasmas.

Indeed, we can always add back to (2.46) the term $f^{\text{cap}}(d)$ subtracted by the truncation of the correlation function. This term reads

$$\begin{aligned} f^{\text{cap}}(d) &= \int d\mathbf{1} \int d\mathbf{2} \int d\mathbf{y} e_{\gamma_1} e_{\gamma_2} (\partial_x v_{AB})(1, 2, \mathbf{y}) \rho_A(1) \rho_B(2) \\ &= 2\pi \left[\int dx_1 c_A(x_1) \right] \left[\int dx_2 c_B(x_2) \right], \end{aligned} \quad (2.47)$$

where $c_A(x_1)$ and $c_B(x_2)$ are the mean charge densities. The second equality in (2.47) results from the fact that

$$\int d\mathbf{y} (\partial_x v_{AB})(1, 2, \mathbf{y}) = -2\pi \text{sign}(x_1 - x_2 - d) = 2\pi, \quad (2.48)$$

as can be seen from Formula (B.8) in Appendix B, evaluated at $\mathbf{k} = \mathbf{0}$. Thus (2.47) vanishes from the assumed global neutrality (2.2) of the plasmas:

$$f^{\text{cap}}(d) \equiv 0. \quad (2.49)$$

Nonneutral plasmas: If these neutralities are not assumed, the only change in the total force between the plasmas is the addition of the force by unit surface (2.47) (in Gaussian units) to the Casimir, fluctuation-induced, force (2.46). As the densities are of order $O(1)$ as $d \rightarrow \infty$, the contribution $f^{\text{cap}}(d)$ is mainly independent of the separation d , and corresponds to the well-known force between a capacitor's plates whose surface charge densities are not necessarily opposite, but respectively $\int dx_1 c_A(x_1)$ and $\int dx_2 c_B(x_2)$ (Schwinger et al., 1998, Form. (11.75)–(11.76)).

The force in a suitable form for a large-distance analysis

In preparation for an analysis of (2.46) in the large-separation limit $d \rightarrow \infty$, the y -integral is written in the (partial) Fourier space \mathbf{k} (see Appendix B), and the change of variable $\mathbf{k} = \mathbf{q}/d$ is performed.

This change of variable has the effect of disentangling nonuniformities present in the A – B electrostatic force — and remaining in the correlation function — between the variables \mathbf{k} and d . Indeed, as seen on its partial Fourier transform (B.8), the electrostatic force bears the factor $e^{-k|x_1-x_2-d|} \leq e^{-kd}$ ($k = |\mathbf{k}|$). The dominant contribution to the integral in (2.46) at large d will thus come from small values of \mathbf{k} . They are more easily investigated at $\mathbf{k} = \mathbf{q}/d$, for then

$$(\partial_x v_{AB})(1, 2, \frac{\mathbf{q}}{d}) = 2\pi e^{-q} e^{-\frac{q|x_1|}{d}} e^{-\frac{q|x_2|}{d}} \quad (2.50)$$

is expandable in power series of $1/d$ while still being integrable on \mathbf{q} .

In a form suitable for a large-distance analysis, the Casimir force therefore reads

$$f(d) = \frac{1}{d^2} \int d1 \int d2 \int \frac{d\mathbf{q}}{(2\pi)^2} e_{\gamma_1} e_{\gamma_2} (\partial_x v_{AB})(1, 2, \frac{\mathbf{q}}{d}) \rho_A(1) \rho_B(2) h_{AB}(1, 2, \frac{\mathbf{q}}{d}), \quad (2.51)$$

with $(\partial_x v_{AB})(1, 2, \frac{\mathbf{q}}{d})$ given by (2.50).

From this formula, the Casimir force $f(d)$ will turn out to be $O(d^{-3})$. The electrostatic force (2.50) is of order $O(1)$ as $d \rightarrow \infty$. The mean densities ρ_A and ρ_B are averaged in the system of the two plasmas under mutual influence; they will tend to the densities ρ_A^0 and ρ_B^0 of the single, individual plasmas. In the next section, the correlation $h_{AB}(\frac{\mathbf{q}}{d})$ between the plasmas will be seen to vanish in the limit as $O(d^{-1})$.

The issue resides in extracting the dominant contribution of the correlation $h_{AB}(1, 2, \frac{\mathbf{q}}{d})$ between the plasmas A and B as they become more distant, but also in understanding how the universality of the Casimir force emerges from this microscopic calculation. We will show that this A – B correlation function asymptotically

involves correlation functions pertaining to the single individual plasmas and that universality results from the perfect screening sum rules that the latter functions satisfy on their own.

2.5.2 Introduction to Mayer graphs and their resummation

Meaningful insights into the Ursell function of our charged system are expected to be gained by the mean-field (linearised) Debye–Hückel approximation (see Section 2.3.5). In the bulk, this theory describes screening very simply for classical Coulomb matter. The effective mean-field potential (2.26) is exponentially damped over the screening length κ^{-1} (2.25). Density and charge correlations exhibit exponential clustering and satisfy the perfect screening sum rule. Moreover, the Debye–Hückel regime is known to be asymptotically correct in the strict limit of low density or high temperature (Brydges & Federbush, 1980). The method of *resummed Mayer graphs*, presented below, provides a natural way for going beyond this approximation while keeping its most pleasant feature: the screening potential.

Mayer graphs in activity

The basic idea behind the expansion of the classical Ursell function $h(\mathbf{1}, \mathbf{2})$ in Mayer graphs *in activity* relies on a simple rewriting of the interacting part of its Gibbs weight (occurring in a representation of h similar to (2.19) in the grand-canonical ensemble):

$$e^{-\beta \sum_{i<j} V(i,j)} = \prod_{i<j} [f(i,j) + 1], \quad f(i,j) = e^{-\beta V(i,j)} - 1 \quad (2.52)$$

(V represents the total pairwise interaction). The product $\prod_{i<j}$ is fully expanded in a series of terms containing a certain combination of multiplied functions f . To form $h(\mathbf{1}, \mathbf{2})$, these terms are integrated over all variables, except the two arguments $\mathbf{1}$ and $\mathbf{2}$, with weights $z(i)$ including the activity and the external potentials:

$$\begin{aligned} h(\mathbf{1}, \mathbf{2}) &= \sum_{\Gamma} \frac{1}{S_{\Gamma}} \int d\mathbf{3} \dots \int d\mathbf{m} z(3) \dots z(m) \prod_{(i,j) \in \Gamma} f(i,j) \\ &= \text{○}_1 \text{---} \text{○}_2 + \text{○}_1 \text{---} \text{○} \text{---} \text{○}_2 + \text{○}_1 \text{---} \text{○} \text{---} \text{○} \text{---} \text{○}_2 + \text{○}_1 \text{---} \text{○} \text{---} \text{○} \text{---} \text{○} \text{---} \text{○}_2 + \dots \end{aligned} \quad (2.53)$$

Each of these terms is graphically represented by a **diagram**, or **graph** (a lattice of linked points) Γ , accordingly: it has two root points ($\mathbf{1}$ and $\mathbf{2}$), a number m of intermediate points representing activity-weighted integrals, and links between the points representing the factors $f(i,j)$ as they occur in the term. The function $f(i,j)$ is called the **Mayer bond**.

Mayer graphs in density

To obtain, instead, an expansion of $h(\mathbf{1}, \mathbf{2})$ in terms of graphs whose integrated points are weighted by the *density*, one has to write a similar expansion in activity for the density $\rho(i)$ and eliminate the activities between the two representations. This elimination process can be made systematically, and is called “topological reduction” because it involves a simplification in the diagrams’ structure (they become free of articulation points).

As a result, the classical Ursell correlation function $h(\mathbf{1}, \mathbf{2})$ is expanded in a formal power series of the density by means of such graphs:

$$\begin{aligned}
 h(\mathbf{1}, \mathbf{2}) &= \sum_{\Gamma'} \frac{1}{S_{\Gamma'}} \int d\mathbf{3} \dots \int d\mathbf{m} \rho(\mathbf{3}) \dots \rho(\mathbf{m}) \prod_{\{i,j\} \in \Gamma'} f(i, j) \\
 &= \text{○} \text{---} \text{○} + \text{○} \text{---} \text{○} \text{---} \text{○} + \dots
 \end{aligned} \tag{2.54}$$

Each graph is an integral over an arbitrary number of intermediate points \mathbf{m} weighted by the local mean density $\rho(\mathbf{m})$, and operating on a product of links $f(\mathbf{i}, \mathbf{j})$ (2.52) between the points. The two root points $\mathbf{1}$ and $\mathbf{2}$ are not integrated over. The series is made up of all graphs of one piece, connecting the root points, and whose network is such that none of the points (whether integrated or root) is an articulation point. Namely, there is no point whose removal would split the graph into pieces not all connected to a root point. Mechanically speaking, there are no “pivotable arms” in the graph when the root points are maintained fixed. [Compare the graphs of the series (2.53) to those of the series (2.54).]

A presentation of these developments can be found, *e.g.*, in (Hansen & McDonald, 1986, Sec. 4.5, 5.3), and some rigorous results about convergence issues of activity and density expansions in the thermodynamic limit, in (Ruelle, 1989, Sec. 4.3).

Resummation of the Coulomb divergencies

In Coulomb fluids, where the interaction is $V(\mathbf{i}, \mathbf{j}) = e_{\gamma_i} e_{\gamma_j} v(\mathbf{i}, \mathbf{j}) + v_{\text{SR}}(\mathbf{i}, \mathbf{j})$, the long range of the Coulomb potential induces the nonintegrability at infinity of the Mayer bond. Every diagram in the Mayer graph series consequently diverges in the thermodynamic limit. However, taken together, they form the Ursell correlation function, which is expected to be well-defined in this limit. Divergencies arising from individual graphs cancel out in their sum, so that partial resummations are devised. One expects these cancellations to occur through the establishment in the plasma of screening mechanisms that reduce the effective range of interaction. To systematically deal with them in the graphs, one “resums” the Coulomb

potentials into the Debye–Hückel potential, according to the following idea. [See (Meeron, 1958; Abe, 1959) or, *e.g.*, (Balescu, 1975, Sec. 6.5), and references therein.]

One may rewrite the Poisson–Boltzmann differential equation (2.25) defining the Debye–Hückel potential Φ (generalised for an inhomogeneous density) as an integral equation, namely

$$\Phi(\mathbf{i}, \mathbf{j}) \equiv v(\mathbf{i}, \mathbf{j}) - \int d\mathbf{1} \frac{\kappa^2(1)}{4\pi} v(\mathbf{i}, \mathbf{1})\Phi(\mathbf{1}, \mathbf{j}), \quad (2.55)$$

$$\kappa^2(1) = 4\pi\beta \sum_{\gamma_1} e_{\gamma_1}^2 \rho(1), \quad (2.56)$$

as can be checked by applying the Laplacian $\nabla_{\mathbf{r}_i}^2$ to it.⁵ Multiplied by $-\beta e_{\gamma_i} e_{\gamma_j}$ and recursively iterated, this integral equation represents an infinite series of convolution chains of bonds $-\beta e_{\gamma_1} e_{\gamma_2} v(\mathbf{1}, \mathbf{2})$ weighted by the density:

$$i \circ \xrightarrow{F = -\beta e_i e_j \Phi} \circ j \equiv \circ \cdots \xrightarrow{-\beta e_i e_j v} \circ + \circ \cdots \xrightarrow{\rho(1)} \bullet \cdots \circ + \circ \cdots \bullet \cdots \bullet \cdots \circ + \dots \quad (2.57)$$

The idea is to prominently give rise in the Mayer graphs to such chain series and regroup them into the quantity $F = -\beta e_{\gamma_i} e_{\gamma_j} \Phi$. To that purpose, the Mayer bonds $f(\mathbf{i}, \mathbf{j})$ are written as the sum of their Coulomb, long-ranged, part $-\beta e_{\gamma_i} e_{\gamma_j} v$, and the rest, $f^R = e^{-\beta e_{\gamma_i} e_{\gamma_j} v - \beta v_{SR}} - 1 + \beta e_{\gamma_i} e_{\gamma_j} v$. Their product in (2.54) is expanded and the resulting new graphs reorganized into subseries, so that chain convolutions (2.57) between two specific points are exhibited, like in

$$\begin{array}{c} f^R \\ \diagdown \quad \diagup \\ \circ \quad \circ \\ \diagup \quad \diagdown \\ f^R \quad -\beta v \end{array} + \begin{array}{c} \quad \quad \quad \\ \diagdown \quad \diagup \\ \circ \quad \circ \\ \diagup \quad \diagdown \\ \bullet \quad \bullet \end{array} + \begin{array}{c} \quad \quad \quad \\ \diagdown \quad \diagup \\ \circ \quad \circ \\ \diagup \quad \diagdown \\ \bullet \quad \bullet \end{array} + \dots = \begin{array}{c} \quad \quad \quad \\ \diagdown \quad \diagup \\ \circ \quad \circ \\ \diagup \quad \diagdown \\ \bullet \quad \bullet \end{array} \quad (2.58)$$

We explain in more detail this procedure in Appendix A. The result is the following.

The new diagrams, so-called **resummed Mayer graphs**, are then made of links chosen among the two types

$$F(\mathbf{i}, \mathbf{j}) = -\beta e_{\gamma_i} e_{\gamma_j} \Phi(\mathbf{i}, \mathbf{j}), \quad (2.59)$$

$$F^R(\mathbf{i}, \mathbf{j}) = e^{-\beta(e_{\gamma_i} e_{\gamma_j} \Phi + v_{SR})(\mathbf{i}, \mathbf{j})} - 1 + \beta e_{\gamma_i} e_{\gamma_j} \Phi(\mathbf{i}, \mathbf{j}). \quad (2.60)$$

⁵The boundary conditions supplementing the Poisson–Boltzmann equation (especially at interfaces) are in fact derived from the integral relation.

The bond F is proportional to the Debye–Hückel potential (2.55). The bond F^R sums up the contributions from the shorter-ranged part of the original Mayer bonds. The Ursell function reads

$$h(\mathbf{1}, \mathbf{2}) = \sum_{\Pi} \frac{1}{S_{\Pi}} \int d\mathbf{3} \rho(\mathbf{3}) \cdots \int d\mathbf{m} \rho(\mathbf{m}) \prod_{\{i,j\} \in \Pi} \mathcal{F}(i, j), \quad (2.61)$$

where Π denotes a resummed Mayer graph with m points, two of which being the root points $\mathbf{1}$ and $\mathbf{2}$, and a symmetry number S_{Π} . It is made of (simple) links $\mathcal{F} \in \{F, F^R\}$ and there are no articulation points. The only additional topological constraint on the resummed graphs is that convolution chains of links F are forbidden: they would redundantly count original chain convolutions of $-\beta e_{\gamma_i} e_{\gamma_j} v$, in view of (2.57).

Remarks

- The resummation procedure can be seen as effectively replacing the Coulomb interactions between the charges by the screened, integrable, Debye–Hückel potential Φ . It is not to be confounded with a coarse-grained scheme that would *ab initio* average out some of the microscopic phase-space degrees of freedom by introducing the mean-field potential. Our approach remains fine-grained and exact: the presence of the bond F^R in the graph series representation of h is the price to pay for dealing with the Debye–Hückel potential.
- This development is, however, not rigorous: infinite quantities have been manipulated in such a way that they cancel out. One could perform these steps before the thermodynamic limit is taken, rearranging only finite quantities. But it would not be justified to take first the thermodynamic limit on the series (2.57) or (2.55), leading to fast decaying, thus integrable, bonds F and F^R , and then conclude that the remaining integrals in the graph (operating on F and F^R) are well-defined when also extended (in a second step) to an infinite domain.⁶

2.5.3 Asymptotic correlations between the plasmas

Having now at disposal a tool (the resummed Mayer graphs) explicitly incorporating collective screening effects for the two-point density correlations, we come

⁶Furthermore, even though the resummed Mayer series might converge, it would not do so to the true correlation function h , for the latter is known to contain nonanalytic terms in the plasma parameter $\Gamma' = \frac{1}{2}\beta e^2 \kappa$ near the strict Debye–Hückel limit $\Gamma' = 0$, of the form $e^{-C/\Gamma'}$ (Brydges & Martin, 2000, Sect. II.C). Nevertheless, expanding around this Debye–Hückel limit — like we do with the resummed Mayer graph series of h — is believed to lead to physically correct results.

back to the force (2.51).

To extract the asymptotic large-distance behaviour of the Ursell correlation function $h_{AB}(1, 2, \frac{\mathbf{q}}{d})$, we select the class of its graphs that give the dominant contribution by analysing them one by one.

In the limit $d \rightarrow \infty$, the integrated bonds of a graph have very different behaviours depending on whether their arguments both lie in the same plasma, or not, in which latter case they account for interactions at a distance at least d . Therefore, we decompose every integrated point \mathbf{i} in (2.61) — running over the whole system — explicitly into an A and a B contribution, namely

$$\int d\mathbf{i} \rho(\mathbf{i})\dots = \int d\mathbf{i} \rho_A(\mathbf{i})\dots + \int d\mathbf{i} \rho_B(\mathbf{i})\dots \quad (2.62)$$

This specialises the bonds F and F^R into F_{AA} , F_{AB} , F_{BA} , F_{BB} and F_{AA}^R , F_{AB}^R , F_{BA}^R , F_{BB}^R contributions, according to the then known location of their arguments.⁷ Note that for every type of link \mathcal{F} ,

$$\mathcal{F}_{BA}(1, 2, \mathbf{y}) = \mathcal{F}_{AB}(2, 1, -\mathbf{y}), \quad \text{and} \quad \mathcal{F}_{BA}(1, 2, \mathbf{k}) = \mathcal{F}_{AB}(2, 1, -\mathbf{k}) \quad (2.63)$$

by space-inversion invariance. We will refer to these BA bonds as being AB bonds as well.

Only *traversing bonds* AB can be held responsible for the decay of h_{AB} to zero (note that every graph of h_{AB} has at least such a bond). The other bonds tend towards those of the single plasmas. The more crossing bonds there are in a graph, the faster it is expected to decay.

The most simple graphs of $h_{AB}(1, 2, \frac{\mathbf{q}}{d})$ are the single links $F_{AB}(1, 2, \frac{\mathbf{q}}{d})$ and $F_{AB}^R(1, 2, \frac{\mathbf{q}}{d})$. Their decay rate needs to be determined.

The Debye–Hückel potential at large separation

The resummed Mayer bonds F and F^R are given in (2.59) and (2.60) in terms of the Debye–Hückel potential Φ . This potential, yet unknown, is solution of the integral equation (2.55), or the Poisson–Boltzmann differential equation (2.25) (generalised to a local inverse screening length $\kappa(1)$).

It is difficult to solve the Poisson–Boltzmann differential equation in the two-plasma system for two reasons:

1. the first is that the density profiles $\rho(1)$ entering into the definition of the local screening length $\kappa^{-1}(1)$ are not explicitly known. This is a serious issue,

⁷We recall that positions along x in plasma B are measured from its inner boundary.

preventing the determination of Φ to be complete, presumably.⁸ However, this problem turns out irrelevant for the determination of the dominant behaviour of the potential as $d \rightarrow \infty$;

2. the second is rather technical: the potential must be solved piecewise in several regions (inside the plates, in the vacuum regions, and on each side of the Dirac source), and the matching of the individual solutions at these regions' boundaries leads to cumbersome algebra.


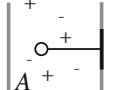
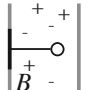
In the article of Chapter 3, this resolution has nevertheless been undertaken. The plates have been taken semi-infinite to relax the second difficulty (except in Appendix 3.A, where one plate is of finite width). It has the advantage of providing an explicit bound for $\Phi(1, 2, \mathbf{k})$ (in particular, uniform in \mathbf{k}) at sufficiently weak coupling.

Result: Under the assumption that the densities of the interacting two-plasma system tend to those of the isolated plasmas, *i.e.*,

$$\rho_A(1) \xrightarrow{d \rightarrow \infty} \rho_A^0(1), \quad \rho_B(2) \xrightarrow{d \rightarrow \infty} \rho_B^0(2), \quad (2.64)$$

the dominant behaviour of the effective potential $\Phi(1, 2, \frac{\mathbf{q}}{d})$ between a charge in plasma *A* and a charge in plasma *B* reads

$$\Phi_{AB}(1, 2, \frac{\mathbf{q}}{d}) \stackrel{d \rightarrow \infty}{\sim} \frac{1}{d} \frac{q}{4\pi \sinh q} \Phi_A^0(1, 0, \mathbf{0}) \Phi_B^0(0, 2, \mathbf{0}). \quad (2.65)$$

It is factorized into the effective potentials Φ_A^0 and Φ_B^0 (at a Fourier vector $\mathbf{k} = \mathbf{0}$) of the single plasmas with one position evaluated at their inner surface. The effective interaction between the plasmas thus occurs through intraplasma interactions with particles close to separating space.

The advantage of having introduced $\mathbf{q} = \mathbf{k}d$ in (2.51) is clearly displayed on this asymptotic formula: all variables of Φ_{AB} are disentangled into factorized dependencies. Note that although the Coulomb potential $v(x, \mathbf{k} = \mathbf{0})$ diverges, in conformity to its long range as $|\mathbf{y}| \rightarrow \infty$ (Appendix B), this is not the case of the resummed — thus shorter ranged — potentials by their uniform bound with respect to \mathbf{k} .

⁸The unknown density profiles $\rho(m)$ can in principle be determined self-consistently from the first equation of the Born–Green–Yvon hierarchy, which is, in addition to the resummed Mayer expansion representing h , another equation relating the unknown local density and density correlation function. See also Section 3.8.

Alternative method: Here we devise a simpler reasoning capable of retrieving (2.65) based on the integral equation (2.55) rather than the Poisson–Boltzmann differential equation. It will prove useful when considering more elaborate models, and does not lead to the difficulty 2 above.

One can establish (2.65) by noticing a similar factorization in the Coulomb potential $v_{AB}(x, \mathbf{k})$ and then resumming only the dominant convolution chains defining $\Phi_{AB}(1, 2, \frac{\mathbf{q}}{d})$.

The series of Coulomb chain convolutions resulting from the iterated integral equation (2.55) reads

$$\Phi(i, j, \mathbf{k}) = v(i, j, \mathbf{k}) - \int d1 \frac{\kappa^2(1)}{4\pi} v(i, 1, \mathbf{k})v(1, j, \mathbf{k}) + \dots \quad (2.66)$$

It is equal to (2.57) up to a factor $-\beta e_{\gamma_i} e_{\gamma_j}$, and written here in partial Fourier representation. Taking $i \in A$ and $j \in B$, we split every integrated point into an A and a B contribution, as in (2.62) for the Mayer graphs before. The chain convolutions are thus expanded into products of AA , BB , AB or BA Coulomb potentials. Representing a traversing bond as a double headed arrow, a typical chain of $\Phi_{AB}(i, j, \mathbf{k})$ then looks like

$$\begin{array}{ccccccc} \circ^A & \cdots & \bullet^A & \leftarrow & \bullet^B & \cdots & \bullet^B & \cdots & \bullet^B & \circ^B \\ & & v_{AA} & & v_{AB} & & v_{BB} & & v_{BB} & \end{array}, \quad (2.67)$$

with weights $-\kappa_A^2(1)/4\pi$ at an A -integrated point 1, and $-\kappa_B^2(2)/4\pi$ at a B -integrated point 2. Every such chain of Φ_{AB} must contain an odd number of traversing bonds (v_{AB} or v_{BA}).

From the partial Fourier representation of the Coulomb potential (B.7), Appendix B, one has

$$\begin{aligned} v_{AB}(1, 2, \mathbf{k}) &= \frac{2\pi}{k} e^{-k|x_1-x_2-d|} = \frac{ke^{-kd}}{2\pi} \left(\frac{2\pi}{k} e^{-k|x_1|} \right) \left(\frac{2\pi}{k} e^{-k|x_2|} \right) \\ &= \frac{ke^{-kd}}{2\pi} v_{AA}(1, 0, \mathbf{k}) v_{BB}(0, 2, \mathbf{k}) \quad \forall \mathbf{k}. \end{aligned} \quad (2.68)$$

Evaluated at $\mathbf{k} = \mathbf{q}/d$, this structure is very similar to (2.65); this is not surprising, since $v_{AB}(1, 2, \frac{\mathbf{q}}{d})$ is the first “chain” of $\Phi_{AB}(1, 2, \frac{\mathbf{q}}{d})$. The Coulomb potentials $v_{AA}(1, 0, \mathbf{k})$ and $v_{BB}(0, 2, \mathbf{k})$ are not well-defined at $\mathbf{k} = \mathbf{0}$, but they will be convoluted in chain to form the factors $\Phi_A^0(1, 0, \mathbf{k})\Phi_B^0(0, 2, \mathbf{k})$, which are.

Because of this divergency of $v_{AA}(\frac{\mathbf{q}}{d})$ and $v_{BB}(\frac{\mathbf{q}}{d})$ with $d \rightarrow \infty$, chains with any (odd) number of crossing bonds will contribute to the asymptotic behaviour of $\Phi_{AB}(1, 2, \frac{\mathbf{q}}{d})$. Let $\Phi_{AB}^{(2n+1)}$ be the sum of chains (2.67) containing $2n + 1$ traversing bonds.

To compute $\Phi_{AB}^{(1)}$, let us represent the Coulomb factorization (2.68) as

$$\circ \left\langle \overset{v_{AB}}{\dots} \right\rangle \circ = \frac{ke^{-kd}}{2\pi} \circ \overset{v_{AA}}{\dots} | \quad | \overset{v_{BB}}{\dots} \circ, \quad (2.69)$$

and insert it into all chains of the type (2.67) containing only one bond v_{AB} . The sum of all of these chains leads to the construction on each side (A or B) of sums of v_{AA} -chains or v_{BB} -chains. Hence, at $\mathbf{k} = \mathbf{q}/d$,

$$\Phi_{AB}^{(1)}(i, j, \frac{\mathbf{q}}{d}) = \frac{qe^{-q}}{2\pi d} \widetilde{\Phi}_{AA}(i, 0, \frac{\mathbf{q}}{d}) \widetilde{\Phi}_{BB}(0, j, \frac{\mathbf{q}}{d}), \quad (2.70)$$

where

$$\widetilde{\Phi}_{AA}(i, 0, \frac{\mathbf{q}}{d}) \equiv \circ \overset{v_{AA}}{\dots} | + \circ \overset{v_{AA}}{\dots} \bullet \overset{v_{AA}}{\dots} | + \circ \overset{v_{AA}}{\dots} \bullet \bullet \overset{v_{AA}}{\dots} | + \dots \quad (2.71)$$

(and likewise for $\widetilde{\Phi}_{BB}$). The introduced potential $\widetilde{\Phi}_{AA}$ represents an intermediate quantity between Φ_{AA} , the Debye–Hückel potential between two points of A in the interacting two-plasma system, and Φ_A^0 , the effective potential between two points of the isolated plasma A . Indeed, it collects all chains of Φ_{AA} that do not vanish in the limit $d \rightarrow \infty$ (the other chains of Φ_{AA} contain (at least two) crossing v_{AB} links and are of order $O(d^{-1})$), but differs from Φ_A^0 by having weights $-\kappa_A^2(1)/4\pi$ instead of

$$-\frac{(\kappa_A^0)^2(1)}{4\pi} \equiv \lim_{d \rightarrow \infty} \frac{-\kappa_A^2(1)}{4\pi} \quad (2.72)$$

at each integrated point [see (2.64)]. The definition (2.71) can equivalently be written as (2.66) or (2.55) but with $\kappa_A^2(1)$ in place of $\kappa^2(1)$. From (2.72) and its B counterpart, one has

$$\lim_{d \rightarrow \infty} \widetilde{\Phi}_{AA}(1, 2, \frac{\mathbf{q}}{d}) = \Phi_A^0(1, 2, \mathbf{0}), \quad (2.73)$$

$$\lim_{d \rightarrow \infty} \widetilde{\Phi}_{BB}(1, 2, \frac{\mathbf{q}}{d}) = \Phi_B^0(1, 2, \mathbf{0}). \quad (2.74)$$

To obtain $\Phi_{AB}^{(3)}(i, j, \frac{\mathbf{q}}{d})$, one can resum first, among all chains containing three crossing Coulomb links, those whose extremal v_{AA} and v_{BB} chains are the same. This gives rise to no more than $\Phi_{BA}^{(1)}$ in the center, as in

$$\circ \overset{v_{AA}}{\dots} \bullet \overset{v_{AB}}{\dots} \left\langle \overset{\Phi_{BA}^{(1)}}{\dots} \right\rangle \overset{v_{AB}}{\dots} \bullet \overset{v_{BB}}{\dots} \circ. \quad (2.75)$$

The quantity $\Phi_{AB}^{(3)}(i, j, \frac{\mathbf{q}}{d})$ is thus retrieved by attaching one traversing Coulomb bond to each extremities of $\Phi_{BA}^{(1)}$ and summing the remaining v_{AA} and v_{BB} chains

on each side, as before. Using the factorization (2.68) of v_{AB} , this will lead to the formation of $\tilde{\Phi}_{AA}$ and $\tilde{\Phi}_{BB}$ at the extremities:

$$\left(\frac{qe^{-q}}{2\pi d}\right)^2 \circ \tilde{\Phi}_{AA} \left| \begin{array}{c} \text{---} \\ \text{---} \\ \text{---} \end{array} \right| \begin{array}{c} \text{---} \\ \text{---} \\ \text{---} \end{array} \left| \begin{array}{c} \text{---} \\ \text{---} \\ \text{---} \end{array} \right| \tilde{\Phi}_{BB} \circ. \quad (2.76)$$

With the factorization of $\Phi_{BA}^{(1)}(i, j, \frac{q}{d})$ similar to (2.70), one has

$$\begin{aligned} \Phi_{AB}^{(3)}(i, j, \frac{q}{d}) &= \left(\frac{qe^{-q}}{2\pi d}\right)^3 \tilde{\Phi}_{AA}(i, 0, \frac{q}{d}) \left[-\int d1 \frac{\kappa_B^2(1)}{4\pi} v_{BB}(0, 1, \frac{q}{d}) \tilde{\Phi}_{BB}(1, 0, \frac{q}{d}) \right] \\ &\quad \times \left[-\int d2 \frac{\kappa_A^2(2)}{4\pi} \tilde{\Phi}_{AA}(0, 2, \frac{q}{d}) v_{AA}(2, 0, \frac{q}{d}) \right] \tilde{\Phi}_{BB}(0, j, \frac{q}{d}). \end{aligned} \quad (2.77)$$

By definition of $\tilde{\Phi}_{AA}$ and $\tilde{\Phi}_{BB}$, the brackets in (2.77) reduce to

$$\tilde{\Phi}_{BB}(0, 0, \frac{q}{d}) - v_{BB}(0, 0, \frac{q}{d}) = -\frac{2\pi d}{q} + O(1), \quad (2.78)$$

$$\tilde{\Phi}_{AA}(0, 0, \frac{q}{d}) - v_{AA}(0, 0, \frac{q}{d}) = -\frac{2\pi d}{q} + O(1). \quad (2.79)$$

On the right hand sides of (2.78) and (2.79), the dominant terms come from the Coulomb potentials, while the estimates $O(1)$ reflect the fact that $\Phi(1, 2, \mathbf{k})$, and also $\tilde{\Phi}_{AA}(1, 2, \mathbf{k})$ and $\tilde{\Phi}_{BB}(1, 2, \mathbf{k})$ are bounded uniformly in \mathbf{k} . We borrow this result from Chapter 3, Formula (3.49). We will see below that it is equivalent to the fact that these Debye–Hückel potentials satisfy the perfect screening sum rule by themselves. Equation (2.77) thus has, in the limit $d \rightarrow \infty$, a prefactor

$$\left(\frac{qe^{-q}}{2\pi d}\right)^3 \left(\frac{2\pi d}{q}\right)^2 = \frac{qe^{-q}}{2\pi d} e^{-2q}, \quad (2.80)$$

so that

$$\Phi_{AB}^{(3)}(i, j, \frac{q}{d}) \stackrel{d \rightarrow \infty}{\sim} \frac{qe^{-q}}{2\pi d} e^{-2q} \tilde{\Phi}_{AA}(i, 0, \frac{q}{d}) \tilde{\Phi}_{BB}(0, j, \frac{q}{d}). \quad (2.81)$$

By induction on n , one easily sees that $\Phi_{AB}^{(2n+1)}(i, j, \frac{q}{d})$ receives, instead, a prefactor $\frac{qe^{-q}}{2\pi d} e^{-2nq}$. Summing over $n = 1, 2, 3, \dots$ and taking the limit $d \rightarrow \infty$ on $\tilde{\Phi}_{AA}$ and $\tilde{\Phi}_{BB}$ gives the final result (2.65).

The Debye–Hückel graph

The asymptotic factorization (2.65) of Φ_{AB} gives to the Mayer graph constituted by the bond F_{AB} alone its asymptotic behaviour:

$$F_{AB}(1, 2, \frac{q}{d}) \stackrel{d \rightarrow \infty}{\sim} \frac{-1}{\beta d} \frac{q}{4\pi \sinh q} \frac{F_A^0(1, 0, \mathbf{0})}{e_{\alpha_0}} \frac{F_B^0(0, 2, \mathbf{0})}{e_{\beta_0}}, \quad (2.82)$$

where e_{α_0} and e_{β_0} are the charges situated at the inner surface of the plasmas in F_A^0 and F_B^0 . We will see that this graph alone already provides the full asymptotic value of the Casimir force.

Dominant graphs and asymptotic behaviour of h_{AB}

Since the dominant graphs of the Ursell function are those containing the least number of crossing links, and that $F^R(\mathbf{1}, \mathbf{2}) \approx \frac{1}{2}F^2(\mathbf{1}, \mathbf{2})$ is of shorter range than F , the asymptotic behaviour of h_{AB} is given by all graphs having exactly one bond F_{AB} . These are formed by binding any type of AA and BB links to the corresponding extremities of F_{AB} in compliance with the diagrammatic rules. Because F -type bonds cannot be convoluted in chains [see the paragraph after Equation (2.61)], subgraphs which bind to F_{AB} by a single F_{AA} or F_{BB} bond (depending on the extremity) are not allowed. The sum of these contributions thus reads [see also (3.77)]

$$\circlearrowleft \left(\circlearrowleft + \frac{F_{AA}}{\rho_A} \bullet \circlearrowleft + \frac{\delta}{\rho_A} \right) \bullet \xleftrightarrow{F_{AB}} \bullet \left(\circlearrowleft + \circlearrowleft \frac{F_{BB}}{\rho_B} + \frac{\delta}{\rho_B} \right) \circlearrowleft, \quad (2.83)$$

where the symbol $\circlearrowleft \circlearrowleft$ represents the sum of all subgraphs (in A or B) having neither of their two root points connected to a single bond F only. The delta terms on both sides of F_{AB} in (2.83) allow the latter's extremities to be the root points of the whole graph (nothing attached).

Upon using the asymptotic factorization of F_{AB} (2.82), the contribution (2.83) can as well be factorized into a product of A and B correlation functions. This provides us with the asymptotic behaviour of $h_{AB}(1, 2, \frac{\mathbf{q}}{d})$:

$$h_{AB}(1, 2, \frac{\mathbf{q}}{d}) \stackrel{d \rightarrow \infty}{\sim} \frac{-1}{\beta d} \frac{q}{4\pi \sinh q} \frac{G_A^0(1, 0, \mathbf{0})}{e_{\alpha_0}} \frac{G_B^0(0, 2, \mathbf{0})}{e_{\beta_0}}, \quad (2.84)$$

with

$$G_A^0 = \circlearrowleft \left(\circlearrowleft + \frac{F_A^0}{\rho} \bullet \circlearrowleft + \frac{\delta}{\rho} \right) \bullet \frac{F_A^0}{\rho} \circlearrowleft = \circlearrowleft \bullet \circlearrowleft + \circlearrowleft \bullet \bullet \circlearrowleft + \circlearrowleft \circlearrowleft \quad (2.85)$$

and $G_B^0 = \circlearrowleft \circlearrowleft + \circlearrowleft \bullet \bullet \circlearrowleft + \circlearrowleft \bullet \circlearrowleft$. The latter entities are correlation functions similar to the Ursell function of the isolated plasmas. In particular, they satisfy the perfect screening sum rule like h in (2.31). They have their inner root point located at the plasma's surface like F_A^0 and F_B^0 in (2.82).

2.5.4 Validity of the perfect screening sum rules

In spite of the temptation to insert (2.82) or (2.84) right away into the force formula (2.51), let us first discuss how the perfect screening sum rule (2.31) for the

Debye–Hückel potential Φ_A^0 and the Ursell function h_A^0 of the single plasma A can be shown to be valid. Indeed, they will be the keys to universality in the Casimir force.

Perfect screening on the Debye–Hückel level

Once it is known that the Debye–Hückel potential $\Phi_A^0(1, 2, \mathbf{k})$ is bounded uniformly with respect to \mathbf{k} , one can show the perfect screening sum rule (2.29) or (2.30) satisfied by it without having an explicit expression. A first way is to proceed as in the article in Chapter 3 by integrating the Poisson–Boltzmann equation. Alternatively, one can start from the integral equation (2.55), divide it by the Coulomb potential, and consider

$$\lim_{\mathbf{k} \rightarrow \mathbf{0}} \frac{\Phi_A^0(i, j, \mathbf{k})}{v_{AA}(i, j, \mathbf{k})} = 1 - \lim_{\mathbf{k} \rightarrow \mathbf{0}} \int d\mathbf{l} \frac{(\kappa_A^0)^2(1)}{4\pi} \frac{v_{AA}(i, 1, \mathbf{k})}{v_{AA}(i, j, \mathbf{k})} \Phi_A^0(1, j, \mathbf{k}). \quad (2.86)$$

The left hand side vanishes by the $\sim 1/k$ divergency of $v_{AA}(i, j, \mathbf{k})$ in this limit, and the boundedness of Φ_A^0 . Since $\Phi_A^0(1, j, \mathbf{k})$ has well-integrable properties on 1 even at $\mathbf{k} = \mathbf{0}$ [see (3.49)], and since

$$\frac{v_{AA}(i, 1, \mathbf{k})}{v_{AA}(i, j, \mathbf{k})} = \frac{e^{-k|x_i - x_1|}}{e^{-k|x_i - x_j|}} \leq \frac{1}{e^{-k|x_i - x_j|}}, \quad \lim_{\mathbf{k} \rightarrow \mathbf{0}} \frac{v_{AA}(i, 1, \mathbf{k})}{v_{AA}(i, j, \mathbf{k})} = 1, \quad (2.87)$$

the limit can be taken on the integrand by dominated convergence (for fixed x_i and x_j), so that the perfect screening sum rule on the Debye–Hückel level

$$\int d\mathbf{l} \frac{(\kappa_A^0)^2(1)}{4\pi} \Phi_A^0(1, j, \mathbf{k} = \mathbf{0}) = 1 \quad (2.88)$$

is satisfied, whether the thickness of plasma A be finite or infinite.

This method clearly displays the interplay between the shielding of the long range of the Coulomb potential incorporated into the resummed potential $\Phi_A^0(\mathbf{k})$ (which no longer exhibits the singularity $\sim 1/k$), and the perfect screening of charges reflected by the sum rule.

Perfect screening rule for the Ursell function

In (Martin, 1988, Sec. III), it is shown that the classical two-point correlation function of a plasma confined to a slab of finite or semi-infinite thickness, satisfies the perfect screening sum rule (2.31).

In fact, it is only necessary for its validity that it holds at the Debye–Hückel level. The proof proceeds by distinguishing the graphs of h_A^0 according to whether their root points are attached to the rest of the graph by a single F bond or not.

This calculation is performed in the article of chapter 3, see Formula (3.68). We will also present it in the quantum case (Section 5.3.6).

The same technique allows to establish that the partial correlation functions G_A^0 and G_B^0 in (2.84) above also satisfy the electroneutrality sum rule (2.31), see (3.82)–(3.84).

2.5.5 The asymptotic force

Knowing the asymptotic behaviour of the correlations across the plasmas at large separation and their screening property, we can at last finalise the calculation of the Casimir force in the limit $d \rightarrow \infty$.

The force in the Debye–Hückel approximation

Approximating h_{AB} by F_{AB} in the force formula (2.51), and using the limiting values of the densities (2.64) and of F_{AB} (2.82), one finds that

$$\begin{aligned} f(d) &\stackrel{d \rightarrow \infty}{\sim} \frac{1}{d^2} \int d1 \int d2 \int \frac{d\mathbf{q}}{(2\pi)^2} 2\pi e^{-q} \rho_A^0(1) \rho_B^0(2) F_{AB}(1, 2, \frac{\mathbf{q}}{d}) \\ &\stackrel{d \rightarrow \infty}{\sim} \frac{-1}{4\pi\beta d^3} \left[\int_{-a}^0 dx_1 \frac{(\kappa_A^0)^2(x_1)}{4\pi} \Phi_A^0(x_1, 0, \mathbf{0}) \right] \left[\int_0^b dx_2 \frac{(\kappa_B^0)^2(x_2)}{4\pi} \Phi_B^0(0, x_2, \mathbf{0}) \right] \int_0^\infty dq \frac{q^2 e^{-q}}{\sinh q} \\ &= -\frac{\zeta(3)}{8\pi\beta d^3}. \end{aligned} \quad (2.89)$$

Last equality results from the perfect screening sum rule (2.88), and the value $\zeta(3)/2$ of the q -integral. By the universality of the result, *i.e.*, its independence upon material parameters of the plates (in particular, upon the coupling parameters and the screening lengths), one can expect it to hold beyond the Debye–Hückel approximation.

The full Casimir force

Indeed, upon insertion of the asymptotic component of h_{AB} (2.84) into the force formula (2.51), one obtains, similarly,

$$\begin{aligned} f(d) &\stackrel{d \rightarrow \infty}{\sim} -\frac{1}{4\pi\beta d^3} \left[\int d1 e_{\gamma_1} \rho_A^0(1) \frac{G_A^0(1, 0, \mathbf{0})}{e_{\alpha_0}} \right] \left[\int d2 e_{\gamma_2} \rho_B^0(2) \frac{G_B^0(0, 2, \mathbf{0})}{e_{\beta_0}} \right] \int_0^\infty dq \frac{q^2 e^{-q}}{\sinh q}. \\ &\quad \left[\begin{array}{c} - \\ + \\ - \\ - \\ + \\ A \end{array} \right] \left[\begin{array}{c} - \\ - \\ - \\ - \\ - \\ \oplus \\ - \\ - \\ - \\ - \end{array} \right] \quad \left[\begin{array}{c} + \\ + \\ - \\ - \\ - \\ \oplus \\ - \\ - \\ - \\ - \\ + \\ B \end{array} \right] \end{aligned} \quad (2.90)$$

The two brackets in (2.90) are associated to the integrals of the screening clouds induced around fixed charges at the inner surfaces of the plasmas, as suggested by the picture. By the sum rule (2.31) that the correlation functions G_A^0 and G_B^0 satisfy on their own, these brackets are equal to -1 (the fixed charges are perfectly screened) and we thus have

$$f(d) \stackrel{d \rightarrow \infty}{\sim} -\frac{\zeta(3)}{8\pi\beta d^3}. \quad (2.91)$$

In addition to the comments of Section 2.4.1, let us mention a few points.

- The perfect screening sum rules are fundamental to wipe out the microscopic details of the plasmas. Their validity reflects that the plasmas are in conducting states, which is known to be the case, in particular, in the weak-coupling regime. This regime is attained at high temperatures and large distances, as discussed in Section 2.3.4. Note that only the screening of charges at the surfaces close to the interspace is involved. This explains why the asymptotic force is independent of the thicknesses a and b of the plasmas.⁹ Furthermore, the same formula is also obtained if a and b are taken infinite before letting $d \rightarrow \infty$, by virtue of the good decaying properties in the bulk of the resummed Debye–Hückel potentials. (The case of *ab initio* semi-infinite plasmas is explicitly dealt with in Chapter 3.)
- Exact knowledge about the local densities is not needed to calculate the dominant behaviour of the Ursell function (and of the Casimir force) at large distances. The speed at which they tend to the densities of the single plasmas as $d \rightarrow \infty$ will be necessary to determine subdominant terms (see next point).
- The question of subdominant terms is of considerable interest. We will see at the end of chapter 3 that $O(d^{-4})$ terms in the force do not necessitate the consideration of new Mayer graphs in the series representation of the Ursell function. Rather, these terms will be associated to the deviation of the $O(d^{-1})$ dominant graphs (2.83) of h_{AB} to their limiting value (2.84) $\propto d^{-1}$ as $d \rightarrow \infty$.

As a last remark, and to establish a link with the fundamental considerations about the model at the beginning of this chapter, let us consider the **gravitational contribution** to the total force exerting between the two metallic plates (still disregarding intraplasma gravitational forces.)

⁹This independence holds as long as the thicknesses are large enough to allow screening to take place, *i.e.*, $\lambda_D/a \lesssim 1$ and $\lambda_D/b \lesssim 1$. See also Appendix 3.A

In the two-plates geometry, if the mass densities ρ_A^{mass} and ρ_B^{mass} are supposed constant, the gravitational force by unit surface acting on plasma B reads

$$-2\pi G(\rho_A^{\text{mass}} a)(\rho_B^{\text{mass}} b), \quad (2.92)$$

similarly to the capacitor's force (2.47). This dominant contribution of the gravitational attractive force is not very interesting: it is independent of the separation d , and also well-known¹⁰, so that its subtraction is easily done. Naturally, there is a separation distance above which it dominates the Casimir force, in spite of the weakness of the coupling constant $G \approx 6.7 \cdot 10^{-8} \text{cm}^3 \text{g}^{-1} \text{s}^{-1}$. As an example, for two plates of thickness $a = b \approx 50 \text{nm}$, mass densities $\approx 10^4 \text{kg/m}^3$, corresponding to the experimental setup of Bressi et al. (2002), this gravitational contribution is $\approx 10^{-16} \text{dyne/cm}^2$. At $T \approx 300 \text{K}$, it overcomes the high-temperature Casimir contribution (2.90) for distances $\gtrsim 1 \text{cm}$!¹¹

2.5.6 Generalisation of the method to quantum plasmas and field-coupled quantum plasmas

To this point, the calculation presented has been carried out for classical plasmas. It retrieves [see (2.90)] the well-known expression (1.4) for the Casimir force in the semi-classical regime, which is expected to be correct in view of the discussion of the physical parameters ruling the plasmas (Section 2.3.4).

Nevertheless, by its very formulation, this model cannot be really related to other calculations that chiefly attribute the Casimir force (1.4) to the fluctuations of the electromagnetic field. Indeed, the radiation part of the field disappears from our description at the beginning, as a consequence of the Bohr–van Leeuwen decoupling theorem. Our result (2.90) includes exclusively the longitudinal part of the field. The force is built up by the thermal fluctuations of the atomic entities inside the globally neutral metals through purely electrostatic interactions.

Because of the actual controversy about the factor 2 discrepancy between the two results (1.4) and (1.3), investigating a more complete model that includes quantum-mechanics and the radiation part of the field is of strong interest.

Our result is that the expression (2.90) is *unchanged by such a generalisation*. Although new contributions to the Ursell function h_{AB} show up at $O(d^{-1})$, the perfect screening sum rule cancels them when integrated into the force. Note that by a simple dimensional analysis, one sees that in accordance to the Bohr–van

¹⁰See, however, the discussion in the introduction about probing short-range gravitational forces.

¹¹This is without taking into account the gravitational attraction of the plates' supports in the experiments. Note also that this range shrinks fast for thicker plates.

Leeuwen theorem, the force could have been supplemented at dominant order $O(d^{-3})$ by terms of the type

$$\frac{1}{d^3} \frac{\hbar c}{\lambda}, \quad (2.93)$$

where λ is a (classical) length (like the plasmas' thickness a , b , the mean inter-particle distance a_ρ , etc). Such terms would vanish in the limit $\hbar \rightarrow 0$ of classical plasmas, for which the field decouples and plays no role in the Casimir force. We have shown that they do not appear at all.

We give in this last section a few hints on how the method exposed above can be generalised to include the quantum-mechanical treatment of the particles, and the inclusion of a classical radiation field. The details of this calculation are to be found in Chapter 5. It relies on tools that are presented in Chapter 4.

Extension of the Mayer expansion to quantum systems

Dealing with the $1/r$ long range of the Coulomb potential in statistical systems is notoriously difficult. General theorems about the thermodynamic limit or low-density expansions usually rely on the assumption of integrable potentials. Fortunately, by the sign of this interaction, screening mechanisms take place and its effective range is short.

We have seen that the mean-field potential of Debye and Hückel is an adequate way to exhibit screening systematically in the Ursell correlation function, by resumming the Coulomb divergencies in the Mayer graphs. It has proven an essential tool in the analysis leading to the result (2.90).

Yet, the Mayer series expansion of the Ursell function relies on a classical form of the Gibbs integral, see Section 2.5.2. Such a classical form can be retrieved in quantum systems when making use of the Feynman–Kac path integral formalism. This point of view has been developed by Ginibre (1965a, 1965b, 1965c). It introduces an auxiliary statistical system, that of **loops** (or “polymers”), which are classical but extended objects of random Brownian shape. This shape represents the quantum-mechanical fluctuations of the positions of the particles. A Mayer-like series of the correlations of these classical-like objects can be developed by the same classical methods overviewed in Section 2.5.2. Rigorous results on the convergence of this Mayer series, for integrable (non-Coulombic) potentials, are stated in (Ruelle, 1989, Sec. 4.6).

The same problems as in classical statistical mechanics arise when the interaction is Coulombic. Due to its long range, every Mayer diagram flagrantly diverges. The resummation of the Mayer-like series can be worked out as well. It leads similarly to Debye–Hückel-type potentials. This procedure has been used to derive

various properties of quantum plasmas, in particular, their large-distance correlations (Cornu, 1996a, 1996b). Reviews on this topic can be found in (Alastuey, 1994; Brydges & Martin, 1999). See also (Ballenegger, Martin, & Alastuey, 2002).

The quantum plasmas considered in the above works concern purely electrostatic matter only. Adding the radiation field $\mathbf{A}(\mathbf{r})$ can be achieved by supplying the formalism with the Itô path integral, which is the subject presented in Chapter 4.

We only mention hereafter the main characteristics of this formalism.

The loop formalism

The quantum-mechanical statistical system of the charges is mapped exactly into an auxiliary, classical-like statistical system. The particles' quantum phase space is replaced by the phase space of loops. Every loop consists of a position \mathbf{r} , a species index γ , an integral charge number q and a closed Brownian shape $\mathbf{X}(\cdot)$. Integrating on these degrees of freedom means, in particular, integrating on all shapes $\mathbf{X}(\cdot)$ by means of a Wiener (Gaussian) functional integral.

These objects interact with one another through a pairwise potential derived from the initial interaction between the particles. This potential differs slightly, but fundamentally, from summing up all interactions between every element of line of the loops' shape. The most striking consequence of this difference arises for Coulomb fluids in their large-distance correlations. Indeed, these asymptotic correlations no longer exhibit exponential clustering. Instead, they decorrelate algebraically at large distances ($\sim r^{-6}$), illustrating the fact that *the quantum-mechanical fluctuations of the charges effectively prevent the screening of multipoles*. Perfect screening of monopoles, however, expressed by the electroneutrality sum rule, still holds.

We will see in Chapter 4 that when the transverse field's degrees of freedom are added to the statistical system, the same developments can be made. When averaging microscopic observables not concerned by the radiation field, like the density, or the density correlation function, or when considering the total free energy, these new degrees of freedom can be exactly integrated out. They result in a new, effective, "magnetic" potential between the loops.

Calculating the force in this formalism

Essentially the same techniques developed for the classical two-plasma system can be used, thanks to the similitude of the statistical system of loops and the classical system of charges. Namely:

1. The total free energy is expressed in terms of the auxiliary system of loops. When the radiation field is included, differentiating it with respect to d provides new microscopic contributions to the Casimir force, representing the magnetic part of the whole Lorentz forces exerting between the two metallic plates. However, averaging these magnetic contributions turns out to only result in contributions to the force of order $O(d^{-5})$ as $d \rightarrow \infty$. The force is expressed as averages of two-body observables in the phase space of loops.
2. The averages of these two-body observables are expressed as integrals on the Ursell function of the statistical system of loops. The truncation of the correlation is allowed when the plasmas are globally neutral. Otherwise, a capacitor-like force, mainly constant, is added.
3. The loop Ursell function is represented in resummed Mayer graph series. Because of the form of the interaction potential between the loops and the effective magnetic potential, the large-distance asymptotic analysis performed on the resummed series provides a class of structurally new dominant terms. These new terms represent, in particular, asymptotic correlations mediated by the radiation field and residual correlations resulting from the imperfect screening of the multipoles in the quantum plasma.
4. When inserted into the force, the first class of the dominant resummed diagrams builds up the classical result (2.90). Universality is obtained as in the classical case by the perfect screening sum rule. The second, new, class of dominant diagrams is found to provide only subleading contributions to the force, because they are shielded away by the same perfect screening sum rule.

As a consequence, the result (2.90) is retrieved, namely, the force between quantum-mechanical plasmas coupled to a classical radiation field reads

$$f(d) = -\frac{\zeta(3)}{8\pi\beta d^3} + O(d^{-4}), \quad d \rightarrow \infty. \quad (2.94)$$

The subdominant $O(d^{-4})$ terms depend in particular on the de Broglie wavelength λ_{part} and the thermal photon wavelength λ_{ph} .

Chapter 3

The Casimir force between classical plasmas

Contents

Microscopic origin of universality in Casimir forces, <i>J. Stat. Phys.</i> , 119, 273–307 (2005)	63
3.1 Introduction	63
3.2 Description of the model	67
3.3 Mayer series for inhomogeneous charged fluids	69
3.4 Debye-Hückel theory	72
3.5 Contributions of the other graphs	78
3.6 Plasma in front of a macroscopic dielectric medium	83
Appendix 3.A: Slab of finite thickness	87
Appendix 3.B: Bounds for the Debye-Hückel potential	89
Appendix 3.C: Decay of Mayer graphs at large slab separation	91
References	93
3.7 Decay analysis of Mayer graphs	95
3.7.1 Decay of Mayer graphs at large separation	95
3.7.2 Illustration on a specific example	96
3.7.3 Determination of the factor $d^{-2I} = d^{-2(L-C)}$	98
3.8 Towards subleading orders of the force	100
3.8.1 Leading and subleading orders of the Ursell function	100
3.8.2 On subleading contributions to the classical force	103

This chapter chiefly consists in the reproduction of the article presenting the calculation of the Casimir force between two classical plasmas [Microscopic origin of universality in Casimir forces, *J. Stat. Phys.*, 119, 273–307, (2005); p. 63]. It is supplemented with additional sections at the end of the chapter (see below).

The calculation presented in the article is parallel to that exposed in Section 2.5. Let us point out its main differences:

- Instead of reasoning on the integral relation defining the resummed Debye–Hückel potential as a chain series of the Coulomb interaction, the Poisson–Boltzmann differential equation is considered. In addition to the difficulty of not knowing explicitly the density profiles, this method imposes matching conditions of piecewise solutions at several interfaces, which leads to cumbersome algebra. Its advantage is to provide an exact bound for the Debye–Hückel potential $\Phi(x, x', \mathbf{k})$ in partial Fourier representation.
- The force between the plasmas is defined from the beginning as the average value of the microscopic Coulomb forces exerting between the two plasmas. This starting point is equivalent to differentiate the free energy of the total system, by virtue of the Bohr–van Leeuwen theorem which proclaims the decoupling of classical matter and field (see Section 2.5). This force has been denoted by $\langle f \rangle$ and defined with the **opposite sign** as the force $f(d)$ of Section 2.5.
- Two viewpoints are exposed to generalise the result obtained in the Debye–Hückel theory so as to include the full correlations. The first uses integral equations to appropriately exhibit the Debye–Hückel potential at the root points of the Ursell function. Assumptions of integrable clustering for related quantities are needed. The second viewpoint proceeds by an analysis of the decay rate of the resummed Mayer graphs constituting h_{AB} .

Note that in the abstract and in the introduction, we assert that the factor two discrepancy is due to the fact that the model does not include the magnetic part of the Lorentz forces. In view of the calculation performed in the field-coupled model (Chapter 5), this turns out to be false.

Dealing with unknown density profiles

The strategy employed to analyse the Poisson–Boltzmann equation for the Debye–Hückel potential $\Phi(\mathbf{r}, \mathbf{r}')$ even though the density profiles $\rho(x_1, \gamma_1)$ are not explicitly known, is to introduce an auxiliary potential, $\varphi(\mathbf{r}, \mathbf{r}')$, solution of the same differential problem but with *piecewise-flat mean densities* along the space: constant inside the plasmas (equal to that of the bulk, or to the space-averaged density

in case of a finite width), and vanishing outside. This kind of simplified Debye–Hückel potential has already been used to calculate weak-coupling expansions of density profiles in wall-constrained plasmas (Jancovici, 1982; J.-N. Aqua & Cornu, 2001a, 2001b). Our method differs by coming back to the Debye–Hückel Φ (defined for the exact structured profiles) in a convenient way.

The explicit solution φ has the advantage of already showing up the main characteristics of the correlations across the two plasmas, in particular, their *asymptotic factorization* into A and B entities. To simplify the calculations, it is calculated for two semi-infinite plasmas in a first stage. In Appendix 3.A, it is given when one of the plates has a finite thickness.

The Debye–Hückel potential Φ is obtained from φ by a convenient chain series, much in the same way as it is defined originally from the Coulomb interaction. This allows to transpose the properties of φ to Φ . Furthermore, the convergence of the series is established at sufficiently weak-coupling. The proof shows that $\Phi(x, x', \mathbf{k})$ is bounded uniformly in \mathbf{k} by an explicit function $\varphi^>(x, x')$ [Equation (3.49)]. This function decays exponentially in the bulk on the range $\kappa = \min\{\kappa_A, \kappa_B\}$, where κ_A and κ_B are the inverse screening lengths corresponding to the flat densities.

Plasma in front of a macroscopic dielectric medium

Section 3.6 of the article deals with a slightly different version of the two-plate system. We calculate with the same method the force exerting between a plasma of charges on one side, and a *macroscopic dielectric plate* on the other side. This generalises the force to a situation in which one of the plates is nonconducting. The nonconducting plate is described on the macroscopic level by a dielectric constant ϵ . It generates images of the plasma's fluctuating charges, that embody the continuity conditions imposed to the electrostatic potential at the dielectric's surface.

The main difference of this calculation resides in the fact that the correlation function involved in the force concerns two charges of the same plasma: the image charges are paired to the real charges. This correlation hence does not vanish as the dielectric plate is sent away to infinity, and one needs to analyse its deviation to its limit value.

The force thus retrieved depends on the dielectric constant and coincides with a particular case of Lifshitz' formula. It is independent of the material constitution of the metallic plate because of screening, and corresponds to the expression obtained between the two plasmas when $\epsilon \rightarrow \infty$.

On the decay of Mayer graphs and subleading orders to the force

In Appendix 3.C of the article, the decay rates of Mayer graphs are discussed. We go back to this discussion in more detail after the reproduction of the article, in Section 3.7, and conclude by a discussion on the subleading orders of the Ursell function and of the classical Casimir force.

Microscopic origin of universality in Casimir forces

Pascal R. Buenzli¹ and Philippe A. Martin

Received July 30, 2004; accepted September 28, 2004

The microscopic mechanisms for universality of Casimir forces between macroscopic conductors are displayed in a model of classical charged fluids. The model consists of two slabs in empty space at distance d containing classical charged particles in thermal equilibrium (plasma, electrolyte). A direct computation of the average force per unit surface yields, at large distance, the usual form of the Casimir force in the classical limit (up to a factor 2 due to the fact that the model does not incorporate the magnetic part of the force). Universality originates from perfect screening sum rules obeyed by the microscopic charge correlations in conductors. If one of the slabs is replaced by a macroscopic dielectric medium, the result of Lifshitz theory for the force is retrieved. The techniques used are Mayer expansions and integral equations for charged fluids.

Key words: Casimir forces, classical charged fluid, universality, Mayer expansion

PACS numbers: 05.20.-y, 61.20.-p

3.1 Introduction

It is well known that the fluctuation-induced forces between macroscopic conductors have a universal character: they only depend on the shapes of the bodies, but not on their material constitution. This observation originates from the celebrated paper of H. B. G. Casimir calculating the force between two parallel

¹E-mail: pascal.buenzli@epfl.ch

metallic plates due to the fluctuations of the quantum electromagnetic field in vacuum at zero temperature. The literature produced since then is so vast that we will only quote in the sequel a number of papers relevant to our purpose. Many references can be found for instances in the books and reviews (Milonni, 1994) (Mostepanenko & Trunov, 1997) (Plunien, Müller, & Greiner, 1986) (Duplantier & Rivasseau, 2003).

Regarding the extension of Casimir's result to non zero temperature T , Balian and Duplantier provide the general form of the free energy in presence of ideal conductors of arbitrary shapes (Balian & Duplantier, 1977, 1978). The theory of Lifshitz and coworkers generalizes the calculations to dielectric bodies characterized by their dielectric functions (Lifshitz, 1955), (Landau, Lifshitz, & Pitaevskii, 1984, §90), (Dzyaloshinskii, Lifshitz, & Pitaevskii, 1961) (see also (Schwinger, DeRaad, & Milton, 1978)). The ideal conductor situation can be recovered from the latter theory by letting the dielectric constants tend to infinity. From these studies one can obtain the asymptotic behaviour of the attractive force between two planar conductors at distance d at high temperature (or equivalently at large separation d)²

$$f \sim \frac{k_B T \zeta(3)}{4\pi d^3}, \quad d \rightarrow \infty \quad (3.1)$$

where ζ is the Riemann ζ -function. In this regime the force is exclusively due to thermal fluctuations and the result may be called classical since it does not depend on Planck's constant. In the above mentioned theories the conductors are treated at the level of macroscopic physics. In fact they are represented by surfaces, called ideal conductors, on which the electromagnetic field has to satisfy the metallic boundary conditions. The purpose of this work is to gain an understanding of the microscopic mechanisms in the conductor that lead to the universality of the force (3.1).

To this end we analyse a simple model where the conductors are described in fully microscopic terms. The conductors consist of two slabs at distance d containing fluids of classical charges (e.g. classical electrolytes or plasmas). The slabs are globally neutral but their material composition (charges and masses of the particles) can be different. The space external to the slabs is empty. The system of the two slabs, considered as a whole, is at thermal equilibrium with a Gibbs weight that includes pairwise interactions between all the particles, consisting of Coulomb potentials plus short-range repulsions. In this setting we present an exact computation of the asymptotic behaviour of the average force per unit surface between the two (infinitely thick) slabs giving

$$\langle f \rangle \sim \frac{k_B T \zeta(3)}{8\pi d^3}, \quad d \rightarrow \infty. \quad (3.2)$$

²The relevant dimensionless parameter is $d k_B T / \hbar c$, c is the speed of light, \hbar the Planck constant, k_B the Boltzmann constant.

It is also checked that (3.2) still holds for slabs of finite thickness (appendix 3.A).

One may notice that the usual approaches consider the fluctuating electromagnetic fields as primary objects. The thermal fluctuations of these fields originate from the fact that they are in equilibrium with the matter constituting the conductors, but as a consequence of universality, the microscopic degrees of freedom of the charges in the conductors do not need to be explicitly incorporated in the description. Here we adopt another point of view: we start from the thermal configurational fluctuations of the charges to provide a direct calculation of the average force without recourse to the field statistics. Then the origin of universality can be traced back to the specific sum rules obeyed by the correlations of Coulombic matter (Martin, 1988).

Universal properties of a variety of classical models of conductor have been studied in (Forrester, Jancovici, & Téllez, 1996) (Jancovici & Téllez, 1996). In (Forrester et al., 1996) the authors consider a statistical mechanical system of charges confined to a plane at distance d of another ideal planar conductor and establish the result (3.2). In (Jancovici & Téllez, 1996), they show that replacing the above ideal conductor by fluctuating charges does not alter (3.2). A recent work (Jancovici & Šamaj, 2004) considers the situation where the space between the two slabs is filled by a third Coulomb fluid, causing a screening of the Casimir force.

The value (3.1) arising from the electromagnetic field fluctuations calculations is twice larger than that obtained in the purely electrostatic models considered here, as well as in (Forrester et al., 1996) (Jancovici & Téllez, 1996) (Jancovici & Šamaj, 2004). This point has been the subject of several discussions in the literature, in particular in (Schwinger, 1975) (Schwinger et al., 1978). In (Schwinger, 1975) Schwinger performs a calculation of the Casimir force mediated by scalar photons (corresponding to the sole electric degree of freedom of an electromagnetic wave) leading to the result (3.2). In (Schwinger et al., 1978) the authors show that taking the magnetic degree of freedom of the field property into account multiplies the expression (3.2) by 2. In its very formulation our model does not include the magnetic part of the Lorentz force induced by fluctuating currents in the conductors, whose effect has the same magnitude as that of the Coulomb force. Although such purely electrostatic models of conductors do not account for the physically correct value of the force at large distance, they already nicely reveal the microscopic mechanisms occurring in conductors that guarantee its universality.

The calculation of the force requires the knowledge of the charge correlation function across the two slabs separation, which is the main object of our study. At large separation it remarkably factorizes into three parts. There is a first factor independent of the slabs' material constitution and two other factors, each solely associated to one of the conductors. More precisely, the latter factors involve the

charge density of the screening cloud induced by a charge located at the boundary of a single conductor in empty space. Then the universality of the force results from the perfect screening sum rule that holds in any conducting phase.

In this work we use the technique of Mayer expansion and integral equations for charged fluids. In Section 3.2, we specify the system under study and express the force by unit surface between two infinitely extended slabs in terms of the microscopic charge correlation between them, taking the existence of the thermodynamic limit for granted.

The general formalism used is recalled in Section 3.3: the charge correlation function is written in terms of the Ursell function subjected to a Mayer expansion. The prototype graphs entering in this expansion involve screened Coulomb bonds resulting from chain summations (Debye-Hückel mean-field potential) and density weights at vertices (Meeron, 1958, 1961) (Aqua & Cornu, 2003). The weights are the exact inhomogeneous densities that have to be self-consistently determined from the first BGY equation. We do not treat here the full self-consistent problem because it turns out that the detailed structure of density profiles is not needed (see (Aqua & Cornu, 2001a) (Aqua & Cornu, 2001b) for a thorough study of density profiles near boundaries). We only have to introduce weak and plausible assumptions on the convergence of the profiles to their bulk value.

It is shown in Section 3.4 that the asymptotic value (3.2) of the force is already obtained at the level of the Debye-Hückel theory. The main tool is the explicit form of the mean-field potential for piecewise-flat density profiles, related to the potential for structured profiles by an integral equation. The latter equation is shown to have a convergent perturbative solution in the weak-coupling regime. At large slab separation, the Debye-Hückel potential factorizes into potentials pertaining to individual plasmas obeying electroneutrality sum rules.

We establish in Section 3.5 that the theory beyond mean-field does not provide any additional contribution to the asymptotics (3.2). This is first done non-perturbatively with the help of integral equations corresponding to an appropriate dressing transformation of the Ursell function and under the mild assumption of integrable clustering. Finally the result is recovered once again by selecting and resumming the contribution of dominant Mayer graphs to the full charge correlation at large separation.

We also treat in Section 3.6 a variant situation where one of the slabs is replaced by an ideal macroscopic dielectric medium at distance d (namely generating images of the plasma's fluctuating charges). Using the Green function of the Poisson equation with appropriate dielectric boundary conditions, the Lifshitz result for the mean force is retrieved and reduces to (3.2) as the dielectric constant tends to infinity. It is interesting to observe that it is sufficient for the fluctuations to occur only in one of the bodies to generate the same asymptotic behaviour.

We will come back to the inclusion of magnetic forces and to quantum models

in future works.

3.2 Description of the model

We consider two plasmas A and B of classical point charges confined to two planar slabs $\Lambda_A(L, a)$ and $\Lambda_B(L, b)$ in three-dimensional space. The slabs have thickness a and b , surface L^2 , and are separated by a distance d :

$$\begin{aligned}\Lambda_A(L, a) &:= \{\mathbf{r} = (x, \mathbf{y}) \mid x \in]-a, 0[, \mathbf{y} \in]-\frac{L}{2}, \frac{L}{2}[^2\} \\ \Lambda_B(L, b) &:= \{\mathbf{r} = (x, \mathbf{y}) \mid x \in]d, d + b[, \mathbf{y} \in]-\frac{L}{2}, \frac{L}{2}[^2\}.\end{aligned}\quad (3.3)$$

The plasma A (B) is made of charges e_α (e_β) of species $\alpha \in S_A$ ($\beta \in S_B$) where S_A and S_B are index sets for the species in $\Lambda_A(L, a)$ and $\Lambda_B(L, b)$ respectively. We assume both plasmas to be globally neutral, *i.e.*, carrying no net charge,

$$\sum_a e_{\alpha_a} = \sum_b e_{\beta_b} = 0 \quad (3.4)$$

where \sum_a (\sum_b) extends on all particles in $\Lambda_A(L, a)$ ($\Lambda_B(L, b)$). For a particle located at \mathbf{r} we will use the generic notation $(\gamma \mathbf{r})$ where $\gamma \in S_A$ if $\mathbf{r} \in \Lambda_A(L, a)$ and $\gamma \in S_B$ if $\mathbf{r} \in \Lambda_B(L, b)$. The space external to the slabs is supposed to have no electrical properties, its dielectric constant being taken equal to that of vacuum. The charges are confined in the slabs by hard walls that merely limit the available configuration space to the regions (3.3).

All particles interact via the two-body potential

$$V(\gamma, \gamma', |\mathbf{r} - \mathbf{r}'|) = e_\gamma e_{\gamma'} v(\mathbf{r} - \mathbf{r}') + v_{\text{SR}}(\gamma, \gamma', |\mathbf{r} - \mathbf{r}'|), \quad (3.5)$$

where $v(\mathbf{r} - \mathbf{r}') = 1/|\mathbf{r} - \mathbf{r}'|$ is the Coulomb potential (in Gaussian units) and $v_{\text{SR}}(\gamma, \gamma', \mathbf{r} - \mathbf{r}')$ is a short-range repulsive potential to prevent the collapse of opposite charges and guarantee the thermodynamic stability of the system.

The total potential energy U consists in the sum of all pairwise interactions, separated into three contributions according to whether they take place between two particles of A , of B , or between a particle of A and a particle of B :

$$U = U_A + U_B + U_{AB}. \quad (3.6)$$

On the microscopic level, the force between configurations of charges in the two plasmas is the sum of all pairwise forces exerted by the particles of B on the particles of A :

$$\begin{aligned}\mathbf{F}_{\Lambda_B \rightarrow \Lambda_A} &:= \sum_a \sum_b \left[e_{\alpha_a} e_{\beta_b} \frac{\mathbf{r}_a - \mathbf{r}_b}{|\mathbf{r}_a - \mathbf{r}_b|^3} + \mathbf{F}_{\text{SR}}(\alpha_a, \beta_b, \mathbf{r}_a - \mathbf{r}_b) \right] \\ \mathbf{r}_a &\in \Lambda_A(L, a), \quad \mathbf{r}_b \in \Lambda_B(L, b)\end{aligned}\quad (3.7)$$

and \mathbf{F}_{SR} is the force associated to the short-range potential v_{SR} . For simplicity we assume that the range of v_{SR} is finite so that $\mathbf{F}_{\text{SR}}(\alpha_a, \beta_b, \mathbf{r}_a - \mathbf{r}_b)$ vanishes as soon as d is large enough, and we will omit it in the following.

Both plasmas are supposed to be in thermal equilibrium at the same temperature T . The statistical average $\langle \cdots \rangle_L$ is defined in terms of the Gibbs weight $\exp(-\beta U)$, $\beta = (k_B T)^{-1}$, associated with the total energy (3.6). There is no need to explicitly specify the ensemble used here (canonical or grand canonical) provided that the global neutrality constraint (3.4) is taken into account. The average particle densities $\rho_L(\gamma \mathbf{r})$ are expressed as averages of the microscopic particle densities $\hat{\rho}(\gamma \mathbf{r}) = \sum_i \delta_{\gamma \gamma_i} \delta(\mathbf{r} - \mathbf{r}_i)$ where the sum runs over all particles

$$\rho_L(\gamma \mathbf{r}) = \langle \hat{\rho}(\gamma \mathbf{r}) \rangle_L. \quad (3.8)$$

We keep the index L to remember that averages are taken for the finite-volume slabs (3.3). Hence expressing the sums in (3.7) as integrals on particle densities $\hat{\rho}(\gamma \mathbf{r})$, the average force reads

$$\langle \mathbf{F} \rangle_L = \int_{\Lambda_A(L)} d\mathbf{r} \int_{\Lambda_B(L)} d\mathbf{r}' \frac{\mathbf{r} - \mathbf{r}'}{|\mathbf{r} - \mathbf{r}'|^3} c_L(\mathbf{r}, \mathbf{r}') \quad (3.9)$$

where $c_L(\mathbf{r}, \mathbf{r}')$ is the two-point charge correlation function

$$c_L(\mathbf{r}, \mathbf{r}') = \langle \hat{c}(\mathbf{r}) \hat{c}(\mathbf{r}') \rangle_L, \quad \hat{c}(\mathbf{r}) = \sum_{\gamma} e_{\gamma} \hat{\rho}(\gamma \mathbf{r}). \quad (3.10)$$

We now consider the average force by unit surface between two infinitely extended slabs at distance d by letting their transverse dimension L tend to infinity. We assume that the plasma phases are in fluid states homogeneous and isotropic in the \mathbf{y} directions, namely the charge correlation has an infinite-volume limit of the form

$$\lim_{L \rightarrow \infty} c_L(\mathbf{r}, \mathbf{r}') = \langle \hat{c}(\mathbf{r}) \hat{c}(\mathbf{r}') \rangle = c(x, x', |\mathbf{y} - \mathbf{y}'|). \quad (3.11)$$

For symmetry reasons, $\langle \mathbf{F} \rangle_L$ has no transverse component and is directed along the x axis perpendicular to the plates. We therefore consider the x -component of the force per unit surface

$$\begin{aligned} \langle f \rangle &:= \lim_{L \rightarrow \infty} \frac{\langle F_x \rangle_L}{L^2} = \lim_{L \rightarrow \infty} \frac{1}{L^2} \int_{L^2} d\mathbf{y} \left(\int_{-a}^0 dx \int_d^{d+b} dx' \int_{L^2} d\mathbf{y}' \frac{x - x'}{|\mathbf{r} - \mathbf{r}'|^3} c_L(x, \mathbf{y}, x', \mathbf{y}') \right) \\ &= \int_{-a}^0 dx \int_d^{d+b} dx' \int d\mathbf{y} \frac{x - x'}{[(x - x')^2 + |\mathbf{y}|^2]^{3/2}} c(x, x', |\mathbf{y}|). \end{aligned} \quad (3.12)$$

The last line results from the \mathbf{y} translational invariance of the integrand in the limit $L \rightarrow \infty$. We do not justify the existence of the limit here (which depends

on a uniform control of $c_L(x, \mathbf{y}, x', \mathbf{y}')$ as $|\mathbf{y} - \mathbf{y}'| \rightarrow \infty$, but it will be clear from the subsequent calculations that (3.12) is a well defined quantity, at least in the weak-coupling regime.

Formula (3.12) remains valid if one replaces $c(x, x', |\mathbf{y}|)$ by the truncated charge-charge correlation function

$$S(x, x', \mathbf{y}) = \langle \hat{c}(\mathbf{r}) \hat{c}(\mathbf{r}') \rangle - \langle \hat{c}(\mathbf{r}) \rangle \langle \hat{c}(\mathbf{r}') \rangle, \quad \mathbf{r} = (x, \mathbf{y}), \quad \mathbf{r}' = (x', \mathbf{0}) \quad (3.13)$$

with $\hat{c}(\mathbf{r})$ the microscopic charge density as in (3.10). Indeed, the \mathbf{y} -Fourier transform of the Coulomb force reads

$$\int d\mathbf{y} e^{-i\mathbf{k}\cdot\mathbf{y}} \frac{x - x'}{[(x - x')^2 + |\mathbf{y}|^2]^{3/2}} = 2\pi \operatorname{sign}(x - x') e^{-k|x-x'|} \quad (3.14)$$

and reduces to -2π when $\mathbf{k} = \mathbf{0}$ and $x < x'$. This implies that the charge density profile $\langle \hat{c}(\mathbf{r}) \rangle = c(x)$ does not contribute to the force because of the global neutrality of both plasmas

$$\int_{-a}^0 dx c(x) = \int_d^{d+b} dx c(x) = 0. \quad (3.15)$$

To take full advantage of the translational invariance in the \mathbf{y} direction we represent the \mathbf{y} -integral in (3.12) in Fourier space:

$$\langle f \rangle = -\frac{1}{2\pi} \int_{-a}^0 dx \int_d^{d+b} dx' \int d\mathbf{k} e^{-k|x-x'|} S(x, x', \mathbf{k}), \quad (3.16)$$

where $k = |\mathbf{k}|$ and $S(x, x', \mathbf{k}) = \int d\mathbf{y} e^{-i\mathbf{k}\cdot\mathbf{y}} S(x, x', \mathbf{y})$. The dependence of $\langle f \rangle = \langle f \rangle(d)$ on the separation d between the two slabs occurs in the integration limits in (3.16) as well as in the charge correlation function $S(x, x', \mathbf{k})$. The d dependence of the correlations between the two slabs A and B originates itself from the Coulomb interaction term U_{AB} occurring in the total Gibbs thermal weight. The object of the next sections is to determine the asymptotic behaviour of $\langle f \rangle(d)$ as $d \rightarrow \infty$.

3.3 Mayer series for inhomogeneous charged fluids

We briefly summarise the methods that we use to calculate the charge-charge correlation function of our system. Let us consider a general charged fluid in presence of spatial inhomogeneities caused by an external potential $\Psi^{\text{ext}}(\gamma \mathbf{r})$, e.g. wall potentials confining the system in some region of space. Hard walls without electrical properties (infinite potentials) can be implemented by simply declaring that the density vanishes in the forbidden regions.

It is well-known (e.g. (Hansen & McDonald, 1986)) that the two-point Ursell function, related to the densities $\rho(\mathbf{i}), \rho(\mathbf{j})$ and the two-particle density $\rho(\mathbf{i}, \mathbf{j})$

$$h(\mathbf{i}, \mathbf{j}) := \frac{\rho(\mathbf{i}, \mathbf{j})}{\rho(\mathbf{i})\rho(\mathbf{j})} - 1, \quad (3.17)$$

can be expanded in a formal power series of the densities by means of Mayer graphs. The basic Mayer bonds are

$$f(\mathbf{i}, \mathbf{j}) = e^{-\beta V(\mathbf{i}, \mathbf{j})} - 1 \quad (3.18)$$

where $V(\mathbf{i}, \mathbf{j})$ is the potential (3.5) and the weights at vertices are the densities $\rho(\mathbf{i})$. Here \mathbf{i} is a shorthand notation for the point $(\gamma_i \mathbf{r}_i)$ in configuration space, and integration on configurations $\sum_{\gamma_i} \int d\mathbf{r}_i$ includes the summation on particle species. Diagrams have two root points \mathbf{i} and \mathbf{j} and m internal points which have to be integrated over. Each pair of points is linked by at most one f -bond and there are no articulation points.³ Because of the long-range of Coulomb interaction, the integrals occurring in every diagram diverge in the thermodynamic limit. It is therefore necessary to introduce the screened mean-field potential $\Phi(\mathbf{r}_i, \mathbf{r}_j)$ as usual by resumming the chains built with pure Coulombic interaction bonds $-\beta e_{\gamma_i} e_{\gamma_j} v(\mathbf{r}_i - \mathbf{r}_j)$. Then replacing the bare Coulomb potential by the screened potential leads to a reorganisation of the diagrammatic expansion of the Ursell function resulting in the formula (Aqua & Cornu, 2003)

$$h(\gamma \mathbf{r}, \gamma' \mathbf{r}') = \sum_{\Pi} \frac{1}{S_{\Pi}} \sum_{\gamma_1, \dots, \gamma_m} \int d\mathbf{r}_1 \cdots d\mathbf{r}_m \rho(\gamma_1 \mathbf{r}_1) \cdots \rho(\gamma_m \mathbf{r}_m) \prod_{\{\mathbf{i}, \mathbf{j}\} \in \Pi} \mathcal{F}(\mathbf{i}, \mathbf{j}) \quad (3.19)$$

The first sum runs over all unlabelled topologically different connected diagrams Π (called prototype graphs) with two root points $(\gamma \mathbf{r})$ and $(\gamma' \mathbf{r}')$ and m integrated internal points with density weights (m ranges from 0 to ∞); S_{Π} denotes the symmetry number of a diagram Π . Each pair of points is linked by at most one bond $\mathcal{F} \in \{F, F^R\}$ and there are no articulation points. Moreover, convolutions of F bonds are forbidden to avoid multiple counting of original Mayer graphs. The two possible bonds read

$$F(\mathbf{i}, \mathbf{j}) = -\beta e_{\gamma_i} e_{\gamma_j} \Phi(\mathbf{r}_i, \mathbf{r}_j) \quad (3.20)$$

$$F^R(\mathbf{i}, \mathbf{j}) = \exp[-\beta e_{\gamma_i} e_{\gamma_j} \Phi(\mathbf{r}_i, \mathbf{r}_j) - \beta v_{SR}(\gamma_i, \gamma_j, |\mathbf{r}_i - \mathbf{r}_j|)] - 1 + \beta e_{\gamma_i} e_{\gamma_j} \Phi(\mathbf{r}_i, \mathbf{r}_j). \quad (3.21)$$

³An articulation point, when removed, splits the diagram into two pieces, at least one of which is disconnected from the root points.

These bonds are obtained in terms of the Debye-Hückel screened potential Φ , which is symmetric and defined as the solution of the integral equation

$$\Phi(\mathbf{r}, \mathbf{r}') = v(\mathbf{r} - \mathbf{r}') - \frac{1}{4\pi} \int d\mathbf{r}_1 \kappa^2(\mathbf{r}_1) v(\mathbf{r} - \mathbf{r}_1) \Phi(\mathbf{r}_1, \mathbf{r}') = \Phi(\mathbf{r}', \mathbf{r}) \quad (3.22)$$

or equivalently of the differential equation

$$\Delta\Phi(\mathbf{r}, \mathbf{r}') - \kappa^2(\mathbf{r})\Phi(\mathbf{r}, \mathbf{r}') = -4\pi\delta(\mathbf{r} - \mathbf{r}') \quad (3.23)$$

supplemented by suitable boundary conditions. In (3.22) and (3.23)

$$\kappa(\mathbf{r}) := \left(4\pi\beta \sum_{\gamma} e_{\gamma}^2 \rho(\gamma \mathbf{r}) \right)^{1/2} \quad (3.24)$$

can be interpreted as the local inverse Debye screening length in the inhomogeneous system. The bond $F^R(\mathbf{i}, \mathbf{j})$ includes the short-range contribution and the nonlinear Coulombic part of the original Mayer bond.

The densities $\rho(\gamma \mathbf{r})$ entering in (3.19) and (3.24) have to be determined self-consistently from the first equation of the Born-Green-Yvon hierarchy which links the one-point and the two-point functions. For charged systems, it takes the form (Martin, 1988)

$$\begin{aligned} \nabla\rho(\gamma \mathbf{r}) = & -\beta e_{\gamma}\rho(\gamma \mathbf{r}) \left[\nabla\Psi(\gamma \mathbf{r}) + \int d\mathbf{r}' \left(\sum_{\gamma'} e_{\gamma'}\rho(\gamma' \mathbf{r}') h(\gamma \mathbf{r}, \gamma' \mathbf{r}') \right) \nabla v(\mathbf{r} - \mathbf{r}') \right] \\ & -\beta \sum_{\gamma'} \int d\mathbf{r}' \rho(\gamma \mathbf{r}, \gamma' \mathbf{r}') \nabla v_{\text{SR}}(\gamma, \gamma', |\mathbf{r} - \mathbf{r}'|) \end{aligned} \quad (3.25)$$

where

$$\Psi(\gamma \mathbf{r}) = \Psi^{\text{ext}}(\gamma \mathbf{r}) + \int d\mathbf{r}' c(\mathbf{r}') v(\mathbf{r} - \mathbf{r}') \quad (3.26)$$

is the sum of the external potential and the electrostatic potential caused by the inhomogeneous mean charge density $c(\mathbf{r}')$ in the system. Hence the Ursell function (considered as a functional of the densities through its Mayer expansion (3.19)) together with (3.25) form a closed set of equations whose solution determines in principle the exact densities and two-particle correlations. The differential equation (3.25) has still to be supplemented with appropriate boundary conditions. For instance if the system is asymptotically uniform in some directions, one can fix the corresponding asymptotic bulk densities.

Finally, the charge-charge correlation function (3.13) is related to the Ursell function by

$$S(\mathbf{r}, \mathbf{r}') = \sum_{\gamma, \gamma'} e_\gamma e_{\gamma'} \rho(\gamma \mathbf{r}) \rho(\gamma' \mathbf{r}') h(\gamma \mathbf{r}, \gamma' \mathbf{r}') + \delta(\mathbf{r} - \mathbf{r}') \sum_{\gamma} e_\gamma^2 \rho(\gamma \mathbf{r}) \quad (3.27)$$

The second term in the right hand side of (3.27) is the contribution of coincident points.

We shall use the above formalism to calculate (3.27) as a function of the distance d for two infinitely thick plasmas (i.e $a \rightarrow \infty$ and $b \rightarrow \infty$ in (3.16)) and with hard walls at $x = 0$ and $x = d$. In this situation we take $\Psi^{\text{ext}}(\gamma \mathbf{r}) = 0$ for $x < 0$ and $x > d$, and impose

$$\begin{aligned} \rho(\gamma x) &= 0, \quad 0 \leq x \leq d, \\ \lim_{x \rightarrow -\infty} \rho(\gamma x) &= \rho_{A\gamma}, \quad \lim_{x \rightarrow \infty} \rho(\gamma x) = \rho_{B\gamma} \end{aligned} \quad (3.28)$$

where $\rho_{A\gamma}$ and $\rho_{B\gamma}$ are the bulk particle densities of plasmas A and B . The contribution of coincident points does not enter into the force (3.16) since \mathbf{r} and \mathbf{r}' are always at least separated by the distance d . Therefore, (3.16) reads

$$\langle f \rangle = - \int_{-\infty}^0 dx \int_d^{\infty} dx' \int_0^{\infty} dk k e^{-k|x-x'|} \sum_{\gamma, \gamma'} e_\gamma e_{\gamma'} \rho(\gamma x) \rho(\gamma' x') h(\gamma x, \gamma' x', \mathbf{k}) \quad (3.29)$$

with $h(\gamma x, \gamma' x', \mathbf{k})$ the \mathbf{y} -Fourier transform of the Ursell function.

3.4 Debye-Hückel theory

In this section we show that the simplest contribution to $h(\gamma \mathbf{r}, \gamma' \mathbf{r}')$ given by the sole bond F , namely,

$$h^{\text{DH}}(\gamma \mathbf{r}, \gamma' \mathbf{r}') = -\beta e_\gamma e_{\gamma'} \Phi(\mathbf{r}, \mathbf{r}') \quad (3.30)$$

already leads to the asymptotic value (3.2) of the force. For this we have to find the screened potential by solving (3.23) (written in Fourier form) with the boundary conditions imposed by the slab geometries

$$\left[\frac{\partial^2}{\partial x^2} - k^2 - \kappa^2(x) \right] \Phi(x, x', \mathbf{k}) = -4\pi \delta(x - x'), \quad \kappa(x) = 0, \quad 0 < x < d, \quad (3.31)$$

with $\Phi(x, x', \mathbf{k}) = \int d\mathbf{y} e^{-i\mathbf{k} \cdot \mathbf{y}} \Phi(x, x', \mathbf{y})$. The boundary conditions are $\Phi(x, x', \mathbf{k})$ and $\partial \Phi(x, x', \mathbf{k}) / \partial x$ continuous at $x = 0$ and $x = d$, and $\lim_{x \rightarrow \pm\infty} \Phi(x, x', \mathbf{k}) = 0$. The density profiles entering in $\kappa^2(x)$ by (3.24) are not known (since they have to be determined by self-consistency from (3.25)), but we will not need their explicit form in the sequel.⁴ We only need to assume that their difference to bulk value is

⁴A mean-field approximation to the densities could be obtained by replacing h in (3.25) by h^{DH} . We are not doing so here but deal throughout with the exact densities.

integrable:

$$\begin{aligned}\rho(\gamma x) - \rho_{A\gamma} &= O\left(\frac{1}{|x|^{1+\epsilon}}\right), \quad x \rightarrow -\infty, \\ \rho(\gamma x) - \rho_{B\gamma} &= O\left(\frac{1}{|x|^{1+\epsilon}}\right), \quad x \rightarrow \infty, \quad \epsilon > 0.\end{aligned}\quad (3.32)$$

Integrating (3.31) on x leads to

$$\int_{-\infty}^{\infty} dx \frac{\kappa^2(x)}{4\pi} \Phi(x, x', \mathbf{k}) = 1 - \frac{k^2}{4\pi} \int dx \Phi(x, x', \mathbf{k}). \quad (3.33)$$

In particular, for $\mathbf{k} = \mathbf{0}$

$$\int_{-\infty}^{\infty} dx \frac{\kappa^2(x)}{4\pi} \Phi(x, x', \mathbf{k} = \mathbf{0}) = 1 \quad (3.34)$$

which is nothing else than the electroneutrality sum rule for the charge-charge correlation (3.13), (3.27) within the Debye regime (3.30) (Martin, 1988):

$$\int_{-\infty}^{\infty} dx \int dy S^{DH}(x, x', \mathbf{y}) = 0 \quad (3.35)$$

To solve (3.31) we first consider the simpler problem with piecewise-flat densities $\rho_{A\gamma}$ and $\rho_{B\gamma}$ in each plasma

$$\begin{aligned}\left[\frac{\partial^2}{\partial x^2} - k^2 - \bar{\kappa}^2(x) \right] \varphi(x, x', \mathbf{k}) &= -4\pi\delta(x - x') \\ \bar{\kappa}(x) = \kappa_A, \quad x < 0, \quad \bar{\kappa}(x) = 0, \quad 0 < x < d, \quad \bar{\kappa}(x) = \kappa_B, \quad x > d\end{aligned}\quad (3.36)$$

where

$$\kappa_A = \left(4\pi\beta \sum_{\alpha \in S_A} e_\alpha^2 \rho_{A\alpha} \right)^{1/2}, \quad \kappa_B = \left(4\pi\beta \sum_{\beta \in S_B} e_\beta^2 \rho_{B\beta} \right)^{1/2} \quad (3.37)$$

are the bulk inverse screening lengths. The boundary conditions are the same as for (3.31). Denoting by \mathcal{L} the linear operator acting on Φ on the left hand side of (3.31) and by $\bar{\mathcal{L}}$ the one acting similarly on φ , one has $\mathcal{L}\Phi(x) - \bar{\mathcal{L}}\varphi(x) = \bar{\mathcal{L}}(\Phi - \varphi)(x) - u(x)\Phi(x) = 0$, where $u(x) = \kappa^2(x) - \bar{\kappa}^2(x)$ represents the deviation of the density profiles to their bulk limiting values. Since $-\varphi/4\pi$ is the Green function of $\bar{\mathcal{L}}$, it follows that $\Phi(x, x', \mathbf{k})$ and $\varphi(x, x', \mathbf{k})$ are related by the integral equation

$$\Phi(x, x', \mathbf{k}) = \varphi(x, x', \mathbf{k}) - \frac{1}{4\pi} \int ds u(s) \varphi(x, s, \mathbf{k}) \Phi(s, x', \mathbf{k}) \quad (3.38)$$

which expresses $\Phi(x, x', \mathbf{k})$ as a perturbation of $\varphi(x, x', \mathbf{k})$ by the inhomogeneity $u(x)$ of the plasmas' density profiles.

Solving (3.36) piecewise and connecting the solutions together yields⁵

$$\varphi(x, x', \mathbf{k}) = \begin{cases} \varphi_{AA}(x, x', \mathbf{k}), & x, x' < 0, \\ \varphi_{AB}(x, x' - d, \mathbf{k}), & x < 0 < d < x', \\ \varphi_{BB}(x - d, x' - d, \mathbf{k}), & d < x, x', \end{cases} \quad (3.39)$$

with

$$\varphi_{AA}(x, x', \mathbf{k}) = 2\pi \frac{e^{-k_A|x-x'|}}{k_A} + 2\pi \frac{e^{-k_A|x+x'|}}{k_A} \frac{(k_A-k)(k_B+k)e^{kd} - (k_A+k)(k_B-k)e^{-kd}}{(k_A+k)(k_B+k)e^{kd} - (k_A-k)(k_B-k)e^{-kd}}, \quad (3.40)$$

$$\varphi_{AB}(x, x', \mathbf{k}) = \frac{8\pi k e^{-k_A|x|} e^{-k_B|x'|}}{(k_A+k)(k_B+k)e^{kd} - (k_A-k)(k_B-k)e^{-kd}}, \quad (3.41)$$

$$k_A = \sqrt{k^2 + \kappa_A^2}, \quad k_B = \sqrt{k^2 + \kappa_B^2}. \quad (3.42)$$

The function $\varphi_{BB}(x, x', \mathbf{k})$ is obtained by interchanging the indices A and B in (3.40). Notice that $\varphi(x, x', \mathbf{k}) = \varphi(x', x, \mathbf{k})$ and is invariant under the symmetry $x \leftrightarrow d - x, x' \leftrightarrow d - x', A \leftrightarrow B$.

We discuss a few properties of this solution. The first term in the right hand side of (3.40) corresponds to the bulk Debye-Hückel potential whereas the second term is the modification due to the finite boundaries of both plasmas A and B . As $d \rightarrow \infty$, $\varphi_{AA}(x, x', \mathbf{k})$ reduces to the well-known Debye-Hückel potential $\varphi_A^0(x, x', \mathbf{k})$ of a single semi-infinite plasma in the region $x < 0$ (see Form. (24) in (Guernsey, 1970), and (Jancovici, 1982))

$$\lim_{d \rightarrow \infty} \varphi_{AA}(x, x', \mathbf{k}) = 2\pi \frac{e^{-k_A|x-x'|}}{k_A} + 2\pi \frac{k_A - k}{k_A + k} \frac{e^{-k_A|x+x'|}}{k_A} = \varphi_A^0(x, x', \mathbf{k}) \quad (3.43)$$

uniformly with respect to \mathbf{k} . One observes that $\varphi(x, x', \mathbf{k})$ is an even, infinitely differentiable function of $|\mathbf{k}|$, implying that $\varphi(x, x', \mathbf{y})$ decays along walls directions faster than any inverse power of y . This is to be contrasted with the small \mathbf{k} behaviour of the function (3.43) which has a non analytic $|\mathbf{k}|$ term leading to the algebraic decay y^{-3} along the wall (Jancovici, 1982); see also (Martin, 1988, Sec. III.C.2).

⁵The functions $\varphi_{AB}, \varphi_{BB}$ (depending on d) refer to the system of the two plasmas under mutual influence with the x -location of particles in plasma B measured by their distance from the boundary at d (*i.e.*, from 0 to $+\infty$). In the sequel, the quantities φ_A^0, φ_B^0 (independent of d) refer similarly to the single semi-infinite plasma A and B . [See also Figure 2.4 and the notations of Section 2.5.1.]

The function $\varphi_{AB}(x, x', \mathbf{k})$ (3.41) describes the correlation between the two plasmas. In terms of the scaled dimensionless variable $\mathbf{q} = \mathbf{k}d$, it has the simple factorized asymptotic behaviour

$$\begin{aligned}\varphi_{AB}(x, x', \frac{\mathbf{q}}{d}) &\sim \frac{1}{d} \frac{4\pi q}{\kappa_A \kappa_B \sinh q} e^{-\kappa_A |x|} e^{-\kappa_B |x'|} \\ &= \frac{1}{d} \frac{q}{4\pi \sinh q} \varphi_A^0(x, 0, \mathbf{0}) \varphi_B^0(0, x', \mathbf{0}), \quad d \rightarrow \infty\end{aligned}\quad (3.44)$$

Finally $\varphi(x, x', \mathbf{k})$ obeys the following bound uniformly with respect to \mathbf{k} and d (appendix 3.B)

$$0 \leq \varphi(x, x', \mathbf{k}) \leq \varphi^>(x, x') \leq \frac{4\pi}{\kappa}, \quad \kappa d \geq 1 \quad (3.45)$$

The function $\varphi^>(x, x')$ is defined as in (3.39) with φ_{AA} , φ_{AB} and φ_{BB} replaced by

$$\varphi_{AA}^>(x, x') \doteq \varphi_{BB}^>(x, x') \doteq \frac{2\pi}{\kappa} \left(e^{-\kappa|x-x'|} + e^{-\kappa|x+x'|} \right) \quad (3.46)$$

$$\varphi_{AB}^>(x, x') \doteq \varphi_{BA}^>(x, x') \doteq \frac{4\pi}{\kappa^2 d} e^{-\kappa|x|} e^{-\kappa|x'|}, \quad \kappa := \min\{\kappa_A, \kappa_B\} \quad (3.47)$$

The Debye-Hückel potential $\Phi(x, x', \mathbf{k})$ can be obtained by iterating the integral equation (3.38). Convergence can be established in the weak-coupling regime:

Lemma (see proof in appendix 3.B)

Let

$$r := \frac{1}{\kappa} \int_{-\infty}^{\infty} dx |u(x)| = \frac{1}{\kappa} \int_{-\infty}^{\infty} dx |\kappa^2(x) - \bar{\kappa}^2(x)| \quad (3.48)$$

Then for $r < 1$ (3.38) has a solution with the bound

$$|\Phi(x, x', \mathbf{k})| \leq \frac{1}{1-r} \varphi^>(x, x'). \quad (3.49)$$

As in (3.39) we distinguish various contributions according to the location of the arguments x, x' of $\Phi(x, x', \mathbf{k})$ by setting (see footnote 5)

$$\Phi(x, x', \mathbf{k}) = \begin{cases} \Phi_{AA}(x, x', \mathbf{k}), & x, x' < 0, \\ \Phi_{AB}(x, x' - d, \mathbf{k}), & x < 0 < d < x', \\ \Phi_{BB}(x - d, x' - d, \mathbf{k}), & d < x, x', \end{cases} \quad (3.50)$$

$$\rho(\gamma x) = \begin{cases} \rho_A(\gamma x), & x < 0, \\ \rho_B(\gamma, x - d), & x > d. \end{cases} \quad (3.51)$$

The quantities $\kappa_{A,B}(x)$, $u_{A,B}(x)$ are defined in the same way. Then the integral equation (3.38) splits into

$$\begin{aligned} \Phi_{AA}(x, x', \mathbf{k}) &= \varphi_{AA}(x, x', \mathbf{k}) - \frac{1}{4\pi} \int_{-\infty}^0 ds u_A(s) \varphi_{AA}(x, s, \mathbf{k}) \Phi_{AA}(s, x', \mathbf{k}) \\ &\quad - \frac{1}{4\pi} \int_0^{\infty} ds u_B(s) \varphi_{AB}(x, s, \mathbf{k}) \Phi_{BA}(s, x', \mathbf{k}). \end{aligned} \quad (3.52)$$

$$\begin{aligned} \Phi_{AB}(x, x', \mathbf{k}) &= \varphi_{AB}(x, x', \mathbf{k}) - \frac{1}{4\pi} \int_{-\infty}^0 ds u_A(s) \varphi_{AA}(x, s, \mathbf{k}) \Phi_{AB}(s, x', \mathbf{k}) \\ &\quad - \frac{1}{4\pi} \int_0^{\infty} ds u_B(s) \varphi_{AB}(x, s, \mathbf{k}) \Phi_{BB}(s, x', \mathbf{k}). \end{aligned} \quad (3.53)$$

The density profiles depend on d because of the mutual Coulomb interactions between the two plasmas. We shall examine the asymptotic behaviour of $\Phi(x, x', \mathbf{k})$ as $d \rightarrow \infty$ under the assumption that these density profiles are uniformly bounded with respect to d and tend to those of single semi-infinite plasmas, *i.e.*,

$$\lim_{d \rightarrow \infty} \rho_A(\gamma x) = \rho_A^0(\gamma x), \quad x < 0, \quad \lim_{d \rightarrow \infty} \rho_B(\gamma x) = \rho_B^0(\gamma x), \quad x > 0 \quad (3.54)$$

We denote by $\kappa_{A,B}^0(x)$, $u_{A,B}^0(x)$ the analogous quantities for the single semi-infinite plasmas. Then one concludes from (3.52) that uniformly in \mathbf{k}

$$\lim_{d \rightarrow \infty} \Phi_{AA}(x, x', \mathbf{k}) = \Phi_A^0(x, x', \mathbf{k}), \quad x, x' < 0 \quad (3.55)$$

where $\Phi_A^0(x, x', \mathbf{k})$ is the Debye-Hückel potential of a semi-infinite plasma in the region $x < 0$ determined in terms of the corresponding flat profile potential $\varphi_A^0(x, x', \mathbf{k})$ (3.43) by

$$\Phi_A^0(x, x', \mathbf{k}) = \varphi_A^0(x, x', \mathbf{k}) - \frac{1}{4\pi} \int_{-\infty}^0 ds u_A^0(s) \varphi_A^0(x, s, \mathbf{k}) \Phi_A^0(s, x', \mathbf{k}), \quad x, x' < 0 \quad (3.56)$$

Indeed, in view of the limits (3.43), (3.54) and using dominated convergence with the bounds (3.45), (3.49) the integral equation (3.52) reduces to (3.56) in the limit $d \rightarrow \infty$. One has likewise

$$\lim_{d \rightarrow \infty} \Phi_{BB}(x, x', \mathbf{k}) = \Phi_B^0(x, x', \mathbf{k}), \quad x, x' > 0 \quad (3.57)$$

where $\Phi_B^0(x, x', \mathbf{k})$ is the Debye-Hückel potential of a semi-infinite plasma in the region $x > 0$.

We come now to the correlation $\Phi_{AB}(x, x', \frac{q}{d})$ which is expected to decay as d^{-1} at large separation of the two plasmas. To see this it is useful to write (3.53) in an alternative form such that φ_{AB} appears explicitly in each term of the equation:

$$\begin{aligned} \Phi_{AB}(x, x', \mathbf{k}) &= \varphi_{AB}(x, x', \mathbf{k}) \\ &- \frac{1}{4\pi} \int_{-\infty}^0 ds u_A(s) \widetilde{\Phi}_{AA}(x, s, \mathbf{k}) \varphi_{AB}(s, x', \mathbf{k}) - \frac{1}{4\pi} \int_0^{\infty} ds u_B(s) \varphi_{AB}(x, s, \mathbf{k}) \Phi_{BB}(s, x', \mathbf{k}) \\ &+ \left(\frac{1}{4\pi}\right)^2 \int_{-\infty}^0 ds_1 \int_0^{\infty} ds_2 u_A(s_1) u_B(s_2) \widetilde{\Phi}_{AA}(x, s_1, \mathbf{k}) \varphi_{AB}(s_1, s_2, \mathbf{k}) \Phi_{BB}(s_2, x', \mathbf{k}). \end{aligned} \quad (3.58)$$

Here $\widetilde{\Phi}_{AA}(x, x', \mathbf{k})$ verifies the equation

$$\widetilde{\Phi}_{AA}(x, x', \mathbf{k}) = \varphi_{AA}(x, x', \mathbf{k}) - \frac{1}{4\pi} \int_{-\infty}^0 ds u_A(s) \varphi_{AA}(x, s, \mathbf{k}) \widetilde{\Phi}_{AA}(s, x', \mathbf{k}), \quad (3.59)$$

which is the equation (3.52) with the last term omitted. Equation (3.58) is obtained by iterating (3.53) and resumming the φ_{AA} chains to $\widetilde{\Phi}_{AA}$, or by verifying that it satisfies the basic differential equation (3.31). By the same arguments that led to (3.55), it is clear that $\widetilde{\Phi}_{AA}$ also tends to the potential Φ_A^0 of the semi-infinite plasma.

Introducing the limits (3.44), (3.54), (3.55), (3.57) in (3.58) and using again dominated convergence provided by the bounds (3.47), (3.46), (3.49) we find that

$$\begin{aligned} \lim_{d \rightarrow \infty} d \Phi_{AB}(x, x', \frac{q}{d}) &= \frac{q}{4\pi \sinh q} \\ &\times \left[\varphi_A^0(x, 0, \mathbf{0}) - \frac{1}{4\pi} \int_{-\infty}^0 ds u_A^0(s) \Phi_A^0(x, s, \mathbf{0}) \varphi_A^0(s, 0, \mathbf{0}) \right] \\ &\times \left[\varphi_B^0(0, x', \mathbf{0}) - \frac{1}{4\pi} \int_0^{\infty} ds u_B^0(s) \varphi_B^0(0, s, \mathbf{0}) \Phi_B^0(s, x', \mathbf{0}) \right] \\ &= \frac{q}{4\pi \sinh q} \Phi_A^0(x, 0, \mathbf{0}) \Phi_B^0(0, x', \mathbf{0}) \end{aligned} \quad (3.60)$$

As in (3.44), the limit factorizes into the product of Debye-Hückel potentials for single semi-infinite plasmas evaluated with one point on the boundary. The last line of (3.60) follows from (3.56), the corresponding equation for $\Phi_B^0(x, x', \mathbf{0})$, and the fact that these functions are symmetric in x, x' .

With this result we can determine the leading term in the asymptotic behaviour

of the force (3.16) in the Debye-Hückel regime. From (3.29) and (3.30), one has

$$\begin{aligned} \langle f \rangle^{\text{DH}}(d) &= \frac{1}{\beta} \int_{-\infty}^0 dx \int_d^{\infty} dx' \int_0^{\infty} dk k e^{-k|x-x'|} \frac{\kappa^2(x)}{4\pi} \frac{\kappa^2(x')}{4\pi} \Phi(x, x', \mathbf{k}) \\ &= \frac{1}{\beta d^2} \int_{-\infty}^0 dx \int_0^{\infty} dx' \int_0^{\infty} dq q e^{-\frac{q}{d}|x-x'+d|} \frac{\kappa_A^2(x)}{4\pi} \frac{\kappa_B^2(x')}{4\pi} \Phi_{AB}(x, x', \frac{\mathbf{q}}{d}) \end{aligned} \quad (3.61)$$

To obtain the second line we have set $\mathbf{k}d = \mathbf{q}$, shifted the x' -integration by $-d$, and introduced the notation (3.50),(3.51). As $d \rightarrow \infty$, one can use (3.60) and the bounds (3.46), (3.49) to conclude again by dominated convergence that

$$\begin{aligned} \lim_{d \rightarrow \infty} d^3 \langle f \rangle^{\text{DH}}(d) &= \frac{1}{8\pi\beta} \int_0^{\infty} dq \frac{4q^2 e^{-q}}{e^q - e^{-q}} \left(\int_{-\infty}^0 dx \frac{(\kappa_A^0)^2(x)}{4\pi} \Phi_A^0(x, 0, \mathbf{0}) \right) \\ &\quad \times \left(\int_0^{\infty} dx' \frac{(\kappa_B^0)^2(x')}{4\pi} \Phi_B^0(0, x', \mathbf{0}) \right) = \frac{\zeta(3)}{8\pi\beta} \end{aligned} \quad (3.62)$$

Indeed, because of the charge sum rules (3.34) for the semi-infinite plasmas, both parentheses are equal to 1, whereas the q integral yields the value $\zeta(3)$ where ζ is the Riemann ζ -function.

3.5 Contributions of the other graphs

In this section we show that the single Debye-Hückel bond F saturates the asymptotic behaviour of the force, *i.e.*, taking into account the full set of other diagrams does not modify the result (3.62). For this we use the method of “dressing of the root points” that has been introduced in (Cornu, 1996) (see also (Brydges & Martin, 1999, Sec. VI.A.3)), to analyse the decay of the quantum truncated charge correlation function. Having singled out the contribution of the single resummed bond F , all remaining diagrams constituting $h(\gamma \mathbf{r}, \gamma' \mathbf{r}')$ can be classified into four types, depending on whether their root points are linked to the rest of the diagram by a single bond F or not.⁶ We thus write their sum in the form

$$h^{\text{R}} := h - F = h^{\text{cc}} + h^{\text{cn}} + h^{\text{nc}} + h^{\text{nn}}, \quad (3.63)$$

where h^{cc} stands for the contribution of all graphs that do begin and do end with an F bond (with anything in between), h^{cn} for the contribution of those that do begin but do not end with an F link, and so on. The latter quantities are obviously

⁶A point in a prototype diagram which is linked to the rest of the diagram by exactly one F bond is called a Coulomb point in (Cornu, 1996; Brydges & Martin, 1999).

related to h^{nn} by the following integral equations (notations are as in Section 3.3)

$$\begin{aligned} h^{\text{cn}}(\mathbf{a}, \mathbf{b}) &:= \int d\mathbf{1} F(\mathbf{a}, \mathbf{1}) \rho(\mathbf{1}) h^{\text{nn}}(\mathbf{1}, \mathbf{b}) \\ h^{\text{cc}}(\mathbf{a}, \mathbf{b}) &:= \int d\mathbf{1} \int d\mathbf{2} F(\mathbf{a}, \mathbf{1}) \rho(\mathbf{1}) h^{\text{nn}}(\mathbf{1}, \mathbf{2}) \rho(\mathbf{2}) F(\mathbf{2}, \mathbf{b}) \end{aligned} \quad (3.64)$$

and analogously for h^{nc} . Using these representations in (3.63) together with (3.20) and building the charge-charge correlation corresponding to h^{R} according to (3.27) yields

$$\begin{aligned} S^{\text{R}}(x, x', \mathbf{k}) &= \sum_{\gamma_1} \int dx_1 \sum_{\gamma_2} \int dx_2 \left(\delta(x - x_1) - \frac{\kappa^2(x)}{4\pi} \Phi(x, x_1, \mathbf{k}) \right) \\ &\times e_{\gamma_1} \rho(\gamma_1 x_1) h^{\text{nn}}(\gamma_1 x_1, \gamma_2 x_2, \mathbf{k}) e_{\gamma_2} \rho(\gamma_2 x_2) \left(\delta(x_2 - x') - \frac{\kappa^2(x')}{4\pi} \Phi(x_2, x', \mathbf{k}) \right). \end{aligned} \quad (3.65)$$

The function $h^{\text{nn}}(\gamma_1 x_1, \gamma_2 x_2, \mathbf{k})$ embodies a resummed contribution, not explicitly known at this point, of higher-order graphs. The only assumption needed on this function in the sequel is integrable clustering uniformly with respect to d

$$\int_{-\infty}^{\infty} dx_1 |h^{\text{nn}}(\gamma_1 x_1, \gamma_2 x_2, \frac{\mathbf{q}}{d})| < \infty \quad (3.66)$$

$$\int_{-\infty}^0 dx_1 \int_d^{\infty} dx_2 |h^{\text{nn}}(\gamma_1 x_1, \gamma_2 x_2, \frac{\mathbf{q}}{d})| < \infty \quad (3.67)$$

As a consequence of the bounds (3.45), (3.49) the condition (3.67) obviously holds for the Debye potential Φ , and it is expected to hold for the Ursell function on the ground that as $x_1 \rightarrow -\infty$ ($x_2 \rightarrow \infty$) $h^{\text{nn}}(\gamma_1 x_1, \gamma_2 x_2, \mathbf{k})$ has a fast decay in the bulk part of plasma A (plasma B). Note that integrating (3.65) on x (or x') at $\mathbf{k} = 0$ proves the validity of the charge sum rule for the exact charge-correlation function (see (3.35))

$$\int_{-\infty}^{\infty} dx \int dy S(x, x', \mathbf{y}) = 0, \quad S(x, x', \mathbf{y}) = S^{\text{DH}}(x, x', \mathbf{y}) + S^{\text{R}}(x, x', \mathbf{y}) \quad (3.68)$$

Proceeding as in (3.61) the contribution of $S^{\text{R}}(x, x', \mathbf{y})$ to the average force can be written in the form (permuting the x, x' and x_1, x_2 integrals)

$$\begin{aligned} \langle f \rangle^{\text{R}}(d) &= -\frac{1}{d^2} \int_0^{\infty} dq q \int dx_1 \int dx_2 H_1(x_1, \frac{\mathbf{q}}{d}) \\ &\times \sum_{\gamma_1, \gamma_2} e_{\gamma_1} e_{\gamma_2} \rho(\gamma_1 x_1) \rho(\gamma_2 x_2) h^{\text{nn}}(\gamma_1 x_1, \gamma_2 x_2, \frac{\mathbf{q}}{d}, d) H_2(x_2, \frac{\mathbf{q}}{d}) \end{aligned} \quad (3.69)$$

where

$$\begin{aligned} H_1(x_1, \frac{q}{d}) &= \int_{-\infty}^0 dx \left(\delta(x - x_1) - \frac{\kappa^2(x)}{4\pi} \Phi(x, x_1, \frac{q}{d}) \right) e^{\frac{q}{d}x} \\ H_2(x_2, \frac{q}{d}) &= \int_d^{\infty} dx' \left(\delta(x_2 - x') - \frac{\kappa^2(x')}{4\pi} \Phi(x_2, x', \frac{q}{d}) \right) e^{-\frac{q}{d}x'} \end{aligned} \quad (3.70)$$

The behaviour of $\langle f \rangle^R(d)$ as $d \rightarrow \infty$ is determined by that of the functions H_1 and H_2 , because $h^{\text{nn}}(\gamma_1 x_1, \gamma_2 x_2, \frac{q}{d}, d)$ does not vanish in the limit when the variables x_1 and x_2 are both located in the same plasma, but tends to the corresponding functions associated with a single semi-infinite plasma. Both H_1 and H_2 are $O(1/d)$ so that $\langle f \rangle^R(d) = O(1/d^4)$ does not contribute to the asymptotic behaviour of the force. More precisely, integrating (3.31) on x gives for $x_1 < 0$

$$\begin{aligned} \int_{-\infty}^0 dx \left(\delta(x - x_1) - \frac{\kappa^2(x)}{4\pi} \Phi(x, x_1, \mathbf{k}) \right) &= \int_d^{\infty} dx \frac{\kappa^2(x)}{4\pi} \Phi(x, x_1, \mathbf{k}) + \frac{k^2}{4\pi} \int dx \Phi(x, x_1, \mathbf{k}) \\ &= \int_0^{\infty} dx \frac{\kappa_B^2(x)}{4\pi} \Phi_{BA}(x, x_1, \mathbf{k}) + \frac{k^2}{4\pi} \int dx \Phi(x, x_1, \mathbf{k}) \end{aligned} \quad (3.71)$$

implying with (3.46), (3.49)

$$H_1(x_1, \frac{q}{d}) = O\left(\frac{1}{d}\right) + O\left(\frac{q^2}{d^2}\right), \quad x_1 < 0 \quad (3.72)$$

For $x_1 > d$ one has

$$H_1(x_1, \frac{q}{d}) = - \int_{-\infty}^0 dx e^{qx/d} \frac{\kappa^2(x)}{4\pi} \Phi(x, x_1, \frac{q}{d}) = O\left(\frac{1}{d}\right) e^{-\kappa_B(x_1-d)} \quad (3.73)$$

In the same way

$$\begin{aligned} H_2(x_2, \frac{q}{d}) &= O\left(\frac{e^{-q}}{d}\right) e^{-\kappa_A|x_2|}, \quad x_2 < 0, \\ H_2(x_2, \frac{q}{d}) &= O\left(\frac{e^{-q}}{d}\right) + O\left(\frac{q^2 e^{-q}}{d^2}\right), \quad x_2 > d \end{aligned} \quad (3.74)$$

(the factor e^{-q} comes from $e^{-qx/d} \leq e^{-q}$ for $x \geq d$ in (3.70)). Inserting these estimates in the four integration domains determined in (3.69) by $x_1, x_2 < 0$, $x_1, x_2 > d$ together with the integrability assumptions (3.66), (3.67) on h^{nn} leads to the result

$$\lim_{d \rightarrow \infty} d^3 \langle f \rangle(d) = \lim_{d \rightarrow \infty} d^3 \langle f \rangle^{\text{DH}}(d) + \lim_{d \rightarrow \infty} d^3 \langle f \rangle^R(d) = \frac{\zeta(3)}{8\pi\beta} \quad (3.75)$$

To conclude this section we present an alternative derivation of the result (3.75) by selecting the class of diagrams that give the dominant contribution to the Ursell function as $d \rightarrow \infty$. For this we decompose the bond $F(\gamma x, \gamma' x', \mathbf{k})$ (in Fourier representation) into the sum of four terms according to the location of the arguments x, x'

$$\begin{aligned}
 F &= F_{AA} + F_{AB} + F_{BA} + F_{BB} \\
 F_{AA}(\gamma x, \gamma' x', \mathbf{k}) &= \begin{cases} F(\gamma x, \gamma' x', \mathbf{k}), & x, x' < 0 \\ 0, & \text{otherwise} \end{cases} \\
 F_{AB}(\gamma x, \gamma' x', \mathbf{k}) &= \begin{cases} F(\gamma x, \gamma', x' + d, \mathbf{k}), & x < 0, x' > 0 \\ 0, & \text{otherwise} \end{cases} \quad (3.76)
 \end{aligned}$$

with F_{BA} and F_{BB} defined likewise and the similar decomposition for F^R (x -integrals in plasma B from now on run in the interval $[0, \infty)$, see footnote 5). The set of prototype graphs is then expanded in a larger set of graphs defined in terms of these bonds. It follows from (3.55) that F_{AA} and F_{AA}^R bonds have limits F_A^0 and F_A^{0R} as $d \rightarrow \infty$ where F_A^0 and F_A^{0R} are the bonds corresponding to the semi-infinite plasma A alone and likewise for BB bonds.

It is shown in appendix 3.C that the dominant part of the Ursell function $h_{AB}(\gamma_a \mathbf{r}_a, \gamma_b \mathbf{r}_b)$ as $d \rightarrow \infty$ is constituted by the set of graphs that have exactly one F_{AB} bond. This class is obtained by linking the extremity $\gamma_1 \mathbf{r}_1$ of $F_{AB}(\gamma_1 \mathbf{r}_1, \gamma_2 \mathbf{r}_2)$ to the root point $\gamma_a \mathbf{r}_a$ of $h_{AB}(\gamma_a \mathbf{r}_a, \gamma_b \mathbf{r}_b)$ in plasma Λ_A by all possible subgraphs comprising only AA bonds (otherwise one would introduce additional AB bonds), taking into account the excluded convolution rule for F bonds. In the same way the other extremity $\gamma_2 \mathbf{r}_2$ of $F_{AB}(\gamma_1 \mathbf{r}_1, \gamma_2 \mathbf{r}_2)$ is linked to the root point $\gamma_b \mathbf{r}_b$ in plasma Λ_B by all possible subgraphs made of BB bonds. One finds in this way

$$\begin{aligned}
 h_{AB}(a, b, \mathbf{k}) &\sim \int d1 \int d2 [\delta(a, 1) + (h_{AA}^m(a, 1, \mathbf{k}) + h_{AA}^{cn}(a, 1, \mathbf{k}))\rho_A(1)] \\
 &\quad \times F_{AB}(1, 2, \mathbf{k}) [\delta(2, b) + (h_{BB}^m(2, b, \mathbf{k}) + h_{BB}^{cn}(2, b, \mathbf{k}))\rho_B(2)] \quad (3.77)
 \end{aligned}$$

Here $a = (\gamma_a x_a)$, $1 = (\alpha_1 x_1)$, $2 = (\beta_2 x_2)$, $b = (\gamma_b x_b)$, and the integration $\int d1 = \sum_{\alpha_1} \int_{-\infty}^0 dx_1$ runs on plasma A and $\int d2 = \sum_{\beta_2} \int_0^{\infty} dx_2$ on plasma B . We have also used that the convolution of translation invariant functions in the \mathbf{y} -direction is the product of their Fourier transforms. The functions h_{AA}^{cn} and h_{AA}^m are defined as in (3.63) in terms of AA bonds (similarly for h_{BB}^{cn} and h_{BB}^m in terms of BB bonds). One can write (3.60) in the form

$$F_{AB}(1, 2, \frac{\mathbf{q}}{d}) \sim -\frac{q}{4\pi\beta d \sinh q} \frac{F_A^0(1, a_0, \mathbf{0})}{e_{\alpha_0}} \frac{F_B^0(b_0, 2, \mathbf{0})}{e_{\beta_0}}, \quad d \rightarrow \infty \quad (3.78)$$

where $a_0 = (\alpha_0 0)$ indexes a charge e_{α_0} located at the boundary $x_{a_0} = 0$ of Λ_A and b_0 indexes a charge e_{β_0} at the boundary of Λ_B . Taking also into account that the functions h_{AA}^{cn} and h_{AA}^{mn} approach the corresponding values $(h_A^0)^{cn}$ and $(h_A^0)^{mn}$ of a single semi-infinite plasma, one finds that the leading term $\sim 1/d$ of $h_{AB}(\gamma x, \gamma' x', \frac{\mathbf{q}}{d})$ factorizes as

$$h_{AB}(a, b, \frac{\mathbf{q}}{d}) \sim -\frac{q}{4\pi\beta d \sinh q} \frac{G_A^0(a, a_0)}{e_{\alpha_0}} \frac{G_B^0(b_0, b)}{e_{\beta_0}}, \quad d \rightarrow \infty \quad (3.79)$$

with

$$\begin{aligned} G_A^0(a, a_0) &= F_A^0(a, a_0) + \int d1 \left[(h_A^0)^{mn}(a, 1) + (h_A^0)^{cn}(a, 1) \right] \rho_A^0(1) F_A^0(1, a_0) \\ &= \left(F_A^0 + (h_A^0)^{nc} + (h_A^0)^{cc} \right) (a, a_0) \end{aligned} \quad (3.80)$$

In G_A^0 all functions are evaluated for the single semi-infinite plasma A at $\mathbf{k} = \mathbf{0}$ and \mathbf{k} has been omitted from the notation. The expression for G_B^0 is built in the same way. By the same calculation that led to (3.62) one finds now from (3.29) that

$$\lim_{d \rightarrow \infty} d^3 \langle f \rangle (d) = \frac{\zeta(3)}{8\pi\beta} \left(\frac{\int da e_{\alpha_a} \rho_A^0(a) G_A^0(a, a_0)}{e_{\alpha_0}} \right) \left(\frac{\int db e_{\beta_b} \rho_B^0(b) G_B^0(b_0, b)}{e_{\beta_0}} \right) \quad (3.81)$$

It remains to see that both parentheses are equal to -1 because of the electroneutrality sum rule in semi-infinite plasmas. Indeed, using (3.63) and (3.64), one recognizes from (3.80) that

$$G_A^0(a, a_0) = h_A^0(a, a_0) - \int d1 \left[F_A^0(a, 1) \rho_A^0(1) + \delta(a, 1) \right] (h_A^0)^{nm}(1, a_0). \quad (3.82)$$

The contribution to the force of the second term of (3.82) involves

$$\begin{aligned} &\int da e_{\alpha_a} \rho_A^0(a) \left[F_A^0(a, 1) \rho_A^0(1) + \delta(a, 1) \right] \\ &= e_{\alpha_1} \rho(\alpha_1 x_1) \left(1 - \frac{1}{4\pi} \int_{-\infty}^0 dx_a (\kappa_A^0)^2(x_a) \Phi_A^0(x_a, x_1, \mathbf{k} = \mathbf{0}) \right) = 0 \end{aligned} \quad (3.83)$$

which vanishes because of the sum rule (3.34) in the case of a semi-infinite plasma. The contribution of the first term of (3.82) is

$$\int da e_{\alpha_a} \rho_A^0(a) h_A^0(a, a_0) = \sum_{\alpha_a} \int_{-\infty}^0 dx_a e_{\alpha_a} \rho_A^0(\gamma_a x_a) h_A^0(\alpha_a x_a, \alpha_0 0, \mathbf{k} = \mathbf{0}) = -e_{\alpha_0} \quad (3.84)$$

The left-hand side is the total charge of the screening cloud induced in the semi-infinite plasma Λ_A by the boundary charge e_{α_0} , which equals $-e_{\alpha_0}$ because of perfect screening (Martin, 1988). By the same considerations the second parenthesis in (3.81) also equals -1 , hence the final result (3.75).

3.6 Plasma in front of a macroscopic dielectric medium

In this section we investigate the situation where plasma B is replaced by a semi-infinite macroscopic medium of homogeneous dielectric constant ϵ . The electrostatic potential $V(\mathbf{r}, \mathbf{r}')$ at \mathbf{r} created by a unit charge at $\mathbf{r}' \in \Lambda_A$ is the Green function of the Poisson equation with the conditions that the normal component of $\mathbf{D}(x) = \epsilon(x)\mathbf{E}(x)$, ($\epsilon(x) = \epsilon$, $x \geq d$, $\epsilon(x) = 1$, $x < d$) and the longitudinal component of $\mathbf{E}(x)$ are continuous at the interface (Jackson, 1998; Schwinger, DeRaad, Milton, & Tsai, 1998)

$$V(\mathbf{r}, \mathbf{r}') = \begin{cases} 1/|\mathbf{r} - \mathbf{r}'| + \Delta/|\mathbf{r} - \mathbf{r}'^*|, & x < d, & \Delta = (1 - \epsilon)/(1 + \epsilon) \\ \widetilde{\Delta}/|\mathbf{r} - \mathbf{r}'|, & x > d, & \widetilde{\Delta} = 2/(1 + \epsilon) \end{cases} \quad (3.85)$$

where $\mathbf{r}^* = (2d - x, \mathbf{y})$ is the point symmetric to \mathbf{r} with respect to the dielectric surface. The case of an ideal grounded conducting plate ($\epsilon = \infty$) is formally recovered when $\Delta = -1$, $\widetilde{\Delta} = 0$. In linear electrostatics, the total energy associated to a distribution of charges $\hat{c}(\mathbf{r})$ external to the dielectric is

$$\frac{1}{8\pi} \int d\mathbf{r} \mathbf{E}(\mathbf{r}) \cdot \mathbf{D}(\mathbf{r}) = \frac{1}{2} \int d\mathbf{r} \int d\mathbf{r}' \hat{c}(\mathbf{r}) V(\mathbf{r}, \mathbf{r}') \hat{c}(\mathbf{r}'). \quad (3.86)$$

For a configuration of charges $\{e_{\alpha_i}, \mathbf{r}_i\}$ in Λ_A , $\hat{c}(\mathbf{r}) = \sum_i e_{\alpha_i} \delta(\mathbf{r} - \mathbf{r}_i)$, one finds with (3.85) that the total energy can be written as

$$U = U_A + U_{AB}, \quad (3.87)$$

$$U_A = \sum_{\{i,j\}} \frac{e_{\alpha_i} e_{\alpha_j}}{|\mathbf{r}_i - \mathbf{r}_j|} + v_{\text{SR}}(\alpha_i, \alpha_j, |\mathbf{r}_i - \mathbf{r}_j|), \quad U_{AB} = \frac{\Delta}{2} \sum_{i=1}^N \sum_{j=1}^N \frac{e_{\alpha_i} e_{\alpha_j}}{|\mathbf{r}_i - \mathbf{r}_j^*|}.$$

where we have omitted the (infinite) self-energies of the particles and added a short-range repulsive potential for thermodynamic stability. As in (3.6), U_{AB} refers to the additional energy due to the presence of the dielectric at distance d . The total force exerted by the dielectric on the particles of A is obtained by differentiating U with respect to d

$$F_{B \rightarrow \Lambda_A} = \frac{\partial}{\partial d} U_{AB} = \Delta \sum_{i=1}^N \sum_{j=1}^N e_{\alpha_i} e_{\alpha_j} \frac{x_i - x_j^*}{|\mathbf{r}_i - \mathbf{r}_j^*|^{3/2}}. \quad (3.88)$$

It corresponds to the sum of all pairwise forces between charges in the plasma A and their image-charges Δe_{α_j} . Proceeding as in the derivation leading from (3.7)

to (3.16), the average force along the x direction per unit surface is given by

$$\begin{aligned} \langle f \rangle &= \lim_{L \rightarrow \infty} \frac{\langle F_{B \rightarrow \Lambda_A} \rangle_L}{L^2} = \Delta \int_{-\infty}^0 dx \int_{-\infty}^0 dx' \int dy \frac{x - x'^*}{|\mathbf{r} - \mathbf{r}'^*|^{3/2}} S(x, x', \mathbf{y}) \\ &= \frac{-\Delta}{d^2} \int_{-\infty}^0 dx \int_{-\infty}^0 dx' \int \frac{d\mathbf{q}}{(2\pi)^2} 2\pi e^{-\frac{q}{d}|x+x'|} e^{-2q} S(x, x', \frac{\mathbf{q}}{d}). \end{aligned} \quad (3.89)$$

To obtain the second line we have introduced the Fourier transform (3.14), used $x'^* = 2d - x'$, and set $\mathbf{k} = \mathbf{q}/d$. $S(x, x', \mathbf{y})$ is the truncated charge-charge correlation function of the plasma A defined in terms of the statistical weight $\exp(-\beta U)$ associated to the energy (3.87). The asymptotic analysis of (3.89) differs from that of the previous section on two points: here the function S provides a contribution from coincident points to the integrals and we expect $S(x, x', \frac{\mathbf{q}}{d}, d)$ to tend towards a non-zero limit when $d \rightarrow \infty$, namely

$$\lim_{d \rightarrow \infty} S(x, x', \frac{\mathbf{q}}{d}) = S^0(x, x', \mathbf{0}) \quad (3.90)$$

with $S^0(x, x', \mathbf{0})$ the charge correlation of the semi-infinite plasma in absence of the dielectric. Hence, the leading behaviour of the force as $d \rightarrow \infty$

$$\langle f \rangle \sim \langle f \rangle^{\text{mon.}} + \langle f \rangle^{\text{dip.}} \quad (3.91)$$

comes from the first two terms resulting from the expansion of $\exp\{-q|x+x'|/d\} \sim 1 - q|x+x'|/d$ in (3.89). At leading order in $\langle f \rangle^{\text{dip.}}$ one can replace $S(x, x', \frac{\mathbf{q}}{d})$ by $S^0(x, x', \mathbf{0})$ so that

$$\lim_{d \rightarrow \infty} d^3 \langle f \rangle^{\text{dip.}} = -\Delta \int_0^\infty dq q^2 e^{-2q} \int_{-\infty}^0 dx \int_{-\infty}^0 dx' (x+x') S^0(x, x', \mathbf{0}) = \frac{-\Delta}{16\pi\beta}. \quad (3.92)$$

The first term of the x, x' integrals vanishes because of perfect screening whereas the second one equals $1/(4\pi\beta)$ as a consequence of the dipole sum rule in a semi-infinite plasma (Martin, 1988, Form. (3.9), Sec. C).⁷ Since $\lim_{d \rightarrow \infty} d^2 \langle f \rangle^{\text{mon.}} = 0$ because of perfect screening, one can replace $S(x, x', \frac{\mathbf{q}}{d})$ by $S(x, x', \frac{\mathbf{q}}{d}) - S^0(x, x', \mathbf{0})$ in the monopole contribution $\langle f \rangle^{\text{mon.}}$. It is convenient to further add and subtract $S^0(x, x', \frac{\mathbf{q}}{d})$ and to note that:

$$\lim_{d \rightarrow \infty} d^3 \left\{ \frac{-\Delta}{d^2} \int_{-\infty}^0 dx \int_{-\infty}^0 dx' \int_0^\infty dq q e^{-2q} \left[S^0(x, x', \frac{\mathbf{q}}{d}) - S^0(x, x', \mathbf{0}) \right] \right\} \quad (3.93)$$

$$= -\Delta \int_0^\infty dq q^2 e^{-2q} \left. \frac{d}{dk} \right|_{k=0} \left(\int_{-\infty}^0 dx \int_{-\infty}^0 dx' S^0(x, x', k) \right) = \frac{-\Delta}{16\pi\beta}. \quad (3.94)$$

⁷Here the sign is opposite to that in (Martin, 1988) because the plasma is located in the $x < 0$ half space.

This follows from the small $k = |\mathbf{k}|$ expansion of the x, x' integral that has a linear term $\frac{k}{4\pi\beta}$ (Martin, 1988, Form. (3.24), Sec. C). Collecting (3.92) and (3.94) in (3.91) we see that the large- d behaviour of $\langle f \rangle$ is determined by

$$\langle f \rangle = \frac{-\Delta}{8\pi\beta d^3} - \frac{\Delta}{d^2} \int_{-\infty}^0 dx \int_{-\infty}^0 dx' \int_0^{\infty} dq q e^{-2q} \left[S(x, x', \frac{\mathbf{q}}{d}) - S^0(x, x', \frac{\mathbf{q}}{d}) \right] + o(d^{-3}). \quad (3.95)$$

One can now proceed as in Section 3.3 with Mayer bonds defined in terms of the Green function (3.85). The Debye-Hückel equation (3.31) is supplemented with the boundary condition $\lim_{x \rightarrow d_-} \partial\Phi(x, x', \mathbf{k})/\partial x = \epsilon \lim_{x \rightarrow d_+} \partial\Phi(x, x', \mathbf{k})/\partial x$, and $\kappa(x)$ is as before for $x \leq 0$ but $\kappa(x) = 0$ for $x > 0$. The solution for piecewise-flat densities is (Aqua & Cornu, 2001a, Form. (3.2)-(3.5))⁸

$$\varphi(x, x', \mathbf{k}) = 2\pi \frac{e^{-k_A|x-x'|}}{k_A} + 2\pi \frac{e^{-k_A|x+x'|}}{k_A} \frac{(k_A - k)e^{kd} + \Delta(k_A + k)e^{-kd}}{(k_A + k)e^{kd} + \Delta(k_A - k)e^{-kd}}. \quad (3.96)$$

It is convenient to single out the potential $\varphi^0(x, x', \mathbf{k})$ (3.43) for the semi-infinite plasma in the absence of the dielectric and to split

$$\varphi(x, x', \mathbf{k}) = \varphi^0(x, x', \mathbf{k}) + \varphi_{AB}(x, x', \mathbf{k}), \quad (3.97)$$

where, from (3.43) and (3.96),

$$\varphi_{AB}(x, x', \mathbf{k}) = \frac{8\pi k e^{-k_A|x|} e^{-k_A|x'|} \Delta e^{-kd}}{(k_A + k) [(k_A + k)e^{kd} + (k_A - k)\Delta e^{-kd}]} \quad (3.98)$$

One observes that $\varphi_{AB}(x, x', \mathbf{k})$ has the factorization property analogous to (3.44)

$$\lim_{d \rightarrow \infty} d\varphi_{AB}(x, x', \frac{\mathbf{q}}{d}) = z(q)\varphi^0(x, 0, \mathbf{0})\varphi^0(0, x', \mathbf{0}), \quad (3.99)$$

$$z(q) = \frac{q}{2\pi} \frac{\Delta e^{-2q}}{1 + \Delta e^{-2q}}. \quad (3.100)$$

The potential Φ corresponding to the exact non-uniform profile is related to φ by the integral equation (3.38). With a reasoning similar to that leading to (3.58) and (3.59), it can also be split in two parts

$$\Phi(x, x', \mathbf{k}) \equiv \widetilde{\Phi}(x, x', \mathbf{k}) + \Phi_{AB}(x, x', \mathbf{k}) \quad (3.101)$$

Here $\widetilde{\Phi}$ verifies eq. (3.59) with φ^0 in place of φ_{AA} and tends to the potential Φ^0 of the semi-infinite plasma in vacuum. Φ_{AB} solves eq. (3.58) with u in place of u_A

⁸Here the minimal distance d between a charge and the dielectric wall plays the role of the hard-core diameter in (Aqua & Cornu, 2001a). Notice that we defined Δ with the opposite sign and that our plasma fills the region $x < 0$.

and u_B , $\widetilde{\Phi}$ in place of $\widetilde{\Phi}_{AA}$, and Φ in place of Φ_{BB} . Then using (3.99) and the fact that both Φ and $\widetilde{\Phi}$ tend to Φ^0 leads to the asymptotic factorisation of Φ_{AB}

$$\lim_{d \rightarrow \infty} d\Phi_{AB}(x, x', \frac{\mathbf{q}}{d}) = z(q)\Phi^0(x, 0, \mathbf{0})\Phi^0(0, x', \mathbf{0}). \quad (3.102)$$

We are now ready to evaluate the force (3.95) as $d \rightarrow \infty$ in the Debye-Hückel approximation. From (3.27), (3.24) and (3.30) one has

$$S^{\text{DH}}(x, x', \frac{\mathbf{q}}{d}) = -\frac{1}{\beta} \frac{\kappa^2(x)}{4\pi} \frac{\kappa^2(x')}{4\pi} \Phi(x, x', \frac{\mathbf{q}}{d}) + \delta(x - x') \frac{\kappa^2(x)}{4\pi\beta} \quad (3.103)$$

and the analogous relation for $S^{0\text{DH}}(x, x', \frac{\mathbf{q}}{d})$; some care has to be exercised here since coincident points do contribute when both x, x' are in the same integration range. We subtract and add $\widetilde{\Phi}(x, x', \frac{\mathbf{q}}{d})$ to $\Phi(x, x', \frac{\mathbf{q}}{d})$ in (3.103). This gives two contributions to the force (3.95). The first one is

$$\begin{aligned} & \frac{-\Delta}{8\pi\beta d^3} + \frac{\Delta}{\beta d^2} \int_{-\infty}^0 dx \int_{-\infty}^0 dx' \int_0^{\infty} dq q e^{-2q} \frac{\kappa^2(x)}{4\pi} \frac{\kappa^2(x')}{4\pi} \left[\Phi(x, x', \frac{\mathbf{q}}{d}) - \widetilde{\Phi}(x, x', \frac{\mathbf{q}}{d}) \right] \\ &= \frac{-\Delta}{8\pi\beta d^3} + \frac{\Delta}{\beta d^2} \int_{-\infty}^0 dx \int_{-\infty}^0 dx' \int_0^{\infty} dq q e^{-2q} \frac{\kappa^2(x)}{4\pi} \frac{\kappa^2(x')}{4\pi} \Phi_{AB}(x, x', \frac{\mathbf{q}}{d}). \end{aligned} \quad (3.104)$$

The second one involves the quantity

$$\begin{aligned} & \frac{1}{4\pi\beta} \left[\kappa^2(x) - (\kappa^0)^2(x) \right] \\ &+ \frac{-1}{\beta} \int_{-\infty}^0 dx' \left[\frac{\kappa^2(x)}{4\pi} \frac{\kappa^2(x')}{4\pi} \widetilde{\Phi}(x, x', \frac{\mathbf{q}}{d}) - \frac{(\kappa^0)^2(x)}{4\pi} \frac{(\kappa^0)^2(x')}{4\pi} \Phi^0(x, x', \frac{\mathbf{q}}{d}) \right] \\ &= \frac{q^2}{4\pi\beta d^2} \int dx' \left[\widetilde{\Phi}(x, x', \frac{\mathbf{q}}{d}) - \Phi^0(x, x', \frac{\mathbf{q}}{d}) \right] = \mathcal{O}\left(\frac{1}{d^2}\right). \end{aligned} \quad (3.105)$$

This equality follows from the relation (3.33) for $\widetilde{\Phi}$ (relative to κ) and for Φ^0 (relative to κ^0) since both potentials satisfy the basic differential equation (3.31). Thus the contribution of (3.105) to the force is $\mathcal{O}\left(\frac{1}{d^4}\right)$. With the factorisation (3.102) and using the sum rule (3.34) for Φ^0 , one finds from (3.104) and (3.100) the final result

$$\lim_{d \rightarrow \infty} d^3 \langle f \rangle = \frac{-\Delta}{8\pi\beta} + \frac{\Delta}{\beta} \int_0^{\infty} dq q e^{-2q} z(q) = \frac{1}{8\pi\beta} \sum_{n=1}^{\infty} \frac{(-\Delta)^n}{n^3}. \quad (3.106)$$

It can be shown along the lines presented in Section 3.5 that the non mean-field part of the charge correlation function does not contribute to this asymptotic result. According to (3.101) one splits the bonds $F = \widetilde{F} + F_{AB}$ and $F^R = \widetilde{F}^R + F_{AB}^R$ with

$F_{AB}^R \equiv \exp(F_{AB} - \beta v_{SR}) - 1 - F_{AB}$. The bonds \widetilde{F} and \widetilde{F}^R tend to the bonds F^0 and F^{0R} pertaining to the semi-infinite plasma without dielectric, whereas F_{AB} vanishes in the limit. At large separation, $F_{AB}^R \sim (F_{AB})^2$ vanishes more rapidly than F_{AB} (see appendix 3.A). As in the analysis leading to (3.79), the leading behaviour of the Ursell function comes from graphs having bonds \widetilde{F} , \widetilde{F}^R , a single F_{AB} one, and it takes the factorized form (3.79). The only difference is that both functions G^0 refer to the same plasma A. Then one establishes the validity of (3.106) as in (3.81)-(3.84).

This result coincides with that of Lifshitz. Indeed, a straightforward generalisation of its asymptotic force as $\frac{d}{\beta \hbar c} \gg 1$ (Lifshitz, 1955, Form. (5.5)) to the case of two different homogeneous dielectric media of constants ϵ_1, ϵ_2 yields⁹

$$f \sim \frac{1}{8\pi\beta d^3} \sum_{n=1}^{\infty} \frac{(\Delta_1 \Delta_2)^n}{n^3}, \quad \Delta_i = \frac{1 - \epsilon_i}{1 + \epsilon_i}, \quad i = 1, 2. \quad (3.107)$$

This reduces to (3.106) once one of the slabs is a conductor, i.e $\Delta_1 = -1$. We have therefore provided a derivation of this formula when the conductor is described as a statistical system of fluctuating charges in thermal equilibrium. It is interesting to note that thermal fluctuations in one of the slabs suffice to generate the correct asymptotic value of the force.

Acknowledgements

We thank F. Cornu and B. Jancovici for useful discussions.

Appendix 3.A: Slab of finite thickness

The analysis of Sections 3.2-3.5 applies to infinitely thick slabs. It is interesting to check that the asymptotic behaviour of the force does not depend on the slab thickness. We consider now that the slab Λ_A has finite thickness $a < \infty$, while, for simplicity, we keep the slab Λ_B infinitely thick. The setting of Sections 3.2 and 3.3 remains the same with the x -integration on Λ_A limited to the interval $-a \leq x \leq 0$. We then follow the same route as in Section 3.4 and 3.5 by first considering the equation (3.36) for the piecewise-flat profile

$$\begin{aligned} \bar{\kappa}(x) &= 0, \quad x < -a, & \bar{\kappa}(x) &= \frac{1}{a} \int_{-a}^0 dx \kappa(x) \equiv \kappa_A, \quad -a < x < 0 \\ \bar{\kappa}(x) &= 0, \quad 0 < x < d, & \bar{\kappa}(x) &= \kappa_B, \quad x > d \end{aligned} \quad (3A.1)$$

⁹One generalises Formulae (5.2), (5.3) and finally (5.5) of (Lifshitz, 1955) starting from (2.4) by keeping ϵ_1 and ϵ_2 different.

It is convenient to choose $\bar{\kappa}(x)$ equal to the average of $\kappa(x)$ in Λ_A , since we expect the latter to be close to its mean value at weak-coupling.

Solving equation (3.36) with x' fixed, continuity conditions of $x \mapsto \varphi(x, x', \mathbf{k})$ and of $x \mapsto \partial_x \varphi(x, x', \mathbf{k})$ at $x = -a$, $x = 0$, $x = d$ as well with $\lim_{x \rightarrow \pm\infty} \varphi(x, x', \mathbf{k}) = 0$ yields

$$\varphi(x, x', \mathbf{k}) = \begin{cases} \varphi_{AA}(x, x', \mathbf{k}), & -a < x, x' < 0 \\ \varphi_{AB}(x, x' - d, \mathbf{k}), & -a < x < 0 < d < x' \\ \varphi_{BB}(x - d, x' - d, \mathbf{k}), & d < x, x' \end{cases} \quad (3A.2)$$

where

$$\varphi_{AA}(x, x', \mathbf{k}) = \frac{2\pi}{k_A} \frac{(k_A+k)e^{k_A a} (e^{-k_A|x'-x|}\sigma_1 + e^{-k_A|x'+x|}\sigma_2) + (k_A-k)e^{-k_A a} (e^{k_A|x'-x|}\sigma_2 + e^{k_A|x'+x|}\sigma_1)}{(k_A+k)e^{k_A a}\sigma_1 - (k_A-k)e^{-k_A a}\sigma_2} \quad (3A.3)$$

$$\varphi_{AB}(x, x', \mathbf{k}) = \frac{8\pi k \left[(k_A+k)e^{k_A a} e^{k_A x} + (k_A-k)e^{-k_A a} e^{-k_A x} \right] e^{-k_B x'}}{(k_A+k)e^{k_A a}\sigma_1 - (k_A-k)e^{-k_A a}\sigma_2} \quad (3A.4)$$

$$\varphi_{BB}(x, x', \mathbf{k}) = \frac{2\pi}{k_B} \left(e^{-k_B|x'-x|} + e^{-k_B|x'+x|} \frac{(k_A+k)e^{k_A a}\sigma_3 - (k_A-k)e^{-k_A a}\sigma_4}{(k_A+k)e^{k_A a}\sigma_1 - (k_A-k)e^{-k_A a}\sigma_2} \right) \quad (3A.5)$$

and

$$\sigma_1 = (k_A+k)(k_B+k)e^{kd} - (k_A-k)(k_B-k)e^{-kd} \quad \sigma_2 = (k_A-k)(k_B+k)e^{kd} - (k_A+k)(k_B-k)e^{-kd} \quad (3A.6)$$

$$\sigma_3 = (k_A+k)(k_B-k)e^{kd} - (k_A-k)(k_B+k)e^{-kd} \quad \sigma_4 = (k_A-k)(k_B-k)e^{kd} - (k_A+k)(k_B+k)e^{-kd}$$

$$k_A = \sqrt{k^2 + \kappa_A^2} \quad k_B = \sqrt{k^2 + \kappa_B^2}.$$

One deduces also from the differential equations that for any $a > 0$ both φ and Φ verify the charge sum rule (3.34). As $a \rightarrow \infty$, formulae reduce to those obtained in Section 3.4 for two semi-infinite plasmas.

The main observation to be made on this explicit result is that it obeys exactly the same factorisation property in terms of the scaled variable $\mathbf{q} = \mathbf{k}d$ as (3.44) with the the same factors (here $\varphi_A^0(x, 0, \mathbf{0})$ corresponds to the single plasma A with finite thickness). The rest of the analysis is the same as in section 3.4, with the difference that the above solution verifies a -dependent bounds in place of (3.45)-(3.47), namely (appendix 3.B)¹⁰

$$|\varphi(x, x', \mathbf{k})| \leq \varphi^>(x, x') \leq \frac{4\pi}{\kappa} \coth \kappa a, \quad \kappa d \geq 1, \quad (3A.7)$$

¹⁰See also the note added on p. 106

where $\varphi^>(x, x')$ is defined piecewise from $\varphi_{AA}^>, \varphi_{AB}^>$, etc. as in (3A.2) with

$$\varphi_{AA}^>(x, x') = \frac{2\pi}{\kappa} \frac{\cosh \kappa(a - |x' - x|) + \cosh \kappa(a - |x' + x|)}{\sinh \kappa a} \quad (3A.8)$$

$$\varphi_{AB}^>(x, x') = \frac{4\pi}{\kappa^2 d} \frac{\cosh \kappa(a - |x|)}{\sinh \kappa a} e^{-\kappa x'} \quad (3A.9)$$

$$\varphi_{BB}^>(x, x') = \frac{2\pi}{\kappa} \left(e^{-\kappa|x'-x|} + e^{-\kappa|x'+x|} \right), \quad \kappa := \min\{\kappa_A, \kappa_B\} \quad (3A.10)$$

The potential Φ with structured profiles is related to φ by the integral equation (3.38) and the estimate (3.49) of the lemma becomes

$$|\Phi(x, x', \mathbf{k})| \leq \frac{1}{1 - r(a)} \varphi^>(x, x'), \quad r(a) := r \coth \kappa a \quad (3A.11)$$

where r is defined by (3.48). To have $r(a) < 1$ one needs r sufficiently small (weak-coupling, see appendix 3.B) and κa not too small, *i.e.*, the slab width is larger than the typical screening length in the plasma.¹¹ Then the steps leading to (3.62) are the same as in Section 3.4 and the considerations of Section 3.5 apply as well. The reason for the asymptotic force being independent of the slab thickness is clearly displayed in expressions (3.62) and (3.81): it only depends on the screening cloud associated to charges located at the inner boundaries of the slabs, and thus is insensitive to charge fluctuations elsewhere in the slabs.

Appendix 3.B: Bounds for the Debye-Hückel potential

In this appendix we present some details of the calculations leading to bounds used throughout the paper for the Debye-Hückel potentials φ and Φ and discuss the validity of (3.49) in the weak-coupling regime.

At first, we show the bound (3A.7), which is a generalisation of (3.45) to the case where plasma A is of finite thickness a . Result (3.45) is recovered by taking $a \rightarrow \infty$. From (3A.6), one has $\sigma_1 \geq \sigma_2$; $\sigma_1 \geq \kappa_A \kappa_B (e^{kd} - e^{-kd})$, and $\sigma_2 + \sigma_4 \leq \sigma_1 + \sigma_3$; $\sigma_3 - \sigma_1 \leq \sigma_4 - \sigma_2 < 0$. This implies

$$-1 \leq \frac{(k_A+k)e^{k_A a} \sigma_3 - (k_A-k)e^{-k_A a} \sigma_4}{(k_A+k)e^{k_A a} \sigma_1 - (k_A-k)e^{-k_A a} \sigma_2} \leq 1,$$

which yields the bound (3A.10) for φ_{BB} :

$$|\varphi_{BB}| \leq \frac{2\pi}{k_B} \left(e^{-k_B|x'-x|} + e^{-k_B|x'+x|} \right) \leq \varphi_{BB}^>(x, x').$$

¹¹Notice that the above bounds cannot be uniform in a : $\varphi_A^0(x, x', \mathbf{0})$ diverges as $a \rightarrow 0$ so that its integral over $[-a, 0]$ leads to the constant value $\frac{4\pi}{\kappa_A}$ requested by the charge sum rule.

To obtain the bound (3A.9) for φ_{AB} , we then note that

$$\sigma_1 - \frac{k_A - k}{k_A + k} e^{-2k_A a} \sigma_2 \geq (1 - e^{-2k_A a}) \sigma_1. \quad (3B.1)$$

Thus, $\frac{k}{\sigma_1 - \frac{k_A - k}{k_A + k} e^{-2k_A a} \sigma_2} \leq \frac{1}{1 - e^{-2k_A a}} \frac{1}{\kappa_A \kappa_B d} \frac{kd}{e^{kd} - e^{-kd}} \leq \frac{1}{1 - e^{-2k_A a}} \frac{1}{\kappa^2 d} \frac{1}{2}$, so that

$$0 \leq \varphi_{AB}(x, x', \mathbf{k}) \leq \frac{4\pi}{\kappa^2 d} \frac{e^{k_A(a-|x|)} + e^{-k_A(a-|x|)}}{e^{k_A a} - e^{-k_A a}} e^{-k_B x'} \leq \varphi_{AB}^>(x, x').$$

Last inequality uses

$$\frac{e^{kx} + e^{-kx}}{e^{kX} - e^{-kX}} \leq \frac{e^{\kappa x} + e^{-\kappa x}}{e^{\kappa X} - e^{-\kappa X}}, \quad 0 < x \leq X, \quad k \geq \kappa > 0. \quad (3B.2)$$

Finally, (3B.1), the fact that $|\sigma_2/\sigma_1| \leq 1$ and (3B.2) show the bound (3A.8)

$$\begin{aligned} |\varphi_{AA}(x, x', \mathbf{k})| &\leq \frac{2\pi}{\kappa_A} \frac{\sigma_1 e^{-k_A|x'-x|} + |\sigma_2| e^{-k_A|x'+x|} + e^{-2k_A a} (|\sigma_2| e^{k_A|x'-x|} + \sigma_1 e^{k_A|x'+x|})}{(1 - e^{-2k_A a}) \sigma_1} \\ &\leq \varphi_{AA}^>(x, x'). \end{aligned}$$

Proof of the lemma

To proof the bound (3.49) of $\Phi(x, x', \mathbf{k})$, we proceed as follows. By (3.38) we can develop $\Phi(x, x', \mathbf{k})$ as a perturbation series with respect to $\varphi(x, x', \mathbf{k})$, whose n^{th} term reads

$$\left(\frac{-1}{4\pi}\right)^n \int ds_1 \cdots ds_n u(s_1) \cdots u(s_n) \varphi(x, s_1, \mathbf{k}) \varphi(s_1, s_2, \mathbf{k}) \cdots \varphi(s_n, x', \mathbf{k}). \quad (3B.3)$$

This term is bounded by $r^n \varphi^>(x, x')$, where r is given by (3.48). Indeed, according to (3.45), $\varphi(x, x', \mathbf{k})$ is bounded by $\varphi^>(x, x')$, which itself satisfies

$$\varphi^>(x, s) \varphi^>(s, x') \leq \frac{4\pi}{\kappa} \varphi^>(x, x'), \quad \forall s, x, x'. \quad (3B.4)$$

Consequently, if $r < 1$, the series is absolutely convergent and the lemma holds. Inequality (3B.4) is proven using (3.46), (3.47) and verifying it for each case. As an example,

$$\varphi_{AA}^>(x, s) \varphi_{AB}^>(s, x') = \frac{2\pi}{\kappa} \frac{4\pi}{\kappa^2 d} e^{-\kappa|x'|} \left(e^{-\kappa(|x-s|+|s|)} + e^{-\kappa(|x+s|+|s|)} \right) \quad (3B.5)$$

$$\leq \frac{4\pi}{\kappa} \varphi_{AB}^>(x, x'), \quad (3B.6)$$

because $|x \pm s| + |s| \geq |x|$. Some of the majorations leading to (3B.4) assume $\kappa d \geq 1$.

If plasma A is finitely thick, (3B.4) generalizes to

$$\varphi^>(x, s) \varphi^>(s, x') \leq \frac{4\pi}{\kappa} \coth(\kappa a) \varphi^>(x, x'), \quad \forall x, x', s \quad (3B.7)$$

and we obtain the bound (3A.11) for Φ .

Profiles in weakly-coupled plasmas

The parameter r occurring in the bound (3.49) can be chosen small enough in the weak-coupling regime, defined by $\Gamma = \frac{1}{2}\beta e^2 \kappa \ll 1$ (e is a typical charge of the system). Indeed, to estimate r , the deviations of the density profiles to their bulk values need to be known. In the simplest case of a semi-infinite charge-symmetric plasma¹² in the weak-coupling regime, Jancovici (Jancovici, 1982) finds

$$\frac{\rho_A(\gamma x) - \rho_{A\gamma}}{\rho_{A\gamma}} \simeq \frac{\beta e_\gamma^2}{2} \kappa_A \chi(\kappa_A x), \quad \Gamma \ll 1,$$

where χ is integrable. Integrating over $x < 0$ and forming r according to (3.48) shows that r is proportional to Γ . This also holds if the semi-infinite plasma is not charge-symmetric (Aqua & Cornu, 2001a, Sec. 5). For our two-plasmas system, r will be less than 1 provided Γ is small and d is large.

Appendix 3.C: Decay of Mayer graphs at large slab separation

We consider prototype graphs constituted of bonds (3.76) labelled by the indices AA, AB, BA, BB according to the respective location of the variables x, x' in slab A or in slab B . In view of (3.29) and after the changes $\mathbf{k}d = \mathbf{q}$, $x' \rightarrow x' - d$, the contribution to the force of a graph Π_{AB} with first root point in Λ_A and second root point in Λ_B is

$$\langle f \rangle^{\Pi_{AB}} = -\frac{1}{d^2} \int_{-\infty}^0 dx \int_0^{\infty} dx' \int_0^{\infty} dq q e^{-\frac{q}{d}|x-x'|} e^{-q} \sum_{\gamma, \gamma'} e_\gamma e_{\gamma'} \rho_A(\gamma x) \rho_B(\gamma' x') \Pi_{AB}(\gamma x, \gamma' x', \frac{\mathbf{q}}{d}). \quad (3C.1)$$

A graph Π_{AB} having L bonds of \mathcal{F}_{AB} or \mathcal{F}_{BA} type, written in Fourier space with respect to the \mathbf{y} -variables, is of the general form

$$\begin{aligned} \Pi_{AB}(\gamma x, \gamma' x', \mathbf{k}) &= \frac{1}{S_{\pi_{AB}}} \int d\mathbf{l} \rho(1) \cdots \int d\mathbf{m} \rho(m) \int \prod_{j=1}^L \frac{d\boldsymbol{\ell}_j}{(2\pi)^2} \mathcal{F}_{[AB]}(\boldsymbol{\ell}_j) \\ &\times \int \prod_a \frac{d\mathbf{k}_a}{(2\pi)^2} \mathcal{F}_{AA}(\mathbf{k}_a) \int \prod_b \frac{d\mathbf{k}_b}{(2\pi)^2} \mathcal{F}_{BB}(\mathbf{k}_b) \prod_{n=0}^m (2\pi)^2 \delta[\mathbf{k}, \{\boldsymbol{\ell}_j\}_n, \{\mathbf{k}_a\}_n, \{\mathbf{k}_b\}_n]. \end{aligned} \quad (3C.2)$$

¹²A charge-symmetric plasma has two species with opposite charges and same bulk densities.

Here m is the number of internal points, $i = (\gamma_i, x_i)$ and $\int di$ stands for summation over particle species and integration over x_i . $\mathcal{F}(\mathbf{k})$ stands either for $F(\mathbf{k})$ or $F^R(\mathbf{k})$ and we have omitted the species and x, x' dependencies from the notation.¹³ The product of $m + 1$ δ -functions expresses the conservation of wave numbers at the m internal points plus a relation that fixes the sum of ingoing (or outgoing) wave numbers to \mathbf{k} , as a result of \mathbf{y} -translation invariance. These constitute $m + 1$ linear equations between wave numbers from the sets $\{\ell_j\}, \{\mathbf{k}_a\}, \{\mathbf{k}_b\}$, which imply C independent relations involving only ℓ variables. Depending on the topology of the graph, $1 \leq C \leq L$. Consider, e.g., the graph constituted by a single chain of bonds $F_{AB}(\ell_1)F_{BB}^R(\mathbf{k}_b)F_{BA}(\ell_2)F_{AA}^R(\mathbf{k}_a)F_{BA}(\ell_3)$ with $L = 3$.¹⁴ The conservation laws $\mathbf{k} = \ell_1 = \mathbf{k}_a = \ell_2 = \mathbf{k}_b = \ell_3$ imply the independent relations $\mathbf{k} = \ell_1$, $\ell_1 = \ell_2$, $\ell_2 = \ell_3$ between the ℓ variables, thus $C = 3$. Consider now the graph constituted of two parallel chains $F_{AA}^R(\mathbf{k}_{a1})F_{AB}(\ell_1)F_{BB}^R(\mathbf{k}_{b1})$ and $F_{AA}^R(\mathbf{k}_{a2})F_{AB}(\ell_2)F_{BB}^R(\mathbf{k}_{b2})$ with $L = 2$. The conservation laws are $\mathbf{k} = \mathbf{k}_{a1} + \mathbf{k}_{a2}$, $\mathbf{k}_{a1} = \ell_1 = \mathbf{k}_{b1}$, $\mathbf{k}_{a2} = \ell_2 = \mathbf{k}_{b2}$ implying the single relation $\mathbf{k} = \ell_1 + \ell_2$, thus $C = 1$.

Then we perform the integrations in (3C.2) in the following order. We first carry C integrals on the δ functions corresponding to the above relations between ℓ variables: this expresses the ℓ_j variables $j = 1, \dots, L$ in the integrand as linear combinations of the remaining $L - C$ ones, say $\ell_{C+1}, \dots, \ell_L$. We evaluate now Π_{AB} at $\mathbf{k} = \mathbf{q}/d$ and change the variables $\ell_j = \mathbf{q}_j/d$, $j = C + 1, \dots, L$: the Jacobian provides a factor $d^{-2(L-C)}$. As $d \rightarrow \infty$ the \mathbf{k}_a , \mathbf{k}_b and \mathbf{q} integrals factorize. Indeed in \mathcal{F}_{AA} or \mathcal{F}_{BB} bonds the \mathbf{q} dependences occur in the form $\mathbf{q}/d \rightarrow 0, d \rightarrow \infty$ whereas for \mathcal{F}_{AB} or \mathcal{F}_{BA} bonds we use the asymptotic form (3.60). This yields a factor $d^{-n[AB]}$ if the number of $F_{[AB]}$ bonds is $n[AB]$ and $d^{-4n^R[AB]}$ if the number of $F_{[AB]}^R$ bonds is $n^R[AB]$ (for the latter, see at the end of this appendix). Then the \mathbf{k}_a and \mathbf{k}_b integrals refer to products of \mathcal{F}_{AA} and \mathcal{F}_{BB} as in single semi-infinite plasmas and the \mathbf{q} integrals are carried on product of functions $q/\sinh q$. For the above examples the \mathbf{q} integrals are $\int d\mathbf{q}(q/\sinh q)^3$ and $\int d\mathbf{q}_1 \int d\mathbf{q}_2 (q_1/\sinh q_1)(|q_1 - q_2|/\sinh |q_1 - q_2|)$. As a final result a graph decays as

$$d^{-2(L-C)}d^{-n[AB]}d^{-4n^R[AB]}, \quad d \rightarrow \infty \quad (3C.3)$$

times a factor of order one resulting of the above integrals. It is clear that the minimal decay d^{-1} is obtained when there is only one F_{AB} bond.

It remains to examine the decay of a $F_{[AB]}^R$ bond, which reads in Fourier form, according to (3.21)

$$F_{AB}^R(\mathbf{k}) = \int d\mathbf{y} e^{-i\mathbf{k}\cdot\mathbf{y}} [\exp(-\beta e_1 e_2 \Phi_{AB}(\mathbf{y})) - 1 + \beta e_1 e_2 \Phi_{AB}(\mathbf{y})]. \quad (3C.4)$$

¹³In (3C.2), $\mathcal{F}_{[AB]}$ designates either a \mathcal{F}_{AB} or a \mathcal{F}_{BA} bond. Notice that $\mathcal{F}_{BA}(i, j, \mathbf{k}) = \mathcal{F}_{AB}(j, i, \mathbf{k})$.

¹⁴The F^R bonds are needed because of the excluded convolution rule between F bonds.

The x variables are omitted and $|x_1 - x_2|$ is large enough so that the short range part of the potential does not contribute. In view of (3.60), $\Phi_{AB}(\mathbf{y})$ has the asymptotic form

$$\begin{aligned}\Phi_{AB}(\mathbf{y}) &= \frac{1}{d^2} \int \frac{d\mathbf{q}}{(2\pi)^2} \exp(i\frac{\mathbf{q}}{d} \cdot \mathbf{y}) \Phi_{AB}\left(\frac{\mathbf{q}}{d}\right) \\ &\sim \frac{1}{d^3} f\left(\frac{\mathbf{y}}{d}\right) \quad \text{with} \quad f(\mathbf{y}) = \Phi_A^0 \Phi_B^0 \int \frac{d\mathbf{q}}{(2\pi)^2} e^{i\mathbf{q}\cdot\mathbf{y}} \frac{q}{4\pi \sinh q}.\end{aligned}\quad (3C.5)$$

Hence substituting (3C.5) in (3C.4) and expanding for large d after the change of variable $\mathbf{u} = \mathbf{y}/d$ gives

$$\begin{aligned}F_{AB}^R\left(\frac{\mathbf{q}}{d}\right) &\sim d^2 \int d\mathbf{u} e^{-i\mathbf{q}\cdot\mathbf{u}} \left[\exp\left(-\frac{\beta}{d^3} f(\mathbf{u})\right) - 1 + \frac{\beta}{d^3} f(\mathbf{u}) \right] \\ &\sim \frac{1}{d^4} \int d\mathbf{u} e^{-i\mathbf{q}\cdot\mathbf{u}} (f(\mathbf{u}))^2 = O\left(\frac{1}{d^4}\right).\end{aligned}\quad (3C.6)$$

References

- Aqua, J.-N., and Cornu, F. (2001a). Density profiles in a classical Coulomb fluid near a dielectric wall, I. Mean-field scheme. *J. Stat. Phys.*, *105*, 211–244.
- Aqua, J.-N., and Cornu, F. (2001b). Density profiles in a classical Coulomb fluid near a dielectric wall, II. Weak-coupling systematic expansion. *J. Stat. Phys.*, *105*, 245–283.
- Aqua, J.-N., and Cornu, F. (2003). Dipolar effective interaction in a fluid of charged spheres near a dielectric plate. *Phys. Rev. E*, *68*, 026133, 1–17.
- Balian, R., and Duplantier, B. (1977). Electromagnetic waves near perfect conductors, I. Multiple scattering expansions and distribution of modes. *Ann. Phys.*, *104*, 300–335.
- Balian, R., and Duplantier, B. (1978). Electromagnetic waves near perfect conductors, II. Casimir effect. *Ann. Phys.*, *112*, 165–208.
- Brydges, D. C., and Martin, Ph. A. (1999). Coulomb systems at low density : a review. *J. Stat. Phys.*, *96*, 1163–1330.
- Cornu, F. (1996). Correlations in quantum plasmas. II. Algebraic tails. *Phys. Rev. E*, *53*, 4595–4631.
- Duplantier, B., and Rivasseau, V. (Eds.). (2003). *Poincaré seminar 2002 : Vacuum energy-renormalization* (Vol. 30). Basel: Birkhäuser.
- Dzyaloshinskii, I. E., Lifshitz, E. M., and Pitaevskii, L. P. (1961). The general theory of van der Waals forces. *Adv. Phys.*, *10*, 165–209.
- Forrester, P., Jancovici, B., and Téllez, G. (1996). Universality in some classical Coulomb systems of restricted dimension. *J. Stat. Phys.*, *84*, 359–378.
- Guernsey, R. L. (1970). Correlation effects in semi-infinite plasmas. *Phys. Fluids*, *13*, 2089–2102.

- Hansen, J.-P., and McDonald, I. R. (1986). *Theory of simple liquids* (2nd ed.). London: Academic Press.
- Jackson, J. D. (1998). *Classical electrodynamics* (2nd ed.). New York: Wiley Text Books.
- Jancovici, B. (1982). Classical Coulomb systems near a plane wall. I. *J. Stat. Phys.*, 28, 43–65.
- Jancovici, B., and Šamaj, L. (2004). Screening of Casimir forces by electrolytes in semi-infinite geometries. *J. Stat. Mech.*, P08006. Electronic journal: <http://www.iop.org/EJ/article/1742-5468/2004/08/P08006>.
- Jancovici, B., and Téllez, G. (1996). The ideal conductor limit. *J. Phys. A : Math. Gen.*, 29, 1155–1166.
- Landau, L. D., Lifshitz, E. M., and Pitaevskii, L. P. (1984). Electrodynamics of continuous media. In *Landau course* (2nd ed., Vol. 8). Oxford: Pergamon Press.
- Lifshitz, E. M. (1955). The theory of molecular attractive forces between solids. *J. Exp. Th. Phys. USSR*, 29, 94–110. (English translation : *Sov. Phys. JETP*, 2, 73–83 (1956))
- Martin, Ph. A. (1988). Sum rules in charged fluids. *Rev. Mod. Phys.*, 60, 1075–1127.
- Meeron, E. (1958). Theory of potentials of average force and radial distribution function in ionic solutions. *J. Chem. Phys.*, 28, 630–643.
- Meeron, E. (1961). *Plasma physics*. New York: McGraw-Hill.
- Milonni, P. W. (1994). *The quantum vacuum: An introduction to quantum electrodynamics*. San Diego: Academic Press.
- Mostepanenko, V. M., and Trunov, N. N. (1997). *The Casimir effect and its applications*. Oxford: Clarendon Press.
- Plunien, G., Müller, B., and Greiner, W. (1986). The Casimir effect. *Phys. Reports*, 134, 87–193.
- Schwinger, J. (1975). Casimir effect in source theory. *Lett. Math. Phys.*, 1, 43–47.
- Schwinger, J., DeRaad, L. L., Jr, and Milton, K. A. (1978). Casimir effect in dielectrics. *Ann. Phys.*, 115, 1–23.
- Schwinger, J., DeRaad, L. L., Jr, Milton, K. A., and Tsai, W.-Y. (1998). *Classical electrodynamics*. Boulder: Westview Press.

3.7 Decay analysis of Mayer graphs

The asymptotic value of the Casimir force has been retrieved in the last part of the precedent article by analysing the Mayer graph series of $h_{AB}(1, 2, \frac{q}{d})$ in the large-distance limit. As has been expected in Section 2.5, graphs with the least number of traversing bonds decay the slowest, and give to h_{AB} its dominant contribution. The consideration of more complicated graphs than the simple ones containing a unique F_{AB} bond is not really needed. Nevertheless, as soon as one wants to investigate subleading orders of the force, a more refined analysis of the Mayer graphs is mandatory.

3.7.1 Decay of Mayer graphs at large separation

We come back shortly to the development sketched in Appendix 3.C (p. 91) to retrieve the minimal decay of an arbitrary Mayer graph of h_{AB} . We will illustrate it on a specific example in the next section (3.7.2) and then give a simple way of determining immediately these minimal decays graphically (Section 3.7.3).

We have seen in Appendix 3.C, Formula (3C.3), that the decay of a graph with $L(F_{AB})$ bonds F_{AB} and $L(F_{AB}^R)$ bonds F_{AB}^R is at least

$$d^{-2I} d^{-L(F_{AB})} d^{-4L(F_{AB}^R)}, \quad (3.108)$$

where

$$I = L - C \quad (3.109)$$

depends on the number C of independent constraints there are, that involve only the L Fourier vectors ℓ_1, \dots, ℓ_L of all crossing bonds.

The graph in Fourier representation:

Since we are interested in h_{AB} in Fourier representation, every bond is written in the partial Fourier space \mathbf{k} , yielding (3C.2). Indeed, by the \mathbf{y} -translation invariance of the space, the meeting of bonds at an integrated point implies the presence of a Dirac factor, which depends on the bonds' Fourier variable. When only two bonds meet at a point (like in a chain), one simply has $\delta(\mathbf{k}_1 - \mathbf{k}_2)$. If one of the Fourier integrals, say, on \mathbf{k}_2 , would be readily effectuated, both bonds would be evaluated at the same Fourier vector \mathbf{k}_1 . This is the convolution theorem. When more than two bonds meet at a point, the Dirac factor involves other Fourier variables but only one of them could be readily integrated.

Because the Fourier variables are only added and subtracted in the argument of a Dirac factor, one can state the nonvanishing contribution of the latter as a

conservation law: at the internal point of the graph to which the Dirac factor is associated, the sum of the ingoing Fourier quantities (say, with plus sign) equals the sum of the outgoing ones (with minus sign). This is pretty much the same as the conservation of impulsion in Feynman diagrams, originating from the total space translation invariance.

Strategy/Problem:

The **aim** pursued in the development of Appendix 3.C is — from the Fourier representation (3C.2) of the graph under investigation — to evaluate all traversing bonds F_{AB} and F_{AB}^R at a Fourier vector of the type \mathbf{Q}/d , so that they are expandable in inverse powers of d , like the Coulomb force in (2.50). (Otherwise, they are nonanalytic in $1/d$ and entangle the integrated Fourier variables and d , as seen on the explicit expression of $\varphi_{AB}(x, x', \mathbf{k})$ (3.41)) This aim can be satisfied in essentially two ways. Let us illustrate it in two simple cases:

1. If traversing bonds are convoluted to each other in a simple chain, like in $(F_{AB} * F_{BA}^R * F_{AB})(\frac{\mathbf{q}}{d})$, nothing needs to be done, for, by the convolution theorem, this chain equals $F_{AB}(\frac{\mathbf{q}}{d})F_{BA}^R(\frac{\mathbf{q}}{d})F_{AB}(\frac{\mathbf{q}}{d})$.
2. When there are several parallel chains bent across the root points, only one of them will transmit \mathbf{q}/d to the other side. For the other chains, expressed in Fourier representation, the changes of variables $\ell_l = \mathbf{q}_l/d$ can be performed, each of which providing a supplementary factor d^{-2} .

The **problem** is that simply performing $\ell_l = \mathbf{q}_l/d$ on all L crossing bonds¹⁵ does not result in an overall factor d^{-2L} , as illustrates the example of the chain in point 1 above: a factor $\delta(\ell_l - \frac{\mathbf{q}}{d})$ would become $d^{-2}\delta(\frac{\mathbf{q}_l}{d} - \frac{\mathbf{q}}{d}) = \delta(\mathbf{q}_l - \mathbf{q})$.

One thus needs to know how many independent variables I there are among the L crossing ones: the other crossing variables can be expressed in terms of these I ones, for which performing $\ell_l = \mathbf{q}_l/d$ then achieves the aim.

Since there are L traversing bonds, there has to be a number C of constraints (represented by Dirac factors) involving only them, such that $I = L - C$. This is how this number has been introduced in Appendix 3.C. Before turning to a geometrical determination of C , let us present these concepts on an explicit example.

3.7.2 Illustration on a specific example

We illustrate the precedent discussion on the graph depicted below (Figure 3.1). It is constituted of $M = 2$ internal points (integrated over A), and a total of $N = 5$

¹⁵We do not want such a change of variable on a noncrossing bond, for it would become asymptotically nonintegrable on its Fourier variable.

bonds. Among them, $L = 2$ are crossing bonds; they are represented by dashed lines.

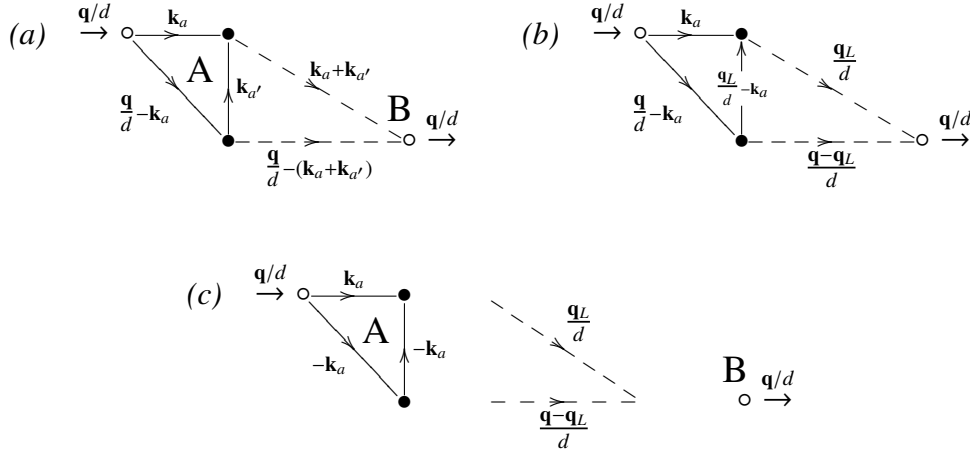


Figure 3.1: Decay analysis of a Mayer graph with $M = 2$ internal points, $N = 5$ bonds, of which $L = 2$ are crossing ones (dashed).

Fig. 3.1(a): From the N initial Fourier variables and the $M + 1$ points imposing an independent conservation law (the first root point, at which \mathbf{q}/d is injected, and the M internal points), there are $N - M - 1 = 2$ independent Fourier variables, that still need to be integrated over to constitute the value of the whole graph.

These two variables are denoted by \mathbf{k}_a and $\mathbf{k}_{a'}$, and have been chosen among the links in accordance with the conservation laws at the internal (black) and root points (white). It is seen, however, that only the combination $\mathbf{k}_a + \mathbf{k}_{a'}$ travels along the crossing bonds. Had we chosen another set of independent variables, we would have had only one ($= I$) independent Fourier vector crossing from A to B . Note that the sum of the traversing Fourier variables must give \mathbf{q}/d .

It is not allowed to perform the changes of variable

$$\mathbf{k}_a = \mathbf{q}_a/d, \quad \text{and} \quad \mathbf{k}_{a'} = \mathbf{q}_{a'}/d. \quad (3.110)$$

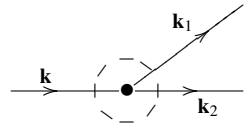
If this is done, the AA bonds become independent of \mathbf{q}_a and $\mathbf{q}_{a'}$ in the limit $d \rightarrow \infty$; integrative factors of the type $\propto e^{-|\mathbf{q}_a + \mathbf{q}_{a'}|}$ are still provided by the AB bonds, but integrating them on, say, \mathbf{q}_a over \mathbb{R}^2 wipes out their dependence upon $\mathbf{q}_{a'}$, and the integral on the latter variable diverges.

Fig. 3.1(b): Here we chose the independent variables \mathbf{k}_a and ℓ_L (e.g., obtained from the previous independent variables $\mathbf{k}_a, \mathbf{k}_{a'}$ in (a) by the simple change $\mathbf{k}_{a'} = \ell_L - \mathbf{k}_a$). We further performed the change of variable $\ell_L = \mathbf{q}_L/d$. Both traversing bonds have thus arguments of the type \mathbf{Q}/d .

Fig. 3.1(c): In taking the limit $d \rightarrow \infty$, AA bonds become independent on \mathbf{q}/d and \mathbf{q}_L/d . They are, however, still dependent on \mathbf{k}_a . Integrability on this variable is assumed to be provided by these links, as in the single plasma. As regards the Fourier integrations, the product of AA links thus factorizes from the rest. The integral on \mathbf{q}_L converges as well, by the integrative factors provided by the AB bonds. Only one change of variable ($\ell_L = \mathbf{q}_L/d$) has been performed (corresponding to $I = 1$). In addition to the factor d^{-2} it provides, factors d^{-1} and d^{-4} arise from the traversing bonds, depending on their type.

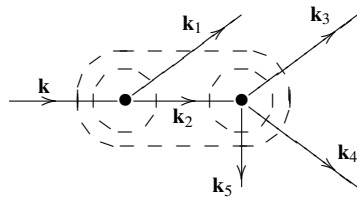
3.7.3 Determination of the factor $d^{-2I} = d^{-2(L-C)}$

We turn now to the determination of the number C , which will allow an immediate characterization of a graph's overall decay merely by looking at it. It is useful to that purpose to introduce a graphical representation of the Fourier conservation laws at the nodes of the diagram. Surrounding the immediate neighbourhood of a node by a closed path, one needs to impose the zero balance of the ingoing (+) and outgoing (−) Fourier vectors encountered along it:



$$\Rightarrow \mathbf{k} - \mathbf{k}_1 - \mathbf{k}_2 = 0. \quad (3.111)$$

Since the Fourier quantities are conserved at each node of the graph, the total amount of the ingoing vectors in a whole subgraph must match the total amount of the outgoing ones. As an example, let us consider two points in a diagram. Summing their two conservation relations yields a third one, necessarily independent of the Fourier variable travelling between the two points:



$$\begin{cases} \mathbf{k} - \mathbf{k}_1 - \mathbf{k}_2 = \mathbf{0} \\ \mathbf{k}_2 - \mathbf{k}_3 - \mathbf{k}_4 - \mathbf{k}_5 = \mathbf{0} \end{cases} \quad (3.112)$$

$$\stackrel{(+)}{\Rightarrow} \mathbf{k} - \mathbf{k}_1 - \mathbf{k}_3 - \mathbf{k}_4 - \mathbf{k}_5 = \mathbf{0}.$$

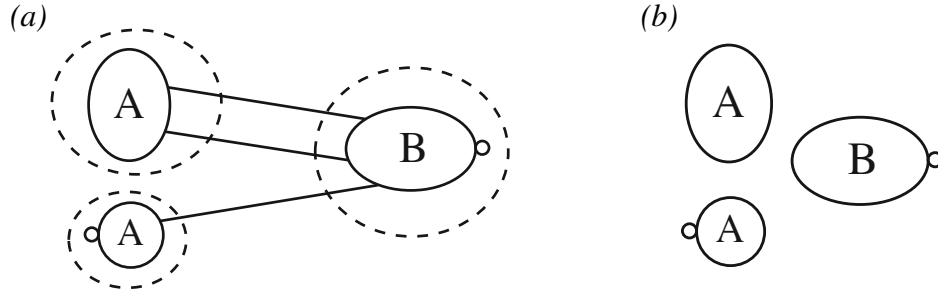


Figure 3.2: (a) A two-point graph with three sectors linked by traversing bonds (full lines). The three sectors are shown separately in (b). Encircling each sector by a closed path (dashed circles) defines relations involving only traversing Fourier variables.

The third equation corresponds graphically to the larger path englobing both points. Note that only two of these three equations (or paths) are independent. Graphically, a closed path is not independent from a second one, if it is deformable into the latter by “adding” (merging) or “subtracting” (detaching) other closed paths. (“Adding” the two dashed circles in (3.112) yields the larger path.)

The determination of the number C of a graph is now immediate. As said before, it corresponds to the number of relations that can be set between the L Fourier variables ℓ_1, \dots, ℓ_L of the crossing links. One thus only needs to determine the number of independent closed paths it is possible to draw in a way that they encounter only crossing bonds. It is clear that each A or B **sector** of the graph, *i.e.*, each piece one receives when cutting every traversing bond, defines such a relation (see Figure 3.2). However, if S is the number of these sectors, only $S - 1$ are independent from each other. Indeed, “adding” all S relations yields the trivial equation $\mathbf{q}/d = \mathbf{q}/d$. It is graphically equivalent to encircling the whole Mayer graph, and just asserts that the Fourier quantity entering the first root point is released at the second one. Consequently,

$$C = S - 1, \quad \implies I = L - S + 1.$$

Thus, the more the A and B sectors are interconnected, the faster the graph decays also by a reason of topology.

In the example presented in Section 3.7.2, the number of sectors is $S = 2$: one is constituted by the A root point together with the two internal points, and the other one by the B root point alone. Since $L = 2$, we recover that $I = 1$.

Note that $L \geq S - 1$ because the graphs are connected. Furthermore, $S \geq 2$ by the fact that the root points lie in different plasmas. These bounds correctly ensure that $0 \leq I \leq L - 1$, or $1 \leq C \leq L$, as stated in the article. The case $I = L - 1$ is obtained, *e.g.*, when there are L parallel AB paths stretched out between the

root points. The case $I = 0$ is of particular interest, since it concerns the slowest decaying diagrams. It is obtained for chains of A and B sectors, like in

$$\dots \xrightarrow{F_{BA}} \bullet \text{---} \underbrace{\hspace{1.5cm}}_A \text{---} \bullet \xrightarrow{F_{AB}} \bullet \text{---} \underbrace{\hspace{1.5cm}}_B \text{---} \bullet \xrightarrow{F_{BA}^R} \dots \quad (3.113)$$

We can show that if the graphs are connected and without articulation points

$$I = 0 \Leftrightarrow \left\| \begin{array}{l} \text{the graph is a chain of } A \text{ and } B \\ \text{sectors like in (3.113).} \end{array} \right. \quad (3.114)$$

Proof: \Rightarrow : from each sector not containing a root point, (at least) two traversing bonds must leave — otherwise, there is an articulation point. Thus, we attach two “half” bonds per such sector. From the two sectors A and B having each one root point, at least one traversing bond must leave — otherwise, there is no path between the two root points, and again an articulation point: the root point itself. We also attach a half bond to each of these root sectors. Having no more bonds at disposal, the only way of assembling the sectors together to recompose whole bonds is to form a chain graph. The direction \Leftarrow is straightforward.

3.8 Towards subleading orders of the force

3.8.1 Leading and subleading orders of the Ursell function

We emphasize that to a graph of h_{AB} is not associated a single power of d^{-1} . The decays (3.108) obtained for the graphs are only minimal. Higher-order contributions are understood.

Dominant graphs

From (3.108), the slowest possible decay of a graph is d^{-1} . It is attained when $I = 0$ and when there is only one crossing bond, a single F_{AB} one. The dominant component of $h_{AB}(1, 2, \frac{\mathfrak{q}}{d})$ is thus given by

$$\mathfrak{d} \left(\bigcirc + \xrightarrow{F_{AA}} \bullet + \frac{\delta}{\rho_A} \right) \bullet \xrightarrow{F_{AB}} \bullet \left(\bigcirc + \bigcirc \xrightarrow{F_{BB}} \bullet + \frac{\delta}{\rho_B} \right) \mathfrak{p}, \quad (3.115)$$

where the symbol $\bigcirc \bullet$ [corresponding to h_{AA}^{nn} or h_{BB}^{nn} in (3.77)] represents the sum of the graphs (in A or B) whose root points are not attached to the rest of the diagram by a single bond of type F [see (2.83), or, (3.77)]. In fact, these graphs build up the whole leading contribution $\propto d^{-1}$ and the whole subleading contribution $\propto d^{-2}$ of h_{AB} , as will be clear from the discussion below.

Minimal decay of the other graphs

An important consequence of the presence of the factor d^{-2I} in (3.108), is that aside from the class of graphs $O(d^{-1})$ building (3.115), *all other graphs are at least*

$$O(d^{-3}). \quad (3.116)$$

Indeed, d^{-2I} supplements a minimal factor d^{-2} except when $I = 0$. In this latter case, the graph is a chain of A and B sectors of the type (3.113), but it has to count an odd number of traversing links because the two root points lie in different plasmas. The graphs having one crossing link either build the contribution (3.115), if the traversing link is F_{AB} , or are $O(d^{-4})$ if it is F_{AB}^R . Having three or more crossing links necessarily results in a graph $O(d^{-3})$.

Leading and subleading orders of the Ursell function

The asymptotic value of the correlation h_{AB} across the two plasmas is given by taking the limit $d \rightarrow \infty$ on (3.115). In that limit, the asymptotic factorization of F_{AB} can be used, and

$$h_{AB}(1, 2, \frac{q}{d}) \stackrel{d \rightarrow \infty}{\sim} - \frac{1}{\beta d} \frac{q}{4\pi \sinh q} \frac{G_A^0(1, 0, \mathbf{0})}{e_{\alpha_0}} \frac{G_B^0(0, 2, \mathbf{0})}{e_{\beta_0}}, \quad (3.117)$$

as already seen in (2.84) or (3.79).

Since the graphs other than (3.115) result in $O(d^{-3})$ contributions to $h_{AB}(1, 2, \frac{q}{d})$, the next order of the Ursell function is contained in the deviation of (3.115) from its limiting value (3.117):

$$\begin{aligned} & \left(\left(\bigcirc + \frac{F_{AA}}{\rho_A} \bullet \bigcirc + \frac{\delta}{\rho_A} \right) \bullet \frac{F_{AB}}{\rho_A} \bullet \left(\bigcirc + \bigcirc \frac{F_{BB}}{\rho_B} + \frac{\delta}{\rho_B} \right) \right) - \frac{(-1)}{\beta d} \frac{q}{4\pi \sinh q} \frac{G_A^0(1, 0, \mathbf{0})}{e_{\alpha_0}} \frac{G_B^0(0, 2, \mathbf{0})}{e_{\beta_0}} \\ & = O(d^{-2}). \end{aligned} \quad (3.118)$$

Determining this deviation is still an open problem. The task is difficult, for the sources leading to an additional factor d^{-1} are numerous:

- all densities $\rho_A(i)$ and $\rho_B(j)$ of the plasmas under mutual influence are likely to tend at a rate $\propto d^{-1}$ towards the densities $\rho_A^0(i)$ and $\rho_B^0(j)$ of the individual plasmas;
- all noncrossing bonds or two-point subgraphs, like $G_{AA}(\frac{q}{d})$ or $G_{BB}(\frac{q}{d})$, depend upon d in two ways: explicitly in their argument, and implicitly by the fact that they tend towards their single plasma counterparts, G_A^0 and G_B^0 ;

- the traversing bond $F_{AB}(\frac{q}{d})$, also tends towards its asymptotic factorization (2.82) at a rate $\propto d^{-1}$.

The problem of characterizing the amplitudes of these $O(d^{-1})$ deviations is difficult to tackle, for these quantities are interrelated: the Mayer bonds are defined by density-weighted convolution chains of the Coulomb potential, and the density depends on the two-point correlation function by the first Born–Green–Yvon equation.

A preliminary analysis of the difference $\rho_A(1) - \rho_A^0(1)$ calculated at lowest order in the coupling parameter, following the methods of J.-N. Aqua and Cornu (2001a, 2001b), has revealed that it indeed vanishes as $O(d^{-1})$ as $d \rightarrow \infty$.

Comment on resummed graphs in activity

An alternative way of analysing the interplasma correlations as $d \rightarrow \infty$ would have been to investigate the resummed Mayer series of $h_{AB}(1, 2, \frac{q}{d})$ in *activity*.

The main advantage of this point of view is that the activity weights

$$z_A(1) = e^{\beta\mu_{\gamma_1}} e^{-\beta V_A^{\text{walls}}(\mathbf{r}_1, \gamma_1)}, \quad z_B(2) = e^{\beta\mu_{\gamma_2}} e^{-\beta V_B^{\text{walls}}(\mathbf{r}_2, \gamma_2)} \quad (3.119)$$

are independent of the separation d (once particles in plasma B are measured from its inner border). The resummation procedure of these graphs makes a second type of weight emerge, which depends on d . Namely, $W(1) = e^{I(1)} - 1$, where $I(1)$ is the sum of Coulomb convolution chains closed in a loop. However, the integrated points of this chain are d -independent activity weights, so that the behaviour as $d \rightarrow \infty$ of $W_A(1)$ and $W_B(2)$ can be investigated easily.

The main drawbacks of graphs in activity is that they can have *articulation points*, and that the perfect screening sum rule involved in the Casimir force implies *density-weighted* integrals (they express the shielding of *charges*). These densities need to be reconstructed by resumming parts of the z -weighted diagrams.¹⁶

Activity-weighted Mayer graphs may be used as an alternative to the first Born–Green–Yvon equation mentioned above to analyse how $\rho_A(1)$ and $\rho_B(2)$ deviate from their limits $\rho_A^0(1)$ and $\rho_B^0(2)$.

¹⁶Consistently, (3.114) no longer holds: nonchain diagrams contribute to the asymptotic correlation. One indeed needs to attach articulated subgraphs at z -integrated points so as to reconstruct the densities involved in the correlations G_A^0 and G_B^0 .

3.8.2 On subleading contributions to the classical force

The complete form of the subdominant term $\propto d^{-4}$ of the Casimir force is naturally as difficult to exhibit. In principle, any length λ can induce a correction of the type

$$\frac{1}{d^3} \frac{\lambda}{d}. \quad (3.120)$$

A microscopic theory like ours provides a vast number of such lengths. They can be the thicknesses a and b , the screening length λ_D , the mean interparticle distance a_ρ , etc., but also less obvious ones like mean dipole lengths of screening clouds (see below). Physically, the difficulty originates in the fact that subdominant orders are not necessarily universal any more. They may involve integrals of correlation functions that do not necessarily reduce to simple values by means of sum rules, as shows the following example.

Multipole moment contributions: a whole series of higher order contributions to the force arise from the expansion of the microscopic Coulomb force $(\partial_x v_{AB})(1, 2, \frac{\mathbf{q}}{d})$ in (2.51):

$$(\partial_x v_{AB})(1, 2, \frac{\mathbf{q}}{d}) = 2\pi e^{-q} e^{-\frac{q|x_1|}{d}} e^{-\frac{q|x_2|}{d}} = 2\pi e^{-q} - 2\pi e^{-q} \frac{q(|x_2|+|x_1|)}{d} + \mathcal{O}(d^{-2}). \quad (3.121)$$

The first term of this expansion was used to retrieve the asymptotic Casimir force. For the contribution of the second term, one can use again the asymptotic factorized form of the Ursell function, resulting in a term

$$\frac{\pi^3}{480\beta d^4} \left[\int_0^b dx_2 |x_2| \sum_{\gamma_2} e_{\gamma_2} \rho_B^0(2) \frac{G_B^0(0, 2, \mathbf{0})}{e_{\beta_0}} + \int_{-a}^0 dx_1 |x_1| \sum_{\gamma_1} e_{\gamma_1} \rho_A^0(1) \frac{G_A^0(1, 0, \mathbf{0})}{e_{\alpha_0}} \right]. \quad (3.122)$$

The macroscopic length constituted by each integral term is associated to the total dipole moment along x carried by the screening cloud around the fixed charge at the boundary. In a bulk geometry, this screening cloud is symmetric and the dipole moment vanishes in average. This result is known as the dipole sum rule (Martin, 1988, Form. (1.22)). Obviously, it no longer can hold when the cloud forms against a wall, so that this dipole moment is nonzero.¹⁷

¹⁷Note, however, that the integrals occurring above involve the functions G_A^0 or G_B^0 , which consist in the Ursell functions h_A^0 or h_B^0 and a subtracted term defined in terms of the Debye–Hückel potential, see (3.82). Still, it is unlikely that a cancellation occurs by this subtraction because the dipole length is nonuniversal: in the simplified Debye–Hückel theory (with flat density profiles), it coincides with the screening length.

One can similarly exhibit higher-order terms in powers of d^{-1} from (3.121). They will involve the multipole moments of the wall-constrained screening cloud induced around the fixed charge.

The other $O(d^{-4})$ contributions to the force necessitate the knowledge of the subdominant orders of the Ursell function.

Debye–Hückel approximation: an explicit expression for the $\propto d^{-4}$ correction to the force can be exhibited on the level of the simplified Debye–Hückel theory with flat profiles (see Section 3.4): one can calculate the $\propto d^{-4}$ contribution given by the approximate correlation $-\beta e_{\gamma_1} e_{\gamma_2} \varphi_{AB}(x, x', \mathbf{k})$ (3.41). Instead of immediately integrating its explicit form in the force formula similarly to what do Jancovici and Šamaj (2004, Form. (3.44)), let us take another route, more prone to a generalisation to the full correlations. On this Debye–Hückel level, the term (3.122) has the functions G_A^0 and G_B^0 (arising from the factorisation of the full correlation) replaced by φ_A^0 and φ_B^0 (emerging from the factorization of φ_{AB}). In this case, the dipole length correction term reads

$$\frac{\pi^3}{480\beta d^4} (\lambda_{D,A} + \lambda_{D,B}), \quad (3.123)$$

where $\lambda_{D,A} = \kappa_A^{-1}$ and $\lambda_{D,B} = \kappa_B^{-1}$ are the screening lengths assumed constant along the semi-infinite plasmas. The remainder of the contribution $\propto d^{-4}$ is contained in the deviation of φ_{AB} from its factorized limit (3.44), say $\varphi_{AB}^{\text{fact.}}$. This deviation is found to be

$$\begin{aligned} (\varphi_{AB} - \varphi_{AB}^{\text{fact.}})(x_1, x_2, \frac{\mathbf{q}}{d}) &= \varphi_{AB}^{\text{fact.}} \left[\frac{\varphi_{AB}}{\varphi_{AB}^{\text{fact.}}} - 1 \right] \\ &\stackrel{d \rightarrow \infty}{\sim} \varphi_{AB}^{\text{fact.}}(x_1, x_2, \frac{\mathbf{q}}{d}) \frac{(-q)}{d} \frac{e^q + e^{-q}}{e^q - e^{-q}} (\lambda_{D,A} + \lambda_{D,B}). \end{aligned} \quad (3.124)$$

This Formula can be proven by using the explicit expressions for φ found in the article. Better, it can also be retrieved by keeping all next subdominant terms in the summation of the dominant Coulomb convolution chains building φ_{AB} , presented in Section 2.5.3 for Φ_{AB} [Equations (2.66)–(2.81)]. In this case, one arrives first at

$$\begin{aligned} \varphi_{AB}(x_1, x_2, \frac{\mathbf{q}}{d}) &= \frac{qe^{-q}}{2\pi d(1 - e^{-2q})} \varphi_A^0(x_1, 0, \frac{\mathbf{q}}{d}) \varphi_B^0(0, x_2, \frac{\mathbf{q}}{d}) \\ &\quad - \frac{q^2 e^{-q} e^{-2q}}{(2\pi d)^2 (1 - e^{-2q})^2} [\varphi_A^0(0, 0, \mathbf{0}) + \varphi_B^0(0, 0, \mathbf{0})] \varphi_A^0(x_1, 0, \mathbf{0}) \varphi_B^0(0, x_2, \mathbf{0}) \\ &\quad + O(d^{-3}). \end{aligned} \quad (3.125)$$

The first term, when evaluated at $\mathbf{q}/d = 0$ corresponds to $\varphi^{\text{fact.}}$. For a single semi-infinite plasma, one can show (using the explicit expression of φ_A^0) that

$$\left. \frac{\partial}{\partial k} \right|_{\mathbf{k}=0} \varphi_A^0(x, x', k) = \frac{-1}{4\pi} \varphi_A^0(x, 0, \mathbf{0}) \varphi_A^0(0, x', \mathbf{0}). \quad (3.126)$$

This result is in accordance with the sum rule (3.24) of (Martin, 1988) on this simplified Debye–Hückel level. Using it to expand the product $\varphi_A^0(\mathbf{q}/d) \varphi_B^0(\mathbf{q}/d)$ at first order in q/d , one reconstructs in (3.125) a term similar to the second term. Thus,

$$\begin{aligned} \varphi_{AB}(x_1, x_2, \frac{\mathbf{q}}{d}) &= \varphi_{AB}^{\text{fact.}}(x_1, x_2, \mathbf{q}, d) \\ &\quad - \left(\frac{q^2 e^{-q}}{8\pi^2 d^2 (1 - e^{-2q})} + \frac{q^2 e^{-q} e^{-2q}}{(2\pi d)^2 (1 - e^{-2q})^2} \right) \\ &\quad \times [\varphi_A^0(0, 0, \mathbf{0}) + \varphi_B^0(0, 0, \mathbf{0})] \varphi_A^0(x_1, 0, \mathbf{0}) \varphi_B^0(0, x_2, \mathbf{0}) + \mathcal{O}(d^{-3}). \end{aligned} \quad (3.127)$$

This expression is equivalent to (3.124) once it has been recognised that

$$\frac{1}{4\pi} \varphi_A^0(0, 0, \mathbf{0}) = \int_{-\infty}^0 dx |x| \frac{(\kappa_A^0)^2(x)}{4\pi} \varphi_A^0(x, 0, \mathbf{0}) = \lambda_{D,A} \quad (3.128)$$

is the mean dipole length of the screening cloud of a charge at the inner surface of the plasma. (The same holds for $\varphi_B^0(0, 0, \mathbf{0})$.) The relation (3.128) is easily obtained by suitably integrating on $(-\infty, 0)$ the Poisson–Boltzmann equation for φ_A^0 .

Inserting the asymptotic deviation (3.124) into the force formula with (3.44) to express $\varphi_{AB}^{\text{fact.}}$ results in

$$\begin{aligned} &\frac{1}{\beta d^4} (\lambda_{D,A} + \lambda_{D,B}) \left[\int \frac{d\mathbf{q}}{(2\pi)^2} 2\pi e^{-q} \frac{q}{4\pi \sinh q} \frac{q(e^q + e^{-q})}{e^q - e^{-q}} \right] \\ &\times \left[\int_{-\infty}^0 dx_1 \frac{\kappa_A^2}{4\pi} \varphi_A^0(x_1, 0, \mathbf{0}) \right] \left[\int_0^{\infty} dx_2 \frac{\kappa_B^2}{4\pi} \varphi_B^0(0, x_2, \mathbf{0}) \right]. \end{aligned} \quad (3.129)$$

The \mathbf{q} integral reduces to $\frac{1}{4\pi} \left[-\frac{\pi^4}{120} + \frac{3\zeta(3)}{2} \right]$. The other integrals give unity by the perfect screening sum rule. Adding this contribution to (3.123) results in the total subdominant term.¹⁸ Consequently,

$$f^{\text{DH,flat}}(d) = -\frac{\zeta(3)}{8\pi\beta d^3} \left[1 - \frac{3}{d} (\lambda_{D,A} + \lambda_{D,B}) + \mathcal{O}(d^{-2}) \right]. \quad (3.130)$$

¹⁸Note the exact cancellation of the dipole term (3.123). Such a cancellation is likely to still occur when taking into account structured profiles. However, other sources of subdominant terms will arise, also if the plasmas are of finite thickness.

This result coincides with (Jancovici & Šamaj, 2004, Form. (3.45)) when the plasmas A and B are taken identical so that $\lambda_{D,A} = \lambda_{D,B}$. We see that although screening mechanisms have been used, a nonuniversal character remains.

Added note in Appendix 3.A

Bound of Φ independent of the thickness: as long as $a \gtrsim \lambda_D$, the bound (3A.11) of $\Phi(x, x', \mathbf{k})$ can be rendered uniform with respect to a , involving a function $\varphi^>(x, x')$ showing good integrability properties in the bulk. This may be useful to commute $\lim_{a \rightarrow \infty}$ limits and spatial integrals of the Debye–Hückel potential by dominated convergence. One can simply bound further the a -dependent function $\varphi^>(x, x', a)$ given in (3A.8)–(3A.10), on the basis that

$$\frac{\cosh \kappa(a - |x|)}{\sinh \kappa a} = \frac{e^{-\kappa|x|}}{1 - e^{-2\kappa a}} + \frac{e^{-2\kappa a} e^{\kappa|x|}}{1 - e^{-2\kappa a}} \stackrel{a \geq |x|}{\leq} \frac{2e^{-\kappa|x|}}{1 - e^{-2\kappa a}} \stackrel{\kappa a \geq 1}{\leq} C e^{-\kappa|x|}. \quad (3.131)$$

This leads to

$$\varphi^>(x, x', a) \leq C \varphi^>(x, x'), \quad (3.132)$$

where $\varphi^>(x, x') = \lim_{a \rightarrow \infty} \varphi^>(x, x', a)$ is the bound obtained for semi-infinite plasmas (3.46)–(3.47) and $C \geq 2/(1 - \exp(-2\kappa a))$.

Chapter 4

Field-coupled quantum plasmas: path integral representation

Contents

Equilibrium correlations in charged fluids coupled to the radiation field, <i>Phys. Rev. E</i> , 73, 036113, 1–14 (2006)	115
4.1 Introduction	115
4.2 The model	118
4.3 The gas of charged loops and the effective magnetic interaction	120
4.4 Two quantum charges in a classical plasma	125
4.5 Particle correlations in the many-body system	128
4.6 Transverse field correlations	132
4.7 Bose and Fermi statistics	136
4.8 Concluding remarks	138
Appendix 4.A	140
Appendix 4.B	141
Appendix 4.C	141
Appendix 4.D	142
References	142

This chapter deviates temporarily — but importantly — from the Casimir force investigation. It constitutes a part on its own, where the formalism necessary to the inclusion of the radiation field into the statistical mechanical description of the charged system is developed. Indeed, we have mentioned in Chapter 2.2.1 that

because of the Bohr–van Leeuwen theorem, matter and field decouple when they are both treated classically. To improve the classical model of electrostatically interacting charges and include the magnetic part of the Lorentz forces exerting between the two slabs, it is necessary to take into account quantum mechanics.

In the article to be found hereunder [Equilibrium correlations in charged fluids coupled to the radiation field, *Phys. Rev. E*, 73, 036113, (2006); see p. 115] the path integral formulation of quantum statistical mechanics for electrostatic matter is extended by including a thermalised radiation field interacting with the charges. The field is kept *classical*, but the particles are *quantum-mechanical*.

Without field, this well-known formalism makes use of the Feynman–Kac path integral to represent the integral kernel of the quantum propagator in imaginary time (corresponding to the integrated Gibbs weight) in terms of an auxiliary statistical system: that of **loops** (or “polymers”). They consist in classical but extended objects of random Brownian shape. This stochastic shape represents the quantum-mechanical fluctuations of the positions of the particles; it is scaled by the thermal de Broglie wavelength. Such a representation has now been long studied. Presentations of it can be found in (Martin, 2003; Høye & Stell, 1994). We will briefly recall its main features below.

The inclusion of field’s degrees of freedom in the loop formalism is performed by means of the Feynman–Kac–Itô path integral. The field intervenes in this representation in a convenient form, that allows its exact (Gaussian) integration. The effect of this integration is to add an effective “magnetic” pair potential between the loops. We will also illustrate these steps below. The same kind of method has been employed by Høye and Stell (1981); Brevik and Høye (1988) in the case of harmonic oscillators interacting with the field by a “spin”-field coupling term. Integration of the field’s degrees of freedom yielded an effective potential between the fluctuating dipoles.

The article comprises the following points:

- The microscopic model is presented in a first stage. This model corresponds to the one exposed in Chapter 2 (except for the geometry).
- It is then exposed how, by the use of the Feynman–Kac–Itô path integral, one comes to integrate field’s degrees of freedom, which yields an effective magnetic pair interaction between loops.
- The method is applied to retrieve the large-distance behaviour of the density correlations in a bulk plasma. It is shown that the algebraic decay $\sim r^{-6}$ induced by the imperfect screening of multipoles in quantum charged systems has its amplitude modified by the inclusion of the field: small contributions of order $O((\beta mc^2)^{-2})$ are added. This is first illustrated between

two quantum charges in a classical plasma, and then extended to the full quantum-mechanical system of charges.

- The formalism proves to be well-adapted too to the investigation of transverse field correlations in the charged fluids. A coupling term linear in the field is added to the Hamiltonian. The field's moments and correlations can then be retrieved by functional differentiation, in particular, after its integration has led to the magnetic effective interaction. Total field correlations are calculated. Because their long range contradicts Landau and Lifshitz' results, it is suggested that spatial dispersion (a wave-dependent dielectric function) should be used in their theories.

This work was mainly the subject of the master thesis of Sami el Boustani (2005). I contributed to it more specifically in the investigation of the asymptotic particle correlations in the many-body system and in the investigation of the transverse field correlations.

Erratum

A small error has been found in the article. It concerns the order of decay when $\hbar \rightarrow 0$ of a constant involved in the asymptotic field correlations. The footnotes 12 and 13 have been added to rectify this decay order from $O(\hbar^4)$ to $O(\hbar^2)$.

The loop formalism without field

We recall the basic formulae at which one arrives when the Feynman–Kac path integral representation of the Gibbs weight is used (*i.e.*, when no radiation field is coupled to matter). We assume in this paragraph that the quantum charges interact via the Coulomb potential, and that they are confined to a finite volume of extension L . In a first stage, we assume that they obey Maxwell–Boltzmann statistics (MB). We will then present the formulae when the Bose or Fermi statistics of the particles is taken into account.

The grand-canonical partition function $Z_L^{\text{MB}}(T, \mu)$ of the quantum system is defined as the trace of the Gibbs weight:

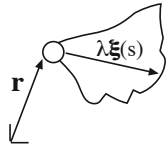
$$Z_L^{\text{MB}}(T, \mu) = \sum_{\{N_\gamma\}}^{0 \dots \infty} \left[\prod_{\gamma} \frac{z(\gamma)^{N_\gamma}}{N_\gamma!} \right] \int d\mathbf{r}_1 \dots d\mathbf{r}_N \langle \mathbf{r}_1 \dots \mathbf{r}_N | e^{-\beta H_N} | \mathbf{r}_1 \dots \mathbf{r}_N \rangle. \quad (4.a)$$

The integral kernel of the Gibbs weight can be conveniently represented by using the Feynman–Kac path integral formalism as follows. The integral kernel of the quantum-mechanical propagator is known to be equal to a functional integral of

the exponential of the action over classical trajectories $\mathbf{r}(t)$ (Feynman & Hibbs, 1965). For one particle subject to an external potential $V^{\text{walls}}(\mathbf{r})$, one has

$$\langle \mathbf{r} | e^{-i\frac{Ht}{\hbar}} | \mathbf{r} \rangle = \int_{\mathbf{r}(0)=\mathbf{r}}^{\mathbf{r}(t)=\mathbf{r}} d[\mathbf{r}(\cdot)] e^{i\int_0^t ds \frac{1}{2} m \dot{\mathbf{r}}(s)^2} e^{-i\int_0^t ds V^{\text{walls}}(\mathbf{r}(s))}. \quad (4.b)$$

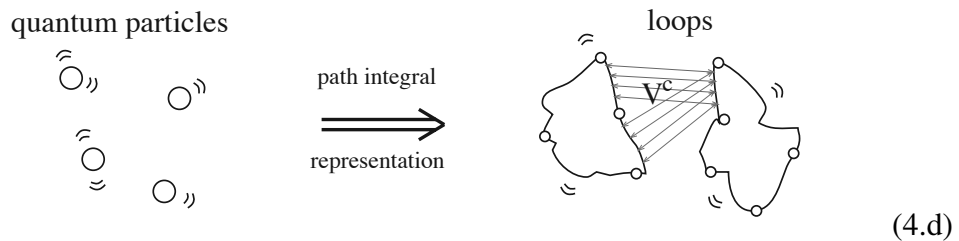
The two exponentials correspond to the “kinetic” and “potential” terms of the Lagrangian. Evaluating this formula at an imaginary time $\beta = it/\hbar$, and after suitable changes of variables, one can express it as

$$\langle \mathbf{r} | e^{-\beta H} | \mathbf{r} \rangle \propto \int \underbrace{d[\boldsymbol{\xi}(\cdot)] e^{-\frac{1}{2} \int_0^1 ds \dot{\boldsymbol{\xi}}(s)^2}}_{D(\boldsymbol{\xi})} \exp \left[-\beta \underbrace{\int_0^1 ds V^{\text{walls}}(\mathbf{r} + \lambda_\gamma \boldsymbol{\xi}(s))}_{\equiv V^{\text{walls}}(\mathbf{r}, \gamma, \boldsymbol{\xi}(\cdot))} \right] \quad (4.c)$$


where $\lambda_\gamma = \hbar \sqrt{\beta/m_\gamma}$ is the de Broglie wavelength of the particle. We can interpret this result by saying that to a quantum particle at \mathbf{r} is associated a closed random path $\mathbf{r} + \lambda_\gamma \boldsymbol{\xi}(s)$ situated at \mathbf{r} , whose extension represents the particle’s quantum-mechanical fluctuations of position. The quantum average of the Gibbs weight then corresponds to integrate over all such random paths [by means of $D(\boldsymbol{\xi})$] the Gibbs weight of the potential felt all along. The normalised Gaussian functional integral $D(\boldsymbol{\xi})$ corresponds to the Wiener integral of a Brownian process. This formula can be easily generalised to several particles.

Then, in the ensemble integrals yielding Z_L^{MB} , one may consider the arising $D(\boldsymbol{\xi}_1) \dots D(\boldsymbol{\xi}_N)$ as being part of the degrees of freedom of extended but classical-like objects, called “loops” or “filaments”, whose interactions are derived from the primitive interactions between the quantum particles, as above.

When the Bose–Fermi statistics of the particles is taken into account, essentially the same holds, except that “loops” will be constituted by gathering in a closed path open Brownian paths of several particles:



The grand-canonical partition function $Z_L(T, \boldsymbol{\mu})$ of the properly symmetrized quan-

tum system can then be exactly represented, in terms of these loops, as

$$Z_L(T, \boldsymbol{\mu}) = \sum_{n=0}^{\infty} \frac{1}{n!} \prod_{i=1}^n d\mathcal{L}_i z(\mathcal{L}_i) e^{-\beta[\sum_{i<j} e_{\gamma_i} e_{\gamma_j} V^c(\mathcal{L}_i, \mathcal{L}_j) + \sum_{i=1}^n V^{\text{walls}}(\mathcal{L}_i)]}. \quad (4.e)$$

A loop $\mathcal{L} = (\mathbf{r}, \chi) = (\mathbf{r}, \gamma, q, \mathbf{X}(\cdot))$ is made of a position \mathbf{r} in the real space, and internal degrees of freedom χ , which comprise a species γ , an integral charge number $q \in 1, 2, \dots$, and a closed Brownian shape $\mathbf{X}(s)$, $s \in [0, q]$, $\mathbf{X}(0) = \mathbf{X}(q) = \mathbf{0}$. The loop's spatial extension is scaled by $\lambda_\gamma = \hbar \sqrt{\beta/m_\gamma}$, so that its path in space reads

$$\mathbf{r}^{[s]} = \mathbf{r} + \lambda_\gamma \mathbf{X}(s), \quad s \in [0, q]. \quad (4.f)$$

The integral number q is the number of original particles that the loop regroups. Their positions are at $\mathbf{r}^{[j]}$, $j = 0, \dots, q-1$. The shape $\mathbf{X}(s)$ is a Gaussian stochastic process whose functional integral has unit normalization, zero mean, and covariance¹

$$\int D(\mathbf{X}) X^\mu(s_1) X^\nu(s_2) = \delta_{\mu\nu} q \left[\min \left\{ \frac{s_1}{q}, \frac{s_2}{q} \right\} - \frac{s_1 s_2}{q^2} \right]. \quad (4.g)$$

Integrating on all internal degrees of freedom of the loop means

$$\int d\mathcal{L} \dots = \int d\mathbf{r} \int d\chi \dots = \int d\mathbf{r} \sum_\gamma \sum_{q=1}^{\infty} \int D(\mathbf{X}) \dots \quad (4.h)$$

The two-loop ‘‘Coulomb’’ potential V^c occurring in (4.e) above, reads

$$V^c(\mathcal{L}_i, \mathcal{L}_j) = \int_0^{q_i} ds_i \int_0^{q_j} ds_j \delta(\tilde{s}_i - \tilde{s}_j) \frac{1}{|\mathbf{r}_i + \lambda_{\gamma_i} \mathbf{X}_i(s_i) - \mathbf{r}_j - \lambda_{\gamma_j} \mathbf{X}_j(s_j)|} \quad (4.i)$$

($\tilde{s} = s \bmod 1$). Note that due to the Feynman–Kac representation, Coulomb interaction only occurs at ‘‘equal times’’ in the unit portions of the two loops, as depicted in (4.d). The confinement of the particles into the volume results in the confinement of the whole loop's path ($\forall s$) into that volume. This loop confinement is represented here by the wall potential $V^{\text{walls}}(\mathcal{L})$. The loop activity $z(\mathcal{L})$ embodies the Bosonic ($\eta_\gamma = +1$) or Fermionic ($\eta_\gamma = -1$) character of the particles, and the loop's self energy, which consists in the interaction energy of the original particles that the loops contains:

$$z(\mathcal{L}) = \frac{(2s_\gamma + 1)(\eta_\gamma)^{q-1}}{q} \frac{(e^{\beta\mu_\gamma})^q}{(2\pi q \lambda_\gamma^2)^{3/2}} e^{-\beta U^{\text{self}}(\mathcal{L})}. \quad (4.j)$$

When the Hamiltonian is spin-independent (which is the case in our models), considering the spin of the particles merely adds to the activity the factor $2s_\gamma + 1$ above.

¹We recall that Gaussian integrals are entirely determined by these three properties.

Inclusion of the field: the effective magnetic potential

One can summarize the steps extending the loop formalism so as to include the field as follows.

The total partition function of matter and field $Z_{K,L}$ (2.12), when normalized by the free field partition function $Z_{0,K}^{\text{rad}}$, can be interpreted as the field-average of the partition function $Z_{K,L}^{\text{mat}}(T, \boldsymbol{\mu}, \mathbf{A})$ of matter embedded in an *external* field $\mathbf{A}(\mathbf{r})$:

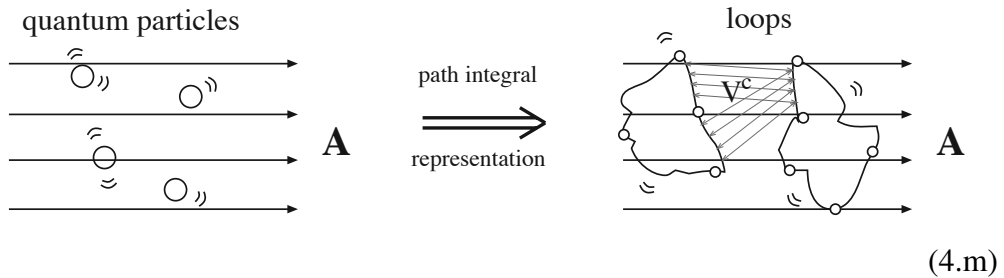
$$\frac{Z_{K,L}}{Z_{0,K}^{\text{rad}}} = \frac{1}{Z_{0,K}^{\text{rad}}} \int \prod_{\mathbf{k},\lambda} \frac{d^2 a_{\mathbf{k},\lambda}}{\pi} e^{-\beta H_0^{\text{rad}}} Z_{K,L}^{\text{mat}}(\mathbf{A}) \equiv \langle Z_{K,L}^{\text{mat}}(\mathbf{A}) \rangle_0^{\text{rad}} \quad (4.k)$$

(the pair \mathbf{k}, λ denotes a field mode in the large enclosing box K).

Loops in external field: at fixed field $\mathbf{A}(\mathbf{r})$, the Feynman-Kac-Itô path integral is used to represent the partition function $Z_{K,L}^{\text{mat}}(\mathbf{A})$ in terms of loops. At this stage, the loops interact with one another via the Coulomb-like potential V^c as above, but also interact with the external field through a one-loop potential. The loop energy is supplemented with

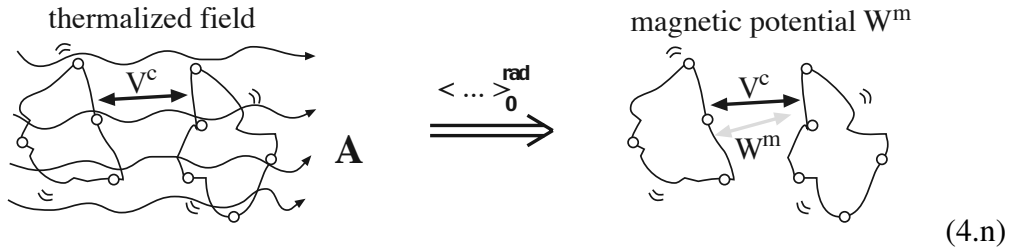
$$i \sum_j \frac{e_{\gamma_j} \lambda_{\gamma_j}}{\hbar c} \int_0^{q_j} d\mathbf{X}_j(s_j) \cdot \mathbf{A}(\mathbf{r}_j + \lambda_{\gamma_j} \mathbf{X}_j(s_j)) \equiv i \sum_{\mathbf{K},\lambda} [\mathbf{J}_{\mathbf{K},\lambda}^* \alpha_{\mathbf{K},\lambda} + \mathbf{J}_{\mathbf{K},\lambda} \alpha_{\mathbf{K},\lambda}^*]. \quad (4.l)$$

On the right hand side, a “loop current” density $\mathbf{J}_{\mathbf{K},\lambda} = \sum_j \mathbf{J}_{\mathbf{K},\lambda}(\mathcal{L}_j)$ is defined. The line-integrals on the left hand side run along the loops’ shape. They can be formally assimilated to the magnetic flux through the loops. Schematically, the system of thermalised quantum particles in an external field is represented by a system of thermalised classical-like loops in the same external field:



An essential advantage of the path integral representation is that the field–loop coupling (4.1) is classical and linear in the field, in contradistinction to the original field–particle coupling.

Loops in thermalised field: the next step is to compute the average of $Z_{K,L}^{\text{mat}}(\mathbf{A})$ in the thermally fluctuating field. The free field Hamiltonian H_0^{rad} is quadratic in the field amplitudes $\alpha_{\mathbf{k},\lambda}$, and the external field potential (4.1) linear in them. The current density $\mathbf{J}_{\mathbf{k},\lambda} = \sum_j \mathbf{J}_{\mathbf{k},\lambda}(\mathcal{L}_j)$ thus represents the vector of the Fourier transform with respect to $\alpha_{\mathbf{k},\lambda}$ of the Gaussian $\exp(-\beta H_0^{\text{rad}})$; the latter transform builds up a Gaussian $\exp[-(J, GJ)]$. By extracting the sums \sum_j included in the J s, this factor can be recast in the form $\exp[-\beta \sum_{i,j} e_{\gamma_i} e_{\gamma_j} W^m(\mathcal{L}_i, \mathcal{L}_j)]$, thereby providing the effective two-loop potential of magnetic origin.



After extending field's enclosing box $K \rightarrow \mathbb{R}^3$, the Fourier modes \mathbf{k} become continuous and one has, explicitly,

$$W^m(\mathcal{L}_i, \mathcal{L}_j) = \frac{1}{\beta \sqrt{m_{\gamma_i} m_{\gamma_j}} c^2} \sum_{\mu, \nu} \int \frac{d\mathbf{k}}{(2\pi)^3} [J_{\mathbf{k}}^\mu(\mathcal{L}_i)]^* J_{\mathbf{k}}^\nu(\mathcal{L}_j) G_{\mu\nu}(\mathbf{k}), \quad (4.o)$$

$$J_{\mathbf{k}}^\mu(\mathcal{L}) = \int_0^q dX^\mu(s) e^{i\mathbf{k} \cdot (\mathbf{r} + \lambda_\gamma \mathbf{X}(s))}, \quad G_{\mu\nu}(\mathbf{k}) = \frac{4\pi}{k^2} \left(\delta_{\mu\nu} - \frac{k_\mu k_\nu}{k^2} \right) |g(\mathbf{k})|^2. \quad (4.p)$$

Remarks

- The auxiliary system of the classical-like loops is an exact representation of the original quantum particles system. There are no approximations involved in this correspondence. It thus consists in a powerful tool, allowing the use of methods from classical statistical mechanics on the loops' system.
- The quantum character of the original particles gives the loops their extension, but also their particular Coulomb interaction, which does not correspond exactly to the classical one that would exert between uniformly charged wires, because of the “equal-time” Dirac condition.

Loop correlations and particle correlations

We recall that one can introduce one-loop, two-loop, *etc.*, correlations as for the particles, by defining the “microscopic loop density”

$$\hat{\rho}(\mathcal{L}) = \sum_{i=1}^n \delta(\mathcal{L}, \mathcal{L}_i), \quad (4.q)$$

where $\delta(\mathcal{L}, \mathcal{L}_i)$ is defined such that $\int d\mathcal{L}_1 \delta(\mathcal{L}, \mathcal{L}_1) \phi(\mathcal{L}_1) = \phi(\mathcal{L})$. The average $\rho(\mathcal{L}) = \langle \hat{\rho}(\mathcal{L}) \rangle$ of the loop density is taken in the phase space of loops. Such densities do not have a real physical meaning before integrating on the involved loop shapes. For example, the one-*particle* and two-*particle* correlation functions are given from the one-loop and two-loop correlations by (Ballenegger et al., 2002, Appendix D)

$$\rho(\mathbf{r}, \gamma) = \sum_{q=1}^{\infty} q \int D(\mathbf{X}) \rho(\mathcal{L}), \quad (4.r)$$

$$\begin{aligned} \rho(\mathbf{r}_1, \gamma_1; \mathbf{r}_2, \gamma_2) &= \sum_{q_1, q_2} q_1 q_2 \int D(\mathbf{X}_1) \int D(\mathbf{X}_2) \rho(\mathcal{L}_1, \mathcal{L}_2) \\ &+ \delta_{\gamma_1 \gamma_2} \sum_{q_2} q_2 \sum_{j=1}^{q_2-1} \int D(\mathbf{X}_2) \delta(\mathbf{r}_2 + \lambda_{\gamma_2} \mathbf{X}_2(j) - \mathbf{r}_1) \rho(\mathcal{L}_2). \end{aligned} \quad (4.s)$$

Equilibrium correlations in charged fluids coupled to the radiation field

Sami El Boustani, Pascal R. Buenzli² and Philippe A. Martin

Received November 22, 2005; accepted January 25, 2006

We provide an exact microscopic statistical treatment of particle and field correlations in a system of quantum charges in equilibrium with a classical radiation field. Using the Feynman-Kac-Itô representation of the Gibbs weight, the system of particles is mapped onto a collection of random charged wires. The field degrees of freedom can be integrated out, providing an effective pairwise magnetic potential. We then calculate the contribution of the transverse field coupling to the large-distance particle correlations. The asymptotics of the field correlations in the plasma are also exactly determined.

PACS numbers:

05.30.-d — Quantum statistical mechanics.

05.40.-a — Fluctuation phenomena, random processes, noise,
and Brownian motion

11.10.Wx — Finite-temperature field theory

4.1 Introduction

Thermal states of non relativistic particles interacting by the sole Coulomb potential are known to provide an adequate description of many states of matter. The introduction of magnetic interactions between the particles poses a novel problem since they are mediated by the coupling to the transverse part of the electromagnetic field. This immediately leads to consider the full system of matter in equilibrium with radiation : the relevant theory becomes then the thermal quantum electrodynamics (thermal QED).

²Electronic address: pascal.buenzli@epfl.ch

In order to go beyond pure electrostatics without facing the full QED, a number of studies rely on the Darwin approximation. Darwin has shown (Darwin, 1920), (Landau, Lifshitz, & Pitaevskii, 1984) that one can eliminate the transverse degrees of freedom of the field within the Lagrangian formalism up to order c^{-2} (c is the speed of light). A nice review of the derivation of the Darwin Lagrangian and a lucid discussion of its consequences can be found in (Essén, 1996). The resulting Darwin Hamiltonian can be used to investigate the equilibrium properties of the so called weakly relativistic plasmas; see the recent works of Appel and Alastuey (Alastuey & Appel, 1997), (Appel & Alastuey, 1998), (Appel & Alastuey, 1999) and earlier references therein. These authors have done a careful analysis of the domain of validity of the Darwin approximation and shown in particular that the predictions of the Darwin Hamiltonian on the tail of particle correlations in thermal states cannot be correct. Indeed the well-known Bohr–van Leeuwen theorem (Alastuey & Appel, 2000) asserts that classical (non-quantum) matter completely decouples from the radiation field. Thus the Darwin Hamiltonian, which treats the particles classically, should not predict any effect of the transverse field when used for thermal equilibrium computations. The Darwin approximation is, however, not deprived of any meaning in statistical physics. Indeed, the authors show in (Appel & Alastuey, 1999) that Darwin predictions about current correlations coincide with those of thermal QED in the restricted window of distances $\lambda_{\text{part}} \ll r \ll \lambda_{\text{ph}}$, where $\lambda_{\text{part}} = \hbar \sqrt{\beta/m}$ is the de Broglie thermal wavelength of the particles and $\lambda_{\text{ph}} = \beta \hbar c$ the thermal wavelength of the photons. But to determine the tail $r \gg \lambda_{\text{ph}}$ of the correlations in the presence of the radiation field, matter has to be treated quantum mechanically to avoid the conclusion of the Bohr–van Leeuwen theorem. The situation is similar to orbital diamagnetism in equilibrium, which is of quantum-mechanical origin.

In this work, we consider equilibrium states of non-relativistic spinless quantum charges coupled with the radiation field in the standard way (Section 4.2). We shall, however, treat the field classically on the ground that the large distances $r \gg \lambda_{\text{ph}}$ are controlled by the small wave numbers $\kappa \sim \frac{1}{r} \ll \frac{1}{\lambda_{\text{ph}}}$, implying $\beta \hbar \omega_{\mathbf{K}} \sim \frac{\lambda_{\text{ph}}}{r} \ll 1$. Hence only long-wavelength photons will contribute to the asymptotics which is expected to be adequately described by classical fields. The full QED model with quantized electromagnetic field will be studied in a subsequent work (see also comments in the concluding remarks, Section 4.8).

Our main tool will be the Feynman-Kac-Itô path integral representation of the degrees of freedom of the charges. The Feynman-Kac integral representation has been widely used to derive various properties of quantum Coulomb systems, in particular to determine the exact large-distance behaviour of the correlations; see (Cornu, 1996a), (Cornu, 1996b), and (Alastuey, 1994), (Brydges & Martin, 1999) for reviews. In this representation quantum charges become fluctuating charged

loops (closed Brownian paths), formally analogous to classical fluctuating wires carrying multipoles of all orders. These fluctuations are responsible for the lack of exponential screening in the quantum plasma and for an algebraic tail $\sim r^{-6}$ of the particle correlations (Alastuey & Martin, 1989).

Adding an external magnetic field produces a phase factor in the Feynman-Kac-Itô formula, whose argument is the flux of the magnetic field across the random loop. Correlations in the case of an homogeneous external magnetic field have been studied in (Cornu, 1998a, 1998b). When the particles are thermalized with the field, the latter becomes itself random and distributed according to the thermal weight of the free radiation. The system can be viewed as a classical-like system of random loops immersed in a random electromagnetic field. At this point, the field degrees of freedom can be exactly integrated out by means of a simple Gaussian integral since the Hamiltonian of free radiation is quadratic in the field amplitudes. One is then left with an effective pairwise current-current interaction between the loops which has a form similar to the magnetostatic energy between a pair of classical currents. For the sake of illustrating the basic mechanisms in a simple setting, this program is carried out in Section 4.3 with particles obeying Maxwell-Boltzmann statistics. Appropriate modifications needed to take into account the particle statistics (Bose or Fermi) are given in Section 4.7.

In Section 4.4 we apply the formalism to the determination of the asymptotic form of the correlation between two quantum particles embedded in a classical plasma. This simple model already illustrates the main features occurring in the general system. The effective magnetic interaction contributes to the r^{-6} tail, but its ratio to the Coulombic contribution is of the order of the square of the relativistic parameter $(\beta mc^2)^{-1} = (\lambda_{\text{part}}/\lambda_{\text{ph}})^2$.

In Section 4.5 we consider the generalization of the results obtained for two particles to the full system of quantum charges. The analysis relies on the technique of quantum Mayer graphs previously developed for Coulomb systems, and we merely point out the few changes that are needed to include the effective magnetic interactions.

Field fluctuations in plasmas have been studied for a long time at macroscopic scales, much larger than interparticle distances; see (Landau et al., 1984), (Felderhof, 1965) and references cited therein. In Section 4.6, we reexamine this question from a microscopic viewpoint and show that electromagnetic field correlations are always long ranged due to the quantum nature of the particles. This is in disagreement with the prediction of macroscopic theories. We come back to this point in the concluding remarks (Section 4.8). However, in the classical limit, we recover the fact already observed in (Felderhof, 1965) that the long-range behaviour of the longitudinal and transverse parts of the electric field correlations compensate exactly.

In Section 4.7, we generalise the formalism developed in Section 4.3 to in-

clude Bose and Fermi particle statistics. This is done as usual by decomposing the permutation group into cycles and grouping particles belonging to a cycle into an extended Brownian loop. When this is combined with the Feynman-Kac-Itô path integral representation of the particles, the system takes again a classical-like form: a collection of Brownian loops immersed in a classical random electromagnetic field. At this point the physical quantities can again be analyzed in terms of Mayer graphs comprising pairwise Coulomb and effective magnetic interactions, as in Section 4.5.

The methods presented in this paper have been applied to the study of the semi-classical Casimir effect (Buenzli & Martin, 2005), (Buenzli & Martin, 2006; Martin & Buenzli, 2006).

4.2 The model

We first consider the QED model for non-relativistic quantum charges (electrons, nuclei, ions) with masses m_γ and charges e_γ contained in a box $\Lambda \in \mathbb{R}^3$ of linear size L and appropriate statistics. The index γ labels the \mathcal{S} different species and runs from 1 to \mathcal{S} . The particles are in equilibrium with the radiation field at temperature T . The field is itself enclosed into a large box K with sides of length R , $R \gg L$. The Hamiltonian of the total finite volume system reads, in Gaussian units,

$$H_{L,R} = \sum_{i=1}^n \frac{\left(\mathbf{p}_i - \frac{e_{\gamma_i}}{c} \mathbf{A}(\mathbf{r}_i)\right)^2}{2m_{\gamma_i}} + \sum_{i<j}^n \frac{e_{\gamma_i} e_{\gamma_j}}{|\mathbf{r}_i - \mathbf{r}_j|} + \sum_{i=1}^n V^{\text{walls}}(\gamma_i, \mathbf{r}_i) + H_0^{\text{rad}}. \quad (4.1)$$

The sums run on all particles with position \mathbf{r}_i , momentum \mathbf{p}_i , and species index γ_i ; $V^{\text{walls}}(\gamma_i, \mathbf{r}_i)$ is a steep external potential that confines a particle in Λ . It can eventually be taken infinitely steep at the wall's position, implying Dirichlet boundary conditions—*i.e.*, vanishing of the particle wave functions at the boundaries of Λ . The electromagnetic field is written in the Coulomb (or transverse) gauge so that the vector potential $\mathbf{A}(\mathbf{r})$ is divergence free and H_0^{rad} is the Hamiltonian of the free radiation field. The Coulomb gauge is usually preferred for simplicity in situations where the particles are non-relativistic and high-energy processes are neglected (Cohen-Tannoudji, Dupont-Roc, & Grynberg, 1989). It has the advantage to clearly disentangle electrostatic and magnetic couplings in the Hamiltonian.

We impose periodic boundary conditions on the faces of the large box K .³ Hence expanding $\mathbf{A}(\mathbf{r})$ and the free photon energy H_0^{rad} in the plane-wave modes

³Periodic conditions are convenient here. We could as well choose metallic boundary conditions. Since the field region K will be extended over all space right away, the choice of conditions on the boundaries of K are expected to make no differences for the particles confined in Λ .

$\mathbf{k} = (\frac{2\pi n_x}{R}, \frac{2\pi n_y}{R}, \frac{2\pi n_z}{R})$ gives

$$\mathbf{A}(\mathbf{r}) = \left(\frac{4\pi\hbar c^2}{R^3}\right)^{1/2} \sum_{\mathbf{K}\lambda} g(\mathbf{k}) \frac{\mathbf{e}_{\mathbf{K}\lambda}}{\sqrt{2\omega_{\mathbf{K}}}} (a_{\mathbf{K}\lambda}^* e^{-i\mathbf{K}\cdot\mathbf{r}} + a_{\mathbf{K}\lambda} e^{i\mathbf{K}\cdot\mathbf{r}}) \quad (4.2)$$

$$H_0^{\text{rad}} = \sum_{\mathbf{K}\lambda} \hbar\omega_{\mathbf{K}} a_{\mathbf{K}\lambda}^* a_{\mathbf{K}\lambda} \quad (4.3)$$

where $a_{\mathbf{K}\lambda}^*$ and $a_{\mathbf{K}\lambda}$ are the creation and annihilation operators for photons of modes $(\mathbf{k}\lambda)$, $\mathbf{e}_{\mathbf{K}\lambda}$ ($\lambda = 1, 2$) are two unit polarization vectors orthogonal to \mathbf{k} , and $\omega_{\mathbf{K}} = cK$, $K = |\mathbf{k}|$. In (4.2), $g(\mathbf{k})$, $g(0) = 1$, is a real spherically symmetric smooth form factor needed to take care of the ultraviolet divergencies. It is supposed to decay rapidly beyond the characteristic wave number $K_c = mc/\hbar$ (see (Cohen-Tannoudji et al., 1989), chap. 3). Since we are interested in the large-distance $r \rightarrow \infty$ asymptotics, related to the small- \mathbf{k} behaviour $K \rightarrow 0$, the final result will be independent of this cut-off function.

The total partition function

$$Z_{L,R} = \text{Tr} e^{-\beta H_{L,R}} \quad (4.4)$$

is obtained by carrying the trace $\text{Tr} = \text{Tr}_{\text{mat}} \text{Tr}_{\text{rad}}$ of the total Gibbs weight over particles' and the field's degrees of freedom: namely, on the particle wave functions with appropriate quantum statistics and on the Fock states of the photons. The average values of observables $\langle O_{\text{mat}} \rangle = Z_{L,R}^{-1} \text{Tr} (e^{-\beta H_{L,R}} O_{\text{mat}})$ concerning only the particle degrees of freedom can be computed from the reduced thermal weight

$$\rho_{L,R} = \frac{\text{Tr}_{\text{rad}} e^{-\beta H_{L,R}}}{Z_{0,R}^{\text{rad}}}, \quad (4.5)$$

where $Z_{0,R}^{\text{rad}} = \text{Tr}_{\text{rad}} \exp(-\beta H_0^{\text{rad}})$ is the partition function of the free radiation field, as follows from the obvious identity

$$\langle O_{\text{mat}} \rangle = \frac{\text{Tr}_{\text{mat}} (O_{\text{mat}} \rho_{L,R})}{\text{Tr}_{\text{mat}} \rho_{L,R}}. \quad (4.6)$$

We shall perform the thermodynamic limit in two stages by first letting $R \rightarrow \infty$. Then $\rho_L = \lim_{R \rightarrow \infty} \rho_{L,R}$ defines the effective statistical weight of the particles in Λ immersed in an infinitely extended thermalized radiation field.

As discussed in the Introduction, in this paper we treat the electromagnetic field classically. This amounts to replacing the photon creation and annihilation operators in (4.2) and (4.3) by complex amplitudes $\alpha_{\mathbf{K}\lambda}^*$ and $\alpha_{\mathbf{K}\lambda}$. In this case, the free field distribution factorizes out as $\exp(-\beta H_{R,L}) = \exp(-\beta H_0^{\text{rad}}) \exp(-\beta H_A)$,

where

$$H_{R,L} = H_A + H_0^{\text{rad}}, \quad H_A = \sum_{i=1}^n \frac{\left(\mathbf{p}_i - \frac{e\gamma_i}{c} \mathbf{A}(\mathbf{r}_i)\right)^2}{2m_{\gamma_i}} + U_{\text{pot}}(\mathbf{r}_1, \gamma_1, \dots, \mathbf{r}_n, \gamma_n), \quad (4.7)$$

and U_{pot} is the total potential energy. Since the free radiation weight $\exp(-\beta H_0^{\text{rad}})$ is Gaussian, $\mathbf{A}(\mathbf{r}) = \mathbf{A}(\mathbf{r}, \{\alpha_{\mathbf{K}\lambda}\})$ can be viewed as a realization of a Gaussian random field, and the term $H_A = H_A(\{\alpha_{\mathbf{K}\lambda}\})$ becomes the energy of the particles in a given realization of the vector potential having Fourier amplitudes $\{\alpha_{\mathbf{K}\lambda}\}$.

The partial trace (4.5) becomes, explicitly,

$$\rho_{L,R} = \left\langle e^{-\beta H_A} \right\rangle_{\text{rad}}, \quad (4.8)$$

where for a general function $F(\{\alpha_{\mathbf{K}\lambda}\})$ of the mode amplitudes $\langle F \rangle_{\text{rad}}$ denotes the normalized Gaussian average over all modes⁴

$$\langle F \rangle_{\text{rad}} = \prod_{\mathbf{K}\lambda} \int \frac{d^2 \alpha_{\mathbf{K}\lambda}}{\pi} \left[\beta \hbar \omega_{\mathbf{K}} e^{-\beta \hbar \omega_{\mathbf{K}} |\alpha_{\mathbf{K}\lambda}|^2} \right] F(\{\alpha_{\mathbf{K}\lambda}\}). \quad (4.9)$$

Note that the stability of Coulombic matter and the existence of thermodynamics for extended systems are assured if at least one of the species obeys Fermi statistics (Lieb, 1976). In the next section, merely as a matter of simplifying the presentation, we compute the effective particle interactions defined by ρ_L ignoring quantum statistics. In this case, Maxwell-Boltzmann statistics requires the presence of an additional short-range repulsive potential $V_{\text{SR}}(\gamma_i, \gamma_j, |\mathbf{r}_i - \mathbf{r}_j|)$ in the Hamiltonian (4.1) to prevent the collapse of opposite charges and guarantee thermodynamical stability. The generalization to Fermi and Bose statistics will be given in Section 4.7.

4.3 The gas of charged loops and the effective magnetic interaction

We now introduce the Feynman-Kac-Itô path integral representation of the configurational matrix element $\langle \mathbf{r}_1, \dots, \mathbf{r}_n | e^{-\beta H_A} | \mathbf{r}_1, \dots, \mathbf{r}_n \rangle$ for the particles interacting with a fixed realization of the field. For a single particle of mass m and charge e in

⁴The classical field is expanded as in (4.2) and (4.3) with dimensionless amplitudes $\alpha_{\mathbf{K}\lambda}$. In fact there will be no \hbar dependence arising from the field, as seen by changing everywhere $\alpha_{\mathbf{K}\lambda} \mapsto \alpha_{\mathbf{K}\lambda} / \sqrt{\hbar}$.

a scalar potential $V^{\text{ext}}(\mathbf{r})$ and vector potential $\mathbf{A}(\mathbf{r})$, we first recall that this matrix element reads (Feynman & Hibbs, 1965), (Roespstorff, 1994), (Simon, 1979)

$$\begin{aligned} \langle \mathbf{r} | \exp \left(-\beta \left[\frac{1}{2m} \left(\mathbf{p} - \frac{e}{c} \mathbf{A}(\mathbf{r}) \right)^2 + V^{\text{ext}}(\mathbf{r}) \right] \right) | \mathbf{r} \rangle &= \left(\frac{1}{2\pi\lambda^2} \right)^{3/2} \int D(\boldsymbol{\xi}) \\ &\times \exp \left(-\beta \left[\int_0^1 ds V^{\text{ext}}(\mathbf{r} + \lambda \boldsymbol{\xi}(s)) - i \frac{e}{\sqrt{\beta m c^2}} \int_0^1 d\boldsymbol{\xi}(s) \cdot \mathbf{A}(\mathbf{r} + \lambda \boldsymbol{\xi}(s)) \right] \right). \end{aligned} \quad (4.10)$$

Here $\boldsymbol{\xi}(s)$, $0 \leq s \leq 1$, $\boldsymbol{\xi}(0) = \boldsymbol{\xi}(1) = \mathbf{0}$, is a closed dimensionless Brownian path and $D(\boldsymbol{\xi})$ is the corresponding conditional Wiener measure normalized to 1. It is Gaussian, formally written as $\exp \left(-\frac{1}{2} \int_0^1 ds \left| \frac{d\boldsymbol{\xi}(s)}{ds} \right|^2 \right) d[\boldsymbol{\xi}(\cdot)]$, with zero mean and covariance

$$\int D(\boldsymbol{\xi}) \xi^\mu(s_1) \xi^\nu(s_2) = \delta^{\mu\nu} (\min(s_1, s_2) - s_1 s_2) \quad (4.11)$$

where $\xi^\mu(s)$ are the Cartesian coordinates of $\boldsymbol{\xi}(s)$. In this representation a quantum point charge looks like a classical charged closed loop denoted by $\mathcal{F} = (\mathbf{r}, \boldsymbol{\xi})$, located at \mathbf{r} and with a random shape $\boldsymbol{\xi}(s)$ having an extension given by the de Broglie length $\lambda = \hbar \sqrt{\beta/m}$ (the quantum fluctuation). The magnetic phase in (4.10) is a stochastic line integral: it is the flux of the magnetic field across the closed loop. The correct interpretation of this stochastic integral is given by the rule of the middle point; namely, the integral on a small element of line $\mathbf{x} - \mathbf{x}'$ is defined by

$$\int_{\mathbf{x}}^{\mathbf{x}'} d\boldsymbol{\xi} \cdot \mathbf{f}(\boldsymbol{\xi}) = (\mathbf{x} - \mathbf{x}') \cdot \mathbf{f} \left(\frac{\mathbf{x} + \mathbf{x}'}{2} \right), \quad \mathbf{x} - \mathbf{x}' \rightarrow 0 \quad (4.12)$$

We shall stick to this rule when performing explicit calculations.⁵ Note the dimensionless relativistic factor $(\beta m c^2)^{-1/2}$ in front of the vector potential term.

This is readily generalized to a system of n interacting particles: The weight in the space of n loops $\mathcal{F}_1 = (\mathbf{r}_1, \gamma_1, \boldsymbol{\xi}_1), \dots, \mathcal{F}_n = (\mathbf{r}_n, \gamma_n, \boldsymbol{\xi}_n)$ coming from the path integral representation of $\langle \mathbf{r}_1, \dots, \mathbf{r}_n | e^{-\beta H_A} | \mathbf{r}_1, \dots, \mathbf{r}_n \rangle$ is $\exp(-\beta U(\mathcal{F}_1, \dots, \mathcal{F}_n, \mathbf{A}))$ where

$$\begin{aligned} U(\mathcal{F}_1, \dots, \mathcal{F}_n, \mathbf{A}) &= \sum_{i < j}^n e_{\gamma_i} e_{\gamma_j} V^c(\mathcal{F}_i, \mathcal{F}_j) \\ &\quad - i \sum_{j=1}^n \frac{e_{\gamma_j}}{\sqrt{\beta m_{\gamma_j} c^2}} \int_0^1 d\boldsymbol{\xi}_j(s) \cdot \mathbf{A}(\mathbf{r}_j + \lambda_{\gamma_j} \boldsymbol{\xi}_j(s)) \end{aligned} \quad (4.13)$$

⁵Other prescriptions are possible for the path integral to correctly represent the quantum mechanical Gibbs weight in presence of a magnetic field. The Itô rule may be used when \mathbf{f} is divergence free (Roespstorff, 1994).

The matrix element $\langle \mathbf{r}_1, \dots, \mathbf{r}_n | e^{-\beta H_{\mathbf{A}}} | \mathbf{r}_1, \dots, \mathbf{r}_n \rangle$ is obtained by integrating $\exp(-\beta U(\mathcal{F}_1, \dots, \mathcal{F}_n, \mathbf{A}))$ over the random shapes ξ_1, \dots, ξ_n of the loops, as in (4.10). In (4.13),

$$V^c(\mathcal{F}_i, \mathcal{F}_j) = \int_0^1 ds \frac{1}{|\mathbf{r}_i + \lambda_{\gamma_i} \xi_i(s) - \mathbf{r}_j - \lambda_{\gamma_j} \xi_j(s)|} \quad (4.14)$$

is the Coulomb potential between two loops, and for the sake of brevity, we have omitted the non electromagnetic terms

$$\sum_{i < j}^n V_{\text{SR}}(\mathcal{F}_i, \mathcal{F}_j) + \sum_{i=1}^n V^{\text{walls}}(\mathcal{F}_i) \quad (4.15)$$

corresponding to the short-range regularization and to the confinement potential. The vector potential term can be written as $-i \int d\mathbf{x} \mathbf{A}(\mathbf{x}) \cdot \mathcal{J}(\mathbf{x})$ in terms of current densities associated with the Brownian loops:

$$\mathcal{J}(\mathbf{x}) = \sum_{i=1}^n \mathbf{j}(\mathcal{F}_i, \mathbf{x}), \quad \mathbf{j}(\mathcal{F}_i, \mathbf{x}) = \frac{e_{\gamma_i}}{\sqrt{\beta m_{\gamma_i} c^2}} \int_0^1 d\xi_i(s) \delta(\mathbf{x} - \mathbf{r}_i - \lambda_{\gamma_i} \xi_i(s)). \quad (4.16)$$

If one interprets the (ill-defined) derivative $\lambda_{\gamma_i} d\xi_i(s)/ds = \mathbf{v}_i(s)$ as the “velocity” of a particle of charge e_{γ_i} moving along the loop $\xi_i(s)$, the quantity $e_{\gamma_i} \mathbf{v}_i(s) \delta(\mathbf{x} - \mathbf{r}_i - \lambda_{\gamma_i} \xi_i(s))$ corresponds to a classical current density. This is just a formal analogy. In subsequent calculations of stochastic integrals arising from (4.16), we will always use the mathematically well-defined rule of the middle point (4.12). Moreover, such “imaginary time” currents appearing in the Feynman-Kac-Itô representation are not the physical “real-time” current observables. Our definition (4.16) also includes the relativistic factor $(\beta m_{\gamma_i} c^2)^{-1/2}$.

A remarkable fact is that the transverse part of the field enters in $\exp(-\beta U(\mathcal{F}_1, \dots, \mathcal{F}_n, \mathbf{A}))$ as a phase factor linear in \mathbf{A} and its Fourier amplitudes (contrary to the Hamiltonian (4.1) written in operatorial form). Since the statistical weight $e^{-\beta H_0^{\text{rad}}}$ (4.3) is a Gaussian function of these Fourier amplitudes, it makes it possible to perform explicitly the partial trace over the field degrees of freedom in (4.8) according to the following steps:

$$\begin{aligned} \left\langle \exp \left[i\beta \int d\mathbf{x} \mathbf{A}(\mathbf{x}) \cdot \mathcal{J}(\mathbf{x}) \right] \right\rangle_{\text{rad}} &= \left\langle \prod_{\mathbf{k}, l} \exp [i(u_{\mathbf{k}l}^* \alpha_{\mathbf{k}l} + u_{\mathbf{k}l} \alpha_{\mathbf{k}l}^*)] \right\rangle_{\text{rad}} = \\ \exp \left[-\frac{\beta}{2R^3} \sum_{\mathbf{k}, l} \frac{4\pi g^2(\mathbf{k})}{k^2} |\mathcal{J}(\mathbf{k}) \cdot \mathbf{e}_{\mathbf{k}l}|^2 \right] &= \exp \left[-\frac{\beta}{2} \int \frac{d\mathbf{k}}{(2\pi)^3} (\mathcal{J}^\mu(\mathbf{k}))^* G^{\mu\nu}(\mathbf{k}) \mathcal{J}^\nu(\mathbf{k}) \right]. \end{aligned} \quad (4.17)$$

The first equality is obtained by introducing the mode expansion (4.2), yielding

$$u_{\mathbf{k}\lambda} = \beta \left(\frac{4\pi\hbar c^2}{R^3} \right)^{1/2} \frac{g(\mathbf{k})}{\sqrt{2\omega_{\mathbf{k}}}} \mathcal{J}(\mathbf{k}) \cdot \mathbf{e}_{\mathbf{k}\lambda}, \quad \mathcal{J}(\mathbf{k}) = \int d\mathbf{x} e^{-i\mathbf{k}\cdot\mathbf{x}} \mathcal{J}(\mathbf{x}) \quad (4.18)$$

The second equality results from (4.8), (4.9) and the Gaussian integral $\int \frac{d^2\alpha}{\pi} e^{-b|\alpha|^2 + i(u^*\alpha + u\alpha^*)} = b^{-1} e^{-b^{-1}|u|^2}$, $b > 0$, whereas the infinite volume limit $R \rightarrow \infty$ and the polarization sum have been performed in the last equality. We have denoted by $G^{\mu\nu}(\mathbf{k})$ the covariance of the free transverse field:

$$G^{\mu\nu}(\mathbf{k}) = \frac{4\pi g^2(\mathbf{k})}{K^2} \delta_{\text{tr}}^{\mu\nu}(\mathbf{k}), \quad \delta_{\text{tr}}^{\mu\nu}(\mathbf{k}) = \delta^{\mu\nu} - \frac{k^\mu k^\nu}{K^2}, \quad k^\mu G^{\mu\nu}(\mathbf{k}) \equiv 0 \quad (4.19)$$

($\delta_{\text{tr}}^{\mu\nu}(\mathbf{k})$ is the transverse Kronecker symbol). In (4.17) and throughout the paper, summation on repeated vector components $\mu, \nu = 1, 2, 3$ is understood. In the configuration space, the asymptotic behaviour of $G^{\mu\nu}(\mathbf{x})$ is obtained by approximating $g^2(\mathbf{k}) \sim 1$ in the inverse Fourier transform of $G^{\mu\nu}(\mathbf{k})$:

$$G^{\mu\nu}(\mathbf{x}) \sim \int \frac{d\mathbf{k}}{(2\pi)^3} e^{i\mathbf{k}\cdot\mathbf{x}} \frac{4\pi}{K^2} \left(\delta^{\mu\nu} - \frac{k^\mu k^\nu}{K^2} \right) = \frac{1}{2r} \left(\delta_{\mu\nu} + \frac{x^\mu x^\nu}{r^2} \right), \quad r = |\mathbf{x}| \rightarrow \infty. \quad (4.20)$$

Decomposing the total current (4.16) into the individual loop currents we see that the effective weight (4.17) takes the form

$$\left\langle \exp \left[i\beta \int d\mathbf{x} \mathbf{A}(\mathbf{x}) \cdot \mathcal{J}(\mathbf{x}) \right] \right\rangle_{\text{rad}} = \prod_{i=1}^n \exp \left(-\frac{\beta e_{\gamma_i}^2}{2} W^{\text{m}}(i, i) \right) \times \exp \left(-\beta \sum_{i<j}^n e_{\gamma_i} e_{\gamma_j} W^{\text{m}}(i, j) \right), \quad (4.21)$$

where for two loops $i = \mathcal{F}_i$ and $j = \mathcal{F}_j$ we have introduced the loop-loop effective magnetic potential

$$\begin{aligned} e_{\gamma_i} e_{\gamma_j} W^{\text{m}}(i, j) &= \int d\mathbf{x} \int d\mathbf{y} (j^\mu(\mathcal{F}_i, \mathbf{x}))^* G^{\mu\nu}(\mathbf{x} - \mathbf{y}) j^\nu(\mathcal{F}_j, \mathbf{y}) = \\ &= \frac{e_{\gamma_i} e_{\gamma_j}}{\beta \sqrt{m_{\gamma_i} m_{\gamma_j}} c^2} \int \frac{d\mathbf{k}}{(2\pi)^3} e^{i\mathbf{k}\cdot(\mathbf{r}_i - \mathbf{r}_j)} \int_0^1 d\xi_i^\mu(s_1) e^{i\mathbf{k}\cdot\lambda_{\gamma_i} \xi_i(s_1)} \int_0^1 d\xi_j^\nu(s_2) e^{-i\mathbf{k}\cdot\lambda_{\gamma_j} \xi_j(s_2)} G^{\mu\nu}(\mathbf{k}). \end{aligned} \quad (4.22)$$

As a consequence of Gaussian integration, one recovers pairwise interactions (4.22) between loops. The product in (4.21) contains the magnetic self-energies of the loops.

It is pleasing and convenient that after averaging over the field modes, the energy of the system of loops becomes an exact and explicit sum of pair potentials

(and self-energies):⁶

$$\left\langle e^{-\beta U(\mathcal{F}_1, \dots, \mathcal{F}_n, \mathbf{A})} \right\rangle_{\text{rad}} = \left[\prod_{i=1}^n e^{-\frac{\beta e_{\gamma_i}^2}{2} W^m(i,i)} \right] e^{-\beta \sum_{i < j} e_{\gamma_i} e_{\gamma_j} (V^c(i,j) + W^m(i,j))}. \quad (4.23)$$

It is interesting to ask for the status of the partial density matrix (4.5) compared to that generated by the Darwin Hamiltonian $\rho_{\text{Darwin}} \propto e^{-\beta H_{\text{Darwin}}}$ or, more generally, if $\rho_{L,R}$ can be cast in the form $\rho_{L,R} \propto e^{-\beta H_{\text{eff}}}$ for some tractable Hamiltonian $H_{\text{eff}}(\{\mathbf{p}_i, \mathbf{r}_i\})$ depending on the canonical variables of the particles. The answer to this last question is very presumably negative. Indeed the magnetic interaction (4.22) is a two times functional of the Brownian loops; namely, it lacks the equal-time constraint occurring in the Coulomb potential (4.14) (see the discussion before (4.26) below) necessary to come back to a simple operator form by using the Feynman-Kac-Itô formula backwards. This is a well-known common feature of interactions resulting from integrating out external degrees of freedom (Feynman & Hibbs, 1965).

The long-distance asymptotics of $W^m(i, j)$ as $|\mathbf{r}_i - \mathbf{r}_j| \rightarrow \infty$ is determined by the small κ behaviour in the integrand of (4.22). Noting that $\int_0^1 d\xi(s) = 0$ for a closed loop (Itô's lemma), one has

$$\int_0^1 d\xi_i^\mu(s) e^{i\mathbf{K} \cdot \lambda_{\gamma_i} \xi_i(s)} \sim i\lambda_{\gamma_i} \int_0^1 d\xi_i^\mu(s) \kappa \cdot \xi_i(s), \quad \kappa \rightarrow 0, \quad (4.24)$$

and thus

$$\begin{aligned} W^m(i, j) &\sim & (4.25) \\ &\sim \frac{\lambda_{\gamma_i} \lambda_{\gamma_j}}{\beta \sqrt{m_{\gamma_i} m_{\gamma_j}} c^2} \int \frac{d\mathbf{k}}{(2\pi)^3} e^{i\mathbf{K} \cdot (\mathbf{r}_i - \mathbf{r}_j)} \int_0^1 d\xi_i^\mu(s_1) (\kappa \cdot \xi_i(s_1)) \int_0^1 d\xi_j^\nu(s_2) (\kappa \cdot \xi_j(s_2)) G^{\mu\nu}(\mathbf{k}) \\ &= \frac{\lambda_{\gamma_i} \lambda_{\gamma_j}}{\beta \sqrt{m_{\gamma_i} m_{\gamma_j}} c^2} \int_0^1 d\xi_i^\mu(s_1) (\xi_i(s_1) \cdot \nabla_{\mathbf{r}_i}) \int_0^1 d\xi_j^\nu(s_2) (\xi_j(s_2) \cdot \nabla_{\mathbf{r}_j}) G^{\mu\nu}(\mathbf{r}_i - \mathbf{r}_j), \end{aligned}$$

as $|\mathbf{r}_i - \mathbf{r}_j| \rightarrow \infty$. Upon using the asymptotic form (4.20) of $G^{\mu\nu}(\mathbf{r}_i - \mathbf{r}_j)$, it is clear that for fixed loop shapes ξ_i and ξ_j the decay of $W^m(i, j)$ is $\sim |\mathbf{r}_i - \mathbf{r}_j|^{-3}$. It is of dipolar type modified by the constraint imposed by the transversality.

The Coulombic part (4.14) of the loop-loop interaction still decays as r^{-1} and deserves the following remark. From the Feynman-Kac formula the potential (4.14) inherits the quantum-mechanical equal-time constraint; *i.e.*, every element of charge $e_{\gamma_i} \lambda_{\gamma_i} d\xi_i(s_1)$ of the first loop does not interact with every other element

⁶We omit again in (4.23) the non-electromagnetic terms (4.15).

$e_{\gamma_j} \lambda_{\gamma_j} d\xi_j(s_2)$ as would be the case in classical physics, but the interaction takes place only if $s_1 = s_2$. It is therefore of interest to split

$$V^c(i, j) = V^{\text{el}}(i, j) + W^c(i, j), \quad (4.26)$$

where

$$V^{\text{el}}(i, j) = \int_0^1 ds_1 \int_0^1 ds_2 \frac{1}{|\mathbf{r}_i + \lambda_{\gamma_i} \xi_i(s_1) - \mathbf{r}_j - \lambda_{\gamma_j} \xi_j(s_2)|} \quad (4.27)$$

is a genuine classical electrostatic potential between two charged loops and

$$W^c(i, j) = \int_0^1 ds_1 \int_0^1 ds_2 (\delta(s_1 - s_2) - 1) \frac{1}{|\mathbf{r}_i + \lambda_{\gamma_i} \xi_i(s_1) - \mathbf{r}_j - \lambda_{\gamma_j} \xi_j(s_2)|} \quad (4.28)$$

is the part of $V^c(i, j)$ due to intrinsic quantum fluctuations ($W^c(i, j)$ vanishes if \hbar is set equal to zero). Because of the identities

$$\int_0^1 ds_1 (\delta(s_1 - s_2) - 1) = \int_0^1 ds_2 (\delta(s_1 - s_2) - 1) = 0, \quad (4.29)$$

the large-distance behaviour of W^c originates again from the term bilinear in ξ_i and ξ_j in the multipolar expansion of the Coulomb potential in (4.28)

$$W^c(i, j) \sim \int_0^1 ds_1 \int_0^1 ds_2 (\delta(s_1 - s_2) - 1) (\lambda_{\gamma_i} \xi_i(s_1) \cdot \nabla_{\mathbf{r}_i}) (\lambda_{\gamma_j} \xi_j(s_2) \cdot \nabla_{\mathbf{r}_j}) \frac{1}{|\mathbf{r}_i - \mathbf{r}_j|}. \quad (4.30)$$

It is dipolar and formally similar to that of two electrical dipoles of sizes $e_{\gamma_i} \lambda_{\gamma_i} \xi_i$ and $e_{\gamma_j} \lambda_{\gamma_j} \xi_j$.

4.4 Two quantum charges in a classical plasma

In order to exhibit the effect of the magnetic potential on the particle correlations, we consider the simple model of two quantum charges e_a and e_b with corresponding loops $\mathcal{F}_a = (\mathbf{r}_a, \xi_a)$ and $\mathcal{F}_b = (\mathbf{r}_b, \xi_b)$ immersed in a configuration ω of classical charges, following Sec. VII of (Alastuey & Martin, 1989) or Sec. IV.C of (Brydges & Martin, 1999). According to (4.26) one can decompose the total energy as $\mathcal{U}(\mathcal{F}_a, \mathcal{F}_b, \omega) = e_a e_b W(\mathcal{F}_a, \mathcal{F}_b) + U_{\text{cl}}(\mathcal{F}_a, \mathcal{F}_b, \omega)$ where $W(\mathcal{F}_a, \mathcal{F}_b) = W^c(\mathcal{F}_a, \mathcal{F}_b) + W^{\text{m}}(\mathcal{F}_a, \mathcal{F}_b)$ is the sum of the electric and magnetic quantum dipolar interactions and $U_{\text{cl}}(\mathcal{F}_a, \mathcal{F}_b, \omega)$ is the purely classical Coulomb energy (4.27) of the two loops \mathcal{F}_a and \mathcal{F}_b together with that of the particles in

the configuration ω . The correlation $\rho(\mathcal{F}_a, \mathcal{F}_b)$ between the loops is obtained by integrating out the coordinates ω of the classical charges:

$$\rho(\mathcal{F}_a, \mathcal{F}_b) = \frac{1}{\Xi_{\text{cl}}} \int_{\Lambda} d\omega e^{-\beta \mathcal{U}(\mathcal{F}_a, \mathcal{F}_b, \omega)} = e^{-\beta e_a e_b W(\mathcal{F}_a, \mathcal{F}_b)} \rho_{\text{cl}}(\mathcal{F}_a, \mathcal{F}_b), \quad (4.31)$$

where Ξ_{cl} is the partition function of the classical plasma and $\rho_{\text{cl}}(\mathcal{F}_a, \mathcal{F}_b)$ is the correlation of the two loops embedded in the plasma interacting with genuine classical Coulomb forces. In the latter quantity, the classical theory of screening applies so that effective interaction between the loops decay exponentially fast.⁷ Thus one can approximate $\rho_{\text{cl}}(\mathcal{F}_a, \mathcal{F}_b)$ in (4.31) by $\rho(\mathcal{F}_a)\rho(\mathcal{F}_b)$ up to a term exponentially decaying as $|\mathbf{r}_a - \mathbf{r}_b| \rightarrow \infty$. Furthermore, integrating $\rho(\mathcal{F}_a, \mathcal{F}_b)$ on the loop shapes leads to the following expression for the positional correlation of the quantum charges

$$\begin{aligned} \rho(\mathbf{r}_a, \mathbf{r}_b) &= \int D(\xi_a) \int D(\xi_b) e^{-\beta e_a e_b W(\mathcal{F}_a, \mathcal{F}_b)} \rho(\mathcal{F}_a) \rho(\mathcal{F}_b) + \mathcal{O}(e^{-C|\mathbf{r}_a - \mathbf{r}_b|}) = \\ &= \rho_a \rho_b - \beta e_a e_b \int D(\xi_a) \int D(\xi_b) W(\mathcal{F}_a, \mathcal{F}_b) \rho(\xi_a) \rho(\xi_b) + \\ &+ \frac{1}{2} \beta^2 e_a^2 e_b^2 \int D(\xi_a) \int D(\xi_b) W^2(\mathcal{F}_a, \mathcal{F}_b) \rho(\xi_a) \rho(\xi_b) + \dots + \mathcal{O}(e^{-C|\mathbf{r}_a - \mathbf{r}_b|}) \end{aligned} \quad (4.32)$$

Since $W(\mathcal{F}_a, \mathcal{F}_b) \sim |\mathbf{r}_a - \mathbf{r}_b|^{-3}$ (see (4.25), (4.30)), the above expansion in powers of W generates algebraically decaying terms at large separation. It is known that in a homogeneous and isotropic phase, the electric dipole part W^c does not contribute at linear order (Alastuey & Martin, 1989), (Brydges & Martin, 1999). The same is true for the magnetic part. To see this, it is convenient to write the linear W^m term of (4.32) as

$$\begin{aligned} & - \beta e_a e_b \int D(\xi_a) \int D(\xi_b) W^m(\mathcal{F}_a, \mathcal{F}_b) \rho(\xi_a) \rho(\xi_b) \\ &= - \frac{\beta e_a e_b}{\sqrt{\beta m_a c^2} \sqrt{\beta m_b c^2}} \int \frac{d^3 \mathbf{k}}{(2\pi)^3} e^{i\mathbf{k} \cdot (\mathbf{r}_a - \mathbf{r}_b)} t_a^{\mu*}(\mathbf{k}) t_b^{\nu}(\mathbf{k}) G^{\mu\nu}(\mathbf{k}). \end{aligned} \quad (4.33)$$

The stochastic ξ_a -line-integral is now included in the definition of the tensor

$$t_a^{\mu}(\mathbf{k}) = \int D(\xi_a) \rho(\xi_a) \int_0^1 d\xi_a^{\mu}(s) e^{-i\lambda_a \mathbf{k} \cdot \xi_a(s)} \quad (4.34)$$

and likewise for $t_b^{\nu}(\mathbf{k})$. Since both the measure $D(\xi_a)$ and $\rho(\xi_a)$ are invariant under a rotation of ξ_a in an isotropic system, $t_a^{\mu}(\mathbf{k})$ transforms in a covariant manner

⁷The usual Debye theory of screening has been rigorously shown to be valid at least at sufficiently high temperature (Brydges & Federbush, 1980).

under rotations of $\mathbf{\kappa}$. Thus it is necessarily of the form $t_a^\mu(\mathbf{\kappa}) = k^\mu f_a(|\mathbf{\kappa}|)$, implying the vanishing of (4.33) because of the transversality of $G^{\mu\nu}(\mathbf{\kappa})$. One concludes that the slowest non-vanishing contribution comes from the W^2 term in (4.32)

$$\rho(\mathbf{r}_a, \mathbf{r}_b) - \rho_a \rho_b = \frac{A(\beta)}{|\mathbf{r}_a - \mathbf{r}_b|^6} + \mathcal{O}\left(\frac{1}{|\mathbf{r}_a - \mathbf{r}_b|^8}\right). \quad (4.35)$$

The temperature-dependent amplitude $A(\beta) = A_{\text{cc}}(\beta) + A_{\text{mm}}(\beta) + A_{\text{cm}}(\beta)$ involves in principle electric and magnetic contributions from W^{c^2} and W^{m^2} , as well as a cross contribution from $2W^c W^m$. These contributions can be calculated explicitly at lowest order in \hbar (or equivalently in the high-temperature limit $\beta \rightarrow 0$). The electric contribution in this limit is known to be (Alastuey & Martin, 1989), (Brydges & Martin, 1999)

$$A_{\text{cc}}(\beta) \sim \hbar^4 \frac{\beta^4}{240} \frac{e_a^2 e_b^2}{m_a m_b} \rho_a \rho_b. \quad (4.36)$$

To compute the magnetic contribution in the same limit, we write the quadratic term

$$\begin{aligned} & \frac{\beta^2 e_a^2 e_b^2}{2} \int \mathcal{D}(\xi_a) \rho(\xi_a) \int \mathcal{D}(\xi_b) \rho(\xi_b) W^{m^2}(\mathcal{F}_a, \mathcal{F}_b) = \frac{e_a^2 e_b^2}{2m_a c^2 m_b c^2} \\ & \times \int \frac{d^3 \mathbf{\kappa}_1}{(2\pi)^3} \int \frac{d^3 \mathbf{\kappa}_2}{(2\pi)^3} e^{i(\mathbf{\kappa}_1 + \mathbf{\kappa}_2) \cdot (\mathbf{r}_a - \mathbf{r}_b)} (T_a^{\mu\nu}(\mathbf{\kappa}_1, \mathbf{\kappa}_2))^* T_b^{\sigma\tau}(\mathbf{\kappa}_1, \mathbf{\kappa}_2) G^{\mu\sigma}(\mathbf{\kappa}_1) G^{\nu\tau}(\mathbf{\kappa}_2) \end{aligned} \quad (4.37)$$

in terms of the tensors

$$T_a^{\mu\nu}(\mathbf{\kappa}_1, \mathbf{\kappa}_2) = \int \mathcal{D}(\xi_a) \rho(\xi_a) \int_0^1 d\xi_a^\mu(s_1) \int_0^1 d\xi_a^\nu(s_2) e^{-i\lambda_a \mathbf{\kappa}_1 \cdot \xi_a(s_1)} e^{-i\lambda_a \mathbf{\kappa}_2 \cdot \xi_a(s_2)} \quad (4.38)$$

and $T_b^{\sigma\tau}(\mathbf{\kappa}_1, \mathbf{\kappa}_2)$, defined likewise. As usual the behaviour at large distances is controlled by that of the integrand of (4.37) at small wave numbers. Expanding (4.38) at lowest order in $\mathbf{\kappa}_1$ and $\mathbf{\kappa}_2$ gives

$$\begin{aligned} T_a^{\mu\nu}(\mathbf{\kappa}_1, \mathbf{\kappa}_2) & \sim \int \mathcal{D}(\xi_a) \rho(\xi_a) \int_0^1 d\xi_a^\mu(s_1) \int_0^1 d\xi_a^\nu(s_2) (-i\lambda_a \mathbf{\kappa}_1 \cdot \xi_a(s_1)) (-i\lambda_a \mathbf{\kappa}_2 \cdot \xi_a(s_2)) \\ & = -\lambda_a^2 k_1^\epsilon k_2^\eta \int \mathcal{D}(\xi_a) \rho(\xi_a) \int_0^1 d\xi_a^\mu(s_1) \int_0^1 d\xi_a^\nu(s_2) \xi_a^\epsilon(s_1) \xi_a^\eta(s_2) \end{aligned} \quad (4.39)$$

and likewise for $T_b^{\sigma\tau}(\mathbf{\kappa}_1, \mathbf{\kappa}_2)$. One sees that because of the factor $\lambda_a^2 \lambda_b^2$, the overall contribution in (4.37) will have a \hbar^4 factor so that at this order we can neglect the quantum fluctuation in the density setting $\rho(\xi_a) \sim \rho_a$ independent of ξ_a . Thus the stochastic integral to be calculated becomes (appendix 5.A)

$$\int \mathcal{D}(\xi) \int_0^1 d\xi^\mu(s) \int_0^1 d\xi^\nu(t) \xi^\epsilon(s) \xi^\eta(t) = \frac{1}{12} (\delta^{\mu\nu} \delta^{\eta\epsilon} - \delta^{\mu\eta} \delta^{\nu\epsilon}), \quad (4.40)$$

leading to

$$\begin{aligned} T_a^{\mu\nu}(\mathbf{k}_1, \mathbf{k}_2) &\sim -\frac{\lambda_a^2 \rho_a}{12} (\delta^{\mu\nu} \mathbf{k}_1 \cdot \mathbf{k}_2 - k_2^\mu k_1^\nu), \\ T_b^{\sigma\tau}(\mathbf{k}_1, \mathbf{k}_2) &\sim -\frac{\lambda_b^2 \rho_b}{12} (\delta^{\sigma\tau} \mathbf{k}_1 \cdot \mathbf{k}_2 - k_2^\sigma k_1^\tau). \end{aligned} \quad (4.41)$$

When this is inserted into (4.37) and summation on vectorial indices are performed, one finds the expression

$$A \int \frac{d\mathbf{k}_1}{(2\pi)^3} \int \frac{d\mathbf{k}_2}{(2\pi)^3} e^{i(\mathbf{K}_1 + \mathbf{K}_2) \cdot (\mathbf{r}_a - \mathbf{r}_b)} (4\pi)^2 |g(\mathbf{k}_1)|^2 |g(\mathbf{k}_2)|^2 \left[1 + \frac{(\mathbf{K}_1 \cdot \mathbf{K}_2)^2}{K_1^2 K_2^2} \right], \quad (4.42)$$

with $A = \frac{\lambda_a^2 \lambda_b^2 e_a^2 e_b^2 \rho_a \rho_b}{288 m_a m_b c^4}$. The first term in the large brackets gives a rapidly decaying contribution since it involves the Fourier transform of the form factor $g^2(\mathbf{k})$. The algebraic large-distance contribution comes from the second term which reads, after Fourier transformation (approximating $g(\mathbf{k}) \sim 1, \mathbf{k} \rightarrow 0$),

$$A \left(\partial_\mu \partial_\nu \frac{1}{|\mathbf{r}_a - \mathbf{r}_b|} \right) \left(\partial_\mu \partial_\nu \frac{1}{|\mathbf{r}_a - \mathbf{r}_b|} \right) = A \frac{6}{|\mathbf{r}_a - \mathbf{r}_b|^6}. \quad (4.43)$$

Finally one checks that there is no cross Coulomb-magnetic contribution $A_{\text{cm}}(\beta)$ at the dominant order \mathbf{r}^{-6} as a consequence of transversality (appendix 5.B). So adding (4.36) and (4.43) gives the final result

$$\rho(\mathbf{r}_a, \mathbf{r}_b) - \rho_a \rho_b \sim \hbar^4 \beta^4 \frac{\rho_a \rho_b e_a^2 e_b^2}{240 m_a m_b} \left[1 + \frac{5}{(\beta m_a c^2)(\beta m_b c^2)} \right] \frac{1}{|\mathbf{r}_a - \mathbf{r}_b|^6} \quad (4.44)$$

as $|\mathbf{r}_a - \mathbf{r}_b| \rightarrow \infty$ and at lowest order in \hbar . One sees from (4.14) and (4.22) that the order of magnitude of the ratio W^m/V^c is $(\beta m c^2)^{-1}$. In an electrolyte at room temperature $T = 300\text{K}$, this ratio is found to be $\approx 10^{-11}$. The magnetic correction to the correlation decay (4.44) is negligible in this case.

4.5 Particle correlations in the many-body system

We apply the formalism developed in Section 4.3 to the determination of the large-distance decay of the particle density correlations in the more general case where all particles are quantum-mechanical, but still obeying Maxwell-Boltzmann statistics.

We show hereafter that the algebraic r^{-6} decay of the (truncated) particle density correlations

$$\rho_T(\gamma_a, \mathbf{r}_a, \gamma_b, \mathbf{r}_b) \sim \frac{A_{ab}(\beta, \{\rho_\gamma\})}{|\mathbf{r}_a - \mathbf{r}_b|^6}, \quad |\mathbf{r}_a - \mathbf{r}_b| \rightarrow \infty \quad (4.45)$$

found in the absence of the radiation field (Cornu, 1996b), (Brydges & Martin, 1999) is not altered, but that the coefficient $A_{ab}(\beta, \{\rho_\gamma\})$ contains in addition small magnetic terms of the order $(\beta mc^2)^{-2}$, as in (4.44). As an illustration, we give the lowest order contribution of this coefficient with respect to Planck's constant \hbar .

By the Feynman-Kac-Itô representation, the full system composed of quantum point charges coupled to the radiation field has reduced to a classical-like system of extended charged loops $\mathcal{F} = (\mathbf{r}, \gamma, \xi)$ for which all the methods of classical statistical mechanics apply. The only novelty comes from the additional magnetic potential W^m . In the following, we merely summarize the arguments since they are essentially the same as those found in (Cornu, 1996b), (Brydges & Martin, 1999) when no radiation field is present.

As usual, we express the truncated two-loop correlation $\rho_T(\mathcal{F}_a, \mathcal{F}_b) = \rho(\mathcal{F}_a)\rho(\mathcal{F}_b)h(\mathcal{F}_a, \mathcal{F}_b)$ in terms of the loop Ursell function $h(\mathcal{F}_a, \mathcal{F}_b)$. The latter function can be expanded in a formal diagrammatic Mayer series of powers of the loop densities $\rho(\mathcal{F})$. One needs to resum the long-range part of the Coulomb potential V^c , which is responsible for the non-integrability of the Mayer bonds $f(\mathcal{F}_i, \mathcal{F}_j) = \exp(-\beta e_{\gamma_i} e_{\gamma_j} [V^c(\mathcal{F}_i, \mathcal{F}_j) + W^m(\mathcal{F}_i, \mathcal{F}_j)]) - 1$ at infinity. Using the decomposition (4.26) we resum the convolution chains built with the purely electrostatic long-range part $V^{\text{el}}(\mathcal{F}, \mathcal{F}')$ into a Debye-Hückel-type screened potential $\Phi(\mathcal{F}, \mathcal{F}')$. Then reorganizing the diagrams leads to a representation of the loop Ursell function by terms of so-called prototype diagrams, built with the two kinds of bonds

$$F(\mathcal{F}, \mathcal{F}') = -\beta e_\gamma e_{\gamma'} \Phi(\mathcal{F}, \mathcal{F}'), \quad (4.46)$$

$$F^R(\mathcal{F}, \mathcal{F}') = e^{-\beta e_\gamma e_{\gamma'} [\Phi(\mathcal{F}, \mathcal{F}') + W(\mathcal{F}, \mathcal{F}')] } - 1 + \beta e_\gamma e_{\gamma'} \Phi(\mathcal{F}, \mathcal{F}'), \quad (4.47)$$

where we have defined $W = W^c + W^m$ as in Section 4.4.⁸

The potential $\Phi(\mathcal{F}, \mathcal{F}')$ has been studied in (Ballenegger, Martin, & Alastuey, 2002). It corresponds to the term $n = 0$ of the full quantum analog of the Debye-Hückel potential given by formula (89) of (Ballenegger et al., 2002). This contribution $n = 0$ is shown to be decaying at infinity faster than any inverse power of $|\mathbf{r} - \mathbf{r}'|$ (see formula (58) of (Ballenegger et al., 2002), and the comment following it).

The asymptotic decay of the two-particle correlation $\rho_T(\gamma_a, \mathbf{r}_a, \gamma_b, \mathbf{r}_b)$ is inferred from that of the loop correlation $\rho_T(\mathcal{F}_a, \mathcal{F}_b)$ by integrating it over the Brownian shapes ξ_a and ξ_b . The bond F is rapidly decreasing, and the asymptotic decay of F^R is dominated by the dipolar decays of W^c and W^m : $F^R(\mathcal{F}, \mathcal{F}') \sim -\beta e_\gamma e_{\gamma'} W(\mathcal{F}, \mathcal{F}')$ as $|\mathbf{r} - \mathbf{r}'| \rightarrow \infty$. We further extract this dipolar part from F^R

⁸Strictly speaking, the short-range repulsive potential needed in the framework of Maxwell-Boltzmann statistics would arise here in the exponent of (4.47). It has no implication in this discussion about long-range behaviours, and we simply omit it.

and define the bond

$$\begin{aligned}\widetilde{F}^{\text{R}}(\mathcal{F}, \mathcal{F}') &= F^{\text{R}}(\mathcal{F}, \mathcal{F}') + \beta e_{\gamma} e_{\gamma'} W(\mathcal{F}, \mathcal{F}') \\ &\sim \frac{1}{2} [\beta e_{\gamma} e_{\gamma'} W(\mathcal{F}, \mathcal{F}')]^2 = \text{O}(|\mathbf{r} - \mathbf{r}'|^{-6})\end{aligned}\quad (4.48)$$

and work now with the three bonds F , \widetilde{F}^{R} , and W .⁹

To find out the slowest-decaying diagrams, we write the truncated two-loop correlation $\rho_{\text{T}}(\mathcal{F}_a, \mathcal{F}_b)$ in an exact Dyson series of convolution chains involving W and H :

$$\begin{aligned}\rho_{\text{T}}(\mathcal{F}_a, \mathcal{F}_b) &= \rho(\mathcal{F}_a) \rho(\mathcal{F}_b) H(\mathcal{F}_a, \mathcal{F}_b) - \beta (K \star W \star K)(\mathcal{F}_a, \mathcal{F}_b) \\ &\quad + \beta^2 (K \star W \star K \star W \star K)(\mathcal{F}_a, \mathcal{F}_b) + \dots\end{aligned}\quad (4.49)$$

where H denotes the sum of the diagrams that remain connected under removal of one W -bond and $K(\mathcal{F}_1, \mathcal{F}_2) = \rho(\mathcal{F}_1) \rho(\mathcal{F}_2) H(\mathcal{F}_1, \mathcal{F}_2) + \delta(\mathcal{F}_1, \mathcal{F}_2) \rho(\mathcal{F}_1)$. This topological constraint ensures that H decays at least as r^{-6} . The series (4.49) is conveniently analysed in Fourier representation with respect to $\mathbf{r}_a - \mathbf{r}_b$. After expanding W into the sum $W^{\text{c}} + W^{\text{m}}$, we have three types of chains: pure W^{c} or W^{m} chains and mixed $W^{\text{c}}, W^{\text{m}}$ chains. It is shown in (Cornu, 1996b), (Brydges & Martin, 1999) that the contribution of pure W^{c} chains to the particle correlation $\rho_{\text{T}}(\gamma_a, \mathbf{r}_a, \gamma_b, \mathbf{r}_b) = \int \text{D}(\xi_a) \int \text{D}(\xi_b) \rho_{\text{T}}(\mathcal{F}_a, \mathcal{F}_b)$ decays strictly faster than $\text{o}(|\mathbf{r}_a - \mathbf{r}_b|^{-6})$.¹⁰ We show below that all other chains containing W^{m} bonds vanish identically as the consequence of transversality. This implies that the longest-range part of the correlations originates from the function H in the first term of the right-hand side of (4.49), hence the result (4.45).

A chain mixing W^{c} and W^{m} bonds must have at least one element $W^{\text{c}} \star K \star W^{\text{m}}$ or $W^{\text{m}} \star K \star W^{\text{c}}$. In Fourier space, one can write, from (4.28) and (4.22),

$$\begin{aligned}(W^{\text{c}} \star K \star W^{\text{m}})(\gamma_a, \xi_a, \gamma_b, \xi_b, \mathbf{k}) &= \int_0^1 ds_a \int_0^1 ds_1 (\delta(s_a - s_1) - 1) \frac{4\pi}{K^2} e^{i\mathbf{k} \cdot \lambda_{\gamma_a} \xi_a(s_a)} \\ &\quad \times [T^{\nu_2}(\mathbf{k}, s_1) G^{\nu_2, \nu_b}(\mathbf{k})] \int_0^1 d\xi_b^{\nu_b}(s_b) e^{-i\mathbf{k} \cdot \lambda_{\gamma_b} \xi_b(s_b)},\end{aligned}\quad (4.50)$$

where

$$\begin{aligned}T^{\nu_2}(\mathbf{k}, s_1) &= \sum_{\gamma_1} \int \text{D}(\xi_1) \sum_{\gamma_2} \int \text{D}(\xi_2) e^{-i\mathbf{k} \cdot \lambda_{\gamma_1} \xi_1(s_1)} K(\gamma_1, \xi_1, \gamma_2, \xi_2, \mathbf{k}) \\ &\quad \times \int_0^1 d\xi_2^{\nu_2}(s_2) e^{i\mathbf{k} \cdot \lambda_{\gamma_2} \xi_2(s_2)}\end{aligned}\quad (4.51)$$

⁹In (Brydges & Martin, 1999), the bond F is further decomposed into a multipole expansion. Our bonds F^{R} and \widetilde{F}^{R} differ formally from their bonds F_1 and \widetilde{F}_1 only by the inclusion of the magnetic contribution W^{m} into W .

¹⁰In this proof, only the invariance of H under rotations is used, which also holds when the magnetic potential is included.

and $K(\gamma_1, \xi_1, \gamma_2, \xi_2, \mathbf{k})$ is the Fourier transform of $K(\mathcal{F}_1, \mathcal{F}_2)$ with respect to $\mathbf{r}_1 - \mathbf{r}_2$. As the measures $D(\xi_1)$ and $D(\xi_2)$ and the function $K(\gamma_1, \xi_1, \gamma_2, \xi_2, \mathbf{k})$ are invariant under spatial rotations, $T^{\nu_2}(\mathbf{k}, s_1)$ transforms as a tensor, implying that it is necessarily of the form $T^{\nu_2}(\mathbf{k}, s_1) = k^{\nu_2} a(k, s_1)$ for some rotationally invariant function a of \mathbf{k} . Using $k^\mu G^{\mu\nu}(\mathbf{k}) \equiv 0$ one deduces immediately that (4.50) vanishes. The case of $W^m \star K \star W^c$ is similar. To see that there are no chains containing only W^m bonds in $\rho_T(\gamma_a, \mathbf{r}_a, \gamma_b, \mathbf{r}_b)$, it is sufficient to notice that the integrated root element $\int D(\xi_a) K \star W^m$ also involves a factor $[T^{\nu_2}(\mathbf{k}) G^{\nu_2, \nu_b}(\mathbf{k})]$ (for another function $T^{\nu_2}(\mathbf{k})$ transforming in a covariant manner), and thereby vanishes for the same reason.

The graphs that do contribute to the coefficient $A_{ab}(\beta, \{\rho_\gamma\})$ of (4.45) are those of H that contain bonds with algebraic decay: namely, \widetilde{F}^R and W . To select the lowest contribution in \hbar , one notes first that W is at least of order \hbar^2 , as seen in (4.25), (4.30) which correspond to the lowest-order terms in the multipolar expansions of W^c and W^m . (Higher-order multipoles generate higher powers of the de Broglie wavelengths.) Since Φ is rapidly decreasing, the algebraic part of \widetilde{F}^R is of order \hbar^4 and is given by $\frac{1}{2}[\beta e_\gamma e_{\gamma'} W(\mathcal{F}, \mathcal{F}')]^2$, as in (4.48). Thus, up to order \hbar^4 , graphs with an algebraic decay can contain only one bond W , two bonds W , or one bond \widetilde{F}^R belonging to paths connecting the two root points. If there is a single such link W , by the topological structure of H there exists another path connecting the root points made of the more rapidly decreasing bonds F and \widetilde{F}^R . Hence the whole graph has a decay faster than r^{-6} . If there are two W bonds in between the root points, as each of them is of order \hbar^2 all the other bonds and vertices can be evaluated in the classical limit $\hbar \rightarrow 0$. Consequently, at least one of the extremities of either bond W is attached to a purely classical part of the graph, which is independent of the Brownian shapes. We call such a point a classical end of W . At such points, integration over the Brownian shape of the loop ‘‘kills’’ the r^{-3} decay of W (see appendix 5.C), leading to an overall decay faster than r^{-6} . Finally, at order \hbar^4 , the only graphs that contribute to (4.45) are constituted by a single \widetilde{F}^R bond linked to the root points by purely classical subgraphs. The sum of such graphs contributes to the particle correlation in the large-distance limit as

$$\begin{aligned} \rho_T(\gamma_a, \mathbf{r}_a, \gamma_b, \mathbf{r}_b) &\sim \sum_{\gamma_1, \gamma_2} \left[\int d\mathbf{r} n_T^{\text{cl}}(\gamma_a, \gamma_1, \mathbf{r}) \right] \left[\int d\mathbf{r} n_T^{\text{cl}}(\gamma_2, \gamma_b, \mathbf{r}) \right] \\ &\times \int D(\xi_1) \int D(\xi_2) \frac{1}{2} \left[\beta e_{\gamma_1} e_{\gamma_2} W^{\text{dip}}(\gamma_1, \xi_1, \gamma_2, \xi_2, \mathbf{r}_a - \mathbf{r}_b) \right]^2, \end{aligned} \quad (4.52)$$

where $W^{\text{dip}} = W^{c, \text{dip}} + W^{m, \text{dip}}$ is the sum of the dipolar parts (4.30) and (4.25) of W^c and W^m , and $n_T^{\text{cl}}(\gamma_a, \gamma_1, \mathbf{r})$ is the classical truncated two-point density correlation (including coincident points). The functional integrals in (4.52) have been

calculated in Section 4.4, see (4.37)-(4.44), yielding the final result

$$\begin{aligned} \rho_T(\gamma_a, \mathbf{r}_a, \gamma_b, \mathbf{r}_b) &\sim \frac{\hbar^4 \beta^4}{240} \sum_{\gamma_1, \gamma_2} \left[\int d\mathbf{r} n_T^{\text{cl}}(\gamma_a, \gamma_1, \mathbf{r}) \right] \left[\int d\mathbf{r} n_T^{\text{cl}}(\gamma_2, \gamma_b, \mathbf{r}) \right] \\ &\times \frac{e_{\gamma_1}^2 e_{\gamma_2}^2}{m_{\gamma_1} m_{\gamma_2}} \left[1 + \frac{5}{\beta m_{\gamma_1} c^2 \beta m_{\gamma_2} c^2} \right] \frac{1}{|\mathbf{r}_a - \mathbf{r}_b|^6} \end{aligned} \quad (4.53)$$

as $|\mathbf{r}_a - \mathbf{r}_b| \rightarrow \infty$ and at lowest order in \hbar . To this order, the only difference with (4.44) is the occurrence of the classical correlation functions n_T^{cl} , a manifestation of the fact that in the quantum many-body problem, every pair of particles contribute to the tail of the correlation function. This generalizes the result of (Alastuey & Martin, 1989), formula (5.12), to the inclusion of the magnetic interactions.

As a final comment, we observe that the inclusion of the transverse degrees of freedom of the field does not modify the charge sum rule in the system of loops and hence it also holds for the charge correlations in the particle system. This sum rule reads

$$\int d\mathbf{r} \int D(\xi) \sum_{\gamma} \frac{e_{\gamma} \rho_T(\mathcal{F}, \mathcal{F}_1)}{\rho(\mathcal{F}_1)} = -e_{\gamma_1}. \quad (4.54)$$

It states that the charge of the cloud of loops induced around a fixed loop \mathcal{F}_1 exactly compensates that of \mathcal{F}_1 . The proof can be carried out word by word as in (Ballenegger et al., 2002, Sec. 6.1.2). It relies exclusively on the long-range part r^{-1} of the Coulomb potential V^c and is not altered by the presence of the magnetic potential W^m .

4.6 Transverse field correlations

A characteristic feature of charged systems is that longitudinal field correlations always remain long ranged in spite of the screening mechanisms that reduce the range of the particle correlations. It has been established on a microscopic basis that the correlations of the longitudinal electric field \mathbf{E}_l behave as (Lebowitz & Martin, 1984), (Martin, 1988)

$$\langle E_l^{\mu}(\mathbf{x}) E_l^{\nu}(\mathbf{y}) \rangle_T \sim -\partial_{\mu} \partial_{\nu} \frac{1}{|\mathbf{x} - \mathbf{y}|} \left[-\frac{2\pi}{3} \int d\mathbf{r} |\mathbf{r}|^2 S(\mathbf{r}) \right], \quad |\mathbf{x} - \mathbf{y}| \rightarrow \infty, \quad (4.55)$$

where $S(\mathbf{r})$ is the (classical or quantum-mechanical) charge-charge correlation function.

In order to obtain the correlations of the transverse fields we first consider correlations $\langle A^{\mu}(\mathbf{x}) A^{\nu}(\mathbf{y}) \rangle_T$ of the vector potential at free points \mathbf{x} and \mathbf{y} in space.

These correlations are easily obtained by functional differentiation, adding to the original Hamiltonian (4.1) a coupling to an external current $\mathcal{J}_{\text{ext}}(\mathbf{x})$

$$H_{L,R}(\mathcal{J}_{\text{ext}}) = H_{L,R} - i \int d\mathbf{x} \mathcal{J}_{\text{ext}}(\mathbf{x}) \cdot \mathbf{A}(\mathbf{x}), \quad (4.56)$$

so that

$$\langle A^\mu(\mathbf{x})A^\nu(\mathbf{y}) \rangle_{\text{T}} = -\frac{1}{\beta^2} \frac{\delta^2}{\delta \mathcal{J}_{\text{ext}}^\mu(\mathbf{x}) \delta \mathcal{J}_{\text{ext}}^\nu(\mathbf{y})} \ln \text{Tr} e^{-\beta H_{L,R}(\mathcal{J}_{\text{ext}})} \Big|_{\mathcal{J}_{\text{ext}}=0}. \quad (4.57)$$

Decomposing $H_{L,R}$ as in (4.7) one can write

$$\begin{aligned} \langle A^\mu(\mathbf{x})A^\nu(\mathbf{y}) \rangle_{\text{T}} &= \\ &= -\frac{1}{\beta^2} \frac{\delta^2}{\delta \mathcal{J}_{\text{ext}}^\mu(\mathbf{x}) \delta \mathcal{J}_{\text{ext}}^\nu(\mathbf{y})} \ln \text{Tr}_{\text{mat}} \left\langle e^{-\beta H_{\Lambda}} e^{i\beta \int d\mathbf{x} \mathcal{J}_{\text{ext}}(\mathbf{x}) \cdot \mathbf{A}(\mathbf{x})} \right\rangle_{\text{rad}} \Big|_{\mathcal{J}_{\text{ext}}=0}. \end{aligned} \quad (4.58)$$

Using the Feynman-Kac formula as in Section 4.3 one sees that the only modification in (4.17) is the replacement of the loop current $\mathcal{J}(\mathbf{x})$ by the total current¹¹

$$\mathcal{J}_{\text{tot}}(\mathbf{x}) = \mathcal{J}(\mathbf{x}) + \mathcal{J}_{\text{ext}}(\mathbf{x}). \quad (4.59)$$

The Gaussian integration on the field variables replaces (4.17) by

$$\begin{aligned} \exp \left\{ -\frac{\beta}{2} \int \frac{d\mathbf{k}}{(2\pi)^3} (\mathcal{J}_{\text{tot}}^\mu(\mathbf{k}))^* G^{\mu\nu}(\mathbf{k}) \mathcal{J}_{\text{tot}}^\nu(\mathbf{k}) \right\} &= \exp \left\{ -\frac{\beta}{2} \int \frac{d\mathbf{k}}{(2\pi)^3} G^{\mu\nu}(\mathbf{k}) \right. \\ &\times \left. \left[(\mathcal{J}^\mu)^* \mathcal{J}^\nu + (\mathcal{J}_{\text{ext}}^\mu)^* \mathcal{J}^\nu + (\mathcal{J}^\mu)^* \mathcal{J}_{\text{ext}}^\nu + (\mathcal{J}_{\text{ext}}^\mu)^* \mathcal{J}_{\text{ext}}^\nu \right] (\mathbf{k}) \right\}. \end{aligned} \quad (4.60)$$

Therefore, from (4.60), functional differentiation with respect to \mathcal{J}_{ext} according to (4.58) produces two terms

$$\langle A^\mu(\mathbf{x})A^\nu(\mathbf{y}) \rangle_{\text{T}} = \langle A^\mu(\mathbf{x})A^\nu(\mathbf{y}) \rangle_{\text{T}}^0 + \langle A^\mu(\mathbf{x})A^\nu(\mathbf{y}) \rangle_{\text{T}}^{\text{mat}}. \quad (4.61)$$

The first contribution (written in Fourier form)

$$\begin{aligned} \langle A^\mu(\mathbf{x})A^\nu(\mathbf{y}) \rangle_{\text{T}}^0 &= \frac{1}{\beta} \int \frac{d\mathbf{k}}{(2\pi)^3} e^{i\mathbf{k} \cdot (\mathbf{x}-\mathbf{y})} G^{\mu\nu}(\mathbf{k}) \\ &\sim \frac{1}{2\beta r} \left(\delta^{\mu\nu} + \frac{r^\mu r^\nu}{r^2} \right), \quad r \rightarrow \infty, \quad \mathbf{r} = \mathbf{x} - \mathbf{y}, \end{aligned} \quad (4.62)$$

¹¹As a consequence of the imaginary coupling constant in the Hamiltonian (4.56), the total current is real, so that we can still apply the Gaussian integration formula used in (4.17).

arises from the part quadratic in \mathcal{J}_{ext} in (4.60). It describes the thermal fluctuations of the free field, and in view of (4.20), decays as r^{-1} . The second term, coming from the part linear in \mathcal{J}_{ext} ,

$$\begin{aligned} \langle A^\mu(\mathbf{x})A^\nu(\mathbf{y}) \rangle_{\text{T}}^{\text{mat}} &= \\ &= - \int \frac{d\mathbf{k}}{(2\pi)^3} e^{i\mathbf{k}\cdot\mathbf{x}} \int \frac{d\mathbf{k}'}{(2\pi)^3} e^{i\mathbf{k}'\cdot\mathbf{y}} G^{\mu\sigma}(\mathbf{k})G^{\nu\tau}(\mathbf{k}') \langle \mathcal{J}^\sigma(\mathbf{k})\mathcal{J}^\tau(\mathbf{k}') \rangle_{\text{T}}, \end{aligned} \quad (4.63)$$

represents the modification to the free-field fluctuations caused by the presence of matter. It involves the loop current correlation function $\langle \mathcal{J}^\sigma(\mathbf{k})\mathcal{J}^\tau(\mathbf{k}') \rangle_{\text{T}}$ where the average is taken with respect to the thermal weight (4.23) for the statistical-mechanical system of loops. Expressing the currents $\mathcal{J}(\mathbf{k}) = \int d\mathcal{F} \mathbf{j}(\mathcal{F}, \mathbf{k})\hat{\rho}(\mathcal{F})$ in terms of the density of loops $\hat{\rho}(\mathcal{F}) = \sum_i \delta(\mathcal{F}, \mathcal{F}_i)$ (see (4.16)), one can write this current correlation in terms of the loop density correlation function $n_{\text{T}}(\gamma_1, \boldsymbol{\xi}_1, \gamma_2, \boldsymbol{\xi}_2, \mathbf{k})$ (including the contribution of coincident points):

$$\begin{aligned} \langle \mathcal{J}^\sigma(\mathbf{k})\mathcal{J}^\tau(\mathbf{k}') \rangle_{\text{T}} &= (2\pi)^3 \delta(\mathbf{k} + \mathbf{k}') \\ &\times \sum_{\gamma_1, \gamma_2} \int D(\boldsymbol{\xi}_1) \int D(\boldsymbol{\xi}_2) \mathcal{T}^\sigma(\gamma_1, \boldsymbol{\xi}_1, \mathbf{k})(\mathcal{T}^\tau(\gamma_2, \boldsymbol{\xi}_2, \mathbf{k}))^* n_{\text{T}}(\gamma_1, \boldsymbol{\xi}_1, \gamma_2, \boldsymbol{\xi}_2, \mathbf{k}). \end{aligned} \quad (4.64)$$

The $\delta(\mathbf{k} + \mathbf{k}')$ is the manifestation of the translational invariance of the state, and we have set

$$\mathcal{T}^\sigma(\gamma_i, \boldsymbol{\xi}_i, \mathbf{k}) = \frac{e\gamma_i}{\sqrt{\beta m_{\gamma_i} c^2}} \int_0^1 d\xi_i^{\sigma}(s_i) e^{i\lambda_{\gamma_i} \mathbf{k} \cdot \boldsymbol{\xi}_i(s_i)}. \quad (4.65)$$

When (4.64) is introduced into (4.63), one obtains the final form

$$\langle A^\mu(\mathbf{x})A^\nu(\mathbf{y}) \rangle_{\text{T}}^{\text{mat}} = - \int \frac{d\mathbf{k}}{(2\pi)^3} e^{i\mathbf{k}\cdot(\mathbf{x}-\mathbf{y})} G^{\mu\sigma}(\mathbf{k})G^{\nu\tau}(\mathbf{k})Q^{\sigma\tau}(\mathbf{k}), \quad (4.66)$$

where $Q^{\sigma\tau}(\mathbf{k})$ is the tensor

$$Q^{\sigma\tau}(\mathbf{k}) = \sum_{\gamma_1, \gamma_2} \int D(\boldsymbol{\xi}_1) \int D(\boldsymbol{\xi}_2) \mathcal{T}^\sigma(\gamma_1, \boldsymbol{\xi}_1, \mathbf{k})(\mathcal{T}^\tau(\gamma_2, \boldsymbol{\xi}_2, \mathbf{k}))^* n_{\text{T}}(\gamma_1, \boldsymbol{\xi}_1, \gamma_2, \boldsymbol{\xi}_2, \mathbf{k}). \quad (4.67)$$

To obtain the long-distance behaviour of this correlation we examine the integrand in (4.67) at small \mathbf{k} . Because of isotropy, the tensor $Q^{\sigma\tau}(\mathbf{k})$ transforms covariantly under the rotations, and thus is of the form

$$Q^{\sigma\tau}(\mathbf{k}) = a(k)\delta^{\sigma\tau} + b(k)k^\sigma k^\tau, \quad k = |\mathbf{k}| \quad (4.68)$$

The term $k^\sigma k^\tau$ does not contribute to (4.67) since $G^{\mu\sigma}(\mathbf{k})$ is transversal. Because of Itô's lemma, $\mathcal{T}^\sigma(\gamma_i, \xi_i, \mathbf{k})$ is linear in \mathbf{k} as $\mathbf{k} \rightarrow 0$, implying $a(\kappa) = a \kappa^2[1 + o(\kappa)]$. Hence, using $\delta_{tr}^{\mu\sigma}(\mathbf{k})\delta_{tr}^{\nu\sigma}(\mathbf{k}) = \delta_{tr}^{\mu\nu}(\mathbf{k})$ one finds

$$G^{\mu\sigma}(\mathbf{k})G^{\nu\tau}(\mathbf{k})Q^{\sigma\tau}(\mathbf{k}) = 4\pi a \frac{4\pi}{\kappa^2} \delta_{tr}^{\mu\nu}(\mathbf{k})[1 + o(\kappa)] = 4\pi a G^{\mu\nu}(\mathbf{k})[1 + o(\kappa)] \quad (4.69)$$

as $\mathbf{k} \rightarrow 0$. This shows that $\langle A^\mu(\mathbf{x})A^\nu(\mathbf{y}) \rangle_{\text{T}}^{\text{mat}}$ has the same type of decay as the free field part (4.62) with a modified amplitude. Summing up the two contributions (4.61) gives

$$\langle A^\mu(\mathbf{x})A^\nu(\mathbf{y}) \rangle_{\text{T}} \sim \frac{1}{2r} \left(\delta^{\mu\nu} + \frac{r^\mu r^\nu}{r^2} \right) \left(\frac{1}{\beta} - 4\pi a \right), \quad r \rightarrow \infty. \quad (4.70)$$

For $\mathbf{B}(\mathbf{x}) = \nabla \times \mathbf{A}(\mathbf{x})$, one finds, from (4.70),

$$\langle B^\mu(\mathbf{x})B^\nu(\mathbf{y}) \rangle_{\text{T}} \sim \left(\partial_\mu \partial_\nu \frac{1}{r} \right) \left(\frac{1}{\beta} - 4\pi a \right), \quad r \rightarrow \infty. \quad (4.71)$$

The constant $a = a(\hbar, \beta, \rho)$ embodies the effects of matter on the transverse field fluctuations. It has a relativistic factor $(mc^2)^{-1}$ and vanishes in the classical limit $\hbar \rightarrow 0$ (in accordance to the Bohr–van Leeuwen decoupling) as $O(\hbar^4)$ (see appendix 4.D).¹²

In order to find the correlations of the transverse electric field

$$\begin{aligned} \mathbf{E}_t(\mathbf{x}) &= -\frac{1}{c} \frac{\partial \mathbf{A}(\mathbf{x}, t)}{\partial t} \Big|_{t=0} \\ &= -\left(\frac{4\pi\hbar c^2}{R^3} \right)^{1/2} \sum_{\mathbf{k}\lambda} g(\mathbf{k}) \frac{\mathbf{e}_{\mathbf{k}\lambda}}{\sqrt{2\omega_{\mathbf{k}}}} \left(\frac{i\omega_{\mathbf{k}}}{c} \alpha_{\mathbf{k}\lambda}^* e^{-i\mathbf{k}\cdot\mathbf{x}} - \frac{i\omega_{\mathbf{k}}}{c} \alpha_{\mathbf{k}\lambda} e^{i\mathbf{k}\cdot\mathbf{x}} \right), \end{aligned} \quad (4.72)$$

we couple the latter to an external polarisation $\mathcal{P}_{\text{ext}}(\mathbf{x})$,

$$H_{L,R}(\mathcal{P}_{\text{ext}}) = H_{L,R} - i \int d\mathbf{x} \mathcal{P}_{\text{ext}}(\mathbf{x}) \cdot \mathbf{E}_t(\mathbf{x}), \quad (4.73)$$

and proceed as after (4.56). This amounts to replacing everywhere $\mathcal{J}_{\text{ext}}(\mathbf{k})$ by $i\kappa \mathcal{P}_{\text{ext}}(\mathbf{k})$ so that the right-hand side of equation (4.60) is changed into

$$\begin{aligned} &\exp \left\{ -\frac{\beta}{2} \int \frac{d\mathbf{k}}{(2\pi)^3} G^{\mu\nu}(\mathbf{k}) \right. \\ &\quad \left. \times \left[(\mathcal{J}^\mu)^* \mathcal{J}^\nu - i\kappa (\mathcal{P}_{\text{ext}}^\mu)^* \mathcal{J}^\nu + i\kappa (\mathcal{J}^\mu)^* \mathcal{P}_{\text{ext}}^\nu + \kappa^2 (\mathcal{P}_{\text{ext}}^\mu)^* \mathcal{P}_{\text{ext}}^\nu \right] (\mathbf{k}) \right\}. \end{aligned} \quad (4.74)$$

¹²The $O(\hbar^4)$ decay is erroneous. In fact, a vanishes as $O(\hbar^2)$. See footnote 13.

As $\mathcal{P}_{\text{ext}}(\mathbf{r})$ and $\mathcal{J}(\mathbf{r})$ are real, $\mathcal{P}_{\text{ext}}^*(\mathbf{k}) = \mathcal{P}_{\text{ext}}(-\mathbf{k})$ and likewise for \mathcal{J} . From the change of variable $\mathbf{k} \mapsto -\mathbf{k}$, one sees that the second term in the integrand in (4.74) is exactly compensated by the third term. Only the term quadratic in \mathcal{P}_{ext} remains, which is responsible upon functional differentiation for the thermal fluctuations of the free field, as in (4.62). Hence, the correlations of the transverse part of the electric field are decoupled from matter and one finds

$$\langle E_t^\mu(\mathbf{x})E_t^\nu(\mathbf{y}) \rangle_T = \langle E_t^\mu(\mathbf{x})E_t^\nu(\mathbf{y}) \rangle_T^0 \sim \left(\partial_\mu \partial_\nu \frac{1}{r} \right) \frac{1}{\beta}, \quad r \rightarrow \infty. \quad (4.75)$$

The asymptotic correlation of the complete electric field $\mathbf{E}(\mathbf{x}) = \mathbf{E}_l(\mathbf{x}) + \mathbf{E}_t(\mathbf{x})$ follows from (4.55) and (4.75) (one can check by similar calculations that the cross correlation $\langle E_l^\mu(\mathbf{x})E_t^\nu(\mathbf{y}) \rangle_T$ vanishes identically):

$$\begin{aligned} \langle E^\mu(\mathbf{x})E^\nu(\mathbf{y}) \rangle_T &= \langle E_l^\mu(\mathbf{x})E_l^\nu(\mathbf{y}) \rangle_T + \langle E_t^\mu(\mathbf{x})E_t^\nu(\mathbf{y}) \rangle_T \\ &= \left(\partial_\mu \partial_\nu \frac{1}{r} \right) \left(\frac{2\pi}{3} \int d\mathbf{r} |\mathbf{r}|^2 S(\mathbf{r}) + \frac{1}{\beta} \right), \quad r \rightarrow \infty. \end{aligned} \quad (4.76)$$

In the classical limit, $S(\mathbf{r})$ satisfies the second-moment Stillinger–Lovett sum rule (Martin, 1988) $-\frac{2\pi}{3} \int d\mathbf{r} |\mathbf{r}|^2 S(\mathbf{r}) = 1/\beta$. Hence, the asymptotic longitudinal electric field correlations in the matter are exactly compensated by those of the free radiation part, as noted in (Felderhof, 1965). However, this no longer holds for quantum plasmas. As an illustration, for the quantum one-component plasma (jellium), one has (Pines & Nozières, 1966)

$$-\frac{2\pi}{3} \int d\mathbf{r} |\mathbf{r}|^2 S(\mathbf{r}) = \frac{\hbar\omega_p}{2} \coth\left(\frac{\hbar\omega_p\beta}{2}\right) = \frac{1}{\beta} + \frac{\beta}{3} \left(\frac{\hbar\omega_p}{2}\right)^2 + \mathcal{O}(\hbar^4), \quad (4.77)$$

where ω_p is the plasmon frequency. The long range of the electric field correlations is thus a purely quantum-mechanical effect. These findings are further discussed in the concluding remarks (Section 4.8).

4.7 Bose and Fermi statistics

In this final section we introduce the needed modifications when the Fermionic or Bosonic particle statistics are taken into account.

The Bose or Fermi statistics of the particles can be incorporated in the formalism following the same procedure as described in (Cornu, 1996a), (Brydges & Martin, 1999, Sec. V). The matrix elements of (4.8), which is still an operator depending on the particle variables, are to be evaluated with properly symmetrized (antisymmetrized) states. When combining the decomposition of the permutation

into cycles with the Feynman-Kac-Itô path integral representation this leads to generalize the previous loops $\mathcal{F} = (\mathbf{r}, \gamma, \xi)$ to Brownian loops $\mathcal{L} = (q, \mathbf{r}, \gamma, \mathbf{X})$ that carry q particles (a set of particles labeled by indices belonging to a permutation cycle of length q). The loop is located at \mathbf{r} and has a random shape which is a Brownian bridge $\mathbf{X}(s)$, $0 \leq s \leq q$, $\mathbf{X}(0) = \mathbf{X}(q) = \mathbf{0}$ with zero mean and covariance

$$\int \mathbf{D}(\mathbf{X}) X_\mu(s_1) X_\nu(s_2) = \delta_{\mu\nu} q \left[\min\left(\frac{s_1}{q}, \frac{s_2}{q}\right) - \frac{s_1 s_2}{q^2} \right]. \quad (4.78)$$

We merely give the final formulae since all steps are essentially identical as those presented in the above mentioned works.

The grand canonical partition function of the particle system, with the field degrees of freedom integrated out, takes the following classical-like form in the space of loops

$$\Xi_\Lambda = \sum_{n=0}^{\infty} \frac{1}{n!} \int \prod_{i=1}^n d\mathcal{L}_i z(\mathcal{L}_i) \exp(-\beta \mathcal{U}(\mathcal{L}_1, \dots, \mathcal{L}_n)). \quad (4.79)$$

Integration on phase space means integration over space and summation over all internal degrees of freedom of the loops:

$$\int d\mathcal{L} \dots = \int d\mathbf{r} \sum_{\gamma} \sum_{q=1}^{\infty} \int \mathbf{D}(\mathbf{X}) \dots \quad (4.80)$$

$\mathcal{U}(\mathcal{L}_1, \dots, \mathcal{L}_n)$ is the sum of the pair interactions between two different loops $e_{\gamma_i e_{\gamma_j}} [\mathcal{V}_c(\mathcal{L}_i, \mathcal{L}_j) + \mathcal{W}_m(\mathcal{L}_i, \mathcal{L}_j)]$ with

$$\mathcal{V}_c(\mathcal{L}_i, \mathcal{L}_j) = \int_0^{q_i} ds_1 \int_0^{q_j} ds_2 \delta(\tilde{s}_1 - \tilde{s}_2) \frac{1}{|\mathbf{r}_i + \lambda_{\gamma_i} \mathbf{X}_i(s_1) - \mathbf{r}_j - \lambda_{\gamma_j} \mathbf{X}_j(s_2)|} \quad (4.81)$$

the Coulomb potential, and

$$\begin{aligned} \mathcal{W}_m(\mathcal{L}_i, \mathcal{L}_j) &= \frac{1}{\beta \sqrt{m_{\gamma_i} m_{\gamma_j}} c^2} \int \frac{d\mathbf{k}}{(2\pi)^3} e^{i\mathbf{k} \cdot (\mathbf{r}_i - \mathbf{r}_j)} \\ &\times \int_0^{q_i} dX_i^\mu(s_1) e^{i\mathbf{k} \cdot \lambda_{\gamma_i} \mathbf{X}_i(s_1)} \int_0^{q_j} dX_j^\nu(s_2) e^{-i\mathbf{k} \cdot \lambda_{\gamma_j} \mathbf{X}_j(s_2)} G^{\mu\nu}(\mathbf{k}) \end{aligned} \quad (4.82)$$

the effective magnetic potential obtained after integrating out the field variables. Here $\tilde{s} = s \bmod 1$ and $\delta(\tilde{s}) = \sum_{n=-\infty}^{\infty} e^{2i\pi n s}$ is the periodic Dirac function of period 1 that takes into account the equal time constraint imposed by the Feynman-Kac formula. Finally, the activity $z(\mathcal{L}_i)$ of a loop

$$z(\mathcal{L}_i) = \frac{(\eta_{\gamma_i})^{q_i-1}}{q_i} \frac{z_{\gamma_i}^{q_i}}{(2\pi q_i \lambda_{\gamma_i}^2)^{3/2}} \exp(-\beta[\mathcal{U}^{\text{self}}(\mathcal{L}_i) + \mathcal{V}^{\text{walls}}(\mathcal{L}_i)]), \quad z_{\gamma_i} = e^{\beta \mu_{\gamma_i}} \quad (4.83)$$

incorporates the chemical potential μ_{γ_i} of the particle, the effects of quantum statistics ($\eta_{\gamma_i} = 1$ for bosons and $\eta_{\gamma_i} = -1$ for fermions), and the internal interaction $\mathcal{U}^{\text{self}}(\mathcal{L}_i) = \frac{e_i^2}{2}(\mathcal{V}^c + \mathcal{W}^m)(\mathcal{L}_i, \mathcal{L}_i)$ of the particles belonging to the same loop (omitting the infinite Coulomb self-energies of the point particles). The addition of the magnetic potential \mathcal{W}^m is the only modification compared to the formalism previously developed for pure Coulombic interactions. Maxwell-Boltzmann statistics and the potentials (4.22) and (4.14) of Section 4.3 are recovered when only single-particle loops ($q = 1$) are retained.

At this point, due to the classical-like structure of the partition function (4.79), methods of classical statistical mechanics can be used in the auxiliary system of loops, in particular the technique of Mayer graphs, as in Section 4.5. The statistics of the particles affects the coefficients of the tails of the density and field correlations, but not their general forms (4.45), (4.71) and (4.76).

4.8 Concluding remarks

The Feynman–Kac–Itô path integral representation of the Gibbs weight enables one to integrate out the (classical) field variables. This yields an exact pairwise magnetic potential in the space of loops, which is asymptotically dipolar. It generates small ($O((\beta mc^2)^{-2})$) corrections to the tail of the particle correlation due to the pure Coulombic interaction.

A word is necessary about spin interactions that have not been included in the above discussion. Spin-1/2 electrons give rise to the additional term $-\nu \sum_{i=1}^n \boldsymbol{\sigma}_i \cdot \mathbf{B}(\mathbf{r}_i)$ in the Hamiltonian, with $\mathbf{B}(\mathbf{r}) = \nabla \wedge \mathbf{A}(\mathbf{r})$, $\nu = \frac{g_s e \hbar}{4mc}$, g_s the gyromagnetic factor, and $\boldsymbol{\sigma}$ the Pauli matrices. Using spin coherent states (Klauder & Skagerstam, 1985), a functional integral representation of the Gibbs weight can be constructed including the coupling of the spins to the field. Since this coupling is linear with respect to the vector potential, Gaussian integration on the field variables leads again to an effective spin-spin interaction $W_s(i, j)$ and effective cross interactions $W_{\text{sm}}(i, j)$ and $W_{\text{ms}}(i, j)$ between spin and orbital magnetism; details can be found in (Boustani, 2005). One finds that these interactions are of dipolar type $\sim r^{-3}$, $r \rightarrow \infty$ and they have to be added to the magnetic potential $W^m(i, j)$. In a homogeneous and isotropic phase, the spin interaction terms contribute to the r^{-6} tail of the particle correlations with the same amplitude $\frac{\lambda_a^2 \lambda_b^2 e_a^2 e_b^2 \rho_a \rho_b}{m_a m_b c^4}$, up to numerical factors, as that found in Section 4.4 in the case of the magnetic potential W^m .

Regarding the electric field correlations in the plasma, we also find that they have an algebraic decay of dipolar type. This is in disagreement with the macroscopic calculation presented by Landau and Lifshitz (Landau et al., 1984, §88),

based on linear response theory and the fluctuation-dissipation theorem. Indeed, the electric field fluctuations obtained in this theory are short ranged (exponentially fast decaying): unlike in our calculation, the algebraic parts of the longitudinal and transverse correlations compensate exactly in the Landau and Lifshitz formulae (Jancovici, 2005). Understanding the relation between our strictly microscopic approach and the macroscopic theory of field fluctuations is an open problem.

Let us, however, briefly point out some differences between the two approaches. The microscopic approach involves all length scales, whereas Landau and Lifshitz assume that the correlations of the polarisation are local (δ correlated in space) and thus deal with a wave-number-independent dielectric function $\epsilon(\omega)$. Taking into account the wave-number dependence, it is likely that $\epsilon(\mathbf{\kappa}, \omega)$ has terms non-analytic in $\mathbf{\kappa}$, reflecting the fact that Coulombic matter has algebraically decaying correlations. In fact, for the jellium model, the static dielectric function $\epsilon(\mathbf{\kappa}, \omega = 0)$ has a singular term $\sim |\mathbf{\kappa}|$ in its small- $\mathbf{\kappa}$ expansion (Cornu & Martin, 1991). It is possible that in a non-local generalization of the Landau–Lifshitz theory such singular terms also generate power-law decays of the field correlations. Furthermore, the magnetic permeability is usually set equal to that of the vacuum, thus ignoring the magnetization fluctuations, whereas in our calculation the latter are properly included.

We stress again that the results of this paper hold when the electromagnetic field is classical, which is supposed to correctly depict the small-wave-number regime, as said in the Introduction. Hence, the occurrence of the Planck constant originates exclusively from the quantum-mechanical nature of matter. If the field is quantized, we can, however, not exclude an interplay between \hbar_{matter} and \hbar_{field} , which could lead to a modification of the asymptotic formulae presented in the paper.

Acknowledgements

We thank A. Alastuey and B. Jancovici for useful discussions. P.R.B. is supported by the Swiss National Foundation for Scientific Research.

Appendix 4.A

To establish (4.40) according to the middle point prescription (4.12) one has to evaluate the rotationally covariant tensor

$$\begin{aligned}
& \int \mathbf{D}(\xi) \int_0^1 d\xi^\alpha(s) \int_0^1 d\xi^\gamma(t) \xi^\omega(s) \xi^\epsilon(t) = \\
& = \lim_{n,m \rightarrow \infty} \sum_{k,l=1}^{n,m} \int \mathbf{D}(\xi) \left[\xi^\alpha(k_n) - \xi^\alpha(k_n - \frac{1}{n}) \right] \left[\xi^\gamma(l_m) - \xi^\gamma(l_m - \frac{1}{m}) \right] \\
& \times \frac{1}{2} \left[\xi^\omega(k_n) + \xi^\omega(k_n - \frac{1}{n}) \right] \frac{1}{2} \left[\xi^\epsilon(l_m) + \xi^\epsilon(l_m - \frac{1}{m}) \right] = \delta^{\alpha\gamma} \delta^{\omega\epsilon} A_1 + \delta^{\alpha\omega} \delta^{\gamma\epsilon} A_2 + \delta^{\alpha\epsilon} \delta^{\gamma\omega} A_3,
\end{aligned} \tag{4A.1}$$

where $k_n = \frac{k}{n}$ and $l_m = \frac{l}{m}$. Setting $C(s, t) = \delta^{\mu\nu}(\min(s, t) - st)$ (see (4.11)), one has

$$\begin{aligned}
A_1 &= \lim_{n,m \rightarrow \infty} \frac{1}{4} \left[C(k_n, l_m) - C(k_n, l_m - \frac{1}{m}) - C(k_n - \frac{1}{n}, l_m) + C(k_n - \frac{1}{n}, l_m - \frac{1}{m}) \right] \\
& \times \left[C(k_n, l_m) + C(k_n, l_m - \frac{1}{m}) + C(k_n - \frac{1}{n}, l_m) + C(k_n - \frac{1}{n}, l_m - \frac{1}{m}) \right], \\
A_2 &= \lim_{n,m \rightarrow \infty} \frac{1}{4} \left[C(k_n, k_n) + C(k_n, k_n - \frac{1}{n}) - C(k_n - \frac{1}{n}, k_n) - C(k_n - \frac{1}{n}, k_n - \frac{1}{n}) \right] \\
& \times \left[C(l_m, l_m) + C(l_m, l_m - \frac{1}{m}) - C(l_m - \frac{1}{m}, l_m) - C(l_m - \frac{1}{m}, l_m - \frac{1}{m}) \right], \\
A_3 &= \lim_{n,m \rightarrow \infty} \frac{1}{4} \left[C(k_n, l_m) + C(k_n, l_m - \frac{1}{m}) C(k_n - \frac{1}{n}, l_m) - C(k_n - \frac{1}{n}, l_m - \frac{1}{m}) \right] \\
& \times \left[C(l_m, k_n) + C(l_m, k_n - \frac{1}{n}) - C(l_m - \frac{1}{m}, k_n) - C(l_m - \frac{1}{m}, k_n - \frac{1}{n}) \right].
\end{aligned} \tag{4A.2}$$

This results from the application of Wick's theorem to the Gaussian average (4A.1) with covariance (4.11). Expanding $C(k_n - \frac{1}{n}, l_m) = C(k_n, l_m) - \frac{1}{n}(\partial_1 C)(k_n, l_m)$ and $C(k_n, l_m - \frac{1}{m}) = C(k_n, l_m) - \frac{1}{m}(\partial_2 C)(k_n, l_m)$ and taking the limits $n, m \rightarrow \infty$ gives

$$\begin{aligned}
A_1 &= \int_0^1 ds \int_0^1 dt C(s, t) (\partial_1 \partial_2 C)(s, t) = \frac{1}{12}, \\
A_2 &= \frac{1}{4} \left(\int_0^1 ds \frac{d}{ds} C(s, s) \right)^2 = 0, \\
A_3 &= \int_0^1 ds \int_0^1 dt (\partial_1 C)(s, t) (\partial_2 C)(s, t) = -\frac{1}{12},
\end{aligned} \tag{4A.3}$$

hence the result (4.40).

Appendix 4.B

From (4.22) and (4.28) the cross Coulomb-magnetic term is

$$\begin{aligned} & \beta^2 e_a^2 e_b^2 \int D(\xi_a) \rho(\xi_a) \int D(\xi_b) \rho(\xi_b) W^c(\mathcal{F}_a, \mathcal{F}_b) W^m(\mathcal{F}_a, \mathcal{F}_b) = \\ & \frac{\beta e_a^2 e_b^2}{\sqrt{m_a m_b} c^2} \int \frac{d\mathbf{k}_1}{(2\pi)^3} \int \frac{d\mathbf{k}_2}{(2\pi)^3} e^{i(\mathbf{k}_1 + \mathbf{k}_2) \cdot (\mathbf{r}_a - \mathbf{r}_b)} \int_0^1 ds_1 \int_0^1 ds_2 (\delta(s_1 - s_2) - 1) \\ & \times (H_a^\mu)^*(\mathbf{k}_1, \mathbf{k}_2, s_1) H_b^\nu(\mathbf{k}_1, \mathbf{k}_2, s_2) \frac{4\pi}{k_1^2} G^{\mu\nu}(\mathbf{k}_2), \end{aligned} \quad (4B.1)$$

where

$$H_a^\mu(\mathbf{k}_1, \mathbf{k}_2, s_1) = \int D(\xi_a) \rho(\xi_a) e^{-i\lambda_a \mathbf{k}_1 \cdot \xi_a(s_1)} \int_0^1 d\xi_a^\mu(s) e^{-i\lambda_a \mathbf{k}_2 \cdot \xi_a(s)}. \quad (4B.2)$$

Because of the rotational invariance of $D(\xi_a) \rho(\xi_a)$, averages of odd powers of ξ_a vanish. This implies that in the small- $\mathbf{k}_1, \mathbf{k}_2$ expansion of $H_a^\mu(\mathbf{k}_1, \mathbf{k}_2, s_1)$ only odd monomials in $\mathbf{k}_1, \mathbf{k}_2$ occur:

$$\begin{aligned} H_a^\mu(\mathbf{k}_1, \mathbf{k}_2, s_1) & \sim \int D(\xi_a) \rho(\xi_a) \int_0^1 d\xi_a^\mu(s) (i\lambda_a \mathbf{k}_2 \cdot \xi_a(s)) + O_3(\mathbf{k}_1, \mathbf{k}_2) \\ & = \text{const} \times k_2^\mu + O_3(\mathbf{k}_1, \mathbf{k}_2), \end{aligned} \quad (4B.3)$$

where $O_3(\mathbf{k}_1, \mathbf{k}_2)$ represent monomials of order 3 in the components of $\mathbf{k}_1, \mathbf{k}_2$. The same holds for $H_b^\mu(\mathbf{k}_1, \mathbf{k}_2, s_2)$. Since $k_2^\mu G^{\mu\nu}(\mathbf{k}_2) = 0$ by transversality, one concludes that the term (4B.1) decays at least as $|\mathbf{r}_a - \mathbf{r}_b|^{-8}$.

Appendix 4.C

If point i in $W^c(i, j)$ or $W^m(i, j)$ is a classical end, there is no other ξ_i dependence at this point than that arising from these bonds. In the asymptotic formula (4.30) for W^c , this dependence is linear and thereby vanishes upon the space-inversion invariant $D(\xi_i)$ integration. In the case of W^m , from formula (4.22), the $D(\xi_i)$ integration yields the factor

$$\int D(\xi_i) \int_0^1 d\xi_i^\mu(s_1) e^{i\mathbf{K} \cdot \lambda_i \xi_i(s_1)} \propto k^\mu \quad (4C.1)$$

because of covariance under rotation. Hence, this contribution vanishes as a consequence of transversality $k^\mu G^{\mu\nu}(\mathbf{k}) = 0$.

Appendix 4.D

An explicit expression for the constant $a = a(\hbar, \beta, \rho)$ follows from taking the trace in equation (4.69) and using (4.67) expanded for small κ . This yields

$$a = \frac{1}{2} \sum_{\gamma, \gamma'} \frac{e_\gamma \lambda_\gamma e_{\gamma'} \lambda_{\gamma'}}{\beta \sqrt{m_\gamma m_{\gamma'}} c^2} \int \mathcal{D}(\xi) \int \mathcal{D}(\xi') \\ \times \int_0^1 d\xi^\mu(s) \int_0^1 d\xi^\nu(s') (\hat{\mathbf{k}} \cdot \xi(s)) (\hat{\mathbf{k}} \cdot \xi'(s')) \delta_{\text{tr}}^{\mu\nu}(\hat{\mathbf{k}}) n_{\text{T}}(\gamma, \xi, \gamma', \xi', \mathbf{k} = \mathbf{0}), \quad (4\text{D}.1)$$

where $\hat{\mathbf{k}} = \mathbf{k}/\kappa$. As $\lambda_\gamma \lambda_{\gamma'}$ is of order \hbar^2 , at lowest order in \hbar one can set $\hbar = 0$ in the correlation function. The latter becomes independent of the quantum fluctuations ξ, ξ' and reduces to the density correlation function of the corresponding classical system. The remaining functional integrals, of the type $\int \mathcal{D}(\xi) \int_0^1 d\xi^\mu(s) \xi^\sigma(s)$, vanish identically. The terms of order $O(\hbar)$ in n_{T} are necessarily linear in ξ or ξ' . They do not contribute to a since averages of odd powers ξ or ξ' are zero, implying that there are no \hbar^3 -terms in a . We thus conclude that a is $O(\hbar^4)$.¹³

References

- Alastuey, A. (1994). Statistical mechanics of quantum plasmas. Path integral formalism. In G. Chabrier and E. Schatzman (Eds.), *The equation of state in astrophysics* (Vol. 147, pp. 43–77). Cambridge, UK: Cambridge University Press.
- Alastuey, A., and Appel, W. (1997). A model of relativistic one-component plasma with Darwin interactions. *Physica A*, 238, 369–404.
- Alastuey, A., and Appel, W. (2000). On the decoupling between classical Coulomb matter and radiation. *Physica A*, 276, 508–520.
- Alastuey, A., and Martin, Ph. A. (1989). Absence of exponential clustering in quantum Coulomb fluids. *Phys. Rev. A*, 40, 6485–6520.
- Appel, W., and Alastuey, A. (1998). Relativistic corrections for a classical one-component plasma with Darwin interactions. *Physica A*, 252, 238–268.
- Appel, W., and Alastuey, A. (1999). Thermal screening of Darwin interactions in a weakly relativistic plasma. *Phys. Rev. E*, 59, 4542–4551.
- Ballenegger, V., Martin, Ph. A., and Alastuey, A. (2002). Quantum Mayer graphs for Coulomb systems and the analog of the Debye potential. *J. Stat. Phys.*, 108, 169–211.
- Boustani, S. el. (2005). *Corrélations dans un gaz Coulombien à l'équilibre en présence du champ de radiation*. Master's thesis, Swiss Federal Institute of Technology,

¹³This $O(\hbar^4)$ decay is erroneous. In fact, a vanishes as $O(\hbar^2)$ due to the contribution of the coincident points of the correlation function, which have been disregarded in this discussion.

- Lausanne (EPFL), Institute of Theoretical Physics, CH-1015 Lausanne, Switzerland.
- Brydges, D. C., and Federbush, P. (1980). Debye screening. *Commun. Math. Phys.*, *73*, 197–246.
- Brydges, D. C., and Martin, Ph. A. (1999). Coulomb systems at low density : a review. *J. Stat. Phys.*, *96*, 1163–1330.
- Buenzli, P. R., and Martin, Ph. A. (2005). The Casimir force at high temperature. *Europhys. Lett.*, *72*, 42–48.
- Buenzli, P. R., and Martin, Ph. A. (2006). *Microscopic theory of the high-temperature Casimir effect*. In preparation, Swiss Federal Institute of Technology, Lausanne (EPFL), Institute of Theoretical Physics, CH-1015 Lausanne, Switzerland.
- Chabrier, G., and Schatzman, E. (Eds.). (1994). *The equation of state in astrophysics* (Vol. 147). Cambridge, UK: Cambridge University Press.
- Cohen-Tannoudji, C., Dupont-Roc, J., and Grynberg, G. (1989). *Photons and atoms, introduction to quantum electrodynamics*. New York: John Wiley and Sons.
- Cornu, F. (1996a). Correlations in quantum plasmas. I. Resummation in Mayer-like diagrammatics. *Phys. Rev. E*, *53*, 4562–4594.
- Cornu, F. (1996b). Correlations in quantum plasmas. II. Algebraic tails. *Phys. Rev. E*, *53*, 4595–4631.
- Cornu, F. (1998a). Quantum plasmas with or without a uniform magnetic field. I. General formalism and algebraic tails of correlations. *Phys. Rev. E*, *58*, 5268–5292.
- Cornu, F. (1998b). Quantum plasmas with or without a uniform magnetic field. III. Exact low-density algebraic tails of correlations. *Phys. Rev. E*, *58*, 5322–5346.
- Cornu, F., and Martin, Ph. A. (1991). Electron gas beyond the random-phase approximation: algebraic screening. *Phys. Rev. A*, *44*, 4893–4910.
- Darwin, C. G. (1920). The dynamical motion of charged particles. *Philos. Mag.*, *39*, 537–551.
- Essén, H. (1996). Darwin magnetic interaction energy and its macroscopic consequence. *Phys. Rev. E*, *53*, 5228–5239.
- Felderhof, B. U. (1965). On fluctuations and coherence of radiation in classical and semi-classical plasmas. *Physica (Amsterdam)*, *31*, 295–316.
- Feynman, R. P., and Hibbs, A. R. (1965). *Quantum mechanics and path integral*. New York: McGraw-Hill.
- Jancovici, B. (2005). [Private communication].
- Klauder, J. R., and Skagerstam, B.-S. (1985). *Coherent states*. Singapore: World Scientific.
- Landau, L. D., Lifshitz, E. M., and Pitaevskii, L. P. (1984). Electrodynamics of continuous media. In *Landau course* (2nd ed., Vol. 8). Oxford: Pergamon Press.
- Lebowitz, J. L., and Martin, Ph. A. (1984). On potential and field fluctuations in classical charged systems. *J. Stat. Phys.*, *34*, 287–311.
- Lieb, E. H. (1976). The stability of matter. *Rev. Mod. Phys.*, *48*, 533–569.
- Martin, Ph. A. (1988). Sum rules in charged fluids. *Rev. Mod. Phys.*, *60*, 1075–1127.
- Martin, Ph. A., and Buenzli, P. R. (2006). *The Casimir effect*. To appear in the Proceedings

of the 1st Warsaw School of Statistical Physics (June 2005), *Acta Physica Polonica*.
(<http://arxiv.org/abs/cond-mat/0602559>)

Pines, D., and Nozières, Ph. (1966). *The theory of quantum liquids*. New York: Benjamin.

Roespstorff, G. (1994). *Path integral approach to quantum physics. An introduction*.
Berlin: Springer Verlag.

Simon, B. (1979). *Functional integration and quantum physics*. London: Academic
Press.

Chapter 5

The Casimir force between field-coupled quantum plasmas

Contents

The Casimir force at high temperature, <i>Europhys. Lett.</i>, 72, 42–48 (2005)	147
References	155
5.1 The force expressed in the loop formalism	157
5.1.1 The free energy of the full system and its differentiation	157
5.1.2 The force expressed in terms of the loop-correlation	161
5.2 Quantum Mayer graphs	167
5.2.1 Resummation of the “classical” contribution V^{el}	168
5.3 Asymptotic correlations between the plasmas	170
5.3.1 The Debye–Hückel potential Φ_{AB} at large separations	170
5.3.2 The potential W_{AB}^{c} at large separations	171
5.3.3 The magnetic potential W_{AB}^{m} at large separations	171
5.3.4 Behaviour of the Mayer bonds	173
5.3.5 Dominant graphs and asymptotic behaviour of h_{AB}	174
5.3.6 Perfect screening sum rules	176
5.4 The Casimir force in the semi-classical regime: final result	178
5.4.1 Final result	179
Appendix 5.A: Properties of V^{c} and W^{m} regarding loops’ origin	180
Appendix 5.B: Large-distance behaviour of $\overline{W_{AB}^{\text{m}}}$	181
Appendix 5.C: Brownian path integrals on slab geometries . . .	183

In this chapter, we come back to the Casimir force exerting between two plasmas A and B . We apply to this setting the path-integral formalism developed in Chapter 4, so as to improve the basic classical model presented earlier by including quantum mechanics and the thermalised coupling of matter with the radiation field. The main result is that the magnetic Lorentz forces, mediated by the transverse field, turn out to not affect the large-distance asymptotic result of the force, namely,

$$f(d) = -\frac{\zeta(3)}{8\pi\beta d^3} + O(d^{-4}).$$

Interplasma correlations are nevertheless supplemented by new terms of magnetic origin, but these are shielded away by screening effects when integrated into the force.

The object of this chapter has been summed up in a short letter published in *Europhys. Lett.*, 72, 42–48 (2005), and reproduced hereinafter. Its contents is as follows. The complete two-plasma system of nonrelativistic quantum charges interacting with the radiation field is detailed. The field is treated classically on the ground that the correlations it induces across the two plasmas involve only long wavelengths (semi-classical regime; see also the discussion in Section 2.3.4). To simplify the presentation, the quantum particles are said to obey Maxwell–Boltzmann statistics. The Casimir force is defined as the derivative of the free energy with respect to d . To cast the full partition function in a classical-like form, the Feynman–Kac–Itô formalism — which is shortly surveyed — is used. It thus becomes an integral on loops’ degrees of freedom of the Gibbs weight $e^{-\beta U}$, where U contains pairwise loop interactions of Coulomb origin, V^c , and of magnetic origin, W^m . The latter interaction results from the exact integration of the transverse field’s degrees of freedom. Finally, the procedure to arrive at the asymptotic force using resummed Mayer graphs is tersely sketched, and the result is discussed.

In the remaining sections of this chapter, following the article, we present the details of this calculation. Proper Fermi and Bose statistics of the particles will be included.

The calculation is achieved assuming plasmas of finite thickness.

The Casimir force at high temperature

P. R. Buenzli¹ and Ph. A. Martin

Received 20 June 2005; accepted 26 July 2005

The standard expression of the high-temperature Casimir force between perfect conductors is obtained by imposing macroscopic boundary conditions on the electromagnetic field at metallic interfaces. This force is twice larger than that computed in microscopic classical models allowing for charge fluctuations inside the conductors. We present a direct computation of the force between two quantum plasma slabs in the framework of non relativistic quantum electrodynamics including quantum and thermal fluctuations of both matter and field. In the semi-classical regime, the asymptotic force at large slab separation is identical to that found in the above purely classical models, which is therefore the right result. We conclude that when calculating the Casimir force at non-zero temperature, fluctuations inside the conductors can not be ignored. Aspects of this subject are treated in a companion letter by B. Jancovici and L. Šamaj (Jancovici & Šamaj, 2005).

PACS numbers : 05.30.-d — Quantum statistical mechanics.
12.20.-m — Quantum electrodynamics
11.10.Wx — Finite-temperature field theory

Casimir showed in 1948 that the zero-point energy of the quantum electromagnetic field generates an attractive force between two perfectly conducting metallic plates at distance d and zero temperature (Casimir, 1948). In his calculation, the microscopic structure of the conductors is not taken into account. The latter are merely treated as macroscopic boundary conditions for the electromagnetic field requiring the vanishing of the tangential electric field. This geometrical constraint

¹E-mail: pascal.buenzli@epfl.ch

modifies the field eigenmodes depending on d . The d -dependence of the modified zero-point energy is the source of the well known Casimir force

$$f^{\text{vac}}(d) = -\frac{\pi^2 \hbar c}{240 d^4} \quad (5.1)$$

(\hbar denotes Planck's constant, c the speed of light).

The generalisation of Casimir's calculation to thermalized fields was given some years later in (Fierz, 1960; Mehra, 1967), see (Balian & Duplantier, 2003) for a recent account. When the temperature T is different from zero, one can form the dimensionless parameter $\alpha = \beta \pi \hbar c / d$ (the ratio of the thermal wave length of the photon to the conductors separation; β is the inverse temperature). A large value of α (low temperature, short separation) characterizes the quantum regime whereas a small value of α (high temperature, large separation) yields a purely classical asymptotic result (independent of \hbar and c)

$$f = -\frac{\zeta(3)}{4\pi\beta d^3} + O(e^{-b/\alpha}), \quad \alpha \rightarrow 0, \quad b > 0 \quad (5.2)$$

where $\zeta(s)$ is the Riemann zeta function. Each field mode is a thermalized quantum mechanical oscillator with frequencies obtained from the previously described macroscopic boundary conditions. All fluctuations inside the conductors are ignored. We note that in fact, on purely dimensional grounds, a term $\propto d^{-3}$ must also be proportional to $k_B T$, the only issue being the numerical value of the proportionality constant. This issue is the subject of this letter.

In recent times, a number of works have addressed the question of the incidence of the microscopic charge and field fluctuations inside the conductors on the Casimir force (Forrester, Jancovici, & Téllez, 1996), (Jancovici & Téllez, 1996), (Buenzli & Martin, 2005). The considered models are classical : the conductors are represented by slabs (or surfaces) containing mobile charges in thermal equilibrium and interacting through the sole Coulomb potential. These models all yield the same universal result for the mean electrostatic force between the slabs at fixed temperature and large distance

$$\langle f \rangle = -\frac{\zeta(3)}{8\pi\beta d^3} + O(d^{-4}), \quad d \rightarrow \infty \quad (5.3)$$

Universality means that the asymptotic force does not involve any parameter characterizing the material constitution of the conductors: particle charges and masses, densities ρ and slab thicknesses.² In (Forrester et al., 1996), the authors study a statistical mechanical system of charges confined to a plane at distance d of a

²In microscopic conductor models, there is a new energy parameter $e^2/\rho^{-1/3}$, the mean potential energy, so that universality does not follow from a simple dimensional analysis.

macroscopic (non fluctuating) planar conductor. In (Jancovici & Téllez, 1996), they show that replacing the above macroscopic conductor by fluctuating charges does not alter the result (5.3). We provide in (Buenzli & Martin, 2005) a general derivation of (5.3) showing that universality is guaranteed by perfect screening sum rules (Martin, 1988).

If one compares the result (5.3) with (5.2), one sees that the extrapolation of Casimir's calculation to the classical regime is larger by a factor 2 than that obtained in the classical microscopic models. The two approaches are based on different premises : (5.2) was derived from the frequency spectrum of the full electromagnetic field but treating the metals as macroscopic bodies without internal structure. On the contrary, the force in (5.3) is purely electrostatic (longitudinal field) and it originates from the particle fluctuations inside the conductors.

This calls for a more complete model that incorporates the dynamical part of the field (transverse field) in addition to the internal degrees of freedom of the conductors. A preliminary remark is in order: it is well known that classical matter in thermal equilibrium always decouples from the transverse field because of the Bohr–van Leeuwen theorem (Alastuey & Appel, 2000). It is therefore necessary to treat the conductors' charges quantum mechanically. The complete model is formulated as follows. One considers two parallel slabs *A* and *B* of surface L^2 , thickness a and at a distance d apart. They contain non relativistic quantum charges (electrons, ions, nuclei) with appropriate statistics. The total charge in each slab is taken equal to zero. The slabs are immersed in a quantum electromagnetic field, which is itself enclosed into a larger box *K* with sides of length R , $R \gg L, a$. The Hamiltonian of the total finite volume system reads in Gaussian units³

$$H = \sum_i \frac{\left(\mathbf{p}_i - \frac{e_{\gamma_i}}{c} \mathbf{A}(\mathbf{r}_i)\right)^2}{2m_{\gamma_i}} + \sum_{i < j} \frac{e_{\gamma_i} e_{\gamma_j}}{|\mathbf{r}_i - \mathbf{r}_j|} + \sum_i V^{\text{walls}}(\gamma_i, \mathbf{r}_i) + H_0^{\text{rad}} \quad (5.4)$$

The sums run on all particles with position \mathbf{r}_i and species index γ_i ; $V^{\text{walls}}(\gamma_i, \mathbf{r}_i)$ is a steep external potential that confines the particles in the slabs . It can eventually be taken infinitely steep at walls' position implying Dirichlet boundary conditions for the particle wave functions.

The electromagnetic field is written in the Coulomb (or transverse) gauge so that the vector potential $\mathbf{A}(\mathbf{r})$ is divergence free and H_0^{rad} is the Hamiltonian of the free radiation field. For it we impose periodic boundary conditions on the faces of the large box *K*. Hence expanding $\mathbf{A}(\mathbf{r})$ in the plane waves modes $\mathbf{\kappa} =$

³The Pauli coupling terms between spins and magnetic field are not taken into account here.

$(\frac{2\pi n_x}{R}, \frac{2\pi n_y}{R}, \frac{2\pi n_z}{R})$ gives the usual formulae

$$\mathbf{A}(\mathbf{r}) = \left(\frac{4\pi\hbar c^2}{R^3} \right)^{1/2} \sum_{\mathbf{k}, \lambda} g(\mathbf{k}) \frac{\mathbf{e}_{\mathbf{k}}(\lambda)}{\sqrt{2\omega_{\mathbf{k}}}} (a_{\mathbf{k}, \lambda}^* e^{-i\mathbf{k}\cdot\mathbf{r}} + a_{\mathbf{k}, \lambda} e^{i\mathbf{k}\cdot\mathbf{r}}) \quad (5.5)$$

$$H_0^{\text{rad}} = \sum_{\mathbf{k}, \lambda} \hbar\omega_{\mathbf{k}} a_{\mathbf{k}, \lambda}^* a_{\mathbf{k}, \lambda}, \quad \omega_{\mathbf{k}} = c|\mathbf{k}| \quad (5.6)$$

In (5.5), $\mathbf{e}_{\mathbf{k}}(\lambda)$, $\lambda = 1, 2$, are the polarization vectors and $g(\mathbf{k})$, $g(\mathbf{0}) = 1$, is a form factor that takes care of ultra-violet divergences.

We suppose that the matter in the slabs is in thermal equilibrium with the radiation field and therefore introduce the finite volume free energy of the full system at temperature T

$$\Phi_{R,L,d} = -k_B T \ln \text{Tr} e^{-\beta H} \quad (5.7)$$

where the trace $\text{Tr} \equiv \text{Tr}_{\text{mat}} \text{Tr}_{\text{rad}}$ is carried over particles' and field's degrees of freedom. The force between the slabs by unit surface is now defined by

$$f(d) = \lim_{L \rightarrow \infty} \lim_{R \rightarrow \infty} f_{R,L}(d) \quad \text{with} \quad f_{R,L}(d) = -\frac{1}{L^2} \frac{\partial}{\partial d} \Phi_{R,L,d} \quad (5.8)$$

Adding and subtracting the free energy of the free photon field in (5.7) leads to

$$\Phi_{R,L,d} = -k_B T \ln \left(\frac{\text{Tr} e^{-\beta H}}{Z_0^{\text{rad}}} \right) - k_B T \ln Z_0^{\text{rad}} \quad (5.9)$$

where Z_0^{rad} is the partition function of the free photon field in the volume K . Since the last term of (5.9) is independent of d , it does not contribute to the force (5.8). Therefore

$$f(d) = k_B T \lim_{L \rightarrow \infty} \lim_{R \rightarrow \infty} \frac{1}{L^2} \frac{\partial}{\partial d} \ln \left(\frac{\text{Tr} e^{-\beta H}}{Z_0^{\text{rad}}} \right) \quad (5.10)$$

In principle $f(d)$ yields the Casimir force taking into account quantum and thermal fluctuations of both matter and field.

The main result presented in this letter is that, in the semi-classical regime, the dominant term of the large distance behaviour of the force (5.10) is still given by the universal classical behaviour (5.3). This regime is obtained when the particle thermal wave lengths $\lambda_\gamma = \hbar(\beta/m_\gamma)^{1/2}$ are much smaller than the slabs' thickness and separation ($\lambda_\gamma \ll a, d$).

More precisely, the force is of the form

$$f(d) = -\frac{\zeta(3)}{8\pi\beta d^3} + \mathcal{R}(\beta, \hbar, d), \quad \text{where} \quad \mathcal{R}(\beta, \hbar, d) = \mathcal{O}(d^{-4}) \quad (5.11)$$

namely, the quantum corrections included in the remainder $\mathcal{R}(\beta, \hbar, d)$ only occur at the subdominant order d^{-4} . We emphasize that it is far from evident that the dominant d^{-3} term is identical to that of the strictly classical model (5.3) at any fixed temperature. It is indeed known (Cornu, 1996; Brydges & Martin, 1999) that quantum Coulomb correlations have an algebraic decay due to dipolar effective interactions generated by the intrinsic fluctuations of the charges (see below). Such dipolar interactions could contribute to the d^{-3} term, as they would in a dielectric medium. But they do not because of the perfect screening sum rules that hold in conducting phases.

The formalism adapted to the investigation of the high temperature (or semi-classical) regime is the Feynman-Kac-Itô path integral representation of the Gibbs weight. In this formalism a quantum point particle of species γ is represented by a closed Brownian path $\mathbf{r} + \lambda_\gamma \boldsymbol{\xi}(s)$, $0 \leq s < 1$, $\boldsymbol{\xi}(0) = \boldsymbol{\xi}(1) = \mathbf{0}$, starting at \mathbf{r} and of extension λ_γ : it can be viewed as a charged random wire at \mathbf{r} . Thus the ensemble of wires can be treated as a classical-like system with phase space points $(\mathbf{r}_i, \boldsymbol{\xi}_i)$. The wire shape $\lambda_\gamma \boldsymbol{\xi}(s)$ (the quantum fluctuation) plays the role of an internal degree of freedom; see (Brydges & Martin, 1999), section IV, for more details on this formalism. Here, for simplicity, we use Maxwell-Boltzmann statistics for the particles. We also treat the field classically on the ground that the spacing between the dimensionless energy levels $\beta \hbar \omega_{\mathbf{k}}$ of the \mathbf{k} field mode become vanishingly small in the high temperature and large distance asymptotics ($\alpha \ll 1$). A complete presentation will be found in (Boustani, Buenzli, & Martin, 2006), (Buenzli & Martin, 2006).

The Gibbs weight associated to n wires is

$$\exp\left(-\beta \sum_{i < j}^n e_{\gamma_i} e_{\gamma_j} V^c(\mathbf{r}_i, \boldsymbol{\xi}_i, \mathbf{r}_j, \boldsymbol{\xi}_j) + i \sum_{j=1}^n \sqrt{\frac{\beta e_{\gamma_j}^2}{m_{\gamma_j} c^2}} \int_0^1 d\boldsymbol{\xi}_j(s) \cdot \mathbf{A}(\mathbf{r}_j + \lambda_{\gamma_j} \boldsymbol{\xi}_j(s))\right) \quad (5.12)$$

where

$$V^c(\mathbf{r}_i, \boldsymbol{\xi}_i, \mathbf{r}_j, \boldsymbol{\xi}_j) = \int_0^1 ds \frac{1}{|\mathbf{r}_i + \lambda_{\gamma_i} \boldsymbol{\xi}_i(s) - \mathbf{r}_j - \lambda_{\gamma_j} \boldsymbol{\xi}_j(s)|} \quad (5.13)$$

is the Coulomb potential between two wires and the vector potential part a stochastic line integral that represents the flux of the magnetic field across the wire. The vector potential is itself a random field distributed by the normalized Gaussian thermal weight $e^{-\beta H_0^{\text{rad}}} / Z_0^{\text{rad}}$. Then the partial trace $\langle \dots \rangle_{\text{rad}} = \frac{1}{Z_0^{\text{rad}}} \text{Tr}_{\text{rad}}(e^{-\beta H_0^{\text{rad}}} \dots)$

over the transverse field degrees of freedom in (5.10) is easily performed

$$\begin{aligned} & \left\langle \exp \left(i \sum_{j=1}^n \sqrt{\frac{\beta e_{\gamma_j}^2}{m_{\gamma_j} c^2}} \int_0^1 d\xi_j(s) \cdot \mathbf{A}(\mathbf{r}_j + \lambda_{\gamma_j} \xi_j(s)) \right) \right\rangle_{\text{rad}} \\ &= \left(\prod_{i=1}^n e^{-\beta e_{\gamma_i}^2 W^m(\mathbf{0}, \xi_i, \mathbf{0}, \xi_i)} \right) e^{-\beta \sum_{i < j} e_{\gamma_i} e_{\gamma_j} W^m(\mathbf{r}_i, \xi_i, \mathbf{r}_j, \xi_j)} \end{aligned} \quad (5.14)$$

In (5.14) W^m is a double stochastic integral

$$e_{\gamma_i} e_{\gamma_j} W^m(\mathbf{r}_i, \xi_i, \mathbf{r}_j, \xi_j) = \frac{1}{\beta \sqrt{m_{\gamma_i} m_{\gamma_j} c^2}} \int \frac{d\mathbf{k}}{(2\pi)^3} \sum_{\mu, \nu=1}^3 j_{\mu}^*(\mathbf{k}, i) G^{\mu\nu}(\mathbf{k}) j_{\nu}(\mathbf{k}, j) \quad (5.15)$$

where

$$G^{\mu\nu}(\mathbf{k}) = \frac{4\pi |g(\mathbf{k})|^2}{|\mathbf{k}|^2} \delta_{tr}^{\mu\nu}(\mathbf{k}), \quad \delta_{tr}^{\mu\nu}(\mathbf{k}) = \delta^{\mu\nu} - \frac{k^{\mu} k^{\nu}}{|\mathbf{k}|^2} \quad (5.16)$$

is the free field covariance and $\delta_{tr}^{\mu\nu}(\mathbf{k})$ the transverse Kronecker symbol.⁴ In (5.15), $j(\mathbf{k}, i)$ is the Fourier transform of the line current $\mathbf{j}(\mathbf{x}, i) = e_{\gamma_i} \int_0^1 d\xi_i(s) \delta(\mathbf{x} - \mathbf{r}_i - \lambda_{\gamma_i} \xi_i(s))$ associated to the wire i . One sees that the transverse part of the field gives rise to an effective pairwise magnetic interaction W^m that has (up to a factor) the same form as the classical energy of a pair of current wires. Its ratio to the Coulomb energy (5.13) is of the order of $k_B T$ divided by the rest mass energy of the particles. It accounts for orbital diamagnetic effects, which are small in normal conductors. Performing a small \mathbf{k} expansion in the integrand of (5.15) and noting that $\int_0^1 d\xi(s) = \mathbf{0}$ one sees that the large distance behaviour of W^m is dipolar

$$\begin{aligned} e_{\gamma_i} e_{\gamma_j} W^m(\mathbf{r}_i, \xi_i, \mathbf{r}_j, \xi_j) &\sim \frac{1}{\beta \sqrt{m_{\gamma_i} m_{\gamma_j} c^2}} \int_0^1 d\xi_i(s_1) \cdot \int_0^1 d\xi_j(s_2) \\ &\times \left(e_{\gamma_i} \lambda_{\gamma_i} \xi_i(s_1) \cdot \nabla_{\mathbf{r}_i} \right) \left(e_{\gamma_j} \lambda_{\gamma_j} \xi_j(s_2) \cdot \nabla_{\mathbf{r}_j} \right) \frac{1}{|\mathbf{r}_i - \mathbf{r}_j|} \end{aligned} \quad (5.17)$$

Having now identified the basic effective pair interactions between the random wires, namely the Coulomb potential $V^c(i, j)$ (5.13) and the magnetic potential $W^m(i, j)$ (5.15), it is possible to proceed exactly as in the treatment of classical charged fluids (Hansen & McDonald, 1986). One sees that $V^c(i, j)$ differs from the genuine classical electrostatic interaction between two charged wires

$$V^{\text{el}}(i, j) = \int_0^1 ds_1 \int_0^1 ds_2 \frac{1}{|\mathbf{r}_i + \lambda_{\gamma_i} \xi_i(s_1) - \mathbf{r}_j - \lambda_{\gamma_j} \xi_j(s_2)|} \quad (5.18)$$

⁴The product in (5.14) contains the magnetic self energies of the wires.

by the quantum-mechanical “equal-time constraint” imposed by the Feynman-Kac formula. It is therefore useful to split $V^c(i, j) = V^{\text{el}}(i, j) + W^c(i, j)$, where

$$W^c(i, j) = \int_0^1 ds_1 \int_0^1 ds_2 (\delta(s_1 - s_2) - 1) \frac{1}{|\mathbf{r}_i + \lambda_{\gamma_i} \boldsymbol{\xi}_i(s_1) - \mathbf{r}_j - \lambda_{\gamma_j} \boldsymbol{\xi}_j(s_2)|} \quad (5.19)$$

is the part of $V^c(i, j)$ due to intrinsic quantum fluctuations ($W^c(i, j)$ vanishes if \hbar is set equal to zero). Its large distance behaviour originates from the term bilinear in $\boldsymbol{\xi}_1$ and $\boldsymbol{\xi}_2$ in the multipolar expansion of the Coulomb potential in (5.19). It is dipolar and formally similar to that of two electrical dipoles of sizes $e_1 \lambda_1 \boldsymbol{\xi}_1$ and $e_2 \lambda_2 \boldsymbol{\xi}_2$.

$$\begin{aligned} & e_{\gamma_i} e_{\gamma_j} W^c(\mathbf{r}_i, \boldsymbol{\xi}_i, \mathbf{r}_j, \boldsymbol{\xi}_j) \\ & \sim \int_0^1 ds_1 \int_0^1 ds_2 (\delta(s_1 - s_2) - 1) \left(e_{\gamma_i} \lambda_{\gamma_i} \boldsymbol{\xi}_i(s_1) \cdot \nabla_{\mathbf{r}_i} \right) \left(e_{\gamma_j} \lambda_{\gamma_j} \boldsymbol{\xi}_j(s_2) \cdot \nabla_{\mathbf{r}_j} \right) \frac{1}{|\mathbf{r}_i - \mathbf{r}_j|} \end{aligned} \quad (5.20)$$

Introducing the diagrammatic representation of the correlation functions by Mayer graphs, we perform the usual resummations of V^{el} -chains to sum the Coulomb divergences. This provides a short range screened potential $\Phi(i, j)$, as in the classical Debye-Hückel mean-field theory. Mayer graphs are reorganized in integrable prototype graphs with bonds

$$F(i, j) = -\beta e_{\gamma_i} e_{\gamma_j} \Phi(i, j) \quad (5.21)$$

$$F^{\text{R}}(i, j) = \exp[-\beta e_{\gamma_i} e_{\gamma_j} (\Phi(i, j) + W^c(i, j) + W^{\text{m}}(i, j))] - 1 + \beta e_{\gamma_i} e_{\gamma_j} \Phi(i, j) \quad (5.22)$$

with the constraint of excluded convolution rule between $F(i, j)$ bonds, namely chains of F bonds are forbidden to avoid double counting of the original Mayer graphs.

We now sketch the final steps. To obtain the force, one needs to find the asymptotic form of the correlation between a wire in A and a wire in B . Set $F(i, j) = F_{AB}$ (F_{AA}) when particle i belongs to slab A and particle j belongs to slab B (A), and likewise for $F^{\text{R}}(i, j)$. Following the methods of (Buenzli & Martin, 2005), one shows that the bond F_{AB} is responsible for the universal term $-\zeta(3)/(8\pi\beta d^3)$ of (5.11). Some care has to be exercised with the bond F_{AB}^{R} that embodies the effect of field and particle quantum fluctuations through W^{m} and W^c . It has a dipolar long distance behaviour $F^{\text{R}}(i, j) \sim -\beta e_{\gamma_i} e_{\gamma_j} (W^c(i, j) + W^{\text{m}}(i, j)) \sim |\mathbf{r}_i - \mathbf{r}_j|^{-3}$ that might contribute to the force. In forming the complete correlation function of the two slab system, the bonds F_{AB} and F_{AB}^{R} have to be dressed at their extremities by appropriate internal correlations of the individual slabs in conformity with the diagrammatic rules. Thus, the complete expressions that enters in the force formula at large separation are of the form $G_{AA} \star F_{AB} \star G_{BB}$ and

$H_{AA} \star F_{AB}^R \star H_{BB}$. The formation of the slabs' internal correlations G_{AA} and H_{AA} in these terms is not the same because of the excluded convolution rule that applies to F_{AB} but not to F_{AB}^R . Working out the explicit expressions, one sees that perfect screening sum rules in the system of wires applied to $G_{AA} \star F_{AB} \star G_{BB}$ imply the universality of the d^{-3} term in (5.11), but the term $H_{AA} \star F_{AB}^R \star H_{BB}$ yields no contribution at order d^{-3} because of the same sum rules.

Even without going through the detailed calculations, it is clear from the asymptotic forms (5.17), (5.20) that the corrections to the electrostatic result (5.3) due to the quantum nature of the charges and the radiation field are controlled by the thermal wave lengths $\lambda_\gamma = \hbar \sqrt{\beta/m_\gamma}$, thus small at high-temperature. Because of the Bohr-van Leeuwen theorem, the free energy (5.7) of the complete model continuously approaches that of the corresponding pure electrostatic classical system as the λ_γ vanish. The force cannot jump by a factor 2 in this limit.

One must conclude from this analysis that the discrepancy between (5.2) and (5.3) is not due to the omission of the transverse part of the electromagnetic interaction in the classical Coulombic models of refs. (Forrester et al., 1996; Jancovici & Téllez, 1996; Buenzli & Martin, 2005) but should be attributed to the very fact that fluctuations inside the conductors are ignored in the calculation leading to (5.2). Hence (5.3) is the correct asymptotic form of the high-temperature Casimir force. In other words, the description of conductors by mere macroscopic boundary conditions is physically inappropriate whenever the effect of thermal fluctuations on the force are considered.

On the other hand, recent experiments validate the zero temperature formula (5.1). In (Bressi, Carugno, Onofrio, & Ruoso, 2002) the authors find an experimental agreement with the value of Casimir force's strength $\pi^2 \hbar c / 240$ to a 15% precision level. This indicates that fluctuations in conductors are drastically reduced as the temperature tends to zero and possibly have no more effect on the force at $T = 0$. A full understanding of the crossover from the high temperature regime (5.11) to the zero temperature case is an open problem.

Finally we like to comment on the Lifshitz versus Schwinger method to take the metallic limit in their theories of forces between macroscopic dielectric bodies. In (Lifshitz, 1955) Lifshitz obtained the high-temperature large-distance ($\alpha \ll 1$) force between two dielectric slabs having a static dielectric constant ϵ as

$$f(d) \sim -\frac{1}{16\pi\beta d^3} \int_0^\infty ds \frac{s^2}{\Delta^2 e^s - 1}, \quad \Delta = \frac{\epsilon + 1}{\epsilon - 1} \quad (5.23)$$

which is easily seen to reduce to (5.3) in the perfect conductor limit of electrostatics $\epsilon \rightarrow \infty$. In (Schwinger, DeRaad, & Milton, 1978), Schwinger *et al.* have proposed to take the limits in the reverse order, *i.e.*, the perfect conductor limit is taken first and the high-temperature large-distance asymptotics afterwards, re-

sulting in the value (5.2). In the light of the preceding considerations, the Lifshitz procedure is the right one to recover the high temperature regime for conductors.

In a companion letter (Jancovici & Šamaj, 2005), B. Jancovici and L. Šamaj present closely related aspects of the classical Casimir force, in particular the role of field fluctuations in classical conductors as well as a more thorough analysis of the Lifshitz theory.

Acknowledgements

We thank B. Jancovici for very fruitful discussions on the subject of this work.

References

- Alastuey, A., and Appel, W. (2000). On the decoupling between classical Coulomb matter and radiation. *Physica A*, 276, 508–520.
- Balian, R., and Duplantier, B. (2003). Effet Casimir et géométrie. In B. Duplantier and V. Rivasseau (Eds.), *Poincaré seminar 2002 : Vacuum energy-renormalization* (Vol. 30). Basel: Birkhäuser.
- Boustani, S. el, Buenzli, P. R., and Martin, Ph. A. (2006). Equilibrium correlations in charged fluids coupled to the radiation field. *Phys. Rev. E*, 73, 036113, 1–14.
- Bressi, G., Carugno, G., Onofrio, R., and Ruoso, G. (2002). Measurement of the Casimir force between parallel metallic surfaces. *Phys. Rev. Lett.*, 88, 041804, 1–4.
- Brydges, D. C., and Martin, Ph. A. (1999). Coulomb systems at low density : a review. *J. Stat. Phys.*, 96, 1163–1330.
- Buenzli, P. R., and Martin, Ph. A. (2005). Microscopic origin of universality in Casimir forces. *J. Stat. Phys.*, 119, 273–307.
- Buenzli, P. R., and Martin, Ph. A. (2006). *Microscopic theory of the high-temperature Casimir effect*. In preparation, Swiss Federal Institute of Technology, Lausanne (EPFL), Institute of Theoretical Physics, CH–1015 Lausanne, Switzerland.
- Casimir, H. B. G. (1948). On the attraction between two perfectly conducting plates. *Proc. Kon. Ned. Akad. Wet.*, 51, 793–795.
- Cornu, F. (1996). Correlations in quantum plasmas. II. Algebraic tails. *Phys. Rev. E*, 53, 4595–4631.
- Fierz, M. (1960). Zur Anziehung leitender Ebenen im Vakuum. *Helv. Phys. Acta*, 33, 855–858.
- Forrester, P., Jancovici, B., and Téllez, G. (1996). Universality in some classical Coulomb systems of restricted dimension. *J. Stat. Phys.*, 84, 359–378.
- Hansen, J.-P., and McDonald, I. R. (1986). *Theory of simple liquids* (2nd ed.). London: Academic Press.
- Jancovici, B., and Šamaj, L. (2005). Casimir force between two ideal-conductor walls revisited. *Europhys. Lett.*, 72, 35–41.

- Jancovici, B., and Téllez, G. (1996). The ideal conductor limit. *J. Phys. A : Math. Gen.*, 29, 1155–1166.
- Lifshitz, E. M. (1955). The theory of molecular attractive forces between solids. *J. Exp. Th. Phys. USSR*, 29, 94–110. (English translation : *Sov. Phys. JETP*, 2, 73–83 (1956))
- Martin, Ph. A. (1988). Sum rules in charged fluids. *Rev. Mod. Phys.*, 60, 1075–1127.
- Mehra, J. (1967). Temperature correction to the Casimir effect. *Physica*, 37, 145–152.
- Schwinger, J., DeRaad, L. L., Jr, and Milton, K. A. (1978). Casimir effect in dielectrics. *Ann. Phys.*, 115, 1–23.

5.1 The force expressed in the loop formalism

As said in the introduction of this chapter, we expose hereafter the details of the calculations outlined in the preceding letter. Due to the similarity of the loop formalism with the classical system of charges, we follow (see Section 2.5.6) the classical route leading to the asymptotic force.

5.1.1 The free energy of the full system and its differentiation

Classically, the force between the two plasmas defined by the derivative of the free energy

$$f_{K,L}(d) = -\frac{1}{L^2} \frac{\partial}{\partial d} \Phi_{K,L,d}$$

corresponds to the average Coulomb forces between the charges in A and the charges in B . It can thus be written in terms of the particle density correlation function.

If the charges become quantum-mechanical but no radiation field is added, the same holds. The quantum correlation function can readily be expressed in terms of the loop correlation function by Equation (4.s) so that its Mayer expansion can be investigated.

When the coupling of matter with the transverse field is taken into account, however, the loop correlation functions are difficult to exhibit from the average value of the total Lorentz forces. This average involves nondiagonal particle-density matrix elements and field degrees of freedom. As an alternative, one can start from the free energy, represent it in the loop phase space, and differentiate it with respect to d . The averages of the microscopic Coulomb and magnetic forces are in this way directly displayed as integrals over the loop correlation function.

The loop partition function of the two-plasma model

The free energy of the full system is given from the partition function $Z_{K,L,d}$ (2.12). In Chapter 4 [Equation (4.k)], we have seen that the latter takes the form

$$Z_{K,L,d} = Z_{0,K}^{\text{rad}} \Xi_{K,L,d} \quad (5.24)$$

where $Z_{0,K}^{\text{rad}}$ (2.10) is the partition function of the free radiation field, and $\Xi_{K,L,d}$ is the partition function of the auxiliary system of loops, which exhibits a convenient classical form.

Since $Z_{0,K}^{\text{rad}}$ is independent on d , the total force exerting between the plasmas becomes

$$f(d) = \lim_{L \rightarrow \infty} \lim_{K \rightarrow \mathbb{R}^3} \frac{k_B T}{L^2} \frac{\frac{\partial}{\partial d} \Xi_{K,L,d}}{\Xi_{K,L,d}}. \quad (5.25)$$

We stress out that in spite of the analogy of (5.25) to the force in the classical system (2.35), here $\Xi_{K,L,d}$ still contains the degrees of freedom of the radiation field.

In the two-plasma system with ideal walls forbidding the particles to cross the interspace, the loop partition function reads

$$\Xi_{K,L,d} = \sum_{n_A=0}^{\infty} \frac{1}{n_A!} \sum_{n_B=0}^{\infty} \frac{1}{n_B!} \int \prod_a^{n_A} d\mathcal{L}_a z(\mathcal{L}_a) \int \prod_b^{n_B} d\mathcal{L}_b z(\mathcal{L}_b) e^{-\beta U(\{\mathcal{L}_a\}, \{\mathcal{L}_b\})}. \quad (5.26)$$

This expression only differs from (4.79) by the fact that the discernability between the particles in A and the particles in B (which transposes to the loops) has been taken into account.⁵ Accordingly, the total loop energy U is separated into intra and interplasma contributions:

$$U = U_A + U_B + U_{AB} + V_A^{\text{walls}} + V_{B,d}^{\text{walls}}. \quad (5.27)$$

The energies U_A , U_B and U_{AB} are sums of pair interactions

$$e_{\gamma_i} e_{\gamma_j} [V^c(\mathcal{L}_i, \mathcal{L}_j) + W^m(\mathcal{L}_i, \mathcal{L}_j)], \quad (5.28)$$

where V^c is the Coulomb potential (4.81) and W^m the magnetic potential (4.82) embodying the integrated field's degrees of freedom. In U_A , these interactions occur only among the loops confined into plasma A by

$$V_A^{\text{walls}}(\{\mathcal{L}_a\}) = \sum_a V_A^{\text{walls}}(\mathcal{L}_a). \quad (5.29)$$

The ideal confinement of the quantum particles imposed by the wall potentials in the original Hamiltonian (2.3) imposes the ideal confinement (to the same volume) of the whole path of the loops. This is a consequence of the way a general one-particle potential generates a corresponding one-loop potential in the path integral representation: every element of line of the loop feels the particle potential.⁶

⁵For a function $f(\gamma_1, \dots, \gamma_N)$ depending only on the numbers $\{n_\gamma\}$ counting the particles of species γ , one has the summation identity $\sum_{\{n_\gamma\}}^{\dots, \infty} \frac{1}{\prod_\gamma n_\gamma!} f(\{n_\gamma\}) = \sum_{N=0}^{\infty} \frac{1}{N!} \sum_{\gamma_1, \dots, \gamma_N} f(\gamma_1, \dots, \gamma_N)$, where $N = \sum_\gamma n_\gamma$. However, in the two-plate situation, the function f involved in the particle partition function also depends on $|S_A|$ and $|S_B|$, the total number of species in plasma A and B , so that this identity can only be used separately in the two plasmas.

⁶An alternative view, when dealing with ideal confining walls, is to consider that the Brownian shape satisfies the diffusion equation with Dirichlet conditions at the interfaces of the slab (due to the enforcement of Dirichlet conditions on the quantum particles' wavefunction). See Appendix 5.C.

After the limit $L \rightarrow \infty$ will be taken, it will mean that

$$e^{-\beta V_A^{\text{walls}}(\mathcal{L}_a)} = \mathbb{1}_A(\mathcal{L}_a) = \begin{cases} 1, & \text{if } \gamma \in S_A \text{ and } -a < x + \lambda_\gamma X(s) < 0 \quad \forall s \in [0, q] \\ 0, & \text{otherwise.} \end{cases} \quad (5.30)$$

The energy U_B similarly takes into account the pairwise interactions internal to plasma B . The interactions occurring between the two plasmas are contained into

$$U_{AB}(\{\mathcal{L}_a\}, \{\mathcal{L}_b\}) = \sum_a \sum_b e_{\gamma_a} e_{\gamma_b} [V^c(\mathcal{L}_a, \mathcal{L}_b) + W^m(\mathcal{L}_a, \mathcal{L}_b)]. \quad (5.31)$$

The activity $z(\mathcal{L})$, which contains the loop self-energy⁷, is given by

$$z(\mathcal{L}) = \frac{(2s_\gamma + 1)(\eta_\gamma)^{q-1}}{q} \frac{(e^{\beta\mu_\gamma})^q}{(2\pi q \lambda_\gamma^2)^{3/2}} e^{-\beta U^{\text{self}}(\mathcal{L})}. \quad (5.32)$$

In these last sections, we take into account the Bose and Fermi statistics of the particles. Considering their spin s_γ merely adds the factor $(2s_\gamma + 1)$ to the activity in (5.32) (we recall that we omitted the spin-field coupling in the basic Hamiltonian (2.3), see Section 2.1.1).

Two-loop forces

The differentiation of the loop partition function according to (5.25) results in the average value of a pairwise summation of the forces acting between the loop objects.

As in the classical case, the dependence upon d in the partition function is exclusively contained in the confinement of the loops of B . To undertake the differentiation with respect to d , we perform similarly the change of variable

$$x_b \mapsto \tilde{x}_b \equiv x_b - d \quad (5.33)$$

in every positional integral dx_b present in $d\mathcal{L}_b$. Again, this corresponds to measure the positions of the loops in B from the inner surface of the slab (see Figure 2.4). Effectuating the differentiation leads to

$$\begin{aligned} f_{K,L}(d) &= \frac{1}{L^2} \left\langle \sum_a \sum_b e_{\gamma_a} e_{\gamma_b} (\partial_x V^c + \partial_x W^m)(\mathcal{L}_a, \mathcal{L}_b + d) \right\rangle \\ &= f_L^c(d) + f_L^m(d). \end{aligned} \quad (5.34)$$

⁷The loop self-energy is made of a Coulomb and a magnetic contribution (see Section 4.7).

We have denote by $\mathcal{L}_b + d$ a loop whose position along x is shifted by d . The Casimir force is thereby expressed as the average value of two-body loop observables. This average is calculated with the loop Gibbs weight $e^{-\beta U}$ and the partition function (5.26). At this stage, the enclosing box of the field can be taken infinitely extended: $K \rightarrow \mathbb{R}^3$. Doing so replaces the sums on the field modes \mathbf{k} by Fourier integrals in the potential W^m .

We see that two types of terms have emerged from the differentiation. The part $f_L^c(d)$ concerns the Coulomb forces exerted between the loops. Since this part remains when there is no radiation field in the model, it is associated to the average value of the Coulomb forces exerting between the atomic charges. The second contribution, $f_L^m(d)$, contains the magnetic part of the Lorentz forces.

Notations

We set again a few notations. They will stress out further the similarities between the classical system of charges and the system of loops.

- **Loop variables:** we recall first that a loop is a collection $\mathcal{L} = (\mathbf{r}, \chi) = (\mathbf{r}, \gamma, q, \mathbf{X}(\cdot))$ regrouping its position \mathbf{r} , and its internal degrees of freedom χ : species index γ , integral charge number q , and Brownian shape $s \mapsto \mathbf{X}(s)$, $\mathbf{X}(0) = \mathbf{X}(q) = \mathbf{0}$. For convenience, we extend the definition of $\mathbf{X}(s)$, $s \in [0, q]$ by a q -periodic function over $s \in \mathbb{R}$. The path in space of the loop is

$$\mathbf{r}^{[s]} \equiv \mathbf{r} + \lambda_\gamma \mathbf{X}(s), \quad s \in \mathbb{R} \quad (5.35)$$

where λ_γ is the de Broglie wavelength. We will be using the even more condensed notation

$$\mathbf{1} \equiv \mathcal{L}_1, \quad \int d\mathbf{1} \dots \equiv \int d\mathcal{L}_1 \dots = \int d\mathbf{r}_1 \sum_{\gamma_1} \sum_{q_1=1}^{\infty} \int D(\mathbf{X}_1) \dots \quad (5.36)$$

The integral $\int D(\mathbf{X}_1)$ is a normalised Gaussian functional integral of zero mean and covariance (4.78). According to the decomposition $\mathbf{r}_1 = (x_1, \mathbf{y}_1)$ of the positions, we also define

$$\mathbf{1} \equiv (x_1, \chi) = (x_1, \gamma_1, q_1, \mathbf{X}_1(\cdot)), \quad \int d\mathbf{1} \dots \equiv \int dx_1 \sum_{\gamma_1} \sum_{q_1=1}^{\infty} \int D(\mathbf{X}_1) \dots \quad (5.37)$$

- To the separation of the space along the x axis and the \mathbf{y} plane correspond also the following decompositions of the Fourier vectors, and the loops' shape:

$$\mathbf{k} \equiv (k_1, \mathbf{k}), \quad \mathbf{X}(s) \equiv (X(s), \mathbf{Y}(s)) \quad (5.38)$$

- **Indices A, B, AB :** we follow the same convention as in the classical case. Every integral runs over the whole space, but is constrained by characteristic functions $\mathbb{1}_A(\mathbf{1}), \mathbb{1}_B(\mathbf{2})$ of the form (5.30). These characteristic functions are merged in the notation with one-loop and two-loop quantities, exactly like in (2.44): $\rho_A(\mathbf{1}) \equiv \mathbb{1}_A(\mathbf{1})\rho(\mathbf{1})$, *etc.*

5.1.2 The force expressed in terms of the loop-correlation

With these notations, and using the “microscopic loop density” (4.q) (p.113), the two-loop force (5.34) is expressed as

$$f_L(d) = \frac{1}{L^2} \int d\mathbf{1} \int d\mathbf{2} e_{\gamma_1} e_{\gamma_2} (\partial_{x_1} V_{AB}^c + \partial_{x_1} W_{AB}^m)(\mathbf{1}, \mathbf{2}) \rho_{AB}(\mathbf{1}, \mathbf{2}). \quad (5.39)$$

In the limit $L \rightarrow \infty$, the space becomes invariant by translation and rotations in the \mathbf{y} plane. Since $\rho_{AB}(\mathbf{1}, \mathbf{2})$ tends to a function of $\mathbf{y}_1 - \mathbf{y}_2$ only, the surface L^2 cancels with one of the \mathbf{y} -integrals. In the partial Fourier space \mathbf{k} at $\mathbf{k} = \mathbf{q}/d$, we thus have

$$\begin{aligned} f(d) &= \frac{1}{d^2} \int d\mathbf{1} \int d\mathbf{2} \int \frac{d\mathbf{q}}{(2\pi)^2} e_{\gamma_1} e_{\gamma_2} (\partial_{x_1} V_{AB}^c + \partial_{x_1} W_{AB}^m)(\mathbf{1}, \mathbf{2}, \frac{\mathbf{q}}{d}) \rho_{AB}(\mathbf{1}, \mathbf{2}, \frac{\mathbf{q}}{d}) \\ &\equiv f^c(d) + f^m(d). \end{aligned} \quad (5.40)$$

We see here that the loop formalism enables us to retrieve an expression very similar to the purely classical case. Examining the leading contributions of this formula can be carried out basically the same way. Namely, by

1. determining whether the correlation ρ_{AB} can be truncated at no cost, and if necessary, calculating the truncated term;
2. writing the resummed Mayer graph series of the loop Ursell function and analysing the decay rates of its bonds;
3. verifying the validity of the perfect screening sum rule.

Before proceeding to the analysis of the asymptotic loop correlations, we establish that the Coulomb forces between the *loops* as given by $f^c(d)$ coincide with the *atomic* electrostatic forces, *i.e.*, that $f^c(d)$ is the average of the Coulomb part of the Lorentz forces exerting between the charges. Note that this average in the coupled system of radiation and matter still contains radiative contributions.

Electrostatic forces

In addition to provide the physical understanding of the force $f^c(d)$ in terms of the original quantum particles, establishing this correspondence will also provide a simplified formula.

We come back to this purpose to the force before the limit L has been taken. The mean value of the electrostatic forces exerting between the quantum particles is given like in (2.45) by

$$\frac{1}{L^2} \int d\mathbf{r}_1 \int d\mathbf{r}_2 F_x(\mathbf{r}_1 - \mathbf{r}_2) c_{AB}(\mathbf{r}_1, \mathbf{r}_2), \quad F_x(\mathbf{r}) = -\frac{x}{|\mathbf{r}|^3}, \quad (5.41)$$

except that c_{AB} is now the quantum charge correlation function. We can express this correlation in terms of the loop correlation function from Formula (4.s):

$$c_{AB}(\mathbf{r}_1, \mathbf{r}_2) \equiv \sum_{\gamma_1, \gamma_2} e_{\gamma_1} e_{\gamma_2} \sum_{q_1, q_2} q_1 q_2 \int D(\mathbf{X}_1) \int D(\mathbf{X}_2) \rho_{AB}(\mathcal{L}_1, \mathcal{L}_2). \quad (5.42)$$

In the loop language, the mean Coulomb forces thus read

$$\frac{1}{L^2} \int d\mathbf{1} \int d\mathbf{2} e_{\gamma_1} e_{\gamma_2} [q_1 q_2 F_x(\mathbf{r}_1 - \mathbf{r}_2)] \rho_{AB}(\mathbf{1}, \mathbf{2}), \quad (5.43)$$

which is not manifestly equal to the force $f_L^c(d)$ as given by the first term of (5.39): according to (4.81), one has

$$(\partial_x V^c)(\mathbf{1}, \mathbf{2}) = \int_0^{q_1} ds_1 \int_0^{q_2} ds_2 \delta(\tilde{s}_1 - \tilde{s}_2) F_x(\mathbf{r}_1^{[s_1]} - \mathbf{r}_2^{[s_2]}). \quad (5.44)$$

However, we will see that these two forces coincide because of an invariance property with respect to the loops' origin, that renders F_x in (5.44) independent of s_1 and s_2 when integrated into $f_L^c(d)$.

Loops' origin invariance properties: when a loop is formed by gathering particles, the position of one of them is chosen to give it its origin \mathbf{r} . The positions of the remaining particles are specified relatively to this origin by the loop's shape: they are given by $\mathbf{r}^{[j]}$, $j = 1, \dots, q - 1$. A specific invariance of the loop entities is associated to the arbitrariness of this choice. The loop $\mathcal{L} = (\mathbf{r}, \gamma, q, \mathbf{X}(\cdot))$ that has its origin shifted by the vector $\lambda_\gamma \mathbf{X}(u)$, $u \in \mathbb{R}$, is given by

$$\mathcal{L}^{[u]} \equiv (\mathbf{r}^{[u]}, \gamma, q, \mathbf{X}^{[u]}(\cdot)) \equiv (\mathbf{r} + \lambda_\gamma \mathbf{X}(u), \gamma, q, \mathbf{X}(\cdot + u) - \mathbf{X}(u)). \quad (5.45)$$

One easily checks that the paths in space of \mathcal{L} and $\mathcal{L}^{[u]}$ are identical. With this notation, the following invariance properties hold (some have already been used in (Ballenegger et al., 2002, Sec. 5.2); those concerning V^c and W^m are shown in Appendix 5.A, p. 180).

- The confinement of a loop concerns only its path in space, which is not affected by the change of origin. The same holds for the loop's self-energy. Thus,

$$\mathbb{1}_A(\mathcal{L}^{[u]}) = \mathbb{1}_A(\mathcal{L}), \quad U^{\text{self}}(\mathcal{L}^{[u]}) = U^{\text{self}}(\mathcal{L}) \quad \forall u \quad (5.46)$$

- Regarding the Coulomb interaction between loops, one has

$$V^c(\mathcal{L}^{[u]}, \mathcal{L}'^{[u']}) = V^c(\mathcal{L}, \mathcal{L}') \quad \text{if } u - u' \in \mathbb{Z}. \quad (5.47)$$

The restriction $u - u' \in \mathbb{Z}$ is the manifestation that elementary Coulomb interactions occur only at equal times between unit portions of the two loops. Only a relative portion can be chosen arbitrarily for the second loop's origin. (see Figure 4.m)

- Such a constraint does not occur for the magnetic potential and one has

$$W^m(\mathcal{L}^{[u]}, \mathcal{L}'^{[u']}) = W^m(\mathcal{L}, \mathcal{L}') \quad \forall u, u', \quad (5.48)$$

which also holds when $\mathcal{L} = \mathcal{L}'$ and $u = u'$, *i.e.*, for the magnetic self-energy of a loop.

In turn, these properties imply that the total energy of the combined system A and B is such that

$$U(\mathcal{L}_1, \dots, \mathcal{L}_i^{[u]}, \dots, \mathcal{L}_j^{[u']}, \dots, \mathcal{L}_n) = U(\mathcal{L}_1, \dots, \mathcal{L}_n) \quad \text{if } u - u' \in \mathbb{Z} \quad (5.49)$$

for any choice of i and j in A or B , and that the one-point and two-point correlation functions satisfy

$$\rho(\mathcal{L}^{[u]}) = \rho(\mathcal{L}) \quad \forall u, \quad (5.50)$$

$$\rho(\mathcal{L}^{[u]}, \mathcal{L}'^{[u']}) = \rho(\mathcal{L}, \mathcal{L}') \quad \text{if } u - u' \in \mathbb{Z}. \quad (5.51)$$

To take advantage of these properties, let us introduce the two-loop function $g(\mathcal{L}_1, \mathcal{L}_2) \equiv F_x(\mathbf{r}_1 - \mathbf{r}_2)$, which depends only on the loops' position, and rewrite $(\partial_{x_1} V^c)$ in $f_L^c(d)$ as

$$(\partial_x V^c)(\mathcal{L}_1, \mathcal{L}_2) = \int_0^{q_1} ds_1 \int_0^{q_2} ds_2 \delta(\bar{s}_1 - \bar{s}_2) g(\mathcal{L}_1^{[s_1]}, \mathcal{L}_2^{[s_2]}). \quad (5.52)$$

In this integral, $s_1 - s_2$ is forced to be an integer by the Dirac equal times condition. We therefore can, at fixed q_1, q_2, s_1 , and s_2 , replace $\rho_{AB}(\mathcal{L}_1, \mathcal{L}_2)$ by $\rho_{AB}(\mathcal{L}_1^{[s_1]}, \mathcal{L}_2^{[s_2]})$ in the integrand of $f_L^c(d)$. Then, one can perform first the changes of variable

$$\mathbf{r}_1 \mapsto \mathbf{r}_1^{[s_1]}, \quad \mathbf{r}_2 \mapsto \mathbf{r}_2^{[s_2]}, \quad (5.53)$$

of unit Jacobian, and next

$$\mathbf{X}_1(\cdot) \mapsto \mathbf{X}_1^{[s_1]}(\cdot), \quad \mathbf{X}_2(\cdot) \mapsto \mathbf{X}_2^{[s_2]}(\cdot). \quad (5.54)$$

The latter changes are known to leave the Gaussian measures $D(\mathbf{X}_1)$ and $D(\mathbf{X}_2)$ in $d\mathcal{L}_1 d\mathcal{L}_2$ invariant as well, see (Macris, Martin, & Pulé, 1988, Lemma 2) or (Ballenegger et al., 2002, Lemma 1).⁸ As an effect of these transformations, the functions g and ρ_{AB} have become independent of s_1 and s_2 , so that

$$\begin{aligned} f_L^c(d) &= \frac{1}{L^2} \int d\mathcal{L}_1 \int d\mathcal{L}_2 e_{\gamma_1} e_{\gamma_2} \int_0^{q_1} ds_1 \int_0^{q_2} ds_2 \delta(\bar{s}_1 - \bar{s}_2) g(\mathcal{L}_1, \mathcal{L}_2) \rho_{AB}(\mathcal{L}_1, \mathcal{L}_2) \\ &= \frac{1}{L^2} \int d\mathcal{L}_1 \int d\mathcal{L}_2 e_{\gamma_1} e_{\gamma_2} q_1 q_2 F_x(\mathbf{r}_1 - \mathbf{r}_2) \rho_{AB}(\mathcal{L}_1, \mathcal{L}_2), \end{aligned} \quad (5.55)$$

which is equal to (5.41). In the remainder, we will calculate the force $f^c(d)$ by means of this simplified formula. Note that it represents both the particle average of the Coulomb forces and the loop average of the monopole force between the total charges $Q_1 = q_1 e_{\gamma_1}$ and $Q_2 = q_2 e_{\gamma_2}$ carried by the loops.

Magnetic forces

We have seen that $f^c(d)$ consists in the average of the electrostatic microscopic forces. It is thus expected that the part $f^m(d)$ of the Casimir force includes the remaining parts of the Lorentz forces exerting between the plasmas. These remaining parts are (according to our sign convention) the average

$$\left\langle \sum_b e_{\gamma_b} \mathbf{E}_t(\mathbf{r}_b) \right\rangle = \left\langle \sum_b e_{\gamma_b} \frac{-1}{c} \dot{\mathbf{A}}(\mathbf{r}_b) \right\rangle \quad (5.56)$$

of the transverse electric force on plasma B ,⁹ and the magnetic contribution

$$\left\langle \sum_b \frac{e_{\gamma_b}}{c} \mathbf{v}_b \times (\nabla \times \mathbf{A}(\mathbf{r}_b)) \right\rangle. \quad (5.57)$$

In fact, the contribution due to the transverse electric field turns out to average to zero,¹⁰ so that only magnetic contributions are left (which justifies our appellation for this force).

⁸To state it with precision, the random process $\tilde{\mathbf{X}}(s) \equiv \mathbf{X}(s+u) - \mathbf{X}(u)$ is still Gaussian, with the same unit normalization, zero mean, and covariance (4.78) than $\mathbf{X}(s)$.

⁹We recall that the transverse electric field $\mathbf{E}_t = -\dot{\mathbf{A}}/c$ depends on the field's mode amplitudes $\alpha_{\mathbf{K},\lambda}$ by Formula (4.72).

¹⁰Indeed: this average is an integral of the correlation function $\langle \hat{c}_B(\mathbf{r}) \mathbf{E}_t(\mathbf{r}) \rangle$, where $\hat{c}_B(\mathbf{r})$ is the microscopic charge density in plasma B . One can for example use the same technique as in Section 4.6 to calculate this function. The exact decoupling of the transverse electric field from matter occurs here as well, and results in the vanishing of the factorized correlation function even for a nonneutral plasma, because $\langle \mathbf{E}_t(\mathbf{r}) \rangle = \mathbf{0}$.

Note that it is not possible in $f^m(d)$ to make use of similar invariance properties to come back to the particle density correlation. Structurally, this fact originates from the presence of the stochastic line integrals $\int d\mathbf{X}_1^u(s_1) \int d\mathbf{X}_2^v(s_2)$ (in place of the equal time integrals), which allow any value of $s_1 - s_2$. Physically, these magnetic forces are related to the microscopic currents of the plasma (like in magnetostatics). The question of the relation between the loop correlation function and current correlation functions of the particles is of general interest and demands further developments.

Truncation of the loop correlation function

Coulomb part: Regarding the Coulomb part $f^c(d)$, we can truncate the correlation function exactly as in the classical situation from Formula (5.41), see Section 2.5.1. If the plasmas are nonneutral, the capacitor force (2.47), mainly constant, is added.

Magnetic part: The term subtracted in the magnetic part $f^m(d)$ by the truncation of the loop correlation function is

$$\begin{aligned} & \int d1 \int d2 \int d\mathbf{y} e_{\gamma_1} \rho_A(1) e_{\gamma_2} \rho_B(2) (\partial_{x_1} W_{AB}^m)(1, 2, \mathbf{y}) \\ &= \int d1 e_{\gamma_1} \rho_A(1) \int d2 e_{\gamma_2} \rho_B(2) (\partial_{x_1} W_{AB}^m)(1, 2, \mathbf{k} = \mathbf{0}). \end{aligned} \quad (5.58)$$

Evaluating the field covariance $G^{\mu\nu}(\mathbf{k}) = G^{\mu\nu}(k_1, \mathbf{k})$ (4.19) in W^m at $\mathbf{k} = \mathbf{0}$, one sees that it vanishes when $\mu = \nu = 1$, and equals $\delta_{\mu\nu} 4\pi/k_1^2$ otherwise. Hence

$$\begin{aligned} \partial_{x_1} W_{AB}^m(1, 2, \mathbf{0}) &= \frac{1}{\beta \sqrt{m_{\gamma_1} m_{\gamma_2}} c^2} \int_0^{q_1} d\mathbf{Y}_1(s_1) \cdot \int_0^{q_2} d\mathbf{Y}_2(s_2) \int \frac{d\mathbf{k}_1}{2\pi} e^{ik_1(x_1 - x_2 - d)} \\ &\quad \times ik_1 \frac{4\pi}{k_1^2} e^{ik_1 \lambda_{\gamma_1} X_1(s_1)} e^{-ik_1 \lambda_{\gamma_2} X_2(s_2)} |g(k_1, \mathbf{k} = \mathbf{0})|^2. \end{aligned} \quad (5.59)$$

Terms independent of s_1 or s_2 in the integrand do not contribute by Itô's Lemma, stating that the line-integral along a closed loop is zero:

$$\int_0^q d\mathbf{X}(s) = 0. \quad (5.60)$$

This Lemma is a straightforward consequence of the definition (4.12) of the line-integral. (It has been extensively used in Chapter 4 with $q = 1$.) Thus, performing first these stochastic integrals, the unit term of both exponentials in the second line of (5.59) can be left behind. They only begin with their linear term $\propto k_1$. Taking

into account that $g(0, \mathbf{0}) = 1$ is finite, the apparent $1/k_1$ singularity of the integrand as $k_1 \rightarrow 0$ is smoothed out. From the asymptotic analysis of Fourier transforms (see Appendix A), one thus knows that $\partial_{x_1} W_{AB}^m(1, 2, \mathbf{0}) = \partial_{x_1} W_{AB}^m(|x_1 - x_2 - d|)$ decays more rapidly than any inverse power of $|x_1 - x_2 - d|$ as $|x_1 - x_2 - d| \rightarrow \infty$, which prevents any algebraical contribution to $f^m(d)$ as $d \rightarrow \infty$.

We can, however, improve this result as follows: the high-frequency cutoff function $|g(k_1, \mathbf{0})|^2$ can be chosen analytic and even in k_1 . It has to be equal to 1 at $k_1 = 0$ and to vanish for $|k_1| \gtrsim mc/\hbar$ (see Section 2.1.1). This function is not needed to legitimate the k_1 Fourier integral in (5.59), taken in the sense of distributions. We can expand it as a power-series of k_1 and integrate term by term. Representing the multiplications by k_1 occurring in the expansion $|g(k_1, \mathbf{0})|^2 = 1 + O(k_1^2)$ as derivatives ∂_{x_1} of the function in the regular space, and using the result

$$\int \frac{dk_1}{2\pi} e^{ik_1 x} \frac{4\pi}{k_1^2} = -2\pi|x| \quad (5.61)$$

(Jones, 1982, Table of Fourier transforms, p. 529), one concludes that

$$\begin{aligned} \partial_{x_1} W_{AB}^m(1, 2, \mathbf{0}) &= \partial_{x_1} \frac{1}{\beta \sqrt{m_{\gamma_1} m_{\gamma_2} c^2}} \int_0^{q_1} d\mathbf{Y}_1(s_1) \cdot \int_0^{q_2} d\mathbf{Y}_2(s_2) \\ &\quad \times [1 + O(\partial_{x_1}^2)] (-2\pi) |d + x_2^{[s_2]} - x_1^{[s_1]}| \\ &\equiv 0. \end{aligned} \quad (5.62)$$

Indeed, $|x_1^{[s_1]} - x_2^{[s_2]} - d| = d + x_2^{[s_2]} - x_1^{[s_1]}$ so that the double stochastic integral vanishes by Itô's Lemma. Consequently, the truncated term (5.58) never contributes to the force $f^m(d)$.

The force expressed in terms of the loop Ursell function

According to the discussion above, the Casimir force can finally be expressed as

$$\begin{aligned} f(d) &= \frac{1}{d^2} \int d1 \int d2 \int \frac{d\mathbf{q}}{(2\pi)^2} e_{\gamma_1} e_{\gamma_2} (q_1 q_2 \partial_{x_1} v_{AB} + \partial_{x_1} W_{AB}^m)(1, 2, \frac{\mathbf{q}}{d}) \\ &\quad \times \rho_A(1) \rho_B(2) h_{AB}(1, 2, \frac{\mathbf{q}}{d}) \equiv f^c(d) + f^m(d), \end{aligned} \quad (5.63)$$

where $\partial_{x_1} v_{AB}(1, 2, \frac{\mathbf{q}}{d})$ is the bare (monopole) Coulomb force (2.50) and $h_{AB}(1, 2, \frac{\mathbf{q}}{d})$ is the loop Ursell function

$$h_{AB}(1, 2, \frac{\mathbf{q}}{d}) = \frac{\rho_{AB}(1, 2, \frac{\mathbf{q}}{d})}{\rho_A(1) \rho_B(2)} - 1. \quad (5.64)$$

We will now investigate the asymptotic correlations between the loops in A and in B , by expanding this Ursell function in a resummed Mayer-like series.

5.2 Quantum Mayer graphs

Due to the classical-like structure of the partition function (5.26), the loop Ursell function is expandable in a Mayer graph series in the very same way as is done classically. Points in the graphs are integrated over loop's degrees of freedom by means of (5.36), with a local loop-density weight $\rho(1)$. The Mayer bonds are

$$f(\mathbf{i}, \mathbf{j}) = e^{-\beta e_{\gamma_i} e_{\gamma_j} [V^c(\mathbf{i}, \mathbf{j}) + W^m(\mathbf{i}, \mathbf{j})]} - 1. \quad (5.65)$$

The resummation of this series is needed as in the classical situation by the fact that at large distances $|\mathbf{r}_i - \mathbf{r}_j| \rightarrow \infty$, the Coulomb loop interaction $e_{\gamma_i} e_{\gamma_j} V^c(\mathbf{i}, \mathbf{j})$ is dominated by its monopole-monopole contribution $e_{\gamma_i} e_{\gamma_j} q_i q_j / |\mathbf{r}_i - \mathbf{r}_j|$, thus nonintegrable (but fortunately signed).

Resummations in the loop formalism

There are several ways of introducing a resummed potential in this formalism, corresponding to the different ways of extracting a long range tail of the Mayer bond.

In homogeneous (bulk) systems, it is possible to build a screened loop potential from resumming convolution chains of the whole Coulomb loop potential V^c (Ballenegger et al., 2002). The resulting potential encompasses different behavioral regimes depending on the distance scale involved: at short distances, in a dilute system, it reduces to the bare Coulomb interaction between the loops. At intermediate distances, it matches the classical exponentially screened Debye–Hückel potential. However, its asymptotic decay is dipolar-like (algebraical). At that scale, the quantum-mechanical fluctuations of the particle's positions interfere with the arrangement of charges involved in screening, so that the efficiency of the latter is lessened. This is the most striking peculiarity of quantum plasmas. Their large-distance correlations are accordingly no longer exponentially screened, but decay algebraically as $\sim r^{-6}$. Nevertheless, the perfect screening sum rule is still valid: the screening cloud around a fixed charge shields it exactly. The screening of multipoles, on the other hand, no longer holds.

Because of the presence of the magnetic potential W^m , and to disentangle explicitly the classical regimes from the large-distance quantum regime, we carry out the resummation differently.

The “classical” and “quantum” components of V^c

We extract from V^c a genuine quantum-mechanical component W^c which encompasses the equal-time constraint, as follows:

$$V^c(\mathbf{i}, \mathbf{j}) = V^{\text{el}}(\mathbf{i}, \mathbf{j}) + W^c(\mathbf{i}, \mathbf{j}), \quad (5.66)$$

with

$$V^{\text{el}}(\mathbf{i}, \mathbf{j}) = \int_0^{q_i} ds_i \int_0^{q_j} ds_j \frac{1}{|\mathbf{r}_i^{[s_i]} - \mathbf{r}_j^{[s_j]}|}, \quad (5.67)$$

$$W^{\text{c}}(\mathbf{i}, \mathbf{j}) = \int_0^{q_i} ds_i \int_0^{q_j} ds_j (\delta(\tilde{s}_i - \tilde{s}_j) - 1) \frac{1}{|\mathbf{r}_i^{[s_i]} - \mathbf{r}_j^{[s_j]}|}. \quad (5.68)$$

- The contribution V^{el} represents the standard, classical, electrostatic energy which sums up the mutual interactions between the line elements of the two uniformly charged loops \mathcal{L}_i and \mathcal{L}_j . It contains multipole contributions of any order because of the extension in space of the loops. These extensions are still scaled by the quantum-mechanical de Broglie wavelength, but we will consider this contribution as if it were classical.
- The contribution W^{c} contains, on the other hand, the memory of the equal time condition in V^{c} that arises when using the Feynman–Kac formalism. It does not reduce to a classical interpretation of the interaction between charged wires, and vanishes identically when λ_{γ_i} and λ_{γ_j} are set equal to zero, by (4.29). Its large-distance behaviour is dipolar-like (Brydges & Martin, 1999).

5.2.1 Resummation of the “classical” contribution V^{el}

The total loop interaction $V^{\text{c}} + W^{\text{m}}$ in the Mayer bond can now be reorganised as

$$f(\mathbf{i}, \mathbf{j}) = e^{-\beta e_{\gamma_i} e_{\gamma_j} [V^{\text{el}}(\mathbf{i}, \mathbf{j}) + W(\mathbf{i}, \mathbf{j})]} - 1, \quad (5.69)$$

where

$$W(\mathbf{i}, \mathbf{j}) \equiv W^{\text{c}}(\mathbf{i}, \mathbf{j}) + W^{\text{m}}(\mathbf{i}, \mathbf{j}). \quad (5.70)$$

We proceed to the resummation of the part $f^{\text{el}}(\mathbf{i}, \mathbf{j}) \equiv -\beta e_{\gamma_i} e_{\gamma_j} V^{\text{el}}(\mathbf{i}, \mathbf{j})$ of the Mayer bond. The asymptotically dipolar-like interaction W included in the remaining part $f^{\text{R}} \equiv f - f^{\text{el}}$ does not need to be resummed.¹¹

The situation is exactly the same as in classical plasmas (Section 2.5.2) and the steps leading to the resummed Mayer series are identical. The dipolar-like potential W plays the role held before by the regularizing short-range potential, with the difference that its slower decay still demands its consideration into AB correlations.

¹¹Dipolar potentials are at the border of integrability. Finite results are obtained when the angular integrals are performed before the radial one.

Summing all f^{el} -convolution chains defines the resummed bond $F(\mathbf{i}, \mathbf{j}) = -\beta e_{\gamma_i} e_{\gamma_j} \Phi(\mathbf{i}, \mathbf{j})$, where Φ is solution of the integral equation

$$\Phi(\mathbf{i}, \mathbf{j}) = V^{\text{el}}(\mathbf{i}, \mathbf{j}) - \int d\mathbf{1} \frac{\kappa^2(1)}{4\pi} V^{\text{el}}(\mathbf{i}, \mathbf{1}) \Phi(\mathbf{1}, \mathbf{j}), \quad (5.71)$$

$$\kappa^2(1) = 4\pi\beta e_{\gamma_1}^2 \rho(1). \quad (5.72)$$

The new diagrams are made of links \mathcal{F} of either of the two types

$$F(\mathbf{i}, \mathbf{j}) = -\beta e_{\gamma_i} e_{\gamma_j} \Phi(\mathbf{i}, \mathbf{j}) \quad (5.73)$$

$$F^{\text{R}}(\mathbf{i}, \mathbf{j}) = e^{-\beta e_{\gamma_i} e_{\gamma_j} (\Phi+W)(\mathbf{i}, \mathbf{j})} - 1 + \beta e_{\gamma_i} e_{\gamma_j} \Phi(\mathbf{i}, \mathbf{j}), \quad (5.74)$$

and the **resummed Mayer graph series** of the Ursell function reads

$$h(\mathbf{1}, \mathbf{2}) = \sum_{\Pi} \frac{1}{S_{\Pi}} \int d\mathbf{3} \rho(3) \cdots \int d\mathbf{m} \rho(m) \prod_{(\mathbf{i}, \mathbf{j}) \in \Pi} \mathcal{F}(\mathbf{i}, \mathbf{j}). \quad (5.75)$$

Properties:

- The diagrammatic rules for the resummed loop graphs are the same as in the classical case. In particular, they do not have articulation points, and convolutions in chain of the bond F are forbidden.
- The signed charges are responsible for strong cancellations among the infinite series of the long-range contribution V^{el} . Because of the classical form of this potential, the classical theory of screening applies, and the resulting Debye–Hückel potential Φ will decay exponentially at large distances.

Link with the “multipole” graphs: in (Brydges & Martin, 1999, Sec. V.B.2) and earlier works (Cornu, 1996a, 1996a), the contribution V^{el} is decomposed into a multipolar expansion and only its monopole part is resummed. Such a resummation leads to the introduction of several new bonds in the resummed Mayer graph series. However, the resulting screened monopole potential Φ^{mon} has the advantage of differing from the potential that would arise if the charges were classical only by the definition of the screening length.¹² The resummed bonds of this multipolar Mayer series are denoted by F^{cc} , F^{cm} , F^{mc} and F^{mm} . The bond F^{cc} is $-\beta e_{\gamma_i} e_{\gamma_j} \Phi^{\text{mon}}$. If one extracts further the contribution $-\beta e_{\gamma_i} e_{\gamma_j} W$ of F^{mm} , resulting

¹²The screening length arising is $\kappa^{-1}(x) = [4\pi\beta \sum_{\gamma} \sum_{\chi} \int D(\mathbf{X}) q^2 e_{\gamma}^2 \rho(x, \chi)]^{-1/2}$. It does not reduce to the classical expression $4\pi\beta \sum_{\gamma} e_{\gamma}^2 \rho(x, \gamma)$ (with the quantum density) due to the squared q in the summand, except when exchange effects inside a loop are neglected (Brydges & Martin, 1999, Sec. V.B.2).

in the bond $\widetilde{F}^{\text{mm}} = F^{\text{mm}} + \beta e_{\gamma_i} e_{\gamma_j} W$, our Debye–Hückel potential Φ is retrieved as an infinite sum of chain graphs made of bonds F^{cc} , F^{cm} , F^{mc} and $\widetilde{F}^{\text{mm}}$. Except for F^{cc} , these bonds are all given by applying various multipole operators on Φ^{mon} . From our knowledge of the classical Debye–Hückel potential in wall-constrained plasmas, these bonds are thus exponentially damped at large distances, and we can conclude the same of the loop potential Φ , as stated above.

Resumming the full Coulomb potential V^c : aside from the technical difficulty of building a unified resummed potential for all length scales in systems with boundaries, the resummation process we consider is especially appropriate to our situation. Indeed, we will see that the screened potential Φ_{AB} between loops in A and B factorizes into an A and a B contribution as $d \rightarrow \infty$, exactly as its classical counterpart. But this is not the case of the potential W_{AB} . The latter will induce in the correlation function dominant terms of a new type.

5.3 Asymptotic correlations between the plasmas

We follow Section 2.5.3 in the analysis of the loop Ursell function $h_{AB}(1, 2, \frac{\mathbf{q}}{d})$. The graphs' integrals are decomposed into A and B contributions, and we assume that the loop densities tend to their single plasma counterparts. To investigate the asymptotic behaviour of the traversing bonds, we analyse first that of Φ_{AB} , W_{AB}^c and W_{AB}^m .

5.3.1 The Debye–Hückel potential Φ_{AB} at large separations

Iterating the integral relation (5.71) defining Φ represents the latter as a sum of convolution chains of the potential V^{el} . We extract the asymptotic behaviour of Φ_{AB} by keeping only the dominant chains.

Exactly the same steps as in the classical case can be repeated. Indeed, the potential V_{AB}^{el} factorizes as well. With the partial Fourier representation (B.7) of the Coulomb potential, $V^{\text{el}}(1, 2, \mathbf{k})$ reads

$$V^{\text{el}}(1, 2, \mathbf{k}) = \int_0^{q_1} ds_1 \int_0^{q_2} ds_2 e^{i\mathbf{k} \cdot [\lambda_{\gamma_1} \mathbf{Y}_1(s_1) - \lambda_{\gamma_2} \mathbf{Y}_2(s_2)]} \frac{2\pi}{k} e^{-k|x_1^{[s_1]} - x_2^{[s_2]}|}. \quad (5.76)$$

Thus (taking into account the shift by $-d$ of the positions in B):

$$\begin{aligned} V_{AB}^{\text{el}}(1, 2, \mathbf{k}) &= \frac{ke^{-kd}}{2\pi} \left[\int_0^{q_1} ds_1 e^{i\mathbf{k} \cdot \lambda_{\gamma_1} \mathbf{Y}_1(s_1)} \frac{2\pi}{k} e^{-k|x_1^{[s_1]}|} \right] \left[\int_0^{q_2} ds_2 e^{-i\mathbf{k} \cdot \lambda_{\gamma_2} \mathbf{Y}_2(s_2)} \frac{2\pi}{k} e^{-k|x_2^{[s_2]}|} \right] \\ &\equiv \frac{ke^{-kd}}{2\pi} V_{AA}^{\text{el}}(1, 0, \mathbf{k}) V_{BB}^{\text{el}}(0, 2, \mathbf{k}). \end{aligned} \quad (5.77)$$

For simplicity of notation, we have denoted by 0 a loop variable representing a classical charge situated at the inner side of the slab A or B , *i.e.*,

$$0 \equiv (x=0, \alpha_0, q=1, \mathbf{X}(\cdot) \equiv 0) \quad (\text{in } A), \quad (5.78)$$

$$0 \equiv (x'=0, \beta_0, q'=1, \mathbf{X}'(\cdot) \equiv 0) \quad (\text{in } B). \quad (5.79)$$

The factorization (5.77) is formally the same as (2.68). The resummed potential $\Phi(i, j, \mathbf{y})$ decays faster than $V^{\text{el}}(i, j, \mathbf{y})$ as $|\mathbf{y}| \rightarrow \infty$ because it encompasses classical-like screening effects [see the discussion after Equation (5.75)]. In the partial Fourier space, this implies that as $d \rightarrow \infty$, the quantity

$$V^{\text{el}}(0, 0, \frac{\mathbf{q}}{d}) \equiv \frac{2\pi d}{q} \quad (5.80)$$

is dominant over the potentials $\tilde{\Phi}_{AA}(0, 0, \frac{\mathbf{q}}{d})$ and $\tilde{\Phi}_{BB}(0, 0, \frac{\mathbf{q}}{d})$, as in (2.78)–(2.79). Finally, we recover the result [analog to (2.65)]

$$\Phi_{AB}(1, 2, \frac{\mathbf{q}}{d}) \stackrel{d \rightarrow \infty}{\sim} \frac{1}{d} \frac{q}{4\pi \sinh q} \Phi_A^0(1, 0, \mathbf{0}) \Phi_B^0(0, 2, \mathbf{0}). \quad (5.81)$$

5.3.2 The potential W_{AB}^c at large separations

As to W_{AB}^c , one has from (5.68), similarly to the partial Fourier transform of V_{AB}^{el} ,

$$W_{AB}^c(1, 2, \mathbf{k}) = \frac{2\pi e^{-kd}}{k} \int_0^{q_1} ds_1 \int_0^{q_2} ds_2 (\delta(\tilde{s}_1 - \tilde{s}_2) - 1) e^{-k[x_1^{[s_1]} + i\hat{\mathbf{k}} \cdot \lambda_{\gamma_1} \mathbf{Y}_1(s_1)]} e^{k[x_2^{[s_2]} + i\hat{\mathbf{k}} \cdot \lambda_{\gamma_2} \mathbf{Y}_2(s_2)]}, \quad (5.82)$$

where $\hat{\mathbf{k}} \equiv \mathbf{k}/k$. We can extract $e^{-k|x_1|} e^{-k|x_2|}$ from the product of exponentials in the integrand; expanding the remaining exponentials then accounts for a multipole expansion. Terms in this expansion assimilating to a sole function of either s_1 or s_2 — originating from the unit term of each exponential — vanish upon integration over the nonequal-time condition, by virtue of (4.29). In the large-distance limit, after substitution of $\mathbf{k} = \mathbf{q}/d$, one therefore has

$$W_{AB}^c(1, 2, \frac{\mathbf{q}}{d}) \stackrel{d \rightarrow \infty}{\sim} \frac{2\pi q e^{-q} e^{-\frac{q|x_1|}{d}} e^{-\frac{q|x_2|}{d}}}{d} \lambda_{\gamma_1}(-\lambda_{\gamma_2}) \int_0^{q_1} ds_1 \int_0^{q_2} ds_2 (\delta(\tilde{s}_1 - \tilde{s}_2) - 1) \\ \times [X_1(s_1) + i\hat{\mathbf{q}} \cdot \mathbf{Y}_1(s_1)][X_2(s_2) + i\hat{\mathbf{q}} \cdot \mathbf{Y}_2(s_2)]. \quad (5.83)$$

5.3.3 The magnetic potential W_{AB}^m at large separations

The asymptotic behaviour of the magnetic potential W_{AB}^m is less straightforward to calculate, for it involves the cutoff function $g(k_1, \mathbf{k})$, as well as the transverse

Kronecker function $\delta_{\text{tr}}^{\mu\nu}(k_1, \mathbf{k})$ in the field covariance $G^{\mu\nu}(k_1, \mathbf{k})$ (4.19). The unpleasantness occasioned by the latter is merely technical. The difficulty arisen by the former is overcome as when calculating the truncated term of $f^m(d)$: the legitimacy of the Fourier integral, taken in the sense of distributions, does not rely on the presence of this cutoff function; we will expand it in power series of k_1 . From (4.82), we have

$$W_{AB}^m(1, 2, \frac{\mathbf{q}}{d}) = \frac{1}{\beta \sqrt{m_{\gamma_1} m_{\gamma_2}} c^2} \sum_{\mu, \nu} \int_0^{q_1} dX_1^\mu(s_1) \int_0^{q_2} dX_2^\nu(s_2) e^{i\frac{\mathbf{q}}{d} \cdot [\lambda_{\gamma_1} \mathbf{Y}_1(s_1) - \lambda_{\gamma_2} \mathbf{Y}_2(s_2)]} \\ \times \int \frac{d\mathbf{k}_1}{2\pi} e^{ik_1(x_1^{[s_1]} - x_2^{[s_2]} - d)} v^{\mu\nu}(k_1, \frac{\mathbf{q}}{d}) |g(k_1, \frac{\mathbf{q}}{d})|^2, \quad (5.84)$$

where

$$v^{\mu\nu}(k_1, \mathbf{k}) = \frac{4\pi}{k_1^2 + k^2} \delta_{\text{tr}}^{\mu\nu}(k_1, \mathbf{k}) \quad (5.85)$$

is the elementary **transverse Coulomb potential** in Fourier representation.

The cutoff function $|g(k_1, \mathbf{k})|^2$ can be chosen analytic in $|\mathbf{k}|^2 = k_1^2 + k^2$. We thus expand $|g(k_1, \frac{\mathbf{q}}{d})|^2$ as $1 + O(k_1^2 + q^2/d^2)$. Expressing the multiplications by k_1 by derivatives ∂_{x_1} , we have

$$W_{AB}^m(1, 2, \frac{\mathbf{q}}{d}) = \left[1 + O\left(\frac{\partial^2}{\partial x_1^2} + \frac{q^2}{d^2}\right) \right] \overline{W}_{AB}^m(1, 2, \frac{\mathbf{q}}{d}), \quad (5.86)$$

where $\overline{W}_{AB}^m(1, 2, \frac{\mathbf{q}}{d})$ is defined as in (5.84) but with the cutoff function set to unity. This new potential is completely explicit. As shows the known expression for the partial Fourier transform $v^{\mu\nu}(x, \mathbf{k})$ (B.11), its exact spatial dependence (at any d) is made of terms proportional to either

$$\frac{d}{q} e^{-\frac{q|x_1|}{d}} e^{-\frac{q|x_2|}{d}}, \quad \text{or} \quad (d + x_2 - x_1) e^{-\frac{q|x_1|}{d}} e^{-\frac{q|x_2|}{d}}. \quad (5.87)$$

Applying $O(\partial^2/\partial x_1^2)$ to such terms multiplies them by a factor d^{-1} in the worst case. As a consequence, the $O(\partial^2/\partial x_1^2 + q^2/d^2)$ term in (5.86) can be neglected as $d \rightarrow \infty$ and the asymptotic behaviour of W_{AB}^m is equal to that of \overline{W}_{AB}^m .

This behaviour is calculated in Appendix 5.B, p. 181. Itô's Lemma (5.60) is responsible for the suppression of the divergency at $d = \infty$ of (5.87) similarly as the nonequal-time integral does in W_{AB}^c . The result is

$$W_{AB}^m(1, 2, \frac{\mathbf{q}}{d}) \stackrel{d \rightarrow \infty}{\sim} \frac{2\pi q e^{-q} e^{-\frac{q|x_1|}{d}} e^{-\frac{q|x_2|}{d}} \lambda_{\gamma_1}(-\lambda_{\gamma_2})}{\beta \sqrt{m_{\gamma_1} m_{\gamma_2}} c^2 d} \sum_{\mu, \nu} \int_0^{q_1} dX_1^\mu(s_1) \int_0^{q_2} dX_2^\nu(s_2) \\ \times w^{\mu\nu}(\mathbf{X}_1(s_1), \mathbf{X}_2(s_2), \mathbf{q}), \quad (5.88)$$

where $w^{\mu\nu}(\mathbf{X}_1, \mathbf{X}_2, \mathbf{q})$ is a bilinear form in $\mathbf{X}_1, \mathbf{X}_2$, whose coefficients (depending on μ, ν) are polynomials of \mathbf{q} . They are explicitly given in (5B.9–5B.12).

5.3.4 Behaviour of the Mayer bonds

The preceding $O(d^{-1})$ behaviours of W_{AB}^c and W_{AB}^m show that the leading correlations between the plasmas will contain terms of a new type. It will be convenient to subtract from the traversing bond F_{AB}^R the contribution W_{AB} by defining

$$\begin{aligned}\widetilde{F}_{AB}^R(\mathbf{i}, \mathbf{j}) &\equiv F_{AB}^R(\mathbf{i}, \mathbf{j}) + \beta e_{\gamma_i} e_{\gamma_j} W_{AB}(\mathbf{i}, \mathbf{j}) \\ &= e^{-\beta e_{\gamma_i} e_{\gamma_j} (\Phi_{AB} + W_{AB})(\mathbf{i}, \mathbf{j})} - 1 + \beta e_{\gamma_i} e_{\gamma_j} (\Phi_{AB} + W_{AB})(\mathbf{i}, \mathbf{j}).\end{aligned}\quad (5.89)$$

Let us sum up the behaviours of the Mayer bonds.

Traversing bonds

- The behaviour of the bond F_{AB} is given by the asymptotic factorization of Φ_{AB} :

$$F_{AB}(i, j, \frac{\mathbf{q}}{d}) \stackrel{d \rightarrow \infty}{\sim} \frac{-1}{\beta d} \frac{q}{4\pi \sinh q} \frac{F_A^0(i, 0, \mathbf{0})}{e_{\alpha_0}} \frac{F_B^0(0, j, \mathbf{0})}{e_{\beta_0}}. \quad (5.90)$$

- The bond $-\beta e_{\gamma_i} e_{\gamma_j} W_{AB}$ is constituted by W_{AB}^c and W_{AB}^m , which are both $O(d^{-1})$.

$$W_{AB}(i, j, \frac{\mathbf{q}}{d}) = O(d^{-1}) \quad (5.91)$$

- The behaviour of the bond \widetilde{F}_{AB}^R proves to be

$$\widetilde{F}_{AB}^R(i, j, \frac{\mathbf{q}}{d}) = O(d^{-4}). \quad (5.92)$$

Indeed, starting from (5.89), one can follow the same steps as for the classical bond F^R , Equations (3C.4)–(3C.6).

Nontraversing bonds

All types of nontraversing bonds tend to their counterparts of the individual plasmas:

$$F_{AA} \xrightarrow{d \rightarrow \infty} F_A^0, \quad F_{BB} \xrightarrow{d \rightarrow \infty} F_B^0, \quad (5.93)$$

$$F_{AA}^R \xrightarrow{d \rightarrow \infty} (F^R)_A^0, \quad F_{BB}^R \xrightarrow{d \rightarrow \infty} (F^R)_B^0. \quad (5.94)$$

In the partial Fourier space, these behaviours are uniform in \mathbf{k} (*i.e.*, also valid at $\mathbf{k} = \mathbf{q}/d$).

5.3.5 Dominant graphs and asymptotic behaviour of h_{AB}

From the asymptotic properties of the links derived in above, the asymptotic behaviour of the loop Ursell function is straightforward to deduce by summing its dominant graphs as in the classical case. The only difference is that a number of structurally new diagrams arise by the fact that W_{AB} is also $O(d^{-1})$, like F_{AB} .

Dominant graphs constructed with F_{AB}

The rule forbidding chain convolutions of F -type bonds restricts here as well the type of links attached to the extremities of F_{AB} : they are not allowed to be single F_{AA} or F_{BB} bonds. Consequently, the dominant graphs containing F_{AB} are [see (2.83)]

$$\circlearrowleft \left(\circ + \frac{F_{AA}}{\rho_A} \bullet + \frac{\delta}{\rho_A} \right) \bullet \xleftrightarrow{F_{AB}} \bullet \left(\circ + \circ \frac{F_{BB}}{\rho_B} + \frac{\delta}{\rho_B} \right) \circlearrowright. \quad (5.95)$$

The symbol $\circlearrowleft \circ$ is the sum of all subgraphs that do not begin nor end with a single bond F .

Dominant graphs constructed with W_{AB}

The type of the links attached to the extremities of W_{AB} is, however, not restricted by the excluded convolution rule. One can reconstruct on each side any two-point structure in accordance to the diagrammatic rules of the Mayer graphs. These structures are exactly all the graphs of the loop Ursell functions of the single plasma, except that they are built with the densities ρ_A and ρ_B , and the bonds F_{AA} and F_{AA}^R of the plasma A still under the influence of plasma B . This difference disappears in the limit $d \rightarrow \infty$. We denote by $\widetilde{h}_A(i, j, \frac{\mathbf{q}}{d})$ and $\widetilde{h}_B(i, j, \frac{\mathbf{q}}{d})$ the sum of these subgraphs, topologically identical to the Ursell functions h_A^0 and h_B^0 of the individual plasmas. The series of supplementary dominant graphs in the Ursell function then reads

$$\circlearrowleft \left(\widetilde{h}_A + \frac{\delta}{\rho_A} \right) \bullet \xleftrightarrow{W_{AB}} \bullet \left(\widetilde{h}_B + \frac{\delta}{\rho_B} \right) \circlearrowright \quad (5.96)$$

$$= \int d^3\rho_A(3) \int d^4\rho_B(4) \left[\widetilde{h}_A(1, 3, \frac{\mathbf{q}}{d}) + \frac{\delta(1,3)}{\rho_A(3)} \right] (-\beta e_{\gamma_3} e_{\gamma_4}) W_{AB}(3, 4, \frac{\mathbf{q}}{d}) \left[\widetilde{h}_B(4, 2, \frac{\mathbf{q}}{d}) + \frac{\delta(4,2)}{\rho_B(4)} \right]. \quad (5.97)$$

Asymptotic behaviour of h_{AB}

In the limit $d \rightarrow \infty$, the factorization of F_{AB} can be used, as well the behaviours (5.83) and (5.88) for the leading contribution $W_{AB}^{(as)}$ of $W_{AB} = W_{AB}^c + W_{AB}^m$. The

asymptotic behaviour of the Ursell function is

$$h_{AB}(1, 2, \frac{\mathbf{q}}{d}) \stackrel{d \rightarrow \infty}{\sim} - \frac{1}{\beta d} \frac{q}{4\pi \sinh q} \frac{G_A^0(1, 0, \mathbf{0})}{e_{\alpha_0}} \frac{G_B^0(0, 2, \mathbf{0})}{e_{\beta_0}} \quad (5.98)$$

$$+ \int d^3 \rho_A^0(3) \int d^4 \rho_B^0(4) \left[h_A^0(1, 3, \mathbf{0}) + \frac{\delta(1,3)}{\rho_A^0(3)} \right] \times (-\beta e_{\gamma_3} e_{\gamma_4}) W_{AB}^{(as)}(3, 4, \frac{\mathbf{q}}{d}) \left[h_B^0(4, 2, \mathbf{0}) + \frac{\delta(4,2)}{\rho_B^0(4)} \right]. \quad (5.99)$$

The function G_A^0 corresponds to the graphical construction

$$G_A^0(1, 0, \mathbf{0}) \equiv \circ \bullet \circ + \circ \bullet \bullet \circ + \circ \circ. \quad (5.100)$$

Comparing it to h_A^0 , which contains all type of graphs, yields

$$\begin{aligned} G_A^0(1, 0, \mathbf{0}) &= h_A^0(1, 0, \mathbf{0}) - \circ \bullet \bullet \circ - \circ \bullet \circ \\ &= h_A^0(1, 0, \mathbf{0}) - \int d^3 \rho_A^0(3) \left[F_A^0(1, 3, \mathbf{0}) + \frac{\delta(1,3)}{\rho_A^0(3)} \right] (h_A^0)^{nn}(3, 0, \mathbf{0}) \end{aligned} \quad (5.101)$$

(having defined $(h_A^0)^{nn} = \circ \bullet \circ$). Alike relations hold between plasma B 's quantities.

Physical sources of the asymptotic loop correlations: as seen on the asymptotic form of h_{AB} , the correlations between the two systems of loops are conveyed by forces of different origins.

- The term (5.98) corresponds to the electrostatic correlations of the loops taken as classical extended objects.
- The contribution given by W_{AB}^c to (5.99), shows, however, that loops' intrinsic quantum nature adds new terms to these correlations. One can interpret these additional terms as resulting from the imperfect screening of the multipoles in the quantum plasma.
- The radiation field also correlates the loops at leading order by its contribution W_{AB}^m to (5.99). Nevertheless, the ratio of this radiative part to the electrostatic quantum part bears a prefactor $(\beta mc^2)^{-1}$. In effect, it renders this transverse contribution hardly observable in the semi-classical regime, as has already been pointed out after Equation (4.44).

Correlations of the quantum particles: One can come back to the correlations occurring between the original quantum particles of the two-plasma system by the following formula [see Equations (4.s)–(4.r)]

$$\begin{aligned} & \rho_A(x_1, \gamma_1) \rho_B(x_2, \gamma_2) h_{AB}(\gamma_1, x_1, \gamma_2, x_2, \frac{\mathbf{q}}{d}) \\ &= \sum_{q_1, q_2} q_1 q_2 \int \mathbf{D}(\mathbf{X}_1) \int \mathbf{D}(\mathbf{X}_2) \rho_A(x_1, \chi_1) \rho_B(x_2, \chi_2) h_{AB}(x_1, \chi_1, x_2, \chi_2, \frac{\mathbf{q}}{d}). \end{aligned} \quad (5.102)$$

Hence, in contradistinction to the classical particle Ursell function (2.84), the quantum particle Ursell function is no longer fully factorized into an A and a B contribution, because of the term (5.99). Although the contribution (5.98) does lead to a factorized term in the particle correlation, it does not reduce to the expression involving *particle* correlations in the individual slabs.

Integrability on loops' internal degrees of freedom: Let us finally comment on integrability concerns regarding loops' internal degrees of freedom in Mayer graphs. One needs in principle to check that the sums on the particle numbers $q \in 1, 2, 3, \dots$, associated to every integrated point, is convergent. Graphs in activity are known to suffer from such divergencies when summing on these numbers (Ballenegger et al., 2002, Sec. 5.4). This is due to the fact that taken individually, these graphs do not necessarily include the physics of screening. Nonetheless, subseries of them representing real physical quantities must do.

In our approach, we deal with Mayer graphs in density instead. Every integrated point is accompanied by a loop-density weight $\rho(x, \chi)$. This density is expandable in a loop Mayer graph series in activity, see, *e.g.*, (Ballenegger et al., 2002). Even though the loop density is not yet a physical quantity, this series obviously incorporates screening mechanisms among the graphs, for the particle density is obtained by

$$\rho(\mathbf{r}, \gamma) = \sum_{q=1}^{\infty} q \int \mathbf{D}(\mathbf{X}) \rho(x, \chi), \quad (5.103)$$

which shows that $\rho(x, \chi)$ contains an integrative factor about q .

Moreover, we consider individual graphs only at intermediate steps of the calculations. The graphs we are interested in are eventually gathered together. They form loop correlations, whose definitions can be given directly from the original loop partition function (5.26), without having recourse to Mayer diagrammatics.

5.3.6 Perfect screening sum rules

Before inserting the complete asymptotic behaviour (5.98)–(5.99) into the force formula, we need to ascertain the status of the perfect screening sum rule in the

system of loops.

Perfect screening on the Debye–Hückel level

We have seen in Section 5.2.1 that the potential $\Phi(\mathbf{i}, \mathbf{j})$ decays rapidly at large distances. In the partial Fourier space, this has as implication that

$$\lim_{\mathbf{k} \rightarrow \mathbf{0}} \frac{\Phi_A^0(i, j, \mathbf{k})}{V_{AA}^{\text{el}}(i, j, \mathbf{k})} = 0. \quad (5.104)$$

The property (5.104) is equivalent to the fulfillment of the perfect screening sum rule in plasma A at the Debye–Hückel level. This has been shown in the classical case (Section 2.5.4). It applies here as well, with the change that

$$\lim_{\mathbf{k} \rightarrow \mathbf{0}} \frac{V_{AA}^{\text{el}}(i, 1, \mathbf{k})}{V_{AA}^{\text{el}}(i, j, \mathbf{k})} = \frac{q_1}{q_j}, \quad (5.105)$$

leading to the result

$$\int d\mathbf{l} \frac{\kappa_A^{02}(\mathbf{l})}{4\pi} q_1 \Phi_A^0(1, j, \mathbf{k} = \mathbf{0}) = q_j. \quad (5.106)$$

Written in terms of $F_A^0(1, j, \mathbf{k}) = -\beta e_{\gamma_1} e_{\gamma_j} \Phi_A^0(1, j, \mathbf{k})$, this equation takes a form similar to (2.31):

$$\int d\mathbf{l} q_1 e_{\gamma_1} \rho_A^0(\mathbf{l}) F_A^0(1, j, \mathbf{0}) = -q_j e_{\gamma_j}. \quad (5.107)$$

It expresses the screening of the charged loops on the Debye–Hückel level. Note that $q_1 e_{\gamma_1} \equiv Q_1$ is the total charge carried by the loop $\mathbf{1}$.

Perfect screening of the charged loops

The validity of the electroneutrality sum rule on the Debye–Hückel level in the geometry we consider implies that it holds in full generality for the loop Ursell function.

The reasoning, already used in the bulk geometry (Brydges & Martin, 1999), proceeds by “extracting” the Debye–Hückel sum rule from the integrated correlation function h_A^0 , exactly as in Section 3.5. One can conveniently rewrite h_A^0 as an integral on the quantities $(h_A^0)^{\text{nn}} \equiv \circ\circ$ and $(h_A^0)^{\text{nc}} \equiv \circ\bullet\circ$:

$$\begin{aligned} h_A^0(1, 2, \mathbf{0}) &= \circ\circ + \circ\bullet\circ + [\circ\circ] + \circ\bullet\bullet\circ + [\circ\bullet\circ] \\ &= F_A^0(1, 2, \mathbf{0}) + \int d\mathbf{3} \rho_A^0(\mathbf{3}) \left[F_A^0(1, 3, \mathbf{0}) + \frac{\delta(1,3)}{\rho_A^0(\mathbf{3})} \right] [(h_A^0)^{\text{nn}} + (h_A^0)^{\text{nc}}](3, 2, \mathbf{0}). \end{aligned} \quad (5.108)$$

Integrating h_A^0 like F_A^0 in (5.107), the first term obviously yields $-q_j e_{\gamma_j}$. The second term is, by contrast, cancelled by the same sum rule: it involves the integral

$$\int d\mathbf{l} q_1 e_{\gamma_1} \rho_A^0(1) \left[F_A^0(1, 3, \mathbf{0}) + \frac{\delta(1,3)}{\rho_A^0(3)} \right] \equiv 0. \quad (5.109)$$

From (5.101), it is clear for the same reason that $G_A^0(1, j, \mathbf{0})$ also satisfies the sum rule. Hence,

$$\int d\mathbf{l} q_1 e_{\gamma_1} \rho_A^0(1) h_A^0(1, 2, \mathbf{0}) = \int d\mathbf{l} q_1 e_{\gamma_1} \rho_A^0(1) G_A^0(1, 2, \mathbf{0}) = -q_2 e_{\gamma_2}. \quad (5.110)$$

Perfect screening of the charged particles

The perfect screening of the quantum charges is, in turn, a direct consequence of the perfect screening in the loop system, by virtue of (5.102) (Ballenegger et al., 2002, Sec. 6.1).

5.4 The Casimir force in the semi-classical regime: final result

Having analysed the large-distance correlations between the field-coupled quantum plasmas and verified that the perfect screening sum rule holds, we are now in position to proceed to the last steps of the calculation of the Casimir force (5.63).

Magnetic forces $f^m(d)$

The loop Ursell correlation function $h_{AB}(1, 2, \frac{\mathbf{q}}{d})$ brings an asymptotic factor $\propto d^{-1}$ to the Casimir force. We have seen that the magnetic potential $W_{AB}^m(1, 2, \frac{\mathbf{q}}{d})$ is $O(d^{-1})$. Necessarily, the magnetic force between loops $\partial_{x_1} W_{AB}^m(1, 2, \frac{\mathbf{q}}{d})$ decays faster. It is shown at the end of Appendix 5.B that it is indeed $O(d^{-2})$.

Thus, the average of the magnetic part of the microscopic Lorentz forces elicited in Section 5.1 has no impact on the total Casimir force at dominant order:

$$f^m(d) = O(d^{-5}). \quad (5.111)$$

Electrostatic forces $f^c(d)$

On the other hand, the Coulomb term $\partial_{x_1} v_{AB}(1, 2, \frac{\mathbf{q}}{d})$ provides the factor

$$\partial_{x_1} v_{AB}(1, 2, \frac{\mathbf{q}}{d}) = 2\pi e^{-q} e^{-\frac{q|x_1|}{d}} e^{-\frac{q|x_2|}{d}} = O(1). \quad (5.112)$$

The average of the microscopic Coulomb forces exerting between the particles is thus

$$f^c(d) = O(d^{-3}). \quad (5.113)$$

5.4.1 Final result

Let us first calculate the contribution to $f(d) \stackrel{d \rightarrow \infty}{\sim} f^c(d)$ given by the asymptotic correlations conveyed by the potential W_{AB} . Using (5.63) and (5.99), one sees that this contribution vanishes identically by the perfect screening sum rule (5.110). Indeed, integrating according to the force formula on the root points of this part of the correlation exhibits the following integrals

$$\int d1 e_{\gamma_1} q_1 \rho_A^0(1) \left(h_A^0(1, 3, \mathbf{0}) + \frac{\delta(1,3)}{\rho_A^0(3)} \right) = \int d2 e_{\gamma_2} q_2 \rho_B^0(2) \left(h_B^0(4, 2, \mathbf{0}) + \frac{\delta(4,2)}{\rho_B^0(4)} \right) = 0, \quad (5.114)$$

which consist in a rewriting of the perfect screening sum rule in the system of loops.

Only the correlations (5.98) conveyed between the loops by the classical-like electrostatic interaction contribute to the establishment of the leading term $\propto d^{-3}$. With (5.63) and (5.112), we have

$$\begin{aligned} f(d) &\stackrel{d \rightarrow \infty}{\sim} -\frac{1}{4\pi\beta d^3} \left[\int d1 q_1 e_{\gamma_1} \rho_A^0(1) \frac{G_A^0(1,0,\mathbf{0})}{e_{\alpha_0}} \right] \left[\int d2 q_2 e_{\gamma_2} \rho_B^0(2) \frac{G_B^0(0,2,\mathbf{0})}{e_{\beta_0}} \right] \int_0^\infty dq \frac{q e^{-q}}{\sinh q} \\ &= -\frac{\zeta(3)}{8\pi\beta d^3}. \end{aligned} \quad (5.115)$$

Last equality makes use of the sum rule (5.110) holding for the functions G_A^0 and G_B^0 , and of the value $\zeta(3)/2$ of the q -integral. *We thus have recovered the classical result (2.90) of the Casimir force in the semi-classical regime of a system of quantum charges coupled to the (classical) radiation field.*

Physical sources of the leading force: The leading term of the Casimir force in the semi-classical regime originates exclusively from the Coulomb part of the microscopic Lorentz forces. Moreover, only the correlations (5.98) driven by the classical-like electrostatic force between the loops support its establishment. Correlations due to the imperfect screening of the multipoles in the quantum plasmas and those mediated by the radiation field, contained in the term (5.99) prove to be inoperative on these Coulomb microscopic forces at dominant order. They are shielded away by screening mechanisms. The quantum nature of the particles and the coupling of matter to the radiation field will be felt only in subdominant terms $\propto d^{-4}$.

Universality's origin: The universality of the leading term $\propto d^{-3}$ holds exactly in the full system of coupled matter and field. The fundamental origin of this universality lies in the perfect screening sum rule. The rule used here expresses the screening occurring in the auxiliary system of the charged loops. Nevertheless, it reflects the perfect screening of the quantum charges.

As in the classical situation, the result is **independent on the (finite) thicknesses** a and b of the plasmas. This is due to the fact that the sum rules in (5.115) involve only the screening clouds of loops close to the inner surface of the plates. For every macroscopic thickness of the slabs, this cloud is able to screen them exactly.

Appendix 5.A: Properties of V^c and W^m regarding loops' origin

With the notation (5.45) for the loop $\mathcal{L}^{[u]}$ with shifted origin, this appendix aims at showing following covariance properties:

$$V^c(\mathcal{L}^{[u]}, \mathcal{L}'^{[u']}) = V^c(\mathcal{L}, \mathcal{L}'), \quad \text{if } u - u' \in \mathbb{Z} \quad (5A.1)$$

$$W^m(\mathcal{L}^{[u]}, \mathcal{L}'^{[u']}) = W^m(\mathcal{L}, \mathcal{L}'), \quad \forall u, u' \quad (5A.2)$$

From (4.82), one has

$$\begin{aligned} W^m(\mathcal{L}^{[u]}, \mathcal{L}'^{[u']}) &= \frac{1}{\beta \sqrt{m_\gamma m_{\gamma'}} c^2} \int \frac{d\mathbf{k}}{(2\pi)^3} \sum_{\mu, \nu} \int_0^q d(\mathbf{X}^{[u]})^\mu(s) \int_0^{q'} d(\mathbf{X}'^{[u']})^\nu(s') \\ &\quad \times e^{i\mathbf{k} \cdot (\mathbf{r} + \lambda_\gamma \mathbf{X}(s+u) - \mathbf{r}' - \lambda_{\gamma'} \mathbf{X}'(s'+u'))} G^{\mu\nu}(\mathbf{k}) \end{aligned}$$

which shows the result (5A.2) because for any function f ,

$$\begin{aligned} \int_0^q d\mathbf{X}^{[u]}(s) f(\mathbf{X}(s+u)) &= \int_0^q d(\mathbf{X}(s+u)) f(\mathbf{X}(s+u)) \stackrel{s \mapsto s+u}{=} \int_u^{q+u} d\mathbf{X}(s) f(\mathbf{X}(s)) \\ &= \int_0^q d\mathbf{X}(s) f(\mathbf{X}(s)). \end{aligned} \quad (5A.3)$$

Last equality results from having extended $s \mapsto \mathbf{X}(s)$, $s \in [0, q]$ to a q -periodic function over \mathbb{R} . Formula (5A.3) can be proven exactly using the discretization rule of the middle point (4.12) and the periodicity of $\mathbf{X}(s)$.

Regarding V^c , one has from (4.81)

$$\begin{aligned} V^c(\mathcal{L}^{[u]}, \mathcal{L}'^{[u']}) &= \int_0^q ds \int_0^{q'} ds' \delta(\widetilde{s} - \widetilde{s}') \frac{1}{|\mathbf{r} + \lambda_\gamma \mathbf{X}(s+u) - \mathbf{r}' - \lambda_{\gamma'} \mathbf{X}'(s'+u')|} \\ &= \int_u^{q+u} ds \int_{u'}^{q'+u'} ds' \delta(\widetilde{(s-u)} - \widetilde{(s'-u')}) \frac{1}{|\mathbf{r}^{[s]} - \mathbf{r}'^{[s']}|}, \end{aligned} \quad (5A.4)$$

where the changes of variable $s \mapsto s + u$ and $s' \mapsto s' + u'$ have been performed for the second equality. The equal time condition $\delta(\widetilde{s} - \widetilde{s}')$ can equivalently be described by the Dirac comb $\widetilde{\delta}(s - s') \equiv \sum_{n \in \mathbb{Z}} e^{i2\pi n(s - s')}$ (Ballenegger et al., 2002). It is then evident that $\widetilde{\delta}(s - u - s' + u') = \widetilde{\delta}(s - s') = \delta(\widetilde{s} - \widetilde{s}')$ whenever $u - u' \in \mathbb{Z}$. The q and q' periodicity of the integrand in (5A.4) regarding s and s' then shows the property (5A.1).

Appendix 5.B: Large-distance behaviour of \overline{W}_{AB}^m

In this appendix, we calculate the asymptotic behaviour of $\overline{W}_{AB}^m(1, 2, \frac{\mathbf{q}}{d})$, defined like $W_{AB}^m(1, 2, \frac{\mathbf{q}}{d})$ but with the cutoff function $g(k_1, \frac{\mathbf{q}}{d})$ set equal to unity. This asymptotic behaviour determines immediately that of $W_{AB}^m(1, 2, \frac{\mathbf{q}}{d})$ by Formula (5.86).

The inverse Fourier integral in (5.84) can be performed explicitly when $g \equiv 1$, yielding

$$\begin{aligned} \overline{W}_{AB}^m(1, 2, \frac{\mathbf{q}}{d}) &= \frac{1}{\beta \sqrt{m_{\gamma_1} m_{\gamma_2} c^2}} \sum_{\mu, \nu} \int_0^{q_1} dX_1^\mu(s_1) \int_0^{q_2} dX_2^\nu(s_2) e^{i\frac{\mathbf{q}}{d} \cdot [\lambda_{\gamma_1} \mathbf{Y}_1(s_1) - \lambda_{\gamma_2} \mathbf{Y}_2(s_2)]} \\ &\quad \times v^{\mu\nu}(x_1^{[s_1]} - x_2^{[s_2]} - d, \frac{\mathbf{q}}{d}), \end{aligned} \quad (5B.1)$$

where $v^{\mu\nu}(x, \mathbf{k})$ is the partial Fourier transform of the transverse Coulomb potential given by (B.11). Because here $|x_1^{[s_1]} - x_2^{[s_2]} - d| = d + x_2^{[s_2]} - x_1^{[s_1]}$, the exact spatial dependence of $\overline{W}_{AB}^m(1, 2, \frac{\mathbf{q}}{d})$ (at any finite d) is inferred to be made up of terms proportional to

$$\frac{d}{q} e^{-\frac{q|x_1|}{d}} e^{-\frac{q|x_2|}{d}}, \quad \text{or} \quad (d + x_2 - x_1) e^{-\frac{q|x_1|}{d}} e^{-\frac{q|x_2|}{d}}. \quad (5B.2)$$

By Itô's Lemma, the line integrals that multiply these spatial dependences reduce the apparent $\propto d$ divergency to an $O(1/d)$ decay: they provide a factor $O(q^2/d^2)$ (see below) exactly as did the nonequal-time integrals when calculating the asymptotic behaviour of $W_{AB}^c(1, 2, \frac{\mathbf{q}}{d})$.

Differentiating twice with respect to x_1 can only increase these terms' decay with d (in the slowest case, by a factor q/d), so that the asymptotic behaviour of W_{AB}^m is the same as that of \overline{W}_{AB}^m by virtue of (5.86):

$$W_{AB}^m(1, 2, \frac{\mathbf{q}}{d}) = \overline{W}_{AB}^m(1, 2, \frac{\mathbf{q}}{d}) [1 + O(d^{-1})]. \quad (5B.3)$$

The cutoff function (*i.e.*, relativistic effects of the particles), disregarded in \overline{W}_{AB}^m , is seen to step in at the first subdominant order already (mixing with subdominant

orders included in \overline{W}_{AB}^m itself). These subdominant orders can only give rise to contributions to the force at least $O(d^{-5})$.

Hereafter, we calculate the asymptotic $\propto d^{-1}$ term of $\overline{W}_{AB}^m(1, 2, \frac{\mathbf{q}}{d})$. There are only two types of line integrals occurring in (5B.1) to investigate, namely

$$I_1(k', \frac{\mathbf{q}}{d}) \equiv \int_0^{q_1} dX_1^\mu(s_1) \int_0^{q_2} dX_2^\nu(s_2) e^{i\frac{\mathbf{q}}{d} \cdot [\lambda_{\gamma_1} \mathbf{Y}_1(s_1) - \lambda_{\gamma_2} \mathbf{Y}_2(s_2)]} e^{-k'(d+x_2^{[s_2]} - x_1^{[s_1]})} \quad (5B.4)$$

evaluated at $k' = \frac{q}{d}$, as well as $I_2(\frac{q}{d}, \frac{\mathbf{q}}{d}) = \frac{d}{dk'} \Big|_{k'=q/d} I_1(k', \frac{\mathbf{q}}{d})$. Rearranging the exponentials, and using Itô's Lemma to cancel the unit term of their expansion, one has

$$\begin{aligned} I_1(k', \frac{\mathbf{q}}{d}) &= e^{-k'(d+x_2-x_1)} \int_0^{q_1} dX_1^\mu(s_1) \int_0^{q_2} dX_2^\nu(s_2) \\ &\quad \times e^{\lambda_{\gamma_1} [k' X_1(s_1) + i\frac{\mathbf{q}}{d} \cdot \mathbf{Y}_1(s_1)]} e^{-\lambda_{\gamma_2} [k' X_2(s_2) + i\frac{\mathbf{q}}{d} \cdot \mathbf{Y}_2(s_2)]} \\ &= e^{-k'(d+x_2-x_1)} \int_0^{q_1} dX_1^\mu(s_1) \int_0^{q_2} dX_2^\nu(s_2) \\ &\quad \times \sum_{n=1}^{\infty} \frac{1}{n!} (\lambda_{\gamma_1} [k' X_1(s_1) + i\frac{\mathbf{q}}{d} \cdot \mathbf{Y}_1(s_1)])^n \\ &\quad \times \sum_{m=1}^{\infty} \frac{1}{m!} (-\lambda_{\gamma_2} [k' X_2(s_2) + i\frac{\mathbf{q}}{d} \cdot \mathbf{Y}_2(s_2)])^m, \end{aligned} \quad (5B.5)$$

whence $I_2(k', \frac{\mathbf{q}}{d})$ is deduced by differentiation. Evaluating at $k' = \frac{q}{d}$ and selecting the asymptotic terms as $d \rightarrow \infty$, it is seen that

$$\begin{aligned} I_1(\frac{q}{d}, \frac{\mathbf{q}}{d}) &\stackrel{d \rightarrow \infty}{\sim} \frac{q^2 e^{-q} e^{-\frac{q|x_1|}{d}} e^{-\frac{q|x_2|}{d}} \lambda_{\gamma_1} (-\lambda_{\gamma_2})}{d^2} \int_0^{q_1} dX_1^\mu(s_1) \int_0^{q_2} dX_2^\nu(s_2) \\ &\quad \times [X_1(s_1) + i\hat{\mathbf{q}} \cdot \mathbf{Y}_1(s_1)] [X_2(s_2) + i\hat{\mathbf{q}} \cdot \mathbf{Y}_2(s_2)], \end{aligned} \quad (5B.6)$$

$$\begin{aligned} I_2(\frac{q}{d}, \frac{\mathbf{q}}{d}) &\stackrel{d \rightarrow \infty}{\sim} \frac{q e^{-q} e^{-\frac{q|x_1|}{d}} e^{-\frac{q|x_2|}{d}} \lambda_{\gamma_1} (-\lambda_{\gamma_2})}{d} \int_0^{q_1} dX_1^\mu(s_1) \int_0^{q_2} dX_2^\nu(s_2) \\ &\quad \times \left\{ X_1(s_1) [X_2(s_2) + i\hat{\mathbf{q}} \cdot \mathbf{Y}_2(s_2)] + [X_1(s_1) + i\hat{\mathbf{q}} \cdot \mathbf{Y}_1(s_1)] X_2(s_2) \right. \\ &\quad \left. - q [X_1(s_1) + i\hat{\mathbf{q}} \cdot \mathbf{Y}_1(s_1)] [X_2(s_2) + i\hat{\mathbf{q}} \cdot \mathbf{Y}_2(s_2)] \right\}. \end{aligned} \quad (5B.7)$$

Note that $I_1(\frac{q}{d}, \frac{\mathbf{q}}{d})$ always occurs in (5B.1) with a factor d/q , so that it does contribute to the asymptotic behaviour of $\overline{W}_{AB}^m(1, 2, \frac{\mathbf{q}}{d})$. Collecting all dominant contributions given by (5B.6) and (5B.7) in (5B.1) results in the formula

$$\begin{aligned} \overline{W}_{AB}^m(1, 2, \frac{\mathbf{q}}{d}) &\stackrel{d \rightarrow \infty}{\sim} \frac{2\pi q e^{-q} e^{-\frac{q|x_1|}{d}} e^{-\frac{q|x_2|}{d}} \lambda_{\gamma_1} (-\lambda_{\gamma_2})}{\beta \sqrt{m_{\gamma_1} m_{\gamma_2}} c^2 d} \sum_{\mu, \nu} \int_0^{q_1} dX_1^\mu(s_1) \int_0^{q_2} dX_2^\nu(s_2) \\ &\quad \times w^{\mu\nu}(\mathbf{X}_1(s_1), \mathbf{X}_2(s_2), \mathbf{q}), \end{aligned} \quad (5B.8)$$

with

$$w^{\mu\nu}(\mathbf{X}_1, \mathbf{X}_2, \mathbf{q}) = \alpha^{\mu\nu}(\mathbf{q})[X_1 + i\hat{\mathbf{q}} \cdot \mathbf{Y}_1][X_2 + i\hat{\mathbf{q}} \cdot \mathbf{Y}_2] \\ + \beta^{\mu\nu}(\hat{\mathbf{q}})[X_1(X_2 + i\hat{\mathbf{q}} \cdot \mathbf{Y}_2) + (X_1 + i\hat{\mathbf{q}} \cdot \mathbf{Y}_1)X_2], \quad (5B.9)$$

$$\alpha^{11}(\mathbf{q}) = \frac{1+q}{2}, \quad \beta^{11}(\hat{\mathbf{q}}) = -\frac{1}{2}, \quad \mu = \nu = 1, \quad (5B.10)$$

$$\alpha^{\mu 1}(\mathbf{q}) = \frac{iq\hat{q}_\mu}{2}, \quad \beta^{\mu 1}(\hat{\mathbf{q}}) = -\frac{i\hat{q}_\mu}{2}, \quad \mu \neq 1, \nu = 1, \quad (5B.11)$$

$$\alpha^{\mu\nu}(\mathbf{q}) = \delta_{\mu\nu} - (1+q)\frac{\hat{q}_\mu\hat{q}_\nu}{2}, \quad \beta^{\mu\nu}(\hat{\mathbf{q}}) = \frac{\hat{q}_\mu\hat{q}_\nu}{2}, \quad \mu \neq 1, \nu \neq 1. \quad (5B.12)$$

The subdominant terms $\propto 1/d^2$ in (5B.8) have their spatial and \mathbf{q} dependences of the type (disregarding angular dependences $\hat{\mathbf{q}}$)

$$\frac{q^2}{d^2}e^{-q}e^{-\frac{q|x_1|}{d}}e^{-\frac{q|x_2|}{d}}, \quad \frac{q}{d}\frac{q}{d}x_j e^{-q}e^{-\frac{q|x_1|}{d}}e^{-\frac{q|x_2|}{d}}, \quad \text{or} \quad \frac{q^3}{d^2}e^{-q}e^{-\frac{q|x_1|}{d}}e^{-\frac{q|x_2|}{d}}, \quad (5B.13)$$

($j = 1, 2$), which are naturally consistent with (5B.2). They exhibit facilitated integrability properties at $\mathbf{q} = 0$, while not altering that at $q \rightarrow \infty$.

The loop magnetic force $\partial_{x_1} W_{AB}^m(1, 2, \frac{\mathbf{q}}{d})$ is easily seen from (5B.2) — and the $O(q^2/d^2)$ factor supplied by Itô's Lemma — to be $O(d^{-2})$ and given by

$$\frac{\partial}{\partial x_1} W_{AB}^m(1, 2, \frac{\mathbf{q}}{d}) = \frac{\partial}{\partial x_1} \overline{W_{AB}^m}(1, 2, \frac{\mathbf{q}}{d}) [1 + O(d^{-1})] = O(d^{-2}). \quad (5B.14)$$

The dominant terms in $\partial_{x_1} \overline{W_{AB}^m}(1, 2, \frac{\mathbf{q}}{d})$ have the forms

$$\frac{q^2}{d^2}e^{-q}e^{-\frac{q|x_1|}{d}}e^{-\frac{q|x_2|}{d}}, \quad \text{or} \quad \frac{q^3}{d^2}e^{-q}e^{-\frac{q|x_1|}{d}}e^{-\frac{q|x_2|}{d}}, \quad (5B.15)$$

with coefficients made of stochastic line integrals depending on $\hat{\mathbf{q}}$, similar to (5B.8)–(5B.9). Note that the dominant component of $\partial_{x_1} \overline{W_{AB}^m}(1, 2, \frac{\mathbf{q}}{d})$ as $d \rightarrow \infty$ is not simply deduced by differentiating the dominant term of $\overline{W_{AB}^m}(1, 2, \frac{\mathbf{q}}{d})$ given by (5B.8).

Appendix 5.C: Brownian functional integrals in slab geometries

In this appendix we show how weighting the normalized bulk measure $D(\mathbf{X})$ [of zero mean and covariance (4.78)] with $\mathbb{1}_A(x, \chi)$ (5.30) formally provides a functional integral corresponding to a Brownian (Markovian) process satisfying the

diffusion equation with Dirichlet conditions at the interfaces $x = -a, 0$. In fact the latter path integral naturally arises when representing the partition function in the Feynman–Kac–Itô formalism with *ab initio* idealized confinements. In this chapter, we have always represented it by the weighted measure $D(\mathbf{X})\mathbb{1}_A(x, \chi)$ on the ground of this equivalence.

We restrict the discussion to the $X(\cdot)$ component of $\mathbf{X}(\cdot)$. The measure $D(\mathbf{X})$ factorizes into $D(X)D(\mathbf{Y})$ and the transverse component $\mathbf{Y}(\cdot)$ has no boundary constraints in the thermodynamic limit $L \rightarrow \infty$; $D(\mathbf{Y})$ is a 2-dimensional Gaussian bulk measure with covariance (4.78).

The 1-dimensional bulk Brownian process $X(\cdot)$ starting from and returning to the origin in the time $[0, q]$ ($X(0) = X(q) = 0$) has the following sequence of absolute probabilities of passing through X_1 at time t_1 ; ... ; X_N at time t_N

$$W_{0,0}^{0,q}(X_1 t_1, \dots, X_N t_N) = (2\pi q)^{1/2} p_0(0 q|X_N t_N) \dots p_0(X_1 t_1|0 0), \quad (5C.1)$$

where

$$p_0(X_2 t_2|X_1 t_1) = \frac{1}{[2\pi(t_2 - t_1)]^{1/2}} e^{-\frac{1}{2} \frac{(X_2 - X_1)^2}{t_2 - t_1}}. \quad (5C.2)$$

One may formally represent $\mathbb{1}_A(x, \chi)$ as

$$\mathbb{1}_A(x, \chi) = e^{-\int_0^q ds \theta_\infty(x + \lambda_\gamma X(s))}, \quad \theta_\infty(x) = \begin{cases} \infty, & \text{if } x \notin [-a, 0], \\ 0, & \text{if } x \in] -a, 0[. \end{cases} \quad (5C.3)$$

Indeed, by continuity of the Brownian path $X(s)$, the set of times s where $x + \lambda_\gamma X(s)$ is not in $[-a, 0]$, if not empty, is of non-vanishing measure; in that case, the integral of θ_∞ must diverge and $\mathbb{1}_A(x, \chi) = 0$.

Using this representation and (5C.1), one can discretize the confined measure and calculate its moments, as illustrated by following example:

$$\int D(X) \mathbb{1}_A(x, \chi) = \lim_{N \rightarrow \infty} \int dX_1 \dots dX_N W_{0,0}^{0,q}(X_1 t_1, \dots, X_N t_N) \times e^{-\sum_{j=0}^N (t_{j+1} - t_j) \theta_\infty(x + \lambda_\gamma X_j)}, \quad (5C.4)$$

where $t_j = j \frac{q}{N+1}$, and $j = 0, 1, \dots, N+1$, $X_0 = X_{N+1} = 0$. The transition probability $p_0(X_2 t_2|X_1 t_1)$ represents $\langle X_2 | U_0(t_2, t_1) | X_1 \rangle$, the kernel of the propagator $U_0(t_2, t_1) = \exp(-(t_2 - t_1) \hat{H}_0)$ with $\hat{H}_0 = -\frac{1}{2} \partial^2 / \partial X^2$. Applying Trotter's formula on (5C.4) to combine \hat{H}_0 and θ_∞ in a same exponential, one finds

$$\begin{aligned} \int D(X) \mathbb{1}_A(x, \chi) &= (2\pi q)^{1/2} \langle X = 0 | e^{-q(\hat{H}_0 + \hat{\theta}_\infty(x + \lambda_\gamma \cdot))} | X = 0 \rangle \\ &\equiv (2\pi q)^{1/2} p(X = 0, q | X = 0, 0). \end{aligned} \quad (5C.5)$$

This new transition probability $p(X, q|X_0, 0)$ is now the kernel of the propagator $e^{-q(\hat{H}_0 + \hat{\theta}_\infty(x + \lambda_\gamma \cdot))}$, namely, it is solution of the diffusion equation (parametrized by x and a occurring in θ_∞)

$$\frac{\partial}{\partial t} p(X, t|X_0, t_0) = \left(\frac{1}{2} \frac{\partial^2}{\partial X^2} - \theta_\infty(x + \lambda_\gamma X) \right) p(X, t|X_0, t_0) \quad (5C.6)$$

$$\lim_{t \rightarrow t_0} p(X, t|X_0, t_0) = \delta(X - X_0), \quad t \geq t_0. \quad (5C.7)$$

Equation (5C.6) is to be understood as

$$\begin{aligned} \frac{\partial}{\partial t} p(X, t|X_0, t_0) &= \frac{1}{2} \frac{\partial^2}{\partial X^2} p(X, t|X_0, t_0), \quad \text{if } -(a+x)/\lambda_\gamma < X < -x/\lambda_\gamma, \\ p(X, t|X_0, t_0) &\equiv 0, \quad \text{otherwise.} \end{aligned}$$

This corresponds to a diffusion problem constrained by hard walls at $-(a+x)/\lambda_\gamma$ and $-x/\lambda_\gamma$. It can be mapped into a problem with hard walls at $-a$ and 0 (conveniently independent on x) by defining

$$\varrho(\xi, t|\xi_0, t_0) \equiv \frac{1}{\lambda_\gamma} p\left(\frac{\xi-x}{\lambda_\gamma}, t\left|\frac{\xi_0-x}{\lambda_\gamma}, t_0\right.\right), \quad (5C.8)$$

which satisfies

$$\begin{aligned} \frac{\partial}{\partial t} \varrho(\xi, t|\xi_0, t_0) &= \frac{\lambda_\gamma^2}{2} \frac{\partial^2}{\partial \xi^2} \varrho(\xi, t|\xi_0, t_0), \quad \text{if } -a < \xi < 0, \\ \varrho(\xi, t|\xi_0, t_0) &\equiv 0, \quad \text{otherwise,} \\ \lim_{t \rightarrow t_0} \varrho(\xi, t|\xi_0, t_0) &= \delta(\xi - \xi_0), \quad t \geq t_0. \end{aligned} \quad (5C.9)$$

As an illustration, the solution of this latter problem when $a = \infty$ reads (Kleinert, 1990, Chap. 6), (Jancovici, 1980; J. N. Aqua & Cornu, 1999)

$$\varrho(\xi, t|\xi_0, t_0) = \frac{\theta(-\xi)\theta(-\xi_0)}{(2\pi\lambda_\gamma^2(t-t_0))^{1/2}} \left(e^{-\frac{(\xi-\xi_0)^2}{2\lambda_\gamma^2(t-t_0)}} - e^{-\frac{(\xi+\xi_0)^2}{2\lambda_\gamma^2(t-t_0)}} \right). \quad (5C.10)$$

Thus, for the semi-infinite plasma, collecting (5C.5), (5C.8) and (5C.10),

$$\int D(X) \mathbb{1}_A(x, \chi) = \theta(-x) \left(1 - e^{-\frac{(2x)^2}{\lambda_\gamma^2 q}} \right). \quad (5C.11)$$

Following similar steps leading from (5C.4) to (5C.5), one infers that

$$\begin{aligned} \int D(X) \mathbb{1}_A(x, \chi) X(t_1) \dots X(t_n) &= \int dX_1 \dots dX_n (2\pi q)^{1/2} p(0, q|X_n, t_n) \dots \\ &\times p(X_1, t_1|0, 0) X_1 \dots X_n. \end{aligned} \quad (5C.12)$$

The spatial constraints on the Brownian paths prevent $D(X)\mathbb{1}_A(x, \mathcal{X})$ from being a Gaussian measure; it is not determined by its normalization, mean value and covariance only. Nevertheless, the path integral is associated to the stochastic Markovian process of transition amplitude $p(X_2, t_2|X_1, t_1)$ (given by (5C.8) and (5C.10) in the semi-infinite situation), and all moments can in principle be computed by (5C.12).

Chapter 6

Conclusions and outlook

From a microscopic description of the perfect conducting behaviour of two parallel metallic plates at a distance d apart, we calculated the Casimir force by which they are attracted, in the semi-classical regime. The exact statistical methods employed allowed to show that this force by unit surface behaves, at large distances and fixed (high) temperature, as

$$f(d) = -\frac{\zeta(3)k_B T}{8\pi d^3} + R(\hbar, c, T, d), \quad \text{where} \quad R(\hbar, c, T, d) = O(d^{-4}). \quad (6.1)$$

Essentially two models have been investigated:

1. In a first model, the charges were classical and interacting via the Coulomb potential only. The asymptotic correlations could be analysed exactly, by means of the resummed Mayer series.
2. Using the path integral formalism of quantum statistical mechanics, the calculation was generalised to include the quantum nature of the particles and their coupling to the radiation field, so that the whole Lorentz force between the conductors was taken into account. The correlations could then be investigated exactly as in the classical situation.

Both models retrieved the asymptotic universal term in (6.1).

Factor 2 controversy: This approach differs from the previous theories calculating the force in the semi-classical regime — all based on Lifshitz' formula for the force between dielectrics — by the following facts.

- The metallic behaviour is described at the root of the model by the fluctuating charged microscopic constituents of the system. It thus takes fully into account the charge fluctuations inside the conductors.

- It is not the result of a controversial metallic limit of dielectrics described semi-macroscopically.
- It does not require the enforcement of macroscopic boundary conditions to the electromagnetic field at the plates' surfaces.

In conclusion, we affirm that it is the correct formula for the force in this regime. In this sense, we rally to the trend of thought prescribing the use of a vanishing reflection coefficient of the transverse electric (TE) mode at zero frequency in the Lifshitz theory, or equivalently, the use of the Drude model (1.8), at least in the semi-classical regime.

Universality: In addition to providing a more refined analysis of the factor 2 debate, our method also explains the emergence of the universality of the result (6.1) in *microscopic terms*. The asymptotic behaviour of the full interplasma correlation function involves, once integrated into the force, perfect screening sum rules that express the effective shielding of the charges in the individual conductors. These perfect screening sum rules imply, on one hand, the universality of the electrostatic part of the force, whereas they shield away its magnetic part. Furthermore, they involve the screening of charges close to the inner surfaces of the plates, which explains why the force is independent of the plates' thickness a and b (provided they are finite and large enough to allow screening clouds to form, *i.e.*, not microscopic. See also the discussion on thin or thick plasmas below).

Some conclusions more specifically concerned by the path integral loop formalism integrating the radiation field (and by its application to field correlations), developed in the article of Chapter 4, are to be found there.

Open questions and new problems

As usual when a new problem is being investigated, its resolution raises many more questions than it resolves. In spite of the rather refined microscopic models investigated throughout this work, a number of points still call for improvements or clarification.

Quantum field: By calculating the force in the semi-classical regime, we argued that only long wavelengths of the radiation field were important for interactions across the plasmas, thus justifying its classical treatment. However, the full model introduced in the article of Chapter 5 should be solved while keeping the quantum character of the field. Indeed, short wavelengths of the field may

in principle alter particles' intraplasma fluctuations. We suspect the asymptotic result (6.1) to be unchanged by such a generalisation.

Thin or thick plasmas: For every finite thickness a, b of the plates, the asymptotic force as $d \rightarrow \infty$ was seen to be always independent of them. This corresponds to situations where $d \gg (a, b) \gg 1$. The question of whether the regimes $d \gg (a, b) \gg 1$ (thin plasmas) and $a, b \gg d \gg 1$ (thick plasmas) lead to the same asymptotic force should be answered. We have seen that this is the case in the classical model. However, it might not be so when the radiation field is included into the description: indeed, the magnetic effective potential becomes asymptotically nonintegrable as $d \rightarrow \infty$.¹ When semi-infinite plasmas are considered before letting $d \rightarrow \infty$ (corresponding to $a, b \gg d \gg 1$), one needs to integrate this potential before analysing its behaviour as $d \rightarrow \infty$. Relativistic corrections $O((\beta mc^2)^{-1})$ and $O((\beta mc^2)^{-2})$ are likely to add to the $\propto d^{-3}$ asymptotic term.

This question is also related to that of subleading terms (see next point): a perturbative expansion in $a/d \ll 1$ is expected to be well-defined, by the presence of spatial dependencies $e^{-\frac{q|x|}{d}} \approx e^{-\frac{qa}{d}}$ in the Coulomb force for example. On the contrary, one expects an expansion in $d/a \ll 1$ to not be so, since the above spatial factor is nonanalytic in this parameter.

Nevertheless, experimentally, only *thin* coats of metal, of the order of 50nm, are presently deposited (by evaporation) on a support. Compared to separation distances ranging in $\approx 0.5\text{--}3\mu\text{m}$, the regime is clearly $a, b \ll d$ (Bressi et al., 2002). Thicker films lead to undesirable rougher surfaces (already at $\approx 0.3\mu\text{m}$) and there seem to be no experimental data in such regimes (Onofrio, 2006).

Subleading terms: The more general question of the subdominant term included in $R(\hbar, c, T, d) = O(d^{-4})$ is of primordial importance for several reasons. First, it naturally gives the dominant value $\propto d^{-3}$ its range of validity, which is crucial to establish contact with experiments — facing every kind of effects altogether —, even the more so in view of the multiple uncertainties found in the literature about how to take into account the corrections to the ideal, theoretical, asymptotic results. For example, finite conductivity corrections as usually taken into account in Lifshitz' theory appear as subdominant orders scaled by the so-called skin depth δ , the penetration depth of the field into the metals (Milton, 2004, Sec. 3.3.2). It would be of strong interest to be able to exhibit such an $O(\delta/d^4)$ correction in our calculation when the field is included.

We have mentioned, for the investigation of subleading terms, the importance of knowing more accurately properties of the density profiles as $d \rightarrow \infty$ (see Sec-

¹By a bulk symmetry argument, the “quantum component” of the Coulomb potential is seen to be, on the contrary, still integrable.

tion 3.8). Note that the mainly constant capacitor's force (2.47), which cannot be completely “turned off” in experiments, might potentially add $O(d^{-1})$ contributions as well.

Although most experiments aim at measuring the zero temperature Casimir force, they are so far performed at room temperature. Having more accurate limitations to distinguish the low-temperature and the high-temperature (semi-classical) regimes would be useful. This leads to the next question, which deserves a separate attention.

Zero temperature: In principle, as temperature is reduced, the higher-order terms $O(d^{-4})$ contained in $R(\hbar, c, T, d)$ should build up the Casimir vacuum force (1.1) while the classical term $\propto d^{-3}$ in (6.1) disappears. However, the interplay between low temperature and short distances, captured in macroscopic theories by the single parameter α (1.2), is not as simple in our microscopic theory, which involves many other characteristic lengths. An explicit form of the subleading term $\propto d^{-4}$ could give insights into the mechanism of this crossover. Nonetheless, the transition from our charged fluids to crystallised metals at zero temperature would require investigating the problem by means of a new formalism: that of loops is not well-defined at too low temperatures, as loops of very large extension (parametrized by the thermal de Broglie wavelength) would contribute substantially. (Moreover, we assumed translation invariance of the states in the calculations.) The sum rules satisfied by the correlations, expressing the screening effects in a conductive state, hold well beyond the weak-coupling regime. A lower bound of temperature for the validity of our result (T fixed, $d \rightarrow \infty$) may then be given by the requirement that the de Broglie wavelength λ_{part} be much smaller than the plates' width a, b . For plates of width $\approx 50\text{nm}$, temperatures only need to be greater than a few Kelvins. Understanding the crossover to lower temperatures in microscopic theories of *conductors* is an open problem.

The question of whether the quantum fluctuations of the microscopic charged constituents inside the conductors might as well modify Casimir's celebrated zero-temperature result is naturally raised by their importance in the semi-classical regime.

Note that in a coupled regime of low temperature and low density, however, one might — starting from the same microscopic premises as ours — investigate the force like Alastuey et al. (n.d.), who computed the effective van der Waals–London-like interactions in a system of recombined atoms with fractions of ionized charges. When these fractions are strictly zero, one is likely to fall back on the Lifshitz force in dilute media interpreted as the pairwise summation of these van der Waals forces. As soon as free charges are present, contributions from their interactions with atoms should occur, as well as “Casimir-like” con-

tributions resulting from the free charge interacting among themselves. Such a regime, however, does not model the conducting behaviour of real metallic plates at low temperature.

Other problems

The methods used in the present work may be applied to investigate related problems.

Field at an interface: The properties of the thermalised electromagnetic field at an interface with a perfect conductor could be analysed following the methods of Chapter 4, used there to calculate the asymptotic field correlations in a bulk material. Although such an equilibrium analysis would be difficult to put in parallel with the frequency-dependent macroscopic fields at an interface, it might still give insight into why the microscopic charge fluctuations of the conductor lead in effect to the vanishing of the reflection factor of the TE zero mode in the Casimir force problem. The calculation of penetration depths (related to the finite conductivity of the conductor) would require a good knowledge of the density profiles close to the surface, which have been extensively studied (in the absence of radiation) in (J.-N. Aqua & Cornu, 2001a, 2001b, 2004).

Atom-wall, charge-wall problems: The attraction occurring between an atom and a metallic plate is a whole field in itself in fluctuation-induced force, although it presents many similarities with the Casimir effect: Casimir and Polder (1948) investigated this case as a preliminary exercise to the retarded van der Waals interaction between two atoms. Yet, the plate is usually described macroscopically or semi-macroscopically. It would be interesting to describe its perfect conducting behaviour from a microscopic point of view. A large number of experiments measure this force too, see *e.g.*, (Duplantier & Rivasseau, 2003).

A similar problem is that of a single charge in front of a metallic plate. The expected result is to retrieve the very well-known “image charge” description on the conductor’s side, which corresponds (in the macroscopic language) to a specific distribution of a surface charge density bearing the opposite sign as the fixed charge. As a preliminary exercise to the Casimir force, we investigated this problem in the simplified Debye–Hückel approximation perturbing around flat density profiles. The leading force was indeed the one usually considered in macroscopic electrodynamics, *i.e.*, the force exerting between the charge and its “image”. Higher-order terms were involving the screening length of the plasma. This problem could be reanalysed so as to go beyond the Debye–Hückel approximation, and to prominently exhibit the screening mechanisms involved in the

universality of the dominant term. By the fact that an opposite mean charge density is brought “from infinity” at the conductor’s surface, this problem also relates to the notion of grounded conductors in the thermodynamic limit.

Other geometries: The problem of investigating the Casimir force between objects other than parallel slabs with our statistical point of view is expected to be hard; it is hard already with a macroscopic description. The calculation of the force in the two-plate geometry used extensively the partial Fourier representation with respect to the y -plane, which proved very fruitful. This could no longer be used.

Appendix A

Resummation of Mayer graphs in density

We sketch here the procedure to follow in order to resum the long-range part $f^{\text{el}}(\mathbf{i}, \mathbf{j}) \equiv -\beta e_{\gamma_i} e_{\gamma_j} v(\mathbf{i}, \mathbf{j})$ of the bond $f(\mathbf{i}, \mathbf{j}) = e^{-\beta(e_{\gamma_i} e_{\gamma_j} v + v_{\text{SR}})(\mathbf{i}, \mathbf{j})} - 1$ in Mayer graphs, giving rise to the resummed Mayer graphs series. (Notations are as in Section 2; v_{SR} denotes the short-range potential (2.20) between the classical charges.) This resummation is needed for Coulombic matter when the thermodynamic limit is taken, for the electrostatic Coulomb potential $v(\mathbf{i}, \mathbf{j})$ is nonintegrable at infinity. Due to the embodiment of screening in the resummation process, infinite spatial integrations in the new graphs are then well-defined. Only Mayer graphs in density are considered. The resummation procedure is slightly more complicated for Mayer graphs in activity, as they allow articulation points.

The principle of the resummation is to give prominence to chain convolutions of the long-range part f^{el} between two specific points. The sum of these chains defines the screened Debye–Hückel-like potential (2.57). However, the remaining part of the Mayer bond $f^{\text{R}} \equiv f - f^{\text{el}}$ and topological issues (the possibility of having two convolution chains in parallel but not two single bonds f across the same points) imply the playing of a second type of link in the resummed series. Hereafter, we call the intermediate points of f^{el} -convolution chains “Coulomb points”. These points disappear from the original graphs in the resummation process.

After splitting all the Mayer bonds f into $f^{\text{el}} + f^{\text{R}}$, one expands their product. In one of these expanded graphs, consider two non-Coulomb points that are linked by a two-point function made of a subgraph that contains only Coulomb points (if any). We resum the whole class of diagrams that differ from this chosen graph only by the internal structure of this two-point function. This process is recursively repeated between every other such pair of non-Coulomb points to provide the new graph series.

We distinguish two categories of subgraph structures for this two-point func-

tion. The first category links the two points by either f^{el} or a f^{el} -convolution chain: $f^{\text{el}} * f^{\text{el}}$, $f^{\text{el}} * f^{\text{el}} * f^{\text{el}}$, *etc.* The second category takes into account every other possibility, namely

- (a) one link f^{R}
- (b) $n \geq 2$ parallel paths of convolution chains $f^{\text{el}} * f^{\text{el}}$, $f^{\text{el}} * f^{\text{el}} * f^{\text{el}}$, *etc.*
- (c) one link f^{el} or f^{R} with in parallel $n \geq 1$ convolution chains like in (b).

Note that having two single f^{el} bonds or two single f^{R} bonds in parallel is not allowed. Resummation of subgraphs of the first category provides the screened bond F (2.57). Convoluting F in chains is then no longer allowed. Resummation of subgraphs of the second category gives rise to another bond:

$$F^{\text{R}} = \underbrace{f^{\text{R}}}_{(a)} + \underbrace{\sum_{n=2}^{\infty} \frac{(F - f^{\text{el}})^n}{n!}}_{(b)} + \underbrace{(f^{\text{el}} + f^{\text{R}}) \sum_{n=1}^{\infty} \frac{(F - f^{\text{el}})^n}{n!}}_{(c)}. \quad (\text{A.1})$$

The factors $1/n!$ take into account the changes in the graphs' symmetry number occasioned by the presence of parallel convolution chains. Reorganizing the different terms, one arrives at

$$\begin{aligned} F^{\text{R}} &= f^{\text{R}} + e^{F - f^{\text{el}}} - 1 - F + f^{\text{el}} + f(e^{F - f^{\text{el}}} - 1) \\ &= (e^{F - f^{\text{el}}} - 1)(1 + f) + f - F \end{aligned} \quad (\text{A.2})$$

$$= e^{F - \beta v_{\text{SR}}} - 1 - F. \quad (\text{A.3})$$

The resummation of all these internal structures yields bonds $F + F^{\text{R}}$, which are expanded to finally provide graphs built with either F or F^{R} by the same diagrammatic rules than the original graphs, except that convolution chains of F are forbidden.

Appendix B

Some Fourier transforms

The importance of Fourier transform in asymptotic analyses comes from the relation between the singularities of a function and the behaviour at infinity of its Fourier transform (or inverse Fourier transform). A nice and simple review of this important result, as well as of the meaning of Fourier transforms in the sense of distributions, can be found (in one dimension) in (Lighthill, 1996, especially Chap. 4). For the generalisation to several dimensions, see (Jones, 1982, especially Chap. 9).

Our definitions and notations for Fourier transforms are the following. We recall that we use the notation $\mathbf{r} = (x, \mathbf{y})$ and $\mathbf{k} = (k_1, \mathbf{k})$.

$$f(\mathbf{k}) = \int d\mathbf{r} e^{-i\mathbf{K}\cdot\mathbf{r}} f(\mathbf{r}), \quad (\text{B.1})$$

$$f(\mathbf{r}) = \int \frac{d\mathbf{k}}{(2\pi)^3} e^{i\mathbf{K}\cdot\mathbf{r}} f(\mathbf{k}), \quad (\text{B.2})$$

$$f(x, \mathbf{k}) = \int d\mathbf{y} e^{-i\mathbf{k}\cdot\mathbf{y}} f(x, \mathbf{y}) \quad (\text{B.3})$$

$$= \int \frac{dk_1}{2\pi} e^{ik_1 x} f(\mathbf{k}). \quad (\text{B.4})$$

We use the same symbol to denote a function and its Fourier transforms. These different entities are distinguished by inspection of their arguments.

Hereafter, some Fourier transforms used in this report are provided, as well as hints of how to derive them. Note that these Fourier transforms are taken in the sense of distributions, for the Coulomb potential is naturally not integrable.

Coulomb potential v

$$v(\mathbf{r}) = \frac{1}{|\mathbf{r}|} \quad (\text{B.5})$$

$$v(\mathbf{k}) = \frac{4\pi}{k^2} \quad (\text{B.6})$$

$$v(x, \mathbf{k}) = \frac{2\pi}{k} e^{-k|x|} \quad (\text{B.7})$$

$$\partial_x v(x, \mathbf{k}) = -2\pi \text{sign}(x) e^{-k|x|} \quad (\text{B.8})$$

Formula (B.7) is easily obtained using (B.4) on (B.6) and the Residue theorem. Its differentiation leads to (B.8).

Transverse Coulomb potential $v^{\mu\nu}$

$$v^{\mu\nu}(\mathbf{k}) = \frac{4\pi}{k^2} \delta_{\text{tr}}^{\mu\nu}(\mathbf{k}) = \frac{4\pi}{k^2} \left(\delta_{\mu\nu} - \frac{k_\mu k_\nu}{k^2} \right) \quad (\text{B.9})$$

$$v^{\mu\nu}(\mathbf{r}) = \frac{1}{2r} \left(\delta_{\mu\nu} + \frac{x_\mu x_\nu}{r^2} \right) \quad (\text{B.10})$$

$$v^{\mu\nu}(x, \mathbf{k}) = \frac{\pi}{k} e^{-k|x|} \times \begin{cases} \delta_{\mu\nu} + k|x|, & \nu = \mu = 1, \\ \delta_{\mu\nu} - ik_\mu x, & \mu \neq 1, \nu = 1, \\ 2\delta_{\mu\nu} - (1 + k|x|) \frac{k_\mu k_\nu}{k^2}, & \mu \neq 1, \nu \neq 1. \end{cases} \quad (\text{B.11})$$

$$\partial_x v^{\mu\nu}(x, \mathbf{k}) = -\pi e^{-k|x|} \times \begin{cases} kx, & \nu = \mu = 1, \\ -ik_\mu |x| + i \frac{k_\mu}{k}, & \mu \neq 1, \nu = 1, \\ \text{sign}(x) (2\delta_{\mu\nu} - k|x| \frac{k_\mu k_\nu}{k^2}), & \mu \neq 1, \nu \neq 1. \end{cases} \quad (\text{B.12})$$

The full Fourier transform (B.1) of the nondiagonal term in (B.10) (yielding part of (B.9)) can be computed using $\frac{x_\mu x_\nu}{r^3} = x_\mu \partial_\nu \left(\frac{1}{r} \right)$, partial integrations, and (B.6). Similar calculations, starting from the same identity (specialized according to the values of μ and ν) and making use of the partial Fourier transform (B.3) lead to (B.11). Differentiation, again, provides (B.12).

Bibliography

- Abe, R. (1959). Giant cluster expansion theory and its application to high temperature plasma. *Progr. Theor. Phys.*, 22, 213–226.
- Alastuey, A. (1994). Statistical mechanics of quantum plasmas. Path integral formalism. In G. Chabrier and E. Schatzman (Eds.), *The equation of state in astrophysics* (Vol. 147, pp. 43–77). Cambridge, UK: Cambridge University Press.
- Alastuey, A., and Appel, W. (1997). A model of relativistic one-component plasma with Darwin interactions. *Physica A*, 238, 369–404.
- Alastuey, A., and Appel, W. (2000). On the decoupling between classical Coulomb matter and radiation. *Physica A*, 276, 508–520.
- Alastuey, A., Cornu, F., and Martin, Ph. A. (n.d.). *Van der Waals forces in a partially recombined Hydrogen plasma*. In preparation. (The results are presented in (Martin and Buenzli, 2006))
- Alastuey, A., and Martin, Ph. A. (1989). Absence of exponential clustering in quantum Coulomb fluids. *Phys. Rev. A*, 40, 6485–6520.
- Appel, W., and Alastuey, A. (1998). Relativistic corrections for a classical one-component plasma with Darwin interactions. *Physica A*, 252, 238–268.
- Appel, W., and Alastuey, A. (1999). Thermal screening of Darwin interactions in a weakly relativistic plasma. *Phys. Rev. E*, 59, 4542–4551.
- Aqua, J. N., and Cornu, F. (1999). Classical and quantum algebraic screening in a Coulomb plasma near a wall: A solvable model. *J. Stat. Phys.*, 97, 173–207.
- Aqua, J.-N., and Cornu, F. (2001a). Density profiles in a classical Coulomb fluid near a dielectric wall, I. Mean-field scheme. *J. Stat. Phys.*, 105, 211–244.
- Aqua, J.-N., and Cornu, F. (2001b). Density profiles in a classical Coulomb fluid near a dielectric wall, II. Weak-coupling systematic expansion. *J. Stat. Phys.*, 105, 245–283.
- Aqua, J.-N., and Cornu, F. (2003). Dipolar effective interaction in a fluid of charged spheres near a dielectric plate. *Phys. Rev. E*, 68, 026133, 1–17.
- Aqua, J.-N., and Cornu, F. (2004). Density profiles in a quantum Coulomb fluid near a hard wall. *J. Stat. Phys.*, 115, 997–1036.
- Aristotle. (350 B.C.). *Historia Animalium*. (English translation : D’A. W. Thompson (1918) Oxford : Clarendon. (http://classics.mit.edu/Aristotle/history_anim.html))
- Autumn, K., Liang, Y. A., Hsieh, S. T., Zesch, W., Chan, W. P., Kenny, T. W., et al. (2000).

- Adhesive force of a single Gecko foot-hair. *Nature*, 405, 681–685.
- Autumn, K., Sitti, M., Liang, Y. A., Peattie, A. M., Hansen, W. R., Sponberg, S., et al. (2002). Evidence for van der Waals adhesion in Gecko Setae. *Proceedings of the National Academy of Sciences*, 99, 12252–12256. (<http://www.pnas.org/cgi/doi/10.1073/pnas.192252799>).
- Balescu, R. (1975). *Equilibrium and nonequilibrium statistical mechanics*. New York: John Wiley & Sons.
- Balian, R., and Duplantier, B. (1977). Electromagnetic waves near perfect conductors, I. Multiple scattering expansions and distribution of modes. *Ann. Phys.*, 104, 300–335.
- Balian, R., and Duplantier, B. (1978). Electromagnetic waves near perfect conductors, II. Casimir effect. *Ann. Phys.*, 112, 165–208.
- Balian, R., and Duplantier, B. (2003). Effet Casimir et géométrie. In B. Duplantier and V. Rivasseau (Eds.), *Poincaré seminar 2002 : Vacuum energy-renormalization* (Vol. 30). Basel: Birkhäuser.
- Ball, Ph. (2006). Popular physics myth is all at sea. Does the ghostly Casimir effect really cause ships to attract each other? *news@nature.com*, 4 May, doi:10.1038/news060501-7. (<http://www.nature.com/news/2006/060501/full/060501-7.html>). (Emailed by F. Pinto to news@nature.com)
- Ballenegger, V., Martin, Ph. A., and Alastuey, A. (2002). Quantum Mayer graphs for Coulomb systems and the analog of the Debye potential. *J. Stat. Phys.*, 108, 169–211.
- Boersma, S. L. (1996). A maritime analogy of the Casimir effect. *Am. J. Phys.*, 64, 539–541.
- Bordag, M. (2006). *The Casimir effect for a sphere and a cylinder in front of plane and corrections to the proximity force theorem*. Preprint. (<http://arxiv.org/abs/hep-th/0602295>)
- Bordag, M., Mohideen, U., and Mostepanenko, V. M. (2001). New developments in the Casimir effect. *Phys. Rep.*, 353, 1–205.
- Boustani, S. el. (2005). *Corrélations dans un gaz Coulombien à l'équilibre en présence du champ de radiation*. Master's thesis, Swiss Federal Institute of Technology, Lausanne (EPFL), Institute of Theoretical Physics, CH-1015 Lausanne, Switzerland.
- Boustani, S. el, Buenzli, P. R., and Martin, Ph. A. (2006). Equilibrium correlations in charged fluids coupled to the radiation field. *Phys. Rev. E*, 73, 036113, 1–14.
- Bressi, G., Carugno, G., Onofrio, R., and Ruoso, G. (2002). Measurement of the Casimir force between parallel metallic surfaces. *Phys. Rev. Lett.*, 88, 041804, 1–4.
- Brevik, I., Aarseth, J. B., Høye, J. S., and Milton, K. A. (2005). Temperature dependence of the Casimir effect. *Phys. Rev. E*, 71, 056101, 1–8.
- Brevik, I., Ellingsen, S. A., and Milton, K. A. (2006). *Thermal corrections to the Casimir effect*. Preprint. (<http://arxiv.org/abs/quant-ph/0605005>)
- Brevik, I., and Høye, J. S. (1988). Van der Waals force derived from a quantum statistical mechanical path integral method. *Physica A*, 153, 420–440.

- Brown-Hayes, M., Dalvit, D. A. R., Mazzitelli, F. D., Kim, W. J., and Onofrio, R. (2005). Towards a precision measurement of the Casimir force in a cylinder-plane geometry. *Phys. Rev. A*, *72*, 052102, 1–11.
- Brydges, D. C., and Federbush, P. (1980). Debye screening. *Commun. Math. Phys.*, *73*, 197–246.
- Brydges, D. C., and Martin, Ph. A. (1999). Coulomb systems at low density : a review. *J. Stat. Phys.*, *96*, 1163–1330.
- Brydges, D. C., and Martin, Ph. A. (2000). Survey of exact results in low density Coulomb systems. *J. Phys. IV France*, *10*, Pr5, 53–63.
- Buenzli, P. R., and Martin, Ph. A. (2005a). Microscopic origin of universality in Casimir forces. *J. Stat. Phys.*, *119*, 273–307.
- Buenzli, P. R., and Martin, Ph. A. (2005b). The Casimir force at high temperature. *Europhys. Lett.*, *72*, 42–48.
- Buenzli, P. R., and Martin, Ph. A. (2006). *Microscopic theory of the high-temperature Casimir effect*. In preparation, Swiss Federal Institute of Technology, Lausanne (EPFL), Institute of Theoretical Physics, CH–1015 Lausanne, Switzerland.
- Casimir, H. B. G. (1948). On the attraction between two perfectly conducting plates. *Proc. Kon. Ned. Akad. Wet.*, *51*, 793–795.
- Casimir, H. B. G. (1949). Sur les forces van der Waals–London. *J. Chim. Physique*, *46*, 407–410.
- Casimir, H. B. G., and Polder, D. (1948). The influence of retardation on the London–van der Waals forces. *Phys. Rev.*, *73*, 360–372.
- Caussé, P. C. (1836). *l'Album du marin : contenant les diverses positions du bâtiment à la mer*. Nantes: Charpentier. (Reproduced in fac-simile in 1990 by Inter-livres, Paris; cited by Boersma (1996))
- Chabrier, G., and Schatzman, E. (Eds.). (1994). *The equation of state in astrophysics* (Vol. 147). Cambridge, UK: Cambridge University Press.
- Chan, H. B., Aksyuk, V. A., Kleiman, R. N., Bishop, D. J., and Capasso, F. (2001). Quantum mechanical actuation of microelectromechanical systems by the Casimir force. *Science*, *291*, 1941–1944.
- Cohen-Tannoudji, C., Dupont-Roc, J., and Grynberg, G. (1989). *Photons and atoms, introduction to quantum electrodynamics*. New York: John Wiley and Sons.
- Cornu, F. (1996a). Correlations in quantum plasmas. I. Resummation in Mayer-like diagrammatics. *Phys. Rev. E*, *53*, 4562–4594.
- Cornu, F. (1996b). Correlations in quantum plasmas. II. Algebraic tails. *Phys. Rev. E*, *53*, 4595–4631.
- Cornu, F. (1998a). Quantum plasmas with or without a uniform magnetic field. I. General formalism and algebraic tails of correlations. *Phys. Rev. E*, *58*, 5268–5292.
- Cornu, F. (1998b). Quantum plasmas with or without a uniform magnetic field. III. Exact low-density algebraic tails of correlations. *Phys. Rev. E*, *58*, 5322–5346.
- Cornu, F., and Martin, Ph. A. (1991). Electron gas beyond the random-phase approximation: algebraic screening. *Phys. Rev. A*, *44*, 4893–4910.
- Darwin, C. G. (1920). The dynamical motion of charged particles. *Philos. Mag.*, *39*,

- 537–551.
- Debye, P., and Hückel, E. (1923a). Zur Theorie der Elektrolyte. I. Gefrierpunktserniedrigung und verwandte Erscheinungen. *Physik. Zeitschr.*, *24*, 185–206.
- Debye, P., and Hückel, E. (1923b). Zur Theorie der Elektrolyte. II. Das Grenzgesetz für die elektrische Leitfähigkeit. *Physik. Zeitschr.*, *24*, 305–325.
- Derjaguin, B. (1934). Untersuchungen über die Reibung und Adhäsion, iv. *Kolloid-Z.*, *69*, 155–164.
- Duplantier, B., and Rivasseau, V. (Eds.). (2003). *Poincaré seminar 2002 : Vacuum energy-renormalization* (Vol. 30). Basel: Birkhäuser.
- Dzyaloshinskii, I. E., Lifshitz, E. M., and Pitaevskii, L. P. (1961). The general theory of van der Waals forces. *Adv. Phys.*, *10*, 165–209.
- Elizade, E., and Romeo, A. (1991). Essentials of the Casimir effect and its computation. *Am. J. Phys.*, *59*, 711–719.
- Essén, H. (1996). Darwin magnetic interaction energy and its macroscopic consequence. *Phys. Rev. E*, *53*, 5228–5239.
- Fefferman, C. (1985). The atomic and molecular nature of matter. *Rev. Mat. Iberoam.*, *1*, 1–44.
- Felderhof, B. U. (1965). On fluctuations and coherence of radiation in classical and semi-classical plasmas. *Physica (Amsterdam)*, *31*, 295–316.
- Feynman, R. P., and Hibbs, A. R. (1965). *Quantum mechanics and path integral*. New York: McGraw–Hill.
- Fierz, M. (1960). Zur Anziehung leitender Ebenen im Vakuum. *Helv. Phys. Acta*, *33*, 855–858.
- Fischbach, E., and Talmadge, C. L. (1999). *The search for non-Newtonian gravity*. New York: Springer.
- Forrester, P., Jancovici, B., and Téllez, G. (1996). Universality in some classical Coulomb systems of restricted dimension. *J. Stat. Phys.*, *84*, 359–378.
- Ginibre, J. (1965a). Reduced density matrices of quantum gases I. Limit of infinite volume. *J. Math. Phys.*, *6*, 238–251.
- Ginibre, J. (1965b). Reduced density matrices of quantum gases II. Cluster property. *J. Math. Phys.*, *6*, 252–262.
- Ginibre, J. (1965c). Reduced density matrices of quantum gases III. Hard-core potentials. *J. Math. Phys.*, *6*, 1423–1446.
- Guernsey, R. L. (1970). Correlation effects in semi-infinite plasmas. *Phys. Fluids*, *13*, 2089–2102.
- Hansen, J.-P., and McDonald, I. R. (1986). *Theory of simple liquids* (2nd ed.). London: Academic Press.
- Høye, J. S., and Brevik, I. (1998). Van der Waals force between dielectric plates derived from the quantum statistical mechanical path integral method. *Physica A*, *259*, 165–182.
- Høye, J. S., Brevik, I., and Aarseth, J. B. (2005). *What is the temperature dependence of the Casimir effect?* Preprint. (<http://arxiv.org/abs/quant-ph/0506025>)
- Høye, J. S., Brevik, I., Aarseth, J. B., and Milton, K. A. (2003). Does the transverse

- electric zero mode contribute to the Casimir effect for a metal? *Phys. Rev. E*, *67*, 056116, 1–17.
- Høye, J. S., and Stell, G. (1981). Quantum statistical mechanical model for polarizable fluids. *J. Chem. Phys.*, *75*, 5133–5142.
- Høye, J. S., and Stell, G. (1994). Path integral formulation for quantized fermion and boson fluids. *J. Stat. Phys.*, *77*, 361–381.
- Huber, G., Mantz, H., Spolenak, R., Mecke, K., Jacobs, K., Gorb, S. N., et al. (2005). Evidence for capillarity contributions to gecko adhesion from single spatula nanomechanical measurements. *Proceedings of the National Academy of Sciences*, *102*, 16293–16296. (<http://www.pnas.org/cgi/doi/10.1073/pnas.0506328102>).
- Jackson, J. D. (1998). *Classical electrodynamics* (2nd ed.). New York: Wiley Text Books.
- Jancovici, B. (1980). Diamagnetism of an electron gas and surface currents. *Physica A*, *101*, 324–338.
- Jancovici, B. (1982). Classical Coulomb systems near a plane wall. I. *J. Stat. Phys.*, *28*, 43–65.
- Jancovici, B. (2005). [Private communication].
- Jancovici, B., and Šamaj, L. (2004). Screening of Casimir forces by electrolytes in semi-infinite geometries. *J. Stat. Mech.*, P08006. Electronic journal: <http://www.iop.org/EJ/article/1742-5468/2004/08/P08006>.
- Jancovici, B., and Šamaj, L. (2005). Casimir force between two ideal-conductor walls revisited. *Europhys. Lett.*, *72*, 35–41.
- Jancovici, B., and Téllez, G. (1996). The ideal conductor limit. *J. Phys. A : Math. Gen.*, *29*, 1155–1166.
- Jones, D. S. (1982). *Theory of generalised functions* (2nd ed.). Cambridge, UK: Cambridge University Press.
- Kempf, A. (2006). *Could the Casimir effect explain the energetics of high-temperature superconductors?* Preprint. (<http://arxiv.org/abs/cond-mat/0603318>)
- Klauder, J. R., and Skagerstam, B.-S. (1985). *Coherent states*. Singapore: World Scientific.
- Kleinert, H. (1990). *Path integrals in quantum mechanics, statistics and polymer physics*. Singapore: World Scientific.
- Klimchitskaya, G. L., and Mostepanenko, V. M. (2006). *Comment on "Effects of spatial dispersion on electromagnetic surface modes and on modes associated with a gap between two half spaces"*. Preprint. (<http://arxiv.org/abs/quant-ph/0603128>)
- Lamoreaux, S. K. (1997). Demonstration of the Casimir force force in the 0.6 to 6 μm range. *Phys. Rev. Lett.*, *78*, 5–8. (See also Erratum in (Lamoreaux, 1998))
- Lamoreaux, S. K. (1998). Erratum: Demonstration of the Casimir force in the 0.6 to 6 μm range (Lamoreaux, 1997). *Phys. Rev. Lett.*, *81*, 5475–5476.
- Landau, L. D., Lifshitz, E. M., and Pitaevskii, L. P. (1984). *Electrodynamics of continuous media*. In *Landau course* (2nd ed., Vol. 8). Oxford: Pergamon Press.
- Larrazza, A., and Denardo, B. (1998). An acoustic Casimir effect. *Phys. Lett. A*, *248*,

- 151–155.
- Lebowitz, J. L., and Martin, Ph. A. (1984). On potential and field fluctuations in classical charged systems. *J. Stat. Phys.*, *34*, 287–311.
- Levin, F. S., and Micha, D. A. (Eds.). (1993). *Long-range Casimir forces. Theory and recent experiments on atomic systems*. New York: Plenum Press.
- Lieb, E. H. (1976). The stability of matter. *Rev. Mod. Phys.*, *48*, 533–569.
- Lieb, E. H. (2004). Quantum mechanics, the stability of matter and quantum electrodynamics. *Jahresbericht der Deutschen Mathematiker-Vereinigung (German Mathematical Society, DMV)*, *106*, 93–110. (<http://arxiv.org/abs/math-ph/0401004>.)
- Lieb, E. H., and Loss, M. (2005). The thermodynamic limit for matter interacting with Coulomb forces and with the quantized electromagnetic field: I. The lower bound. *Commun. Math. Phys.*, *258*, 675–695.
- Lifshitz, E. M. (1955). The theory of molecular attractive forces between solids. *J. Exp. Th. Phys. USSR*, *29*, 94–110. (English translation : *Sov. Phys. JETP*, *2*, 73–83 (1956))
- Lighthill, M. J. (1996). *Introduction to Fourier analysis and generalised functions* (Reprint ed.). Cambridge, UK: Cambridge University Press.
- London, F. (1930). Zur Theorie und Systematik der Molekularkräfte. *Z. Physik*, *63*, 245–279.
- Macris, N., Martin, Ph. A., and Pulé, J. V. (1988). Diamagnetic currents. *Commun. Math. Phys.*, *117*, 215–241.
- Mahanty, J., and Ninham, B. W. (1976). *Dispersion forces*. New York: Academic Press.
- Martin, Ph. A. (1988). Sum rules in charged fluids. *Rev. Mod. Phys.*, *60*, 1075–1127.
- Martin, Ph. A. (2003). Quantum Mayer graphs: Application to Bose and Coulomb gases. *Acta Phys. Polonica B*, *34*, 3629–3648. (Presented at the XV Marian Smoluchowski Symposium, Zakopane, September 2002. Available from <http://th-www.if.uj.edu.pl/acta/vol34/abs/v34p3629.htm>)
- Martin, Ph. A., and Buenzli, P. R. (2006). *The Casimir effect*. To appear in the Proceedings of the 1st Warsaw School of Statistical Physics (June 2005), *Acta Physica Polonica*. (<http://arxiv.org/abs/cond-mat/0602559>)
- Meeron, E. (1958). Theory of potentials of average force and radial distribution function in ionic solutions. *J. Chem. Phys.*, *28*, 630–643.
- Meeron, E. (1961). *Plasma physics*. New York: McGraw-Hill.
- Mehra, J. (1967). Temperature correction to the Casimir effect. *Physica*, *37*, 145–152.
- Milonni, P. W. (1994). *The quantum vacuum: An introduction to quantum electrodynamics*. San Diego: Academic Press.
- Milonni, P. W., Cook, R. J., and Goggin, M. E. (1988). Radiation pressure from the vacuum : Physical interpretation of the Casimir force. *Phys. Rev. A*, *38*, 1621–1623.
- Milton, K. A. (2001). *The Casimir effect: Physical manifestations of zero-point energy*. Singapore: World Scientific.
- Milton, K. A. (2004). The Casimir effect: recent controversies and progress. *J. Phys. A:*

- Math. Gen.*, 37, R209–R277.
- Mohideen, U., and Roy, A. (1998). Precision measurement of the Casimir force from 0.1 to 0.9 μm range. *Phys. Rev. Lett.*, 81, 4549–4552.
- Mostepanenko, V. M., Bezerra, V. B., Decca, R. S., Geyer, B., Fischbach, E., Klimchitskaya, G. L., et al. (2005). *Present status of controversies regarding the thermal Casimir force*. Preprint. To appear in *J. Phys. A*. (<http://arxiv.org/abs/quant-ph/0512134>)
- Mostepanenko, V. M., and Trunov, N. N. (1997). *The Casimir effect and its applications*. Oxford: Clarendon Press.
- Olver, F. W. J. (1974). *Asymptotics and special functions*. New York: Academic Press.
- Onofrio, R. (2006). [Private communication].
- Pines, D., and Nozières, Ph. (1966). *The theory of quantum liquids*. New York: Benjamin.
- Plunien, G., Müller, B., and Greiner, W. (1986). The Casimir effect. *Phys. Reports*, 134, 87–193.
- Renne, M. J. (1971a). Microscopic theory of retarded van der Waals forces between macroscopic dielectric bodies. *Physica*, 56, 125–137.
- Renne, M. J. (1971b). Retarded van der Waals interaction in a system of harmonic oscillators. *Physica*, 53, 193–209.
- Roespstorff, G. (1994). *Path integral approach to quantum physics. An introduction*. Berlin: Springer Verlag.
- Ruelle, D. (1989). *Statistical mechanics, rigorous results* (Reprint ed.). New York: Benjamin.
- Schaden, M., and Spruch, L. (2002a). Semiclassical Casimir energies at finite temperature. *Phys. Rev. A*, 65, 022108, 1–8.
- Schaden, M., and Spruch, L. (2002b). Classical Casimir effect: The interaction of ideal parallel walls at a finite temperature. *Phys. Rev. A*, 65, 034101, 1–4.
- Schwinger, J. (1975). Casimir effect in source theory. *Lett. Math. Phys.*, 1, 43–47.
- Schwinger, J., DeRaad, L. L., Jr, and Milton, K. A. (1978). Casimir effect in dielectrics. *Ann. Phys.*, 115, 1–23.
- Schwinger, J., DeRaad, L. L., Jr, Milton, K. A., and Tsai, W.-Y. (1998). *Classical electrodynamics*. Boulder: Westview Press.
- Sernelius, B. E. (2005). Effects of spatial dispersion on electromagnetic surface modes and on modes associated with a gap between two half spaces. *Phys. Rev. B*, 71, 235114-1–235114-13.
- Sernelius, B. E. (2006). *Finite-temperature Casimir force between metal plates: full inclusion of spatial dispersion resolves a long-standing controversy*. Preprint, provided by the author. To appear in *J. Phys. A*.
- Simon, B. (1979). *Functional integration and quantum physics*. London: Academic Press.
- Sommerfeld, A. (1948). Elektrodynamik. In *Vorlesung über theoretische Physik* (Vol. 3). Wiesbaden: Dieterich'sche Verlagsbuchhandlung. (*English translation: Electrodynamics, Lectures in theoretical physics* (Vol. 3), New York: Academic Press (1952))

-
- Sparnaay, M. J. (1958). Measurements of attractive forces between flat plates. *Physica*, 24, 751–764.
- Stanley, H. E. (1971). *Introduction to phase transitions and critical phenomena*. Oxford: Clarendon Press.
- Valeri, L., and Scharf, G. (2005). *Microscopic theory of the Casimir effect*. Preprint. (<http://arxiv.org/abs/quant-ph/0502115>)
- Yurdumakan, B., Raravikar, N. R., Ajayan, P. M., and Dhinojwala, A. (2005). Synthetic gecko foot-hairs from multiwalled carbon nanotubes. *Chem. Commun.*, 30, 3799–3801.

Acknowledgments

I would like to warmly thank my PhD supervisor, Prof. Philippe A. Martin, for giving me the opportunity to work on such an interesting subject and with such a fundamental approach. He has always been of a grand availability, humanness, and patience to me in the large space of freedom I was offered. His invaluable pedagogical explanations and advice, combined with his enthusiasm and regard for exactitude, encouraged me through difficult situations, and have guided me successfully through the completion of this work.


I am very thankful too to Prof. B. Jancovici, who, by his comments, allowed us to improve several points in our articles.

I would also like to thank Prof. Ch. Gruber, who directed me towards Ph. A. Martin, and Prof. H. Kunz and Prof. V. Savona for letting me be assistant to their lectures on Mathematical Physics and Statistical Mechanics, respectively, which consisted in pleasant challenges of pedagogy and interactions with undergraduate students. I am grateful to the Swiss National Science Foundation for having partially supported this research, and to Prof. A. Baldereschi for giving me the opportunity to work at the Institute of Theoretical Physics after my PhD. I acknowledge too Prof. J. S. Høye, Prof. B. Jancovici and Dr. N. Macris for having accepted to participate in the examination committee.

Having now spent a couple of years at the Institute of Theoretical Physics, my acknowledgments also go to all the people I became acquainted with there, especially Gaetano, who brought Italy in our shared office, as well as whistles in my head. Aric, who seeks out life's little challenges. Séverine and Leonor, for having been flowers. But also Claude, Rico, Davide, the peninsular community, George, Samuel B., Mauro and Sébastien, Vincent, Jean-Luc, Laurent, and all the others, for the many breaks and discussions we had together, and for their support.

A special attention goes to my friend Nicolas, as well as to Samuel, for they took me with them in the worlds of philosophy and music. To Fernando, whose will I admire and encourage. And also to Mildred for her unbounded friendship and magnanimity. Finally, I thank my parents Ursula and Jean-Claude, and my funny brothers Daniel and Dominique.

Thanks to all of them — at the first place — for who they all are.

My last thanks — but not at all the least — are for Sam x , who has been everything I dared imagine her to be.
And everything she dared imagine.

Lausanne, Summer 2006

Curriculum Vitae

Pascal (Renato) Bünzli

Born on September 26th, 1976, in Lausanne

EPFL SB ITP GMQ
PH H2 455 (Bâtiment PH)
Station 3
CH-1015 Lausanne
Tel. +41-21-693 34 17

E-mail: Pascal.Buenzli@alumni.ethz.ch

Education:

- 1999 – 2001 Diploma in theoretical physics [computational physics group] at Eidgenössische Technische Hochschule Zürich (ETHZ)
- 1996 – 1999 Undergraduate student in physics at École Polytechnique Fédérale de Lausanne (EPFL)
- 1995 – 1996 Undergraduate student in architecture at EPFL
- 1992 – 1995 High school at Gymnase Cantonal de la Cité, Lausanne
- 1983 – 1992 Elementary school in Cugy (VD) and college in Lausanne

Publications

- Buenzli, P. R., and Martin, Ph. A., Microscopic origin of universality in Casimir forces, *J. Stat. Phys.*, 119, pp. 273–307, (2005)
- el Boustani, S., Buenzli, P. R., and Martin, Ph. A., Equilibrium correlations in charged fluids coupled to the radiation field, *Phys. Rev. E*, 73, pp. 036113, 1–14, (2006)
- Buenzli, P. R., and Martin, Ph. A., The Casimir force at high temperature, *Europhys. Lett.*, 72, pp. 42–48, (2005)

In preparation:

- Buenzli, P. R., and Martin, Ph. A., Microscopic theory of the high-temperature Casimir effect (2006)

Proceedings:

- Martin, Ph. A., and Buenzli, P. R., The Casimir Effect, To appear in the Proceedings of the 1st Warsaw School of Statistical Physics (June 2005), *Acta Physica Polonica*, (2006), url: <http://arxiv.org/abs/cond-mat/0602559>